UNIVERSITÉ DE LIÈGE
FACULTÉ DES SCIENCES APPLIQUÉES

Automatic plastic-hinge analysis and design of 3D steel frames

Par

HOANG Van Long
Docteur en sciences de l'ingénieur de l'Université de Liège

Thèse de doctorat

2008

Thèse défendue, avec succès, le 24 septembre 2008, pour l'obtention du garde de Docteur en sciences de l'ingénieur de l'Université de Liège.

Jury: J.P. JASPART, Professeur à l'Université de Liège, Président
H. NGUYEN-DANG**,** Professeur à l'Université de Liège, Promoteur
R. MAQUOI, Professeur à l'Université de Liège
J.P. PONTHOT, Professeur à l'Université de Liège
J. RONDAL**,** Professeur à l'Université de Liège
I. DOGHRI, Professeur à l'Université Catholique de Louvain
M. DOMASZEWSKI**,** Professeur à l'Université de Technologie de Belfort-Montbéliard
G. MAIER, Professeur à Politecnico di Milano
P. MORELLE, Docteur, SAMTECH Liège

Dedicated to

my parents,
my parents-in-law,
my brother,
my wife,
and my daughter.

Table of contents

Introduction

Each year, a huge volume of steel is used in construction. Each year, ten thousands of researchers, engineers devote their time to determine an appropriate structural solutions respecting safety, serviceability and cost saving. Thank to the development of computer science, the application of modern theories for obtaining automatic solutions becomes the optimal answer to the mentioned questions.

During the last 40 years, the theories of plasticity, stability and computing technology made the great achievements. They permit to adopt the nonlinear design specifications in the Standards of construction. Both conditions and motivations to build-up the numerical tools for structural analysis are taken off since 1970's. The framed structures are always the test bench, many software for this family of structure were early developed in various research centres around the world. For example, in the Department of Structural Mechanics and Stability of Constructions of the University of Liège, two computer programs for frameworks ware established at the end of the 1970's: FINELG program, a finite element computer program for nonlinear step-by-step analysis, was firstly build by F. Frey [50]; and CEPAO program developed by Nguyen-Dang [117], is a package for plastic-hinge direct analysis and optimization of 2-D frames.

In general, either the plastic-zone or the plastic-hinge approach is adopted to capture the both material inelasticity and geometric nonlinearity of a framed structure. In the plastic-zone method, according to the requirement of refinement, a structure member is discretized into a mesh of finite elements, composed of three-dimensional finite-shell elements or fibre elements. Thus, this approach may describe the "actual" behaviour of structures, and it is known as the "quasi-exact" solution. However, although tremendous advances in both computer hardware and numerical technique were achieved, plastic-zone method is still considered as an "expensive" method requiring considerable computing burden.

On the other hand, in the plastic-hinge approach, only one beam-column element per physical member can model the nonlinear properties of the structures. It leads to significant reduction of computation time. Furthermore, the computer program using the plastic-hinge model is familiar to the habit the engineers. With such mentioned advantages, it appears that the plastic-hinge method is more widely used in practice than the plastic zone method. However, the plastic-hinge analysis is not without inconveniences that will be mentioned in Chapter 1 of this thesis. This approach needs then to be improved. Present thesis is oriented in that direction and aims to develop practical software for automatic plastic-hinge analysis and optimisation of 3-D steel frames. The principal basic ideas have been originally adopted in CEPAO package for 2-D frames by Nguyen-Dang [117]. The present work proposes to extend these solutions to 3-D frames. The theory of plasticity, particularly, the theory of limit analysis and the theory of shakedown analysis constitute the fundamental theoretical bases for the numerical implementations. The use of the linear programming technique combined with the finite element method constitutes the two useful pillars of this numerical procedure. This thesis is concretely composed of 10 chapters as follows:

Chapter 1 constitutes an overview of plastic-hinge analysis of frameworks. It aims to highlight the deficiencies of the domain, on about both aspects: model and method. In fact, the main motivations of the present thesis are to overcome these deficiencies.

Chapter 2 describes the plastic behaviours of structures under fixed and repeated loading. Useful theorems for plastic analysis are presented.

Chapter 3 presents the formulation of the thirteen-degree-of-freedom element for 3-D members. This element allows to apply the fundamental equations in both elastic-plastic and rigid-plastic analysis of frames. The compatible matrix (or its transpose the equilibrium matrix) established automatically in this chapter is fundamentally used in all procedures, both analysis and in design aspects of CEPAO package.

Chapter 4 deals with an efficient algorithm for both limit and shakedown analysis of 3-D steel frames based on kinematical method using linear programming technique. Several features in the application of linear programming technique for rigid-plastic analysis of three-dimensional steel frames are discussed. We will mainly tackle the change of the variables, the automatic choice of the initial basic matrix for the simplex algorithm and the direct calculation of the dual variables by primal-dual technique. To highlight the capacity of the proposed techniques, numerical examples and discussions will be presented.

Chapter 5 considers the volume optimization of 3-D steel frames under both fixed loading (limit design) and repeated loading (shakedown design). The conception variables of the problem are the cross sections of 3-D frame members; they are automatically chosen in the database that contains the standard I or H-shaped section of both Europe and USA. Besides, the dimension of rigid-plastic design problem by statical approach using linear programming is considerably reduced. Several special techniques so-called *fixed-push* and *standard-transformation* leading to *semi-direct algorithm* are originally described. The content of this chapter may be considered as the "dual formulation" of which of Chapter 4. The efficiency of the technique is demonstrated with details by some numerical examples.

Chapter 6 concerns the second-order aspect of plastic-hinge analysis. First, a strain hardening rule for 3-D plastic-hinges is proposed in this chapter. The linear strain hardening law is modelled by two parameters: the effective strain and the plastic modulus. The definition of the effective strain as well as the method to fix the value of plastic modulus is described. A conventional second-order elastic-plastic approach taking into account above hardening rule is also considered in the present chapter. Finally, numerical examples are analyzed by using CEPAO. It appears that the new numerical results are in good agreement with benchmarks.

Chapter 7 deals with local buckling check according to Eurocode-3 for the plastic-hinge analysis of 3-D steel frames with I or H-shaped sections. A useful technique for the determination of the stress distribution on the cross-sections under axial force and bi-bending moments is proposed. It permits to the concept of the classification of cross-sections may be directly used. Cross-section requirements for global plastic analysis in Eurocode-3 are applied for the local buckling check. To evaluate the technique, a large number of 3-D plastic hinge have been tested.

Chapter 8 is devoted to semi-rigid steel frames in the level of global plastic analysis and optimization. First, the behaviour and the popular modelling of connexions are briefly reminded. One may see here how CEPAO takes into account the semi-rigid behaviour of connexions in both elastic-plastic and rigid-plastic analysis. Finally, various numerical examples solved by CEPAO are examined. The comparison with some other software is also illustrated.

Chapter 9 presents the application aspect of CEPAO by the input and output systems. It demonstrates the automatic level of CEPAO, with a simple input as in the linear elastic analysis one obtains a rather complete picture of the plastic analysis and design of frames in the output.

Chapter 10 contains the main conclusions and future perspectives.

From Chapter 3 to Chapter 8, all mentioned algorithms were implemented in a united package, written in FORTRAN language. The robustness of code, that is the ability to solve the large-scale frames, constitutes the most important task in the preparation of this thesis. Considerable times are needed to overcome multiple difficulties in the construction of the new CEPAO package.

On the scientific research point of view, according to the author's knowledge, the following points may be considered as the *original contributions* in this thesis:

- The change of variables and the automatic choice of the initial basic matrix for the simplex algorithm allow to reduce the computational cost in both limit and shakedown analysis of 3-D steel frames (Chapter 4).

- To reduce the problem size of limit and shakedown design problem, we propose the following techniques: fixed-push technique, standard-transformation technique and semi-direct algorithm (Chapter 5).

- We did set up a new algorithm for the second-order plastic-hinge analysis of 3-D steel frames taking into account strain hardening behaviour (Chapter 6).

- We propose the formulations to determine the stress state over I or H-shaped sections so that the concept of the classification of cross-sections in Eurocode-3 may be directly used (Chapter 7).

The mentioned points have been already presented in our recent already published or in review for publications [60, 61, 62, 63].

Chapter **1**

An overview of plastic-hinge analysis for steel frames

Generally, there are two principal aspects in the domain of structural analysis: *models* and *methods*. This chapter discusses on models and methods frequently used in the plastic-hinge analysis of frames.

Keywords: *Plastic hinge; Yield surface; Direct methods; Step-by-step methods.*

1.1. Models in plastic-hinge analysis

1.1.1. Discretization of structures

Actually, all structures have three dimensions; their behaviour is the object of the continuum mechanic where the fundamental relationships are written at each point in the structure. However, with their form, the bars have the particular behaviour described by the kinematic hypothesis of Bernoulli: the cross-section of bars remains plan after deformation (see Massonnet (1947)[107]). By this hypothesis, the bars may be reduced to one-dimensional structure. On the large sense, the bars are discretized and modelled by their neutral axis. The state of stress and strains anywhere in the bars may be deduced from the "*axis's stress"* and the "*axis's strain"* also respectively called the *generalized stresses* and the *generalized strains*. The generalized stresses are bending moments, torsional moment, shear force and axial force; the corresponding generalized strains contain rotations, deflections and elongation/shortening. The concept of *generalized stresses* and *generalized strains* were widely used in the structural engineering since the 1950's (see Timoshenko (1951, 1962)[142, 143]).

1.1.2. Definitions of plastic hinge and collapse mechanism

According to many authors (e.g. Neal [114], Massonnet [106]), the notion of *plastic hinge* and *collapse mechanism* were firstly pointed out by Kazinczy in 1914.

Until now, the terminology plastic hinge is used to indicate a section (zero-length) on which all points are in the plastic range. The elastic state and the plastic state of a section are distinguished by a *yield surface* that is written in the space of the generalized stresses.

The terminology collapse mechanism is originally utilized to describe the ultimate state of a frame where it is considered as a deformable geometric system. The last state is based on the idealization: the plastic hinges are replaced by "real" hinges whereas the rest parts of the frame are the rigid-bodies. In the large sense, the collapse mechanism is understood as the collapse state of frames due to the combined plastic deformations at plastic hinges.

1.1.3. Modelling of frames in plastic- hinge analysis

On the behaviour aspect, in the plastic-hinge analysis, the frame is considered as a system of three components: the *joints* (connexions), the *critical sections* and the *bars*. The different behaviour laws are applied onto each component as follows:

Connexions behaviours: Either rigid or semi-rigid behaviour is adopted for the connexions. The behaviour of the semi-rigid connexions depends on their form. It was dealt with in many texts, e.g. Chen (1989, 1991, 1996)[23, 24, 19], Kishi (1990)[82], Bjorhovde (1990)[8], Maquoi (1991, 1992)[105, 104], Jaspart (1991, 1997)[68, 70], Cabrero (2005, 2007)[11, 12], among many others.

Critical section behaviours: the critical sections could exhibit two states: elastic or plastic (plastic hinge). They are distinguished by the yield surface. There are not relative displacements at the elastic sections, while there exist the discontinuities of the displacements at plastic hinges (Fig.1.1). The last phenomenon is due to the fact that the plastic deformations are lumped at plastic hinges (zero length). To model the behaviour of plastic hinges, there are three principal approaches:

1. Considering only the bending effect, the others effects are neglected (Fig.1.2a). By its simplicity, this approach is popularly applied to 2-D steel frames (see Neal (1956)[114], Hodge (1959)[64] and Massonnet (1976)[106]).

2. Considering the effect of axial force by the yield surface but neglecting the plastic axial deformation (Fig.1.2b). The detailed application of this type may be found in Chen (1996)[19]; and several authors recently adopted this model to build up the numerical algorithms for 3-D steel frames (e.g. Kim (2001, 2002, 2003)[81, 79, 80]).

3. The plastic hinge is modelled by the normality rule (Fig.1.2c), it is considered as the most "exact" model. This formulation were adopted by many authors, for example: Lescouarc'h (1975, 1976)[86, 87], Orbison (1982)[126] and present thesis.

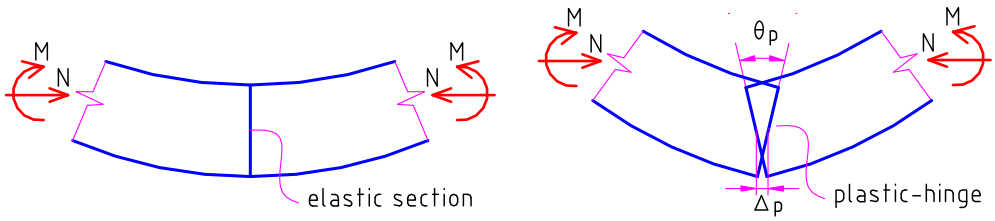

Fig.1.1. Behaviours of critical sections

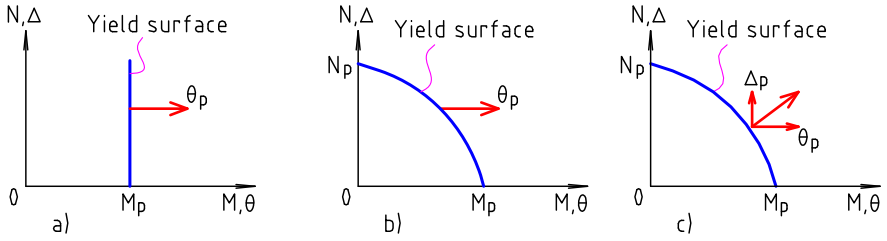

Fig.1.2. Plastic hinge models

Behaviours of bars: in the elastic-plastic plastic-hinge analysis, the bars abide obviously the Hook's law. These behaviours are the object of the strength of material domain. On the other hand, the rigid-plastic analysis assumes the bars are the rigid bodies.

On the concept of the finite element method, in the plastic-hinge analysis, each physical member is modelled by a beam-column element that is modelled again by a line. These elements are connected by the nodes. Herein, the nodes are the point, no behaviour. Therefore, the behaviour of the beam element must include the behaviours of the bars, of two critical sections at its ends and of the concerned semi-rigid connexions.

1.1.4. Advantages and limitations

From the above description, the plastic-hinge model embeds the following features:

- *Advantages*

1. In the plastic-hinge model, a physical member may be modelled by only one beam-column element; the computational cost is then significant reduced, in comparison with plastic-zone methods.

2. The computer program for the global analysis of frames using the plastic-hinge model is familiar with the uses as the engineers.

- *Limitations*

1. Although the formulation of yield surfaces have drawn the attentions of many authors (e.g. Hodge (1959[64], Save (1961, 1972)[136, 135], Sawczuk (1971)[137], Chen (1977)[20], Orbison (1982)[126] and Nguyen-Dang (1984)[122]), it is still difficult to build-up the practical yield surfaces for any shapes of cross-sections. For the practical purpose, a yield surface must be satisfied two conditions: (1) to have a good reflection of the real behaviour of sections; (2) to be suitable to global plastic analysis (not too complicated). The second request means that the yield surface must be convex and must be described by only a few numbers of mathematical equations. In the steel frames, I or H-shaped sections is frequently used. The inherent form of this type sections leads to both mentioned conditions are not easy to satisfy. Up to now, the popular yield surfaces take into account only the bending moments and the axial force, the shear force and torsional moments are ignored; e.g. the sixteen-facet polyhedron of AISC [1] or Orbison's yield surface [126].

2. Because the theory of limit analysis is usually applied to construct the yield surfaces, the local buckling phenomenon of the sections is normally ignored.

3. There are a significant difference between the Euler's bar used in plastic-hinge analysis and the actual bar. The experiments demonstrate that the critical axial force of an actual bar never reached the Euler's value; it's due to the complex member behaviour, such as: distributed plasticity, lateral-torsional effect, local buckling, geometric imperfection, and residual stresses. The mentioned discussions is demonstrated by the difference between the buckling curves and Euler' curve (see Rondal (1979, 1984)[131, 130]).

1.2. Direct methods for plastic analysis and design

Generally, problems of *analysis* and *design* are closely related, but they are not identical. On one hand, the aim of analysis problems is the determination of the maximum *safe load* for a frame that is fully specified. On the other hand, the loads are specified in a design problem, and we must determine the *optimal member-size* (cross-sections) of a frame with the node layout is fixed. In the plastic theory for frameworks, the analysis and design approaches constitute dual problems. It is not complete if we consider only one of them.

1.2.1. Description

Fundamental theorems: The two fundamental theorems of limit analysis, static and kinematic theorems, were first established by Gvozdev in 1938. At the same time, the static shakedown theorem was first proved by Melan in 1938. After 20 years, the kinematic theorem for shakedown analysis of frames was derived by Neal in 1956 [114]. In the same year, this theorem for solids was pointed out by Koiter [83]. The theorems concerning plastic design problems were established, in 1950's, by Foulkes [47] and Neal [114].

Plastic methods: Generally, there are two fundamental theorems: static and kinematic. It leads to two corresponding approaches: *static approach* and *kinematic approach* that are called *direct methods*. The terminology *Direct* means that the load multiplier is directly found without any intermediate state of structures. Both the static method and the kinematic method are

continually exploited and improved since more than 50 years until now. A brief historic landmark of this question for framed structures is described as follows:

- *Classic methods*

In the 1950's, at University of Cambridge, the first plastic methods, e.g. trial and error method; combination of mechanism method; plastic moment distribution method, were proposed by Baker, Neal, Symonds and Horne (see Neal [114]). The method of combined mechanics has become rapidly popular around the world, and it is now still presented as lectures of many universities. Based on the method of combined mechanics, some computer program were established (see Cohn (1969)[31]). However, since 1970, with the developments of application of mathematical programming in the plasticity, the mentioned methods become "classic methods". They are still the best tools for simple frames, less than 20 bars, but it is not suitable for the large real-world structures.

- *Automatic methods using mathematical programming*

The application of mathematical programming to the structural mechanic in generally, and to the engineering plasticity in particularity, is a large and interesting domain. The plastic analysis can be formulated as a problem of mathematical programming, and this powerful tool developed in the mathematical theory of optimization can be applied. With the *simplex method,* proposed by Dantzig in 1949 (see [39]), the linear programming problem is generally well solved. The first connexion of the linear programming – to – the plastic analysis was pointed out by Charnes (1951)[17]. The useful approaches using mathematical programming for all plastic analysis and design problems were developed by Maier (1969, 1970, 1971, 1973)[102, 101, 93, 96, 103, 98], Cohn (1971)[30, 33], Grierson (1971)[55] and Munro (1972)[113]. It is a landmark in the plastic method using mathematical programming for structural analysis. After that, this domain has been exploited with success. We may find a big picture on the application of the mathematical programming to structural analysis in the texts: the state-of-the-art report of Grierson (1974)[54]; the book edited by Cohn (1979)[32]; the state-of-the-art papers and the key note of Maier (1982, 2000)[97, 99, 94]; the book edited by Smith (1990)[140]; and the paper by Cocchetti (2003)[29] . At University of Liège, Nguyen-Dang et al. have obtained the progress to establish the automatic algorithms using the finite element technique (see Nguyen-Dang (1976, 1978, 1980, 1982, 1984)[115, 121, 124, 118, 116, 117], Morelle (1984, 1986, 1989)[111, 110, 109], Bui-Cong (1998)[9], Yan (1999)[150], Vu-Duc (2004)[147] and Hoang-Van (2008)[60, 61, 62, 63]).

During 1970-1990, the researchers aimed to develop the practical software for framed structures. Some interesting computer programs were built up, e.g. DAPS [127], STRUPL-ANALYSIS [49], CEPAO [117, 38]. For this work, seeking of automatic algorithms and of techniques to reduce the computational cost are two most important problems. In general, in order to have an automatic solution, the linear programming technique must combine with the finite element method. The fine combination between the structural behaviour with the linear algebra/linear programming properties leads to a significant reduction of the problem-sizes. Various useful techniques with the archival values are presented in Domaszewski (1979, 1983, 1985)[41, 42, 43] and Nguyen-Dang (1983, 1984)[117, 123]. Not only the determination of the ultimate load factor but also the determination of the displacement field by linear programming has examined, e.g. Grierson (1972)[56], Nguyen-Dang (1983)[125]. Even the second-order analysis using linear programming was also examined (see Baset (1973)[3]). However, unfortunately, after 1990, the research in this direction is sporadic and limited; requirement of practical engineering is not yet satisfied. This situation due to two main reasons: (1) some inconveniences of the direct methods appear (see Section 1.2.2); and (2) the attraction of the step-by-step methods (see Section 1.3.2).

1.2.2. Advantages and limitations of direct methods

Concerning the rigid-plastic analysis and design of frames using linear programming, we may summarize in the following points.

- *Advantages*

It appears that this type of analysis is

1. Capable of taking full advantages of mathematic programming achievements;
2. Suitable to solve the structures under repeated loading (shakedown problem);
3. Possible to unify into unique computer program because the algorithms of direct methods for different procedures are similar, such as: limit or shakedown, analysis or design, frames or plate/shell, etc.
4. Not influenced by the local behaviour of structures, such as the elastic return (a phenomenon often occurs in the step-by-step methods). There exists sometime degenerate phenomenon in simplex method but it was treated by the *lexicographical rule* (see [39]).

- *Limitations*

One may evoke here some drawbacks:

1. The difficulties appear when the geometric nonlinearity conditions are considered. It is a great challenge.
2. The difficulties to solve the large-scale frames. Because the direct methods are "one step" methods.

1.3. Step-by-step methods for plastic-hinge analysis

1.3.1. Description

Step-by-step methods, or elastic-plastic incremental methods, are based on the standard methods of elastic analysis. The loading process is divided into various steps. After each loading step, the stiffness matrix is updated in order to take into account the nonlinear effects. In comparison with the elastic solution, only the physical matrix varies to consider the plastic behaviour. Zienkiewicz (1969)[151] is one pioneer who first introduced the formulation of the elastic-plastic physical matrix into the finite element method. The majority of step-by-step approaches are based on the displacement model, while a few authors have applied the equilibrium approach (e.g. Fraeijs de Veubeke (1965)[48], Nguyen-Dang (1970)[119], Beckers (1972)[7]). Normally, the stiffness matrix is classically updated. However, other authors have proposed to implement the indirect update of structural stiffness matrix using mathematical programming (e.g. Maier (1979)[95]). In summary, the step-by-step methods benefit the long experiences of the linear elastic analysis by the finite element method. One may find many useful computational algorithms and techniques in many text books (e.g. Bathe (1982, 1996)[5, 4], Géradin (1997)[51], Zienkiewicz (1989, 1991)[152, 153], Doghri (2000)[40], among others).

Concerning the plastic-hinge analysis of framed structures, the question to be answer is the formulation of the beam-column element. It must be suitable to the global algorithm, while the complex behaviours of the structures should be taken into account. It means that the improvement of the third limitation (see Section 1.1.4) is the focus in the plastic-hinge analysis of steel frames using step-by-step methods. Some remarks are summarized as follows:

Geometric nonlinearity: Concerning the geometric nonlinearity, there are two theories: the finite-strains (large deformation) and the large-displacements small-strains. The first theory is suitable to model some process of the mechanics, e.g. metal forming (see Cescotto (1978,

1994)[15, 16], Ponthot (1994, 2002)[128, 129]). In general speaking, the maximal deformations occurring at the ultimate state of the building steel frames are in the scope of the large-displacements small-strains theory. With the 3-D frames, the treatment of the finite rotation about an axis is an important subject (see Argyris (1978)[2]). This problem attracts the attention of many authors (e.g. Cardona (1988)[13], Teh (1998)[141], Izzuddin (2001)[65], Battini (2002)[6] and Ridrigues (2005)[132]). However, for the practical purpose, the conventional second-order analysis is widely utilized to capture the geometric nonlinearity of the steel frames. This approach takes into account the P-delta effect (P-Δ and P-δ), and the finite rotations are simply ignored. In order to avoid the member is divided into various elements, the stability functions are widely utilized in the element formulation. The elementary explanations of the method for steel structures may be found in a lot of books, e.g. Chen (1996)[19].

Effect of distributed plasticity: Actually, there is always a plastic zone around the plastic hinge. Their dimensions depend on the slope of the moment diagrams. Moreover, due to initial imperfection (member out of straightness and residual stress), some plastic pieces also appear along the bars. Those phenomena are named "distributed plasticity". They are neglected in the classic plastic-hinge model. In order to take into account the plastic zone effect at plastic hinges, most of authors used the element with spring ends (e.g. Liew (1993)[90], Chan (1997)[18], Hasan (2002)[58], Sekulović (2004)[138], Gong (2006)[53], Gizejowski (2006)[52], Liu (2008)[91], among others). Based on the AISC-LRFD Specification [1], Liew (1993)[90] has proposed the *column effective stiffness* concept to approximate the effect of distributed plasticity along the bars. This technique were recently applied and modified by the utilization of European buckling curves (Landesmann (2005)[85]). When the distributed yielding is considered by the mentioned techniques, the analysis is called the *refined plastic-hinge analysis* (see Liew (1993)[90] and Donald (1993)[44] and Chen (2005)[22]).

Strain hardening behaviour: It seems that the hardening effect is not adequately highlighted in the refined plastic hinge analysis. On the other context, the role of the hardening in steel structures is underlined by recent theoretic development and experimental tests presented by Davies (2002, 2006)[36, 37] and Byfield (2005)[10]. Those authors did study in detail the parameters useful to establish an expression which takes into account the increased bending moment due to a plastic-hinge rotation. By this technique, the strain hardening may be directly considered in the global plastic-hinge analysis of frames. However, their results are only applicable to the elastic-plastic analysis of 2-D steel frames where the bending behaviour is dominant.

Numerical algorithm: In the recent years, many authors concentred their efforts to establish the useful algorithms for the numerical tools to 3-D steel frames. For example: Orbison (1982)[126], Liew (2000, 2001)[88, 89], Kim (2001, 2006)[77, 78], etc. The lateral torsional and local buckling effects were also taken into account in few researches (Kim (2002, 2003)[79, 80]). Generally, these formulations are based on the conventional second-order approach with the concept of refined plastic hinge analysis. On the other hand, it is necessary to mention here several interesting algorithms so-called the *quasi-plastic zone* methods (e.g. Jiang (2002)[71], Chiorean (2005)[28] and Cuong (2006)[35]). They compromise plastic-zone and plastic-hinge methods.

When the global algorithm including the geometric and material nonlinearity is used, the approach is called the *direct design*. It means that the effective length factor concept is not requited (see Chen (2000)[26]).

1.3.2. Advantages and limitations

Compared to the direct methods, the step-by-step methods have the following features:

- *Advantages*

1. The geometric nonlinearity is appropriately taken into account in step-by-step methods.

2. The step-by-step methods furnished the complete redistribution progress prior to collapse of structures.

3. With the progress in both computing hardware and numerical technology, the modelling of structures, even the large-scale 3-D frames, could be dealt with.

- *Limitations*

1. For the case of arbitrary loading histories (shakedown problem), the step-by-step methods are cumbersome and embed many difficulties. It is a great challenge.

2. With the elastic-plastic plastic-hinge analysis of frames, this method is influenced by the local behaviour of structures, such as the elastic return, it can lead to an erroneous solution.

1.4. Computer program aspect

1.4.1. Generality

Computer program is an algorithm written by a computational language (FORTRAN, C, C^{++}, MATLAB, etc.), and the calculation procedures are then automatically realized by computer. There is a great distance from the theory to the computer program but it is the optimal way leading to the target.

Based on the application aspect, one may classed the computer program into three categories: computer program to illustrate the algorithms, computer programs to study and commercial software.

With the mentioned definition, one may see that any research group owns at least one computer program. However, according to the author' knowledge, almost computer programs for plastic-hinge analysis of complicated frames are based on the step-by-step methods. In fact, the large-scale 3-D steel frames under the arbitrary loading histories are not yet carried out.

1.4.2. CEPAO computer program

At the end of the 70's, this computer program was established by Nguyen-Dang et al. in University of Liège. The detailed explanation of this package may be found in Nguyen-Dang (1984)[117]. In the present thesis, only a brief presentation is condensed hereinafter:

Unified package of approaches: CEPAO was a unified package devoted to automatically solve the following problems happened for 2-D frames: Elastic analysis, elastic-plastic analysis, limit analysis with proportional loadings, shakedown analysis with variable repeated loadings, optimal plastic design with fixed loading, optimal plastic design with choice of discrete profiles and stability checks, shakedown plastic design with variable repeated loadings, shakedown plastic design with updating of elastic response in terms of the plastic capacity, optimal plastic design for concrete structures. In CEPAO, both direct and step-by-step methods are used, they give a better view on the behaviour of the structure and also they may mutually make up for their deficiencies. With the multi-results given by multi-approaches, CEPAO is an auto-control computer program.

Package of original techniques: In CEPAO, efficient choice between statical and kinematic formulations is realised leading to a minimum number of variables; also there is a considerable reduction of the dimension of every procedure is performed. The basic matrix of linear programming algorithm is implemented under the form of a reduced sequential vector which is modified during each iteration. An automatic procedure is proposed to build up the

common characteristic matrices of elastic-plastic or rigid-plastic calculation, particularly the matrix of the independent equilibrium equations. Application of duality aspects in the linear programming technique allows direct calculation of dual variables and avoids expensive re-analysis of every problem.

However, in the old version of CEPAO, the necessary techniques to treat some particular cases are not enough. For example, the treatment of the elastic-return phenomenon and the treatment of the degenerate in the simplex method are not efficient. Recently, CEPAO has been re-checked and updated to the case of semi-rigid frames (see Nguyen-Dang (2006)[120]).

Moreover, at the present time, on the point of view of software development, the 2-D bending frame modelling is not yet acclaimed. The actual computing technology permits us to think about the better modern modelling. On the one hand, the advanced analysis gives the results that reflect well the actual behaviour of structures. On the other hand, the engineers are "emancipated" by the conformable software that uses the modern analysis while the application is simple.

1.5. Conclusions

An overview of the global plastic-hinge analysis of steel frames has been presented. The current difficulties of the domain have been highlighted. Among those, there are the great challenges that are not easy to overcome. It appears that using the ideas of CEPAO to develop the practical software for 3-D frames is a research direction of great promise.

Chapter **2**

Inelastic behaviour of frames and fundamental theorems

The inelastic behaviour and the fundamental theorems for structures analysis in generally, and for frames analysis in particularly, were well dealt with in many text books (e.g. Neal (1951) [114], Hodge (1959)[64], Save (1972)[135], Massonnet (1976)[106], Nguyen-Dang (1984)[122], König (1987)[84], Chen (1988)[21], Lubliner (1990)[92], Mróz (1995)[112], Weichert (2000)[148] and Jirásek (2001)[72]). This chapter will first introduce a brief presentation of the plastic behaviour of frames; it is *clear* and *sufficient* to state the *definitions* and the *hypotheses* that are applied in this work. In the second part, the classic theorems are briefly announced without proof explanations, but the *useful comments* for the case of framed structures are underlined.

Keywords: *Simple loading*; *Complex loading*; *Plastic behaviour*; *Lower bound theorem*; *Upper bound theorem*.

2.1. Loading types

In the plasticity theory, the load is classified into two types: *simple loads* and *complex loads*. The simple loads indicate the proportional or fixed loads, while the complex loads denote non-proportional or repeated loads. The complex loads are described by a domain (Fig.2.1a), in which each load varies independently:

$$\mu \bar{f}_k^{\min} \le f_k \le \mu \bar{f}_k^{\max} . \tag{2.1}$$

The simple load is a particular case of the complex load where $f_k^{\min} = f_k^{\max}$, the domain becomes a line (proportional load) or a point (fixed load) as the show on Fig.2.1b,

$$f_k = \mu \bar{f}_k . \tag{2.2}$$

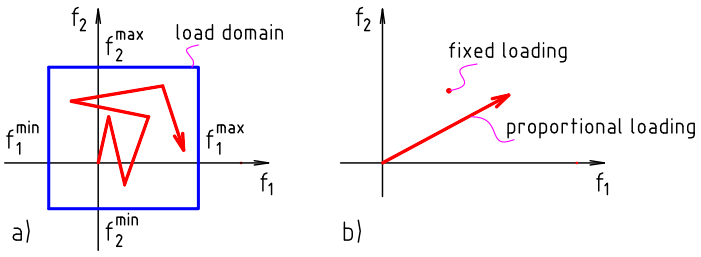

Fig.2.1. Loading type (a-complex loading; b-simple loading)

In Eqs.(2.1) and (2.2), μ is called the *load multiplier*, to be found in the plastic analysis problems.

In practices of construction, a structure may be subjected to various kinds of load, by example: dead load, live load, wind load, effects of earthquake, etc. The dead load consists of the weight of the structure itself and its cladding. The dead load remains constant, but the other loading types continually vary. Those variations are independent and repeated with the arbitrary histories. It is clear that the structure is always subjected to the complex loads. However, up to now, the researches on the structures under complex load do not yet completely answer to the practical requirements, the studies on the structures subjected to simple loads are then still necessary.

2.2. Material behaviour

Under simple loading: Fig.2.2 displays three types of stress – strain diagram that are generally applied in the inelastic analysis of steel structures. They are: the rigid-plastic material (Fig.2.2a), the elastic-perfectly plastic material (Fig.2.2b) and the elastic-plastic-hardened material (Fig.2.2c). The principal characters of the material are: Young'modulus (E); Yield stress (σ_p); Strain hardening modulus (E_{SH}). e.g. for the mild steel, E is about $2.0x10^8$ kN/m^2; σ_p is about from $2.3x10^5$ to $3.5x10^5$ kN/m^2; E_{SH} is about 2% of Young'modulus.

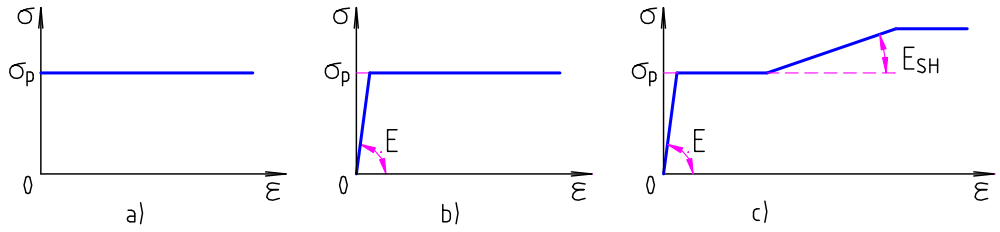

Fig.2.2. Ideal behaviours of mild steel

Under repeated loading (loading, unloading and reloading): Bauschinger effect always occurs in the material; the limit elastic is unsymmetrical in two opposite directions. There are three possibilities of material behaviours as follows:

(1) Material returns to in the elastic range after have some plastic deformations (Fig.2.3a), the material is said to have *shakedown*;

(2) Plastics deformation constitutes a closed cycle (Fig.2.3b), the material is said to have failed by *alternating plasticity*;

(3) Plastic deformation infinitely progress (Fig.2.3c), the material is said to have failed by *incremental plasticity*.

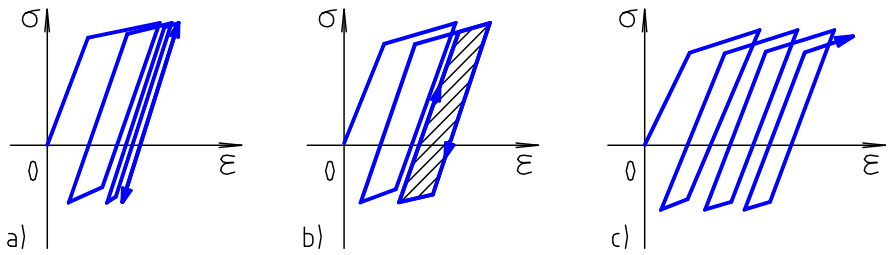

Fig.2.3. Material behaviours under repeated loading

2.3. Structural behaviour

The influence of geometric nonlinearity will be discussed in Chapter 6, the present section mainly describes the plastic behaviour of framed structures.

On the mechanical point of view, the behaviour of a structure is deduced from which of its components. With the plastic-hinge concept, the components of the frame are the critical sections while the components of the critical section are the fibres (material).

2.3.1. Under simple loading

The behaviours of fibres, of sections and of frames are respectively illustrated on Fig.2.4. One may see that the elastic-plastic behaviour may be ignored in components (points, fibres or sections) but it always appears in the behaviour of structures (sections or frames).

On the frame level, there are two load-displacement relationships showing on Figs.2.4g and 2.4h. They represent respectively two types of analysis: rigid-plastic assumed in direct method and elastic-plastic assumed in step-by-step method. In principle, the rigid-plastic analysis and elastic-plastic analysis provide the same load multiplier. All numerical examples in the thesis will confirm this statement.

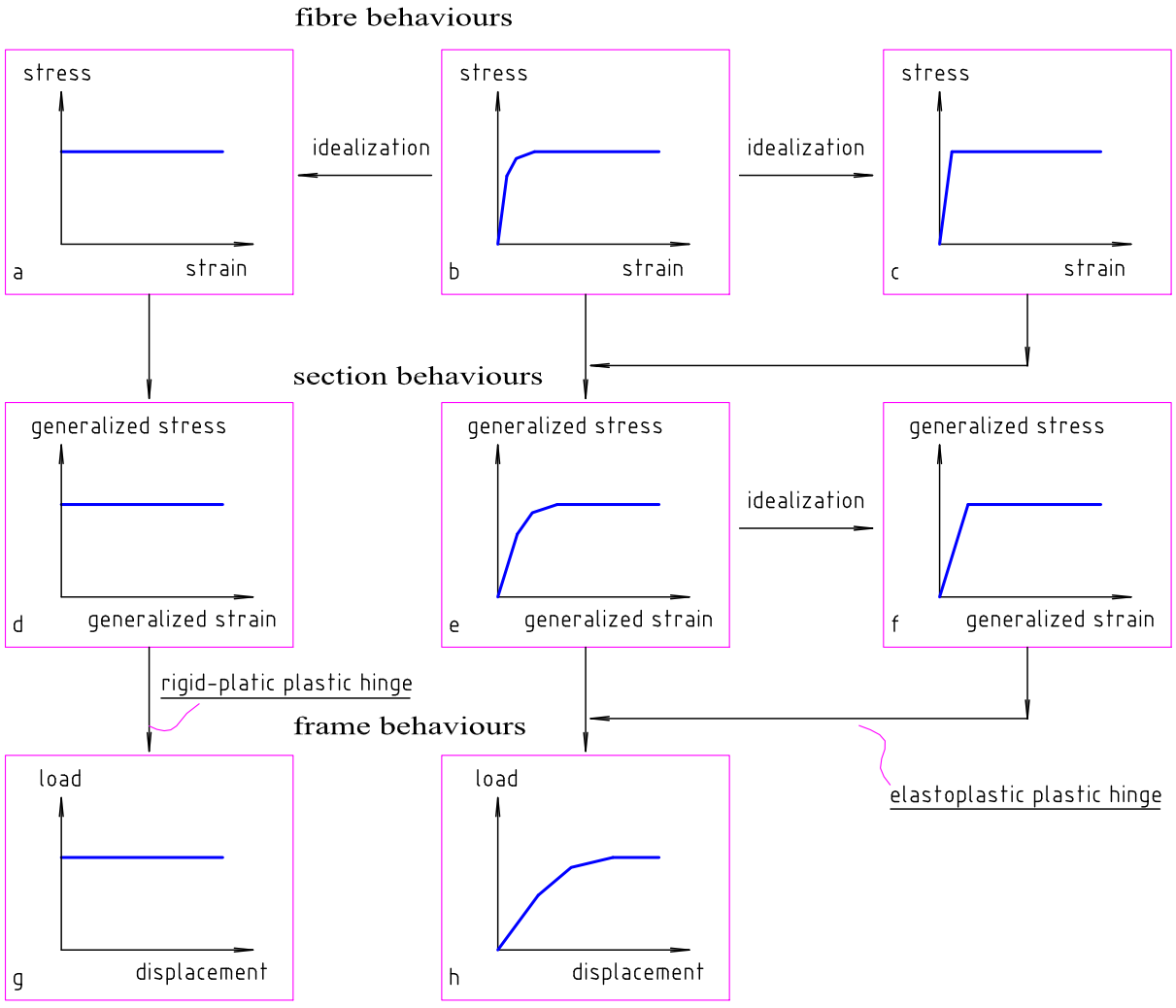

Fig.2.4. From the component behaviours to structure behaviours under simple loading

2.3.2. Under repeated loading

Fig.2.5 shows a sequence from the fibre behaviours to the frame behaviours under repeated loading. The elasto-plastic property and the Bauschinger's effect appear in the structure even they are ignored in the adjacent components. In the present thesis, the behaviour of

sections shown on Fig.2.5d is adopted; it means that the Bauschinger's effect and the elasto-plastic property are ignored in the behaviour of sections.

The states of the structures are deduced from the states of its components as the following:

- *The structure (section/frame) shakes down if the all its components (fibres/sections) shake down.*

- *The structure (section/frame) has the incremental plasticity if at least a component (fibre/section) has the incremental plasticity.*

- *The structure (section or frame) has the alternating plasticity if all its components (fibres of sections) working in the plastic range have the incremental plasticity.*

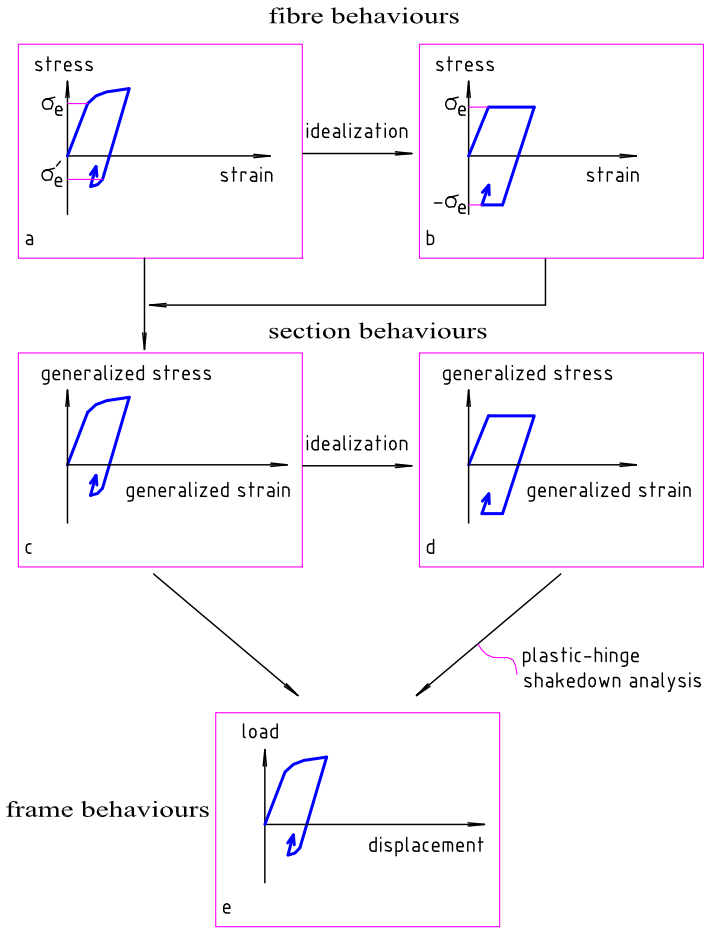

Fig.2.5. From component behaviours to frame behaviour, under repeated loading

2.4. Fundamental theorems

All computational algorithms must be based on fundamental theorems. In the following, the useful theorems for plastic analysis of structures are briefly presented.

2.4.1. Equation of virtual power

- *Static admissible field and kinematic admissible field*

A field of displacements is called a *kinematic admissible field* if it has continuous distribution of displacements and respects the boundary conditions.

A field of internal forces is called a *static admissible field* if it satisfies the *equilibrium condition*, inside and on the boundary.

- *Equation of virtual power*

*For all static admissible field (***s***) and all cinematic admissible field of (***d***), the external power carried out by external load (*$\bar{\mathbf{f}}$*) equals to the internal power absorbed by the internal deformation (***e***)*:

$$\mu \bar{\mathbf{f}}^{\mathrm{T}} \mathbf{d} = \mathbf{s}^{\mathrm{T}} \mathbf{e} , \tag{2.3}$$

- *Static and kinematic relations*

The kinematic admissible field may be expressed by the kinematic relationship between the generalized strains **e** and the displacements **d**. Under matrix formulation, one may write:

$$\mathbf{e} = \mathbf{B}\mathbf{d} , \tag{2.4}$$

where **B** is called compatible matrix or connection matrix.

Substituting Eq.(2.4) in Eq.(2.3), one obtains the equilibrium relationship:

$$\mathbf{s} = \mathbf{B}^{\mathrm{T}} \mu \bar{\mathbf{f}} . \tag{2.5}$$

The establishment of the matrix **B** for 3-D frames will be presented in Chapter 3 of the thesis.

2.4.2. Theorems of limit and shakedown analysis

Before dealing with the rigid-plastic theory, let us recall the following definitions: the *kinematic licit field* and the *static licit field*.

The *kinematic licit field* is the kinematic admissible field for which the external power is non-negative.

The *static licit field* is the static admissible field satisfying the plastic admissible condition (nowhere violates the plastic yield conditions).

2.4.2.1. Lower bound theorem of limit analysis

Giving the structure some licit filed of internal forces, the equilibrium equation of the structure is written as:

$$\mu_l^- \bar{\mathbf{f}} = \mathbf{B}^{\mathrm{T}} \mathbf{s} , \tag{2.6}$$

The upper bound theorem is expressed as: *The safely factor is the largest static multiplier*:

$$\mu_l \geq \mu_l^- . \tag{2.7}$$

2.4.2.2. Upper bound theorem of limit analysis

If the structure is submitted to licit field of displacement rates ($\dot{\mathbf{d}}$), from Eq.(2.3) one obtains a kinematic load multiplier:

$$\mu_l^+ = \frac{\mathbf{s}^{\mathrm{T}}|\dot{\mathbf{e}}|}{\bar{\mathbf{f}}^{\mathrm{T}}\dot{\mathbf{d}}}, \tag{2.8}$$

The upper bound theorem is expressed as: *The safely factor is the smallest kinematic multiplier*:

$$\mu_l \le \mu_l^+ . \tag{2.9}$$

2.4.2.3. Static theorem of shakedown analysis

❖ *Melan's theorem:*

Shakedown occurs, if there is a permanent field of residual internal forces ($\boldsymbol{\rho}$), statically admissible, such that:

$$\Phi(\mathbf{s}_e + \boldsymbol{\rho}) < 0 , \tag{2.10}$$

at all sections.

Shakedown will not occur, if no $\boldsymbol{\rho}$ exists, such that:

$$\Phi(\mathbf{s}_e + \boldsymbol{\rho}) \le 0 , \tag{2.11}$$

at one or several sections.

In Eqs.(2.10) and (2.11), Φ is the yield surface of cross-section; $\mathbf{s}_e$ is the *envelop* of the elastic responses of the considered loading domain (computed as if the structure were purely elastic), it involves two extreme values: positive ($\mathbf{s}_e^{\max}$) and negative ($\mathbf{s}_e^{\min}$).

❖ *Lower bound theorem*

Consider a load multiplier μ_s^- that leads to the elastic response $\mathbf{s}_e$. If one may find a field of residual forces $\boldsymbol{\rho}$ (self-equilibrium) such that Eq.(2.10) is satisfied, μ_s^- is called statically admissible multiplier. Based on Melan's theorem, lower bound theorem of shakedown induces: *The safety factor is the largest statically admissible multiplier:*

$$\mu_s \ge \mu_s^- . \tag{2.12}$$

2.4.2.4. Kinematic theorem of shakedown analysis

❖ *Koiter's theorem*

Let us consider a cycle load described by a periodic function **f**(t) which period τ, Koiter's theorem can be stated as following:

Shakedown may happen if there is an kinematic admissible plastic deformation cycle $\dot{\mathbf{e}}(t)$, such that:

$$\int_0^\tau \mathbf{f}^{\mathrm{T}}(t)\dot{\mathbf{d}}(t)\mathrm{dt} \le \int_0^\tau \mathbf{s}^{\mathrm{T}}|\dot{\mathbf{e}}(t)|\mathrm{dt} . \tag{2.13}$$

Shakedown cannot happen as long as the following inequality is valid:

$$\int_0^\tau \mathbf{f}^{\mathrm{T}}(t)\dot{\mathbf{d}}(t)\mathrm{dt} > \int_0^\tau \mathbf{s}^{\mathrm{T}}|\dot{\mathbf{e}}(t)|\mathrm{dt} . \tag{2.14}$$

Note that the compatible condition is only required after the complete cycle (i.e. the intermediate increment of $\dot{\mathbf{e}}$ do not have to be compatible):

$$\Delta\dot{\mathbf{e}} = \mathbf{B}\Delta\dot{\mathbf{d}}\,, \tag{2.15}$$

with:

$$\Delta\dot{\mathbf{d}} = \int_0^\tau \dot{\mathbf{d}}(t)\mathrm{dt}, \tag{2.16}$$

$$\Delta\dot{\mathbf{e}} = \int_0^\tau \dot{\mathbf{e}}(t)\mathrm{dt}\,. \tag{2.17}$$

Remark: The frame has *incremental plasticity* if Eq.(2.14) occurs and $\Delta\dot{\mathbf{d}} \neq \mathbf{0}$. The frame has *alternating plasticity* if Eq.(2.14) occurs and $\Delta\dot{\mathbf{d}} = \mathbf{0}$.

❖ *Upper bound theorem*

During the deformation process, there are the time intervals when the generalized strains rate ($\dot{\mathbf{e}}$) are positive and there are the time intervals when they are negative. Let us decompose $\dot{\mathbf{e}}$ into the positive part, $\dot{\mathbf{e}}^+ = (|\dot{\mathbf{e}}| + \dot{\mathbf{e}})/2$ parts, and the negative part, $\dot{\mathbf{e}}^- = (|\dot{\mathbf{e}}| - \dot{\mathbf{e}})/2$, so that $\dot{\mathbf{e}} = \dot{\mathbf{e}}^+ - \dot{\mathbf{e}}^-$. Then, we obtain the following quantities:

$$\Delta\dot{\mathbf{e}}^+ = \int_0^\tau \dot{\mathbf{e}}^+(t)\mathrm{dt}\,, \tag{2.18}$$

$$\Delta\dot{\mathbf{e}}^- = \int_0^\tau \dot{\mathbf{e}}^-(t)\mathrm{dt}\,, \tag{2.19}$$

$$\Delta\dot{\mathbf{e}} = \Delta\dot{\mathbf{e}}^+ - \Delta\dot{\mathbf{e}}^-\,. \tag{2.20}$$

One can prove the following relations:

$$\int_0^\tau \mathbf{s}^{\mathrm{T}} |\dot{\mathbf{e}}(t)| \mathrm{dt} = \mathbf{s}^{\mathrm{T}}(\Delta\dot{\mathbf{e}}^+ + \Delta\dot{\mathbf{e}}^-)\,, \tag{2.21}$$

$$\int_0^\tau \bar{\mathbf{f}}^{\mathrm{T}}(t)\dot{\mathbf{d}}(t)\mathrm{dt} \le (\mathbf{s}_{\mathrm{e}}^{\max})^T \Delta\dot{\mathbf{e}}^+ + (\mathbf{s}_e^{\min})^T \Delta\dot{\mathbf{e}}^-\,. \tag{2.22}$$

Consider now some kinemaric licit field $\dot{\mathbf{d}}$, the following load multiplier

$$\mu_s^+ = \frac{\mathbf{s}^{\mathrm{T}}(\Delta\dot{\mathbf{e}}^+ + \Delta\dot{\mathbf{e}}^-)}{(\mathbf{s}_{\mathrm{e}}^{\max})^{\mathrm{T}} \Delta\dot{\mathbf{e}}^+ + (\mathbf{s}_{\mathrm{e}}^{\min})^{\mathrm{T}} \Delta\dot{\mathbf{e}}^-} \tag{2.23}$$

is called a kinematic admissible load multiplier.

According to Koiter's theorem, the upper bound theorem may be stated as: *The safety factor is the smallest kinematic admissible multiplier:*

$$\mu_s \le \mu_s^+\,. \tag{2.24}$$

The application of mentioned theorems using the linear programming will be described in Chapters 4 and 5.

Chapter **3**

Element formulation

In the mechanic study, there are three fundamental relations: the *compatible,* the *equilibrium* and the *constitutive*. Those equations describe the relationships between the following variables: the displacements, the strains and the stresses. In the finite element method, the fundamental equations are first established for each element, they are then assembled to the whole structure.

With the plastic-hinge concept, the frames are discretized into elements such as the bars including the plastic hinges. In the present work, one element of 3-D steel frames is described by *thirteen-degree-of-freedom* (DOF) with plastic hinges modelled by normality rule. The formulation of this element is detailed in this chapter. The applications of those formulations for the global analysis will be presented in the next Chapters. Taking into account the semi-rigid behaviours of beam-to-column connexions will be dealt with in Chapter 8.

Keywords: *Plastic hinge; Yield surface; Compatible relation*; *Equilibrium relations*; *Constitutive relations*.

3.1. Modelling of plastic hinges

The general presentation of the constitutive laws may be found in many texts (e.g. Nguyen-Dang (1984)[122], Chen (1988)[21], Lubliner (1990)[92], Jirásek (2001)[72], among others). Particularly, the useful discussions on the piecewise linearization constitutive laws were condensed in Maier (1976)[100] where one may also find many others references. Present section deals with the practical constitutive laws at 3-D plastic hinges of steel bars with I or H-shaped, the material properties are assumed to be elastic-perfectly plastic. A physical relation taking into account the strains hardening will be proposed in Chapter 6.

3.1.1. Yield surfaces

The I or H-shaped sections (Fig.3.1a) are often used in steel frames, for which the yield surfaces of Orbison [126] and of AISC [1] are adopted in present work. Orbison's yield surface is a single-smooth-convex-nonlinear function while the AISC yield surface is a sixteen-facet polyhedron. The equations are presented bellows:

- Orbison's yield surface [126](Fig.3.1b):

$$\Phi = 1.15n^2 + m_z^2 + m_y^4 + 3.67p^2m_z^2 + 3p^6m_y^2 + 4.65m_y^2m_z^4 - 1 = 0\,, \tag{3.1}$$

- Yield surface of AISC [1] (Fig.3.1c):

$$|n| + (8/9)|m_y| + (8/9)|m_z| = 1 \text{ for } |n| \geq 0.2\,; \tag{3.2a}$$

$$(1/2)|n| + |m_y| + |m_z| = 1 \text{ for } |n| < 0.2\,; \tag{3.2b}$$

in the Eqs.(3.1) and (3.2); $n=N/N_p$ is ratio of the axial force over the squash load, $m_y=M_y/M_{py}$ and $m_z=M_z/M_{pz}$ are respectively the ratios of the minor-axis and major-axis moments to the corresponding plastic moments.

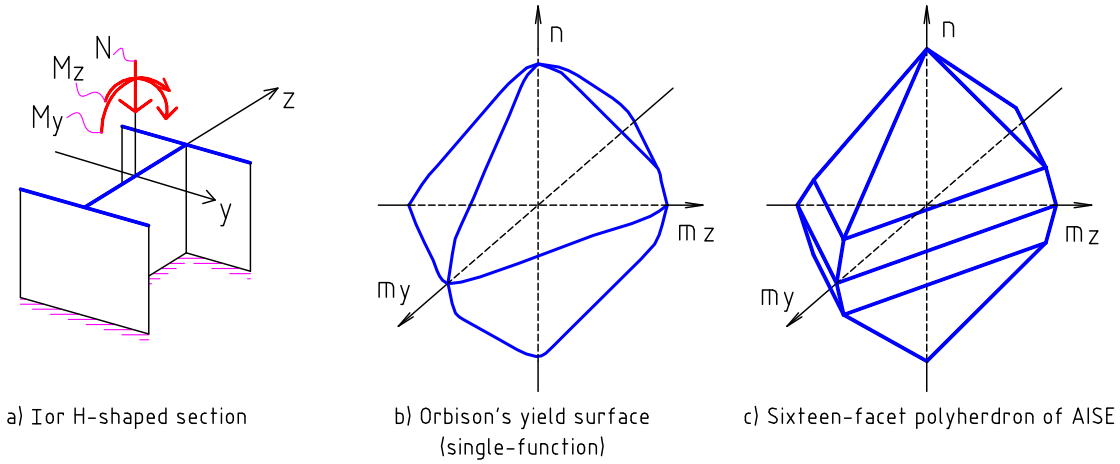

a) I or H-shaped section b) Orbison's yield surface (single-function) c) Sixteen-facet polyherdron of AISE

Fig.3.1. Yield surfaces

Eqs. (3.2a) and (3.2b) may also be written under the form:

$$a_1|N|+a_2|M_y|+a_3|M_z|=S_0 \quad \text{for} \quad |N|\geq 0.2N_p\,; \tag{3.3a}$$

$$a_4|N|+a_5|M_y|+a_6|M_z|=S_0 \quad \text{for} \quad |N|< 0.2N_p\,; \tag{3.3b}$$

with S_0 is a referential value, and $a_1,...,a_6$ are the non-zero coefficients.

The plastic admissibility zone enveloped by the sixteen-facet polyhedron [Eqs.(3.3a) and (3.3b)] may be expressed as:

$$\mathbf{Ys}\leq \mathbf{s}_0\,, \tag{3.4}$$

where matrix $\mathbf{Y}$ contains the coefficients $a_1,...a_6$; $\mathbf{s}$ collects the vector of internal forces (algebraic values); the column matrix $\mathbf{s}_0$ contains the corresponding terms S_0. System (3.4) includes sixteen-inequations that will be written in detail in Chapter 4 (Section 4).

The advantages and difficulties of both nonlinear and piecewise linearization yield surface for general engineering structures were highlighted in Maier (1976)[100]. However, one can probably say that Orbison's yield surface is very suitable to the elastic-plastic analysis by step-by-step method for 3-D steel frames, it has been widely applied (see Orbison (1982)[126], Liew (2000)[88], Kim (2001, 2002, 2003, 2006)[77, 81, 79, 80, 78], Choi (2002)[27], Chiorean (2005)[28], among others). On the other hand, the polyhedrons (e.g. the sixteen-facet polyhedron) obviously are the unique way allowing the use of the linear programming technique in the plastic analysis.

3.1.2. Normality rule

When the effects of two bending moments and axial force are taken into account on the yield surface, the associated generalized strains are: the two rotations and the axial displacement of section (Fig.3.2a). The normality rule was originally proposed by Von Mises in 1928, it may be applied for this case as follows:

$$\begin{Bmatrix} \Delta^p \\ \theta_y^p \\ \theta_z^p \end{Bmatrix} = \lambda \begin{Bmatrix} \partial\Phi / \partial N \\ \partial\Phi / \partial M_y \\ \partial\Phi / \partial M_z \end{Bmatrix}, \tag{3.5}$$

or, symbolically:

$$\mathbf{e}^p = \mathbf{N}_C \lambda . \tag{3.6}$$

where λ is the plastic deformation magnitude; $\mathbf{N}_C$ is a gradient vector at a point of the yield surface Φ; $\mathbf{e}^p$ collects the plastic generalized strains. Fig.3.2b describes the normality rule.

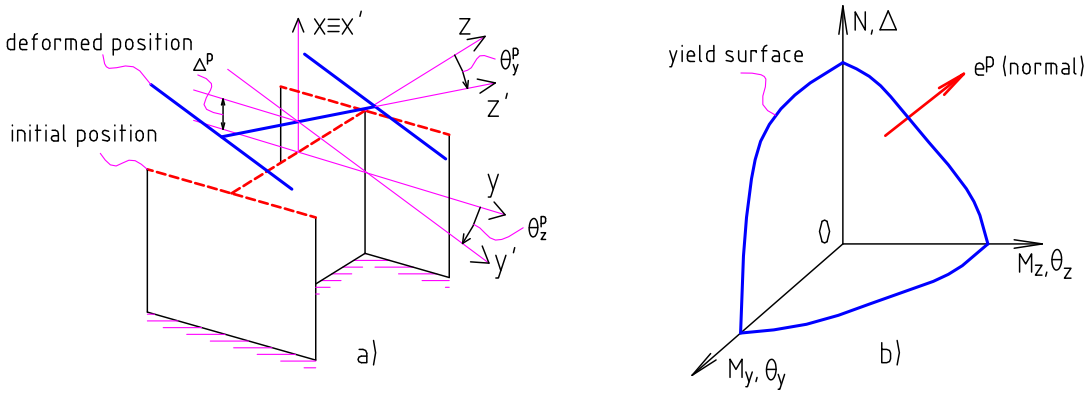

Fig.3.2. Plastic hinge modelling (a-generalized strains at plastic hinges; b-normality rule)

Clearly, each facet of the linearized yield surface is described by one raw of Eq.(3.4); three terms of the same raw of matrix $\mathbf{Y}$ constitutes the outward of this facet (Fig.3.3). In the rigid-plastic analysis where the linearized yield surface is adopted, the active facet is not known a priori. Therefore, we may express the generalized strains rate by a linear combination of outward normal of all facets:

$$\dot{\mathbf{e}} = \mathbf{Y}^T \dot{\boldsymbol{\lambda}} = \mathbf{N}_C \dot{\boldsymbol{\lambda}} . \tag{3.7}$$

where $\dot{\boldsymbol{\lambda}}$ is the vector whose components are equals to the number of facets of the polyhedron. Note that $\mathbf{N}_C$ in Eqs.(3.6) and (3.7) have the same mathematical signification but have the different forms. $\mathbf{N}_C$ in Eq.(3.6) is the gradient vector at a point of the yield surface while $\mathbf{N}_C$ in Eq.(3.7) is a matrix of which each column is a gradient vector of each facet of the linearized yield surface.

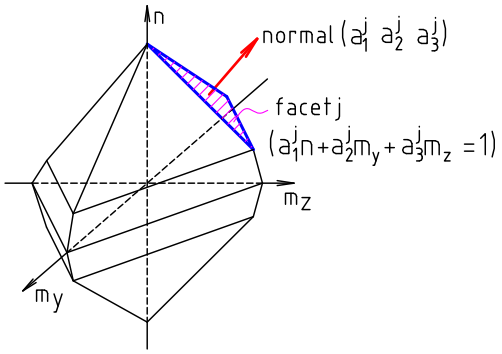

Fig.3.3. Normal vector of a facet

3.1.3. Plastic incremental forces-generalized strains relation

When the plastic loading occurring, the point force is on the yield surface (or subsequence yield surface) $\Phi = 0$. In taking the derivative of this relationship, we obtain:

$$d\Phi = \frac{\partial \Phi}{\partial N} dN + \frac{\partial \Phi}{\partial M_y} dM_y + \frac{\partial \Phi}{\partial M_z} dM_z = 0 . \tag{3.8}$$

By use of Eqs.(3.5), the equation (3.8) becomes:

$$\lambda^{-1} \Delta \mathbf{s}^{\mathrm{T}} \Delta \mathbf{e}^{\mathrm{p}} = 0 . \tag{3.9}$$

Since λ in Eq.(3.9) is arbitrary, one obtains:

$$\Delta \mathbf{s}^{\mathrm{T}} \Delta \mathbf{e}^{\mathrm{p}} = 0 . \tag{3.10}$$

Eq.(3.10) shows the normal relation between the vector of plastic generalized strains increments ($\Delta \mathbf{e}^{\mathrm{p}}$) and the vector of internal force increments ($\Delta \mathbf{s}$) (Fig.3.4). This relationship is applied in the elastic-plastic analysis by step-by-step method (Chapter 6).

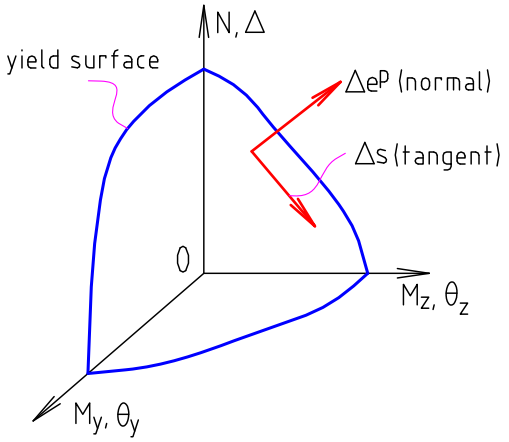

Fig.3.4. Plastic forces-generalized strains relation

3.1.4. Plastic dissipation

In the rigid-plastic analysis, the *plastic dissipation* conception is defined as follows:

$$\dot{D} = \mathbf{s}^{\mathrm{T}} \dot{\mathbf{e}} . \tag{3.11}$$

The plastic dissipation given by Eq.(3.11) is not convenient to apply the kinematic formulation using linear programming, because the vector of internal forces is not a priori known. It was modified. As the plastic deformation occurs only if the yield condition is satisfied at the corresponding facet, one obtains:

$$\dot{\boldsymbol{\lambda}}^{\mathrm{T}} (\mathbf{Y}\mathbf{s} - \mathbf{s}_0) = 0 . \tag{3.12}$$

From Eqs.(3.7), (3.11) and (3.12), the plastic dissipation may be rewritten in the term of plastic deformation magnitude:

$$\dot{D} = \mathbf{s}_0^{\mathrm{T}} \dot{\boldsymbol{\lambda}} . \tag{3.13}$$

Eq.(3.13) shows that the plastic dissipation is uniquely depending on $\dot{\boldsymbol{\lambda}}$ because $\mathbf{s}_0$ is a given constant vector for each critical section.

3.2. Thirteen-DOF element formulation

Generally, twelve-DOF element may be used in the global elastic-plastic analysis of 3-D framework. However, when the axial plastic deformation is taken into account in rigid-plastic analysis, twelve-DOF are not enough to describe the deformation of a beam-column element. Since CEPAO program is a computer code for elastic-plastic and rigid-plastic analysis, thirteen-DOF element must be adopted such that the fundamental compatibility and equilibrium relationships may be applied in every algorithm. Therefore, we present hereafter the thirteen-DOF element formulation.

As both adopted yield surfaces neglect the torsional moment (Eqs.(3.1) and (3.2)), two possibilities remain in the descriptions of the element:

1. Take into account the torsional stiffness of the elements but we neglect the torsional moment in the plastic conditions.

2. Neglect the torsional stiffness of the element then the torsional moment disappears in the frame.

Both above solutions are approximations. However, in our opinion, the second choice has three advantages in comparison with the first one:

1. It leads to the reductions of the problem size;

2. It leans towards secure, because the bending moment are augmented due to the torsional stiffness of the element are ignored;

3. It is suitable to the rigid-plastic analysis.

3.2.1. Compatible and equilibrium relations

Let $\mathbf{d}_k^T = [d_1\ d_2\ d_3\ d_4\ d_5\ d_6\ d_7\ d_8\ d_9\ d_{10}\ d_{11}\ d_{12}\ d_{ek}]$ be the vector of member independent displacements in the global coordinate system OXYZ, as shown in Fig.3.5. Assembling for the whole frameworks we obtain the vector **d.**

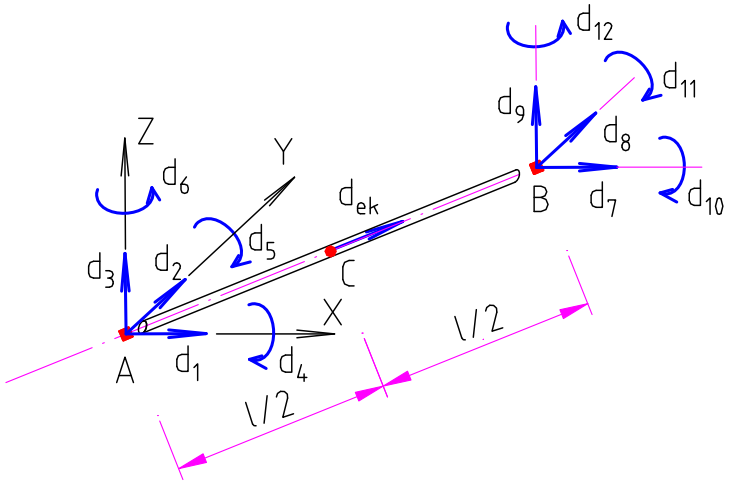

Fig.3.5. Thirteen-DOF element

Let $\mathbf{s}_k^T = [N_A\ M_{yA}\ M_{zA}\ N_B\ M_{yB}\ M_{zB}]$ be the vector of the axial force and bending moments of member end nodes (Fig.3.6a). Assembling in the whole frameworks, it is denoted by **s.**

Let $\mathbf{e}_k^T = [\Delta_A\ \ \theta_{yA}\ \ \theta_{zA}\ \ \Delta_B\ \ \theta_{yB}\ \ \theta_{zB}]$ be the vector of the associated generalized trains at the member end nodes (Fig.3.6b). Assembling for the whole frameworks, it is denoted by **e.**

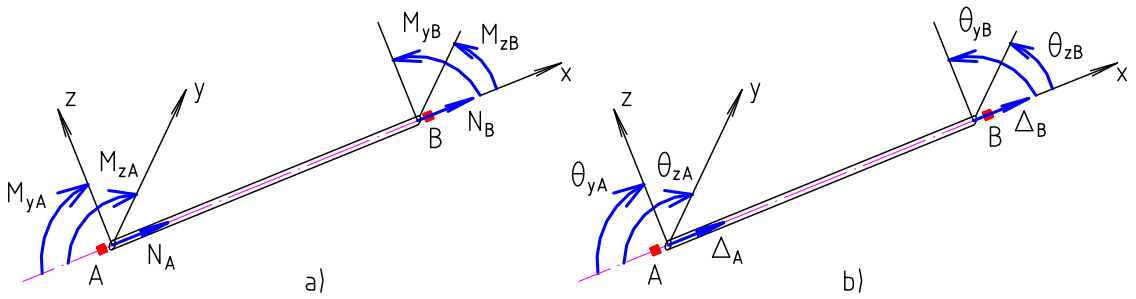

Fig.3.6. Member k (a- internal forces; b-generalized strains)

The compatibility equation is defined as the relationship between the vector of generalized strains and the vector of displacements:

$$\mathbf{e}_k = \mathbf{B}_k \mathbf{d}_k \,, \tag{3.14}$$

where $\mathbf{B}_k$ is called the *kinematic matrix* defined below:

$$\mathbf{B}_k = \mathbf{A}_k \mathbf{T}_k \,. \tag{3.15}$$

where

$$\mathbf{A}_k = \begin{bmatrix} 1 & 0 & 0 & 0 & 0 & 0 & 0 & 0 & 0 & 0 & -1 \\ 0 & 0 & -1/l & 1 & 0 & 0 & 0 & 1/l & 0 & 0 & 0 \\ 0 & -1/l & 0 & 0 & -1 & 0 & 1/l & 0 & 0 & 0 & 0 \\ 0 & 0 & 0 & 0 & 0 & 1 & 0 & 0 & 0 & 0 & -1 \\ 0 & 0 & 1/l & 0 & 0 & 0 & 0 & -1/l & -1 & 0 & 0 \\ 0 & 1/l & 0 & 0 & 0 & 0 & -1/l & 0 & 0 & 1 & 0 \end{bmatrix}, \tag{3.16}$$

$$\mathbf{T}_k = \begin{bmatrix} \mathbf{C}_k & & & & \\ & \mathbf{C}'_k & & & \\ & & \mathbf{C}_k & & \\ & & & \mathbf{C}'_k & \\ & & & & 1 \end{bmatrix}. \tag{3.17}$$

In Eqs.(3.16) and (3.17), l is the length of element k; $\mathbf{C}_k$ is the matrix of direction cosines of element k:

$$\mathbf{C}_k = \begin{bmatrix} c_{11} & c_{12} & c_{13} \\ c_{21} & c_{22} & c_{23} \\ c_{31} & c_{32} & c_{33} \end{bmatrix};$$

$$\mathbf{C}'_k = \begin{bmatrix} c_{21} & c_{22} & c_{23} \\ c_{31} & c_{32} & c_{33} \end{bmatrix}.$$

For the whole frame, the compatible relation is written [Eq.(2.4)]:

$$\mathbf{e} = \mathbf{B}\mathbf{d} \tag{3.18}$$

with

$$\mathbf{B} = \sum_k \mathbf{B}_k \mathbf{L}_k \tag{3.19}$$

where $\mathbf{L}_k$ is a localization Boolean matrix of element k.

As the discussion in Chapter 2 [Eq.(2.5)], the equilibrium is determined as the follows:

$$\mathbf{s} = \mathbf{B}^{\mathrm{T}} \mu \bar{\mathbf{f}} \,. \tag{3.20}$$

$\mathbf{B}^{\mathrm{T}}$ is called the *equilibrium matrix*.

Remark: In the sense of limit analysis, one may think that: d_1, d_2, d_3, d_7, d_8, d_9 are the displacements corresponding to the deflection mechanisms (beam and sideways mechanisms) (Fig.3.7a). d_4, d_5, d_6, d_{10}, d_{11}, d_{12} are the displacements showing the joints mechanisms (Fig.3.7b). d_{ek} is the displacement in the longitudinal direction of middle-point of the span, it describes the bar mechanisms (the bar translates along its axis) (Fig.3.7c). Since the torsional stiffness of the elements is neglected, we must eliminate the degree of freedoms that only provoke pure torsion in the bars (Fig.3.7d). Those degrees of freedom correspond to the columns of matrix **B** in which the all terms are zeros.

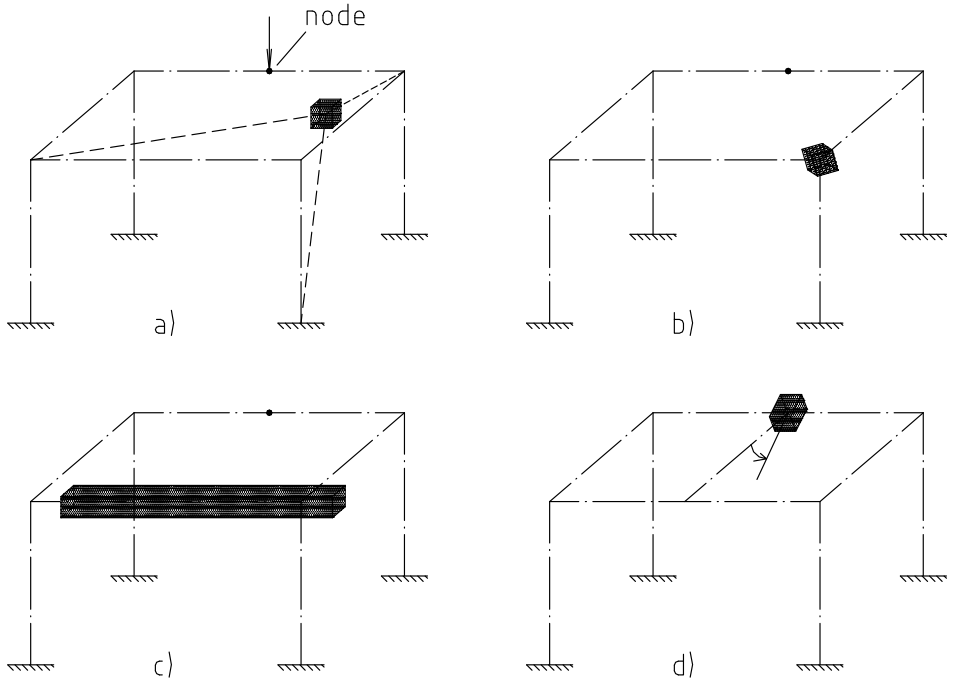

Fig.3.7. Three types of mechanics and the degree of freedom eliminated

3.2.2. Constitutive relation

For the element *k*, Hook's law is written as follows:

$$\mathbf{s}_k = \mathbf{D}_k(\mathbf{e}_k - \mathbf{e}_k^p), \tag{3.21}$$

$(\mathbf{e}_k^p)^T = [\mathbf{e}_{k,A}^p \ \ \mathbf{e}_{k,B}^p]$ is the plastic part of the generalized strains at the element ends; they are determined by Eq.(3.6); $\mathbf{D}_k$ is called the *linear elastic matrix* of the element *k*:

$$\mathbf{D}_k = \frac{1}{l}\begin{bmatrix} 2EA & 0 & 0 & 0 & 0 & 0 \\ 0 & 4EI_y & 0 & 0 & -2EI_y & 0 \\ 0 & 0 & 4EI_z & 0 & 0 & -2EI_z \\ 0 & 0 & 0 & 2EA & 0 & 0 \\ 0 & -2EI_y & 0 & 0 & 4EI_y & 0 \\ 0 & 0 & -2EI_z & 0 & 0 & 4EI_z \end{bmatrix}, \tag{3.22}$$

where E is the Young'modulus; A, I_y, I_z are, respectively, the area, the moment of inertias of the cross-section about y and z axes, respectively;

For the whole structure, we have:

$$\mathbf{s} = \mathbf{D}(\mathbf{e} - \mathbf{e}^p), \tag{3.23}$$

where

$$\mathbf{D} = \sum_{k} \mathbf{D}_k \ , \tag{3.24}$$

The elastic-plastic matrix taking into account P-δ effect will be present in Chapter 6.

Chapter **4**

Limit and shakedown analysis of 3-D steel frames by linear programming

A systematic treatment of the application of linear programming in plastic analysis can be found in a lot of texts (e.g. Cohn (1979)[32] and Smith (1990)[140]). In this chapter, we restrict ourselves to describing some practical aspects of the CEPAO package applied to the case of 3-D steel frames. They are: the further reduction of the kinematic approach (Sections 4.2.2 and 4.3.2), and the direct calculation of the internal force (or residual internal force) distribution (Sections 4.2.3 and 4.3.3). Those techniques were originally proposed by Nguyen-Dang [117] for the 2-D bending frames. In this work, they are extended to 3-D frames. Beside, the determination the specific displacement is originally presented in Section 4.4. Several numerical will demonstrate the efficiency of the proposed algorithm.

Keywords: *Limit analysis*; *Shakedown analysis*; *Plastic-hinge; Space frames; Linear programming.*

4.1. General formulation

In CEPAO, the canonical formulation of the linear programming problem is considered as below:

$$\text{Min } \pi = \mathbf{c}^{\mathrm{T}}\mathbf{x} \;\big|\; \mathbf{W}\mathbf{x} = \mathbf{b}\,. \tag{4.1}$$

where π is the objective function; $\mathbf{x}$, $\mathbf{c}$, $\mathbf{b}$ are respectively the vector of variables, of costs and of second member. $\mathbf{W}$ is called the matrix of constraints. The objective function may have a state variable, and the matrix formulation is arranged such that a way the basic matrix of the initial solution is appeared clearly under the form:

$$\begin{bmatrix} -\mathbf{c}_1^{\mathrm{T}} & 1 & -\mathbf{c}_2^{\mathrm{T}} \\ \mathbf{W}_1 & 0 & \mathbf{W}_2 \end{bmatrix} \begin{bmatrix} \mathbf{x}_1 \\ \pi \\ \mathbf{x}_2 \end{bmatrix} = \begin{bmatrix} 0 \\ \mathbf{b} \end{bmatrix}. \tag{4.2}$$

The basic matrix of initial solution is:

$$\mathbf{X}_0 = \begin{bmatrix} 1 & -\mathbf{c}_2^{\mathrm{T}} \\ 0 & \mathbf{W}_2 \end{bmatrix}. \tag{4.3}$$

Eq. (4.1) can be then written under a general form:

$$\mathbf{W}^*\mathbf{x}^* = \mathbf{b}^*. \tag{4.4}$$

The matrices **W***, **x***, **b*** and $\mathbf{X}_0$ for both limit and shakedown analysis problems will be concretely formulated in the next sections. The relationship (4.4) will be established in Chapter 5 for the plastic design problems.

4.2. Limit analysis by kinematic formulation

The first part of this section reminds the principal ideas of the standard kinematic formulation using simplex method. Some practical techniques used in CEPAO are presented in the second part. Finally, the advantages of the proposed techniques are highlighted.

4.2.1. Standard kinematic approach

Based on the upper bound theorem of limit analysis (see Section 2.4.2.2 in Chapter 2) one may state that: among the licit mechanisms that provide the same external power, the actual mechanism absorbs the minimal dissipation. Therefore, the kinematical formulation of limit analysis can be stated as a linear programming problem [see Eqs. (2.8), (3.7), (3.13) and (3.18)]:

$$\text{Min} \quad \phi = \mathbf{s}_0^{\mathrm{T}}\dot{\boldsymbol{\lambda}} \left| \begin{array}{c} \mathbf{N}_{\mathrm{C}}\dot{\boldsymbol{\lambda}} - \mathbf{B}\dot{\mathbf{d}} = \mathbf{0} \\ \bar{\mathbf{f}}^{\mathrm{T}}\dot{\mathbf{d}} = \xi \\ \dot{\boldsymbol{\lambda}} \geq \mathbf{0} \end{array} \right. . \tag{4.5}$$

By consequence, the safety factor is obtained by:

$$\mu_+ = \phi / \xi \, .$$

In Eq.(4.5), $\dot{\boldsymbol{\lambda}}$ is the vector of the plastic deformation magnitude rate; **B** is the kinematic matrix defined in Chapter 3; $\dot{\mathbf{d}}, \bar{\mathbf{f}}$ are, respectively, the vector of independent displacement rates and the vector of external load; ξ is a positive constant.

The unknowns in Eq.(4.5) are the plastic deformation magnitude rate, $\dot{\boldsymbol{\lambda}}$ (positive), and the independent displacement rate, $\dot{\mathbf{d}}$ (negative or positive). Simplex method requires that all variables must be non-negative. By consequence, the following change of variables is generally adopted:

$$\dot{\mathbf{d}} = \dot{\mathbf{d}}^+ - \dot{\mathbf{d}}^- \text{ with } \dot{\mathbf{d}}^+ \geq \mathbf{0}, \dot{\mathbf{d}}^- \geq \mathbf{0} \, . \tag{4.6}$$

The simplex procedure is a series of the automatic choice of the admissible basis (basic matrix). However, the *initial basis* should be pre-selected. The initial admissible solution is such that the initial value of any variable (except the objective function) must be non-negative. To satisfy this requirement, one uses frequently the unity matrix (**E**) for the initial admissible solution; it is added to the matrix of constraints (see Fig.4.4a in Section 4.2.2.3).

4.2.2. Further reduction of kinematic approach

4.2.2.1. Change of variables

Instead of the change of variables shown in Eq.(4.6), the following change of variables is adopted in CEPAO:

$$\dot{\mathbf{d}}' = \dot{\mathbf{d}} + \mathrm{d}_0 \text{ so that } \dot{\mathbf{d}}' \geq \mathbf{0} \, . \tag{4.7}$$

Section 4.4 will present a way to fix the value of *specific displacement* (d_0), which depends on the actual structure, such that $\dot{\mathbf{d}}'$ are always non-negative. Now, problem of Eq.(4.5) becomes:

$$\text{Min} \quad \phi = \mathbf{s}_0^{\mathrm{T}}\dot{\boldsymbol{\lambda}} \left| \begin{array}{c} \mathbf{N}_C\dot{\boldsymbol{\lambda}} - \mathbf{B}\dot{\mathbf{d}}' = -\mathbf{B}\mathrm{d}_0 \\ \bar{\mathbf{f}}^{\mathrm{T}}\dot{\mathbf{d}}' = \xi + \bar{\mathbf{f}}^{\mathrm{T}}\mathrm{d}_0 \\ \dot{\boldsymbol{\lambda}}, \dot{\mathbf{d}}' \geq \mathbf{0} \end{array} \right. . \tag{4.8}$$

By consequence, vector of variables, vector of right-hand and matrix of constraints corresponding to the problem of Eq. (4.4) for limit analysis are given below:

$$\mathbf{x}^{*\mathrm{T}} = [\pi \quad \mathbf{x}^{\mathrm{T}} \quad \eta] = [\pi \quad \dot{\mathbf{d}}'^{\mathrm{T}} \quad \dot{\boldsymbol{\lambda}}^{\mathrm{T}} \quad \eta] \; ; \; \mathbf{b}^{*\mathrm{T}} = [0 \quad \mathbf{b}^{\mathrm{T}}] = [0 \quad -\mathbf{B}\mathrm{d}_0 \quad \xi + \bar{\mathbf{f}}^{\mathrm{T}} d_0] \; ;$$

$$\mathbf{W}^* = \begin{bmatrix} 1 & \mathbf{0}^{\mathrm{T}} & -\mathbf{s}_0^{\mathrm{T}} & 0 \\ \mathbf{0} & -\mathbf{B} & \mathbf{N}_C & \mathbf{0} \\ 0 & \bar{\mathbf{f}}^{\mathrm{T}} & \mathbf{0}^{\mathrm{T}} & 1 \end{bmatrix} ;$$

where η is an artificial variable which must be taken out of the basic vector in the simplex process.

4.2.2.2. Automatic choice of initial admissible solution

To avoid the addition of the unity matrix to the matrix of constraints, it appears that the following arrangement is appreciated for automatic calculation.

The linearized condition of plastic admissibility for the i[th] section (Eq. (3.4) in Chapter 3) may be expanded as follows:

$$\begin{array}{c} \langle 1\rangle \\ \langle 2\rangle \\ \langle 3\rangle \\ \langle 4\rangle \\ \langle 5\rangle \\ \langle 6\rangle \\ \langle 7\rangle \\ \langle 8\rangle \\ \langle 9\rangle \\ \langle 10\rangle \\ \langle 11\rangle \\ \langle 12\rangle \\ \langle 13\rangle \\ \langle 14\rangle \\ \langle 15\rangle \\ \langle 16\rangle \end{array} \begin{bmatrix} a_1^i & -a_2^i & -a_3^i \\ a_1^i & a_2^i & -a_3^i \\ a_1^i & a_2^i & a_3^i \\ -a_1^i & a_2^i & a_3^i \\ -a_1^i & -a_2^i & a_3^i \\ -a_1^i & -a_2^i & -a_3^i \\ a_1^i & -a_2^i & a_3^i \\ -a_1^i & a_2^i & -a_3^i \\ a_4^i & -a_5^i & -a_6^i \\ a_4^i & a_5^i & -a_6^i \\ a_4^i & a_5^i & a_6^i \\ -a_4^i & a_5^i & a_6^i \\ -a_4^i & -a_5^i & a_6^i \\ -a_4^i & -a_5^i & -a_6^i \\ a_4^i & -a_5^i & a_6^i \\ -a_4^i & a_5^i & -a_6^i \end{bmatrix} \begin{Bmatrix} N^i \\ M_y^i \\ M_z^i \end{Bmatrix} \leq \begin{Bmatrix} S_0^i \\ S_0^i \\ S_0^i \\ S_0^i \\ S_0^i \\ S_0^i \\ S_0^i \\ S_0^i \\ S_0^i \\ S_0^i \\ S_0^i \\ S_0^i \\ S_0^i \\ S_0^i \\ S_0^i \\ S_0^i \end{Bmatrix} \tag{4.9}$$

Fig.4.1 describes the projection of the sixteen-planar facets of the yield surface corresponding to the sixteen-inequalities numbered on Eq. (4.9).

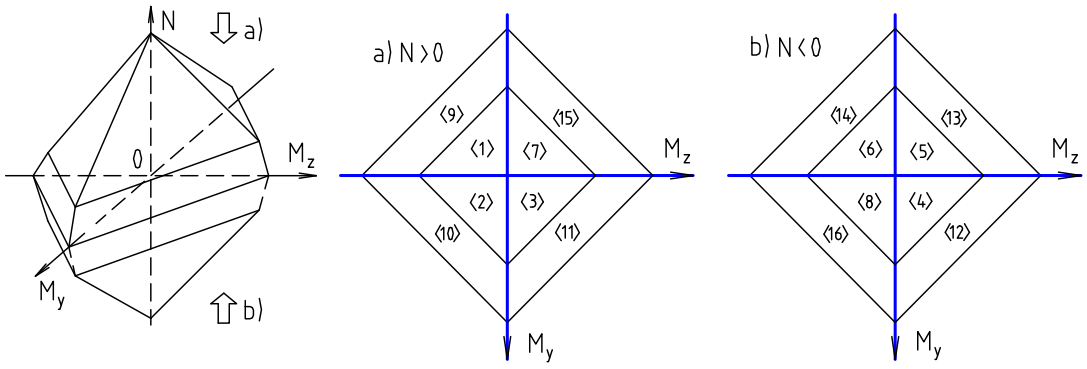

Fig. 4.1. Projection of the yield surface on the plan M_yOM_z

Eq. (4.9) can be written under symbolic formulation [See Eqs.(3.4) and 3.7)]:

$$\mathbf{N}_C^{iT}\mathbf{s}^i \le \mathbf{s}_0^i . \tag{4.10}$$

Fig.4.2 shows the structure of the global matrix $\mathbf{N}_C$ in Eq.(4.5) assembled from the matrix $\mathbf{N}_C^i$ of ith plastic hinge in Eq.(4.10).

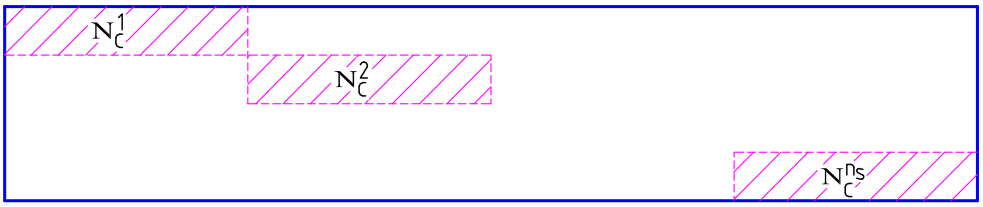

Fig.4.2. The form of matrix $\mathbf{N}_C$ (n_s is the number of critical sections)

Put:

$$\tilde{\mathbf{N}}_C^i = \begin{bmatrix} a_1^i & a_1^i & a_1^i \\ -a_2^i & a_2^i & a_2^i \\ -a_3^i & -a_3^i & a_3^i \end{bmatrix}.$$

Let us note that $\tilde{\mathbf{N}}_C^i$ is always non-singular because a_1^i, a_2^i, a_3^i are positive.

Then, matrix $\mathbf{N}_C^i$ in Eq. (4.10) may be decomposed into three sub-matrices:

$$\mathbf{N}_C^i = [\tilde{\mathbf{N}}_C^i \quad -\tilde{\mathbf{N}}_C^i \quad \bar{\mathbf{N}}_C^i], \tag{4.11}$$

with $\bar{\mathbf{N}}_C^i$ is the rest of $\mathbf{N}_C^i$ after deducting $\tilde{\mathbf{N}}_C^i$ and $-\tilde{\mathbf{N}}_C^i$.

The decomposition of matrix $\mathbf{N}_C^i$ leads then to the following form:

$$\mathbf{s}_0^{iT} = [\tilde{\mathbf{s}}_0^{iT} \quad \tilde{\mathbf{s}}_0^{iT} \quad \bar{\mathbf{s}}_0^{iT}] = [S_0^i \quad \cdots \quad S_0^i];$$

$$\boldsymbol{\lambda}^{iT} = [\tilde{\boldsymbol{\lambda}}^{iT} \quad \tilde{\boldsymbol{\lambda}}_{+3}^{iT} \quad \bar{\boldsymbol{\lambda}}^{iT}],$$

where:

$$\tilde{\boldsymbol{\lambda}}^{iT} = [\lambda_1^i \quad \lambda_2^i \quad \lambda_3^i];$$

$$\tilde{\boldsymbol{\lambda}}_{+3}^{iT} = [\lambda_4^i \quad \lambda_5^i \quad \lambda_6^i];$$

$$\bar{\boldsymbol{\lambda}}^i = [\lambda_7^i \quad \ldots \quad \lambda_{16}^i].$$

Let **E** be a unity matrix of dimension *3x3*; and let $\mathbf{S}^i$ be a diagonal matrix, such that:

$$\mathbf{S}^i = \text{diag}\left[1 \text{ x sign of } \left(\left(\tilde{\mathbf{N}}_C^i\right)^{-1}\mathbf{b}^i\right)\right],$$

with:

$$(\mathbf{b}^i)^T = [b_{3(i-1)+1} \quad b_{3(i-1)+2} \quad b_{3(i-1)+3}];$$

Consider now the distribution of the new plastic deformation magnitude:

$$(\dot{\boldsymbol{\lambda}}^{i'})^T = [(\tilde{\dot{\boldsymbol{\lambda}}}^{i'})^T \quad (\tilde{\dot{\boldsymbol{\lambda}}}_{+3}^{i'})^T \quad (\bar{\dot{\boldsymbol{\lambda}}}^i)^T],$$

in which:

$$\tilde{\boldsymbol{\lambda}}^{i'} = 0.5(\mathbf{E}+\mathbf{S}^i)\tilde{\boldsymbol{\lambda}}^{i} + 0.5(\mathbf{E}-\mathbf{S}^i)\tilde{\boldsymbol{\lambda}}^{i}_{+3}; \tag{4.12}$$

$$\tilde{\boldsymbol{\lambda}}^{i'}_{+3} = 0.5(\mathbf{E}-\mathbf{S}^i)\tilde{\boldsymbol{\lambda}}^{i'} + 0.5(\mathbf{E}+\mathbf{S}^i)\tilde{\boldsymbol{\lambda}}^{i}_{+3}. \tag{4.13}$$

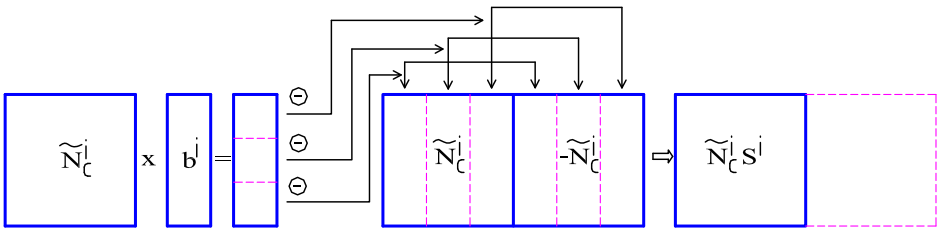

Fig.4.3. Choice of the initial basic

Fig.4.3 explains the arrangement of the columns of constraint matrix allowing to obtain the initial base as described by Eqs.(4.12) and (4.13). With mentioned arrangement, if the case of initial basis of variables is $[(\tilde{\boldsymbol{\lambda}}^{1'})^T \quad (\tilde{\boldsymbol{\lambda}}^{2'})^T ... (\tilde{\boldsymbol{\lambda}}^{n_s'})^T]$, the initial basic matrix may be determined as follows:

$$\mathbf{X}_0 = \begin{bmatrix} 1 & -\tilde{\mathbf{s}}_0^{1T} & -\tilde{\mathbf{s}}_0^{2T} & \dots & -\tilde{\mathbf{s}}_0^{n_sT} & 0 \\ \mathbf{0} & \tilde{\mathbf{N}}_C^1\mathbf{S}^1 & \mathbf{0} & \dots & \mathbf{0} & \mathbf{0} \\ \mathbf{0} & \mathbf{0} & \tilde{\mathbf{N}}_C^2\mathbf{S}^2 & \dots & \mathbf{0} & \mathbf{0} \\ \vdots & \vdots & \vdots & \dots & \vdots & \vdots \\ \mathbf{0} & \mathbf{0} & \mathbf{0} & \dots & \tilde{\mathbf{N}}_C^{n_s}\mathbf{S}^{n_s} & \mathbf{0} \\ 0 & \mathbf{0}^T & \mathbf{0}^T & \dots & \mathbf{0}^T & 1 \end{bmatrix}, \tag{4.14}$$

in which, n_s is the number of critical sections.

Easily, we may demonstrate that the initial solution:

$$\mathbf{x}_0 = \mathbf{X}_0^{-1}\mathbf{b}$$

is certainly *non-negative.*

4.2.2.3. Advantages of proposed techniques

Fig.4.4. shows the matrix of constraints [W^* in Eq.(4.4)] in the standard and reduced formulation. With n_s and n_m are respectively the number of critical sections and the number of independent mechanism. In comparison with standard approach, the number of columns of constraint matrix reduces from $(19n_s+2n_m+1)$ to $(16n_s+n_m+2)$.

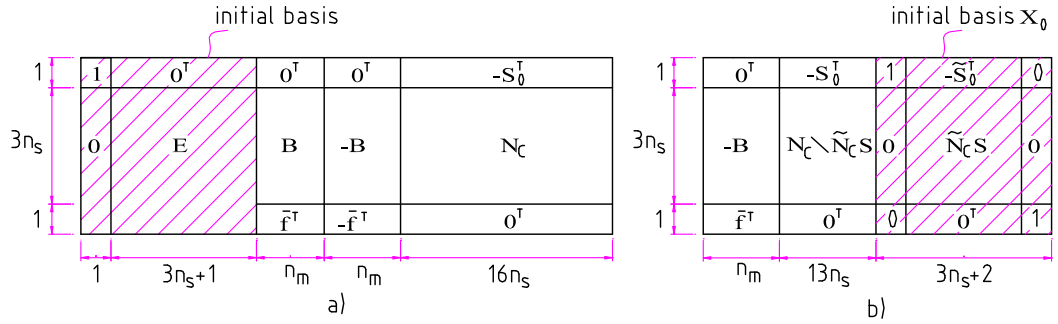

Fig.4.4. Matrix of constraints (a- standard formulation; b- reduced formulation)

4.2.3. Direct calculation of internal force distribution

4.2.3.1. Primal-dual technique

The generalized strain rates at critical sections are chosen as variables in kinematic approach. The load factor and the collapse mechanism are given as output. To obtain the internal

force distribution while avoiding the static approach, the dual properties of linear programming are used. The physical meaning of the dual variables may be established as follows:

The canonical dual form of the linear programming problem of Eq.(4.1) is:

$$\text{Max} \quad (\mathbf{b}^{\mathrm{T}}\mathbf{y} + \mathbf{0}^{\mathrm{T}}\mathbf{h}) \left| \begin{array}{l} \mathbf{W}^{\mathrm{T}}\mathbf{y} + \mathbf{h} = \mathbf{c} \\ \mathbf{h} \geq \mathbf{0} \end{array} \right. , \tag{4.15}$$

in Eq. (4.15), $\mathbf{y}^{\mathrm{T}} = [\mathbf{s}^{\mathrm{T}} \quad \mu\_]$ are the internal forces and the load factor, $\mathbf{h}$ are the non-negative slack variables, vector $\mathbf{c}$ collects the values S_0

$$\mathbf{h}^{\mathrm{T}} = [\mathbf{0}^{\mathrm{T}} \quad \mathbf{h}^{1\mathrm{T}} \quad \mathbf{h}^{2\mathrm{T}} \quad \ldots \mathbf{h}^{n_s\mathrm{T}}], \text{ with } \mathbf{h}^{i\mathrm{T}} = [\tilde{\mathbf{h}}^{i\mathrm{T}} \quad \tilde{\mathbf{h}}_{+3}^{i\mathrm{T}} \quad \bar{\mathbf{h}}^{i}].$$

The constraints in Eq.(4.15) are the plastic conditions. At the optimal solution (in the convergence state) the plastic conditions are written for i^{th} critical sections as follows:

$$\mathbf{N}_{\mathrm{C}}^{i}\mathbf{s}^{i} + \mathbf{h}_{\mathrm{op}}^{i} = \mathbf{s}_{0}^{i},$$

it allows to determinate the internal forces from the slack variables $\mathbf{h}_{\mathrm{op}}$:

$$\mathbf{s}^{i} = \left(\tilde{\mathbf{N}}_{\mathrm{C}}^{i}\right)^{-\mathrm{T}}\left(\tilde{\mathbf{s}}_{0}^{i} - \tilde{\mathbf{h}}_{\mathrm{op}}^{i}\right). \tag{4.16}$$

Let us note that the slack variables $\mathbf{h}_{\mathrm{op}}$ are identified exactly as the reduced cost vector $\bar{\mathbf{c}}$ of the primal problem of Eq.(4.5) (Fig.4.5):

$$\mathbf{h}_{\mathrm{op}} = \bar{\mathbf{c}} = \left(\mathbf{X}_{\mathrm{op}}^{-1}(1,:)\right)\mathbf{W}^{*}$$

where $\mathbf{X}_{\mathrm{op}}^{-1}(1,:)$ is the first row of the inverses basic matrix at the optimal solution (final solution).

The reduced costs $\bar{\mathbf{c}}$ necessary for the convergence test of the simplex algorithm are variables in the output of the primal calculation. The automatic computation by Eq.(4.16) of the internal forces distribution is independent of the type of collapse: partial, complete or over-complete. However, it is necessary to notice that the internal force distribution given by this way is the static licit field (equilibrium and the plastic condition are respected). It may not coincide with the internal force distribution given by the elastic-plastic analysis where the physical condition is included.

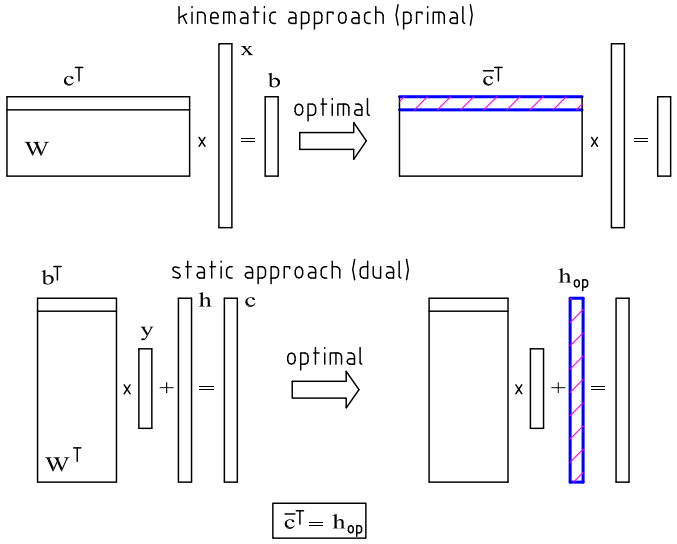

Fig.4.5. Primal-dual technique

4.2.3.2. Advantages of the primal-dual technique

For instance, the direct calculation of the internal force distribution has two advantages:

1. One may obtain the internal force from output of the kinematic approach without re-analyzing by static approach (or by elastic-plastic analysis).

2. The internal forces obtained by this technique are used in the plastic design leading to an important reduction of the problem size (Chapter 5).

4.3. Shakedown analysis by kinematic method

Fortunately, the mentioned techniques may be similarly applied in the kinematic formulation of shakedown analysis. Hereafter, we note only the formulas applied in the case of shakedown analysis without the intermediate explanations (presented in the previous section).

4.3.1. Standard kinematic approach

Based on the upper bound theorem of shakedown analysis [Eq.(2.24)], the safety factor can be determined by minimizing the kinematic admissible multiplier. Since the service load domain is specified by linear constraints, the kinematic approach leads to a linear programming problem:

$$\text{Min} \quad \phi = \mathbf{s}_0^{\mathrm{T}}\dot{\boldsymbol{\lambda}} \left| \begin{array}{c} \mathbf{N}_{\mathrm{C}}\dot{\boldsymbol{\lambda}} - \mathbf{B}\dot{\mathbf{d}} = \mathbf{0} \\ \mathbf{s}_{\mathrm{E}}^{\mathrm{T}}\mathbf{N}_{\mathrm{C}}\dot{\boldsymbol{\lambda}} = \xi \\ \dot{\boldsymbol{\lambda}} \geq \mathbf{0} \end{array} \right. , \tag{4.17}$$

where $\mathbf{s}_{\mathrm{E}}$ is the envelope of the elastic responses of the considered loading domain.

Then, the safety factor is obtained by:

$$\mu_{s+} = \phi / \xi \, .$$

4.3.2. Further reduction of kinematic approach

As in the limit analysis, by an appropriate choice of d_0 such that:

$$\dot{\mathbf{d}}' = \dot{\mathbf{d}} + \mathrm{d}_0 \geq 0 \, .$$

Using the new plastic deformation magnitude distribution, the vector of variables, matrix of constraints and vector of second member corresponding to the problem of Eq.(4.4) for shakedown analysis. We obtain then the following form:

$$\mathbf{x}^{*\mathrm{T}} = [\pi \quad \dot{\mathbf{d}}' \quad \dot{\boldsymbol{\lambda}} \quad \eta] \, ; \; \mathbf{b}^{*\mathrm{T}} = [0 \quad -\mathbf{B}\mathbf{d}_0 \quad \xi] \, ;$$

$$\mathbf{W}^* = \begin{bmatrix} 1 & \mathbf{0}^{\mathrm{T}} & -\mathbf{s}_0^{\mathrm{T}} & 0 \\ \mathbf{0} & -\mathbf{B} & \mathbf{N}_{\mathrm{C}} & \mathbf{0} \\ 0 & \mathbf{0}^{\mathrm{T}} & \mathbf{s}_{\mathrm{E}}^{\mathrm{T}}\mathbf{N}_{\mathrm{C}} & 1 \end{bmatrix} .$$

With initial basic matrix:

$$\mathbf{X}_0 = \begin{bmatrix} 1 & -\widetilde{\mathbf{s}}_0^{1\mathrm{T}} & -\widetilde{\mathbf{s}}_0^{2\mathrm{T}} & \ldots & -\widetilde{\mathbf{s}}_0^{\mathrm{n_s T}} & 0 \\ \mathbf{0} & \widetilde{\mathbf{N}}_{\mathrm{C}}^{1}\mathbf{S}^{1} & \mathbf{0} & \ldots & \mathbf{0} & \mathbf{0} \\ \mathbf{0} & \mathbf{0} & \widetilde{\mathbf{N}}_{\mathrm{C}}^{2}\mathbf{S}^{2} & \ldots & \mathbf{0} & \mathbf{0} \\ \vdots & \vdots & \vdots & \ldots & \vdots & \vdots \\ \mathbf{0} & \mathbf{0} & \mathbf{0} & \ldots & \widetilde{\mathbf{N}}_{\mathrm{C}}^{\mathrm{n_s}}\mathbf{S}^{n_s} & \mathbf{0} \\ 0 & \mathbf{s}_{\mathrm{E}}^{1\mathrm{T}}\left(\widetilde{\mathbf{N}}_{\mathrm{C}}^{1}\mathbf{S}^{1}\right) & \mathbf{s}_{\mathrm{E}}^{2\mathrm{T}}\left(\widetilde{\mathbf{N}}_{\mathrm{C}}^{2}\mathbf{S}^{2}\right) & \ldots & \mathbf{s}_{\mathrm{E}}^{\mathrm{n_s T}}\left(\widetilde{\mathbf{N}}_{\mathrm{C}}^{\mathrm{n_s}}\mathbf{S}^{n_s}\right) & 1 \end{bmatrix} . \tag{4.18}$$

The corresponding initial variables: $[\widetilde{\dot{\boldsymbol{\lambda}}}^{1'\mathrm{T}} \quad \widetilde{\dot{\boldsymbol{\lambda}}}^{2'\mathrm{T}} ... \widetilde{\dot{\boldsymbol{\lambda}}}^{n_s'\mathrm{T}}]$.

Let us notice that the problems of Eqs. (4.5) and (4.17) are similar except for the choice of the initial admissible point in the permissible domain and the shakedown analysis requires preliminary calculation of elastic responses.

4.3.3. Direct calculation of residual internal force distribution

Again the dual form of Eq.(4.15) is re-used with:

$$\mathbf{y}^{\mathrm{T}} = [\boldsymbol{\rho}^{\mathrm{T}} \quad \mu_{s-}]; \ \mathbf{h}^{\mathrm{T}} = [\mathbf{0}^{\mathrm{T}} \quad \mathbf{h}^{1\mathrm{T}} \quad \mathbf{h}^{2\mathrm{T}} \quad ... \mathbf{h}^{n_s\mathrm{T}}]$$

where $\boldsymbol{\rho}$ is the residual internal force vector; μ_{s-} is the load factor.

$$\mathbf{h}^{i\mathrm{T}} = [\widetilde{\mathbf{h}}^{i\mathrm{T}} \quad \widetilde{\mathbf{h}}_{+3}^{i\mathrm{T}} \quad \overline{\mathbf{h}}^{i}].$$

As the Eq.(4.16) in limit analysis, the relationship between the residual internal forces and the slack variables is:

$$\boldsymbol{\rho}^{i} = \left(\widetilde{\mathbf{N}}_{\mathrm{C}}^{i\mathrm{T}}\right)^{-1}\left(\widetilde{\mathbf{s}}_0^{i} - \mu_s \widetilde{\mathbf{N}}_{\mathrm{C}}^{i}\mathbf{s}_{\mathrm{E}} - \widetilde{\mathbf{h}}_{\mathrm{op}}^{i}\right).$$

As $\mathbf{h}_{\mathrm{op}}$ is identified to be the reduced costs of the primal problem of Eq.(4.17), the distribution of the residual internal force is directly obtained without performing a second static analysis.

4.4. Determination of specific displacement

d_0 is some positive number satisfying Eq.(4.7). A method to fix this quantity with the necessary proof is presented below.

Let us suppose that $\overline{\mathbf{d}}$ is the actual displacement field (the actual mechanism), where $\overline{d}_{\max}$ is the largest absolute value. In limit analysis, the safety factor is determined by the equilibrium between the internal power and the external power [see Eq.(4.5)]:

$$\mu_{+} = \mathbf{s}_0^{\mathrm{T}}\boldsymbol{\lambda} / \overline{\mathbf{f}}^{\mathrm{T}}\overline{\mathbf{d}} = \phi / \xi . \tag{4.19}$$

where the symbols are defined as in Eq.(4.5).

Based on the upper bound theorem of limit analysis, we have:

$$\mu_{+} \le \mu^{*}, \tag{4.20}$$

with μ^{*} is a load factor of any licit mechanism. By giving any licit displacement field $\mathbf{d}^{*}$ (for example, only one component equals unity, and every other components are null), μ^{*} may be easily obtained.

From the Eqs.(4.19) and (4.20), one has:

$$\phi / \xi \le \mu^{*}. \tag{4.21}$$

On the point of view of geometry (kinematic), with the actual mechanism, $\overline{\mathbf{d}}$, it exists at least a plastic deformation component, $\overline{e}$, such that:

$$\overline{e} \ge \overline{d}_{\max} / H_{\max},$$

with $H_{\max}$ is the maximum dimension of the structure.

Therefore, a lower bound of the internal power may be evaluated:

$$\phi \geq s_{p\min} \bar{d}_{\max} / H_{\max}, \tag{4.22}$$

in which, $s_{p\min}$ is the smallest among the plastic capacity (N_P , M_{py}, M_{pz}) of all the sections of the structure.

From the Eqs.(4.21) and (4.22), the maximum displacement is constrained by an upper bound:

$$\bar{d}_{\max} \leq \xi \mu^* H_{\max} / s_{p\min}.$$

Then, any value of d_0 that satisfies:

$$d_0 \geq \xi \mu^* H_{\max} / s_{p\min} \geq \bar{d}_{\max},$$

will lead to $\mathbf{d}' = \bar{\mathbf{d}} + d_0$ is *always non negative*.

With the similar argument, the d_0 value for the shakedown analysis may be obtained.

4.5. Numerical examples and discussions

According to the author's knowledge, there is not available benchmark for limit and shakedown analysis of large 3-D steel frames with I or H-shaped sections in the open literatures. In this section, three examples are selected. Two firsts are the 3-D steel frames that are the current benchmarks in the "advanced nonlinear analysis of steel frames" (e.g. Orbison (1982)[126], Liew (2000, 2001)[88, 89], Kim (2001)[81], Jiang (2002)[71], Chiorean (2005)[28] and Cuong (2006)[35]). The last example is a series of 2-D bending frames that already studied by Casciaro (2002)[14].

The results of two 3-D steel frames will be re-evaluated in Chapter 6 by step-by-step method. In addition, various other examples of limit and shakedown analysis will be also presented in Chapter 8 (semi-rigid frames).

Example 4.1a – Six-story space frame: Fig.4.6 shown Orbison's six-story space frame. The yield strength of all members is 250 MPa and Young'modulus is 206 GPa. Uniform floor pressure of $4.8\mu_1$ kN/m^2; wind loads are simulated by point loads of $26.7\mu_2$ kN in the Y-direction at every beam-column joint. In which, μ_1, μ_2 are the factors that define the loading domain.

Example 4.1b – Twenty-story space frame: Twenty-story space frame with dimensions and properties shown in Fig.4.7. The yield strength of all members is 344.8 MPa and Young'modulus is 200 GPa. Uniform floor pressure of $4.8\mu_1$ kN/m^2; the wind loads $=0.96\mu_2$ kN/m^2 are acting in the Y direction.

Concerning the loading domain (for two examples 4.1a and 4.1b), two cases are considered for shakedown analysis: a) $0\leq\mu_1\leq1$, $0\leq\mu_2\leq1$ and b) $0\leq\mu_1\leq1$, $-1\leq\mu_2\leq1$. For fixed or proportional loading, we obviously must have: $\mu_1=\mu_2=1$. The uniformly distributed loads are lumped at the joints of frames.

The load multipliers are shown on Table 4.1 while the collapse mechanisms are reported on Figs. 4.8 and 4.9. The load factor and the collapse mechanisms given by limit analysis will be compared with which of step-by-step method in Chapter 6.

It appears that in the case of symmetric horizontal loading (seismic load or wind load), the alternating plasticity occur; and corresponding load factors are very small in comparison with the case of one-sign load (load domain a).

For the case where the alternating plasticity occur; one may verify the result by a simple verification. For example, with the six-story frame with the load domain b, alternating plasticity occur at section B (Fig.4.6), the necessary parameters are:

Elastic envelop: $M_y^+ = M_y^- = 186.42$ (kNm); $N^+ = N^- = 13.46$ KN; $M_z^+ = M_z^- = 1.22$ (KNm); one may verify those value by the linear elastic analysis with the load factor equal 1.67.

Plastic capacity (W12x53): $M_{py} = 318.70$ (kNm); $N_p = 2525.00$ KN; $M_{pz} = 119.50$ (KNm);

With this simple case (elastic envelop is symmetric), load multiplier is calculated by (Fig.4.10)**:** $\mu = OA/OB = 1.670$ **;** it is agree with the value given in Table 4.1.

Table 4.1: Examples 4.1 - ultimate strengths of the frames given by CEPAO

Type of analysis	Load multiplier		Limit state
	Example 4.1a	Example 4.1b	
Limit analysis	2.412	1.698	Formation of a mechanism
Shakedown analysis, domain load a	2.311	1.614	Incremental plasticity
Shakedown analysis, domain load b	1.670	0.987	Alternating plasticity (*)

(*) alternating plasticity at section B (Figs. 4.6 and 4.7).

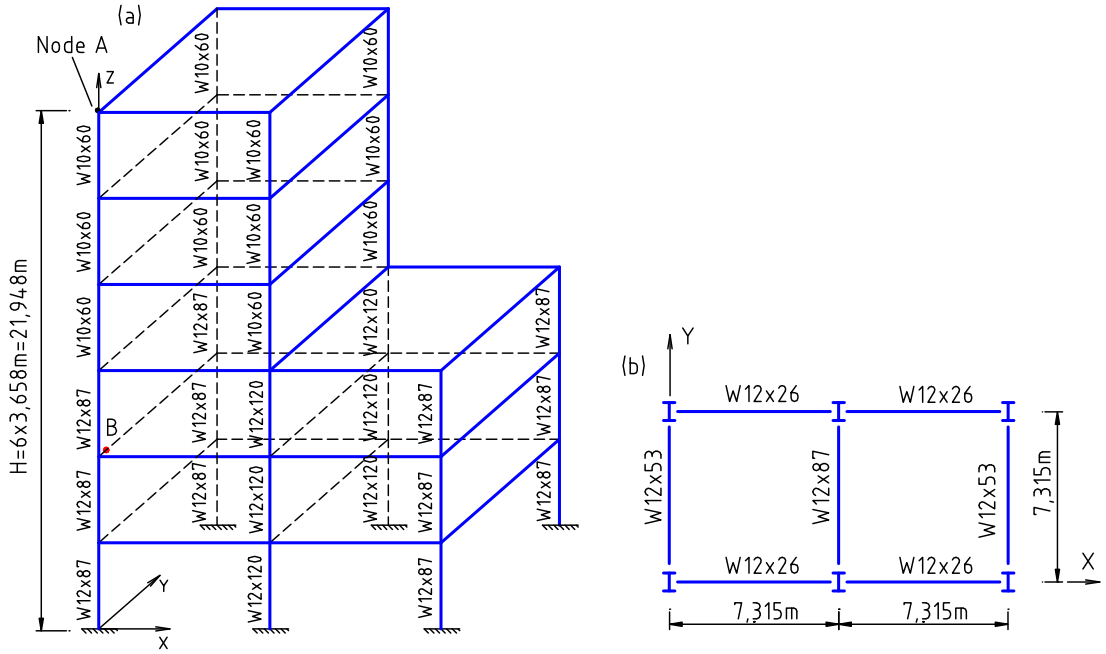

Fig.4.6. Example 4.1a- Six story space frame (a – perspective view, b- plan view)

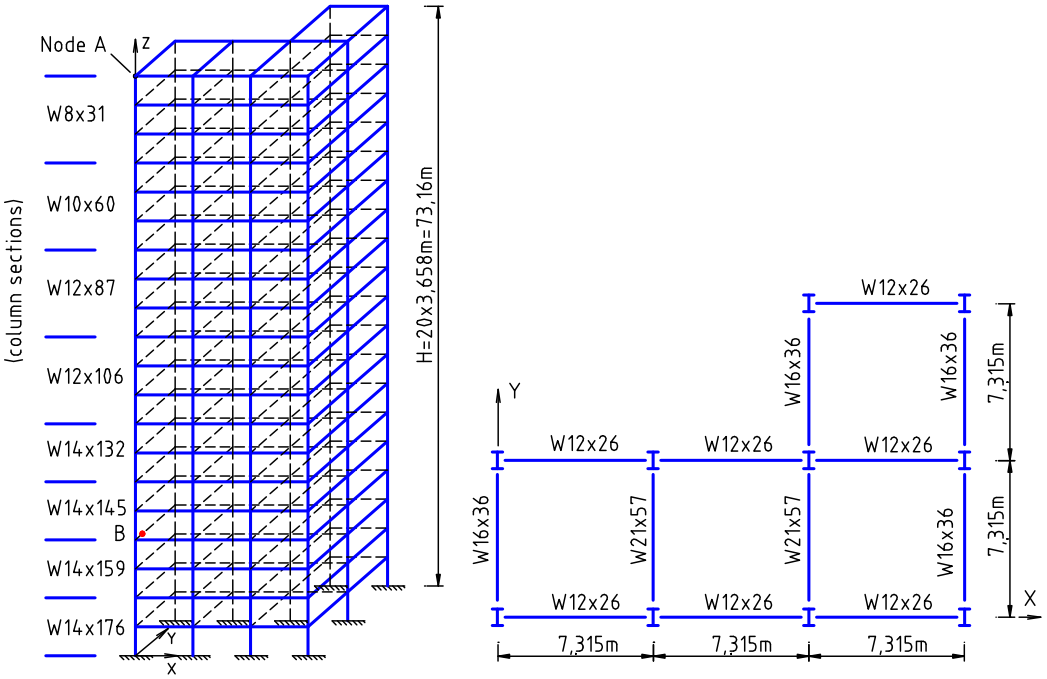

Fig.4.7. Example 4.1b- Twenty story space frame (a- perspective view; b- plan view)

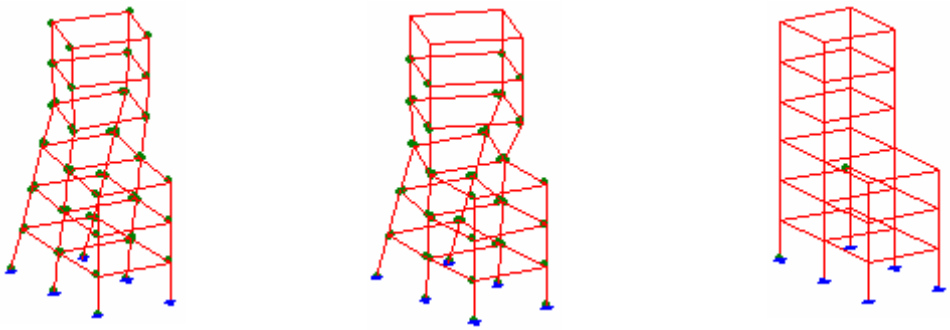

Fig.4.8. Example 4.1a-deformation at limit state given by CEPAO
(left to right: limit analysis; shakedown analysis, load domain a; shakedown analysis, load domain b)

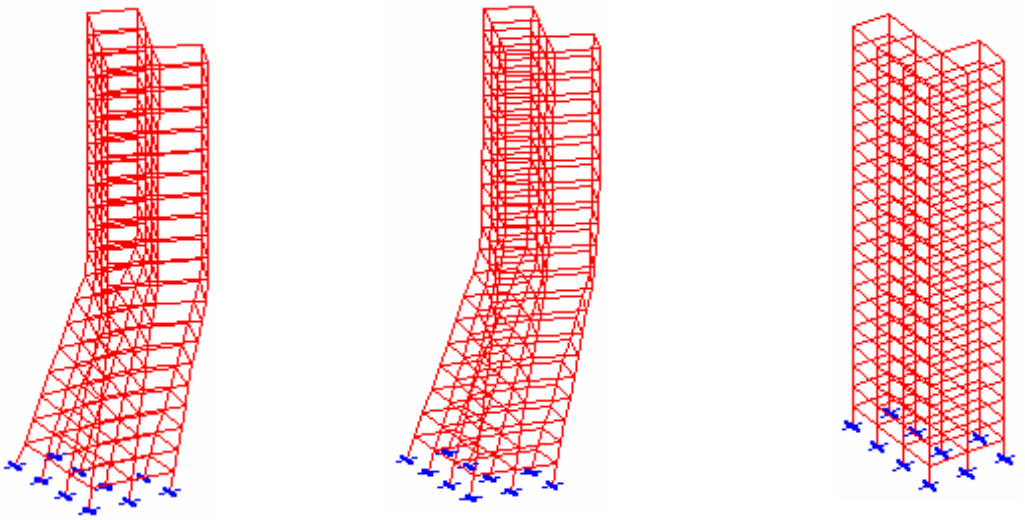

Fig.4.9. ample 4.1b-deformation at limit state given by CEPAO
(left to right: limit analysis; shakedown analysis, load domain a; shakedown analysis, load domain b)

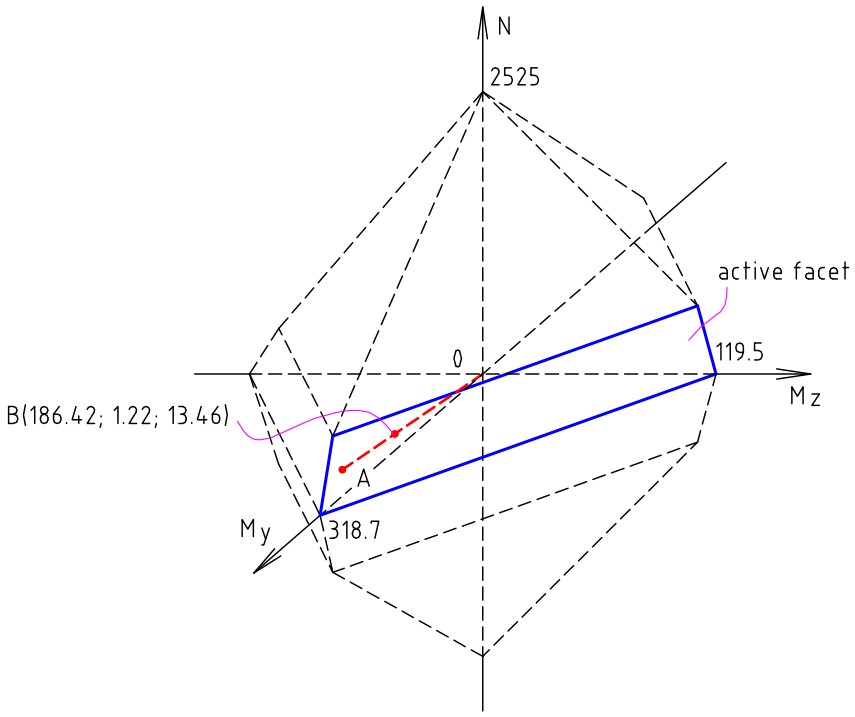

Fig.4.10. State of section B of six-story frame with load domain b

Example 4.2-Limit and shakedown analysis for 2-D bending frame: A series of frames with different numbers of story and bay being already considered by Casciaro (2002)[14] are shown on the Fig.4.11 (the units was not mentioned in [14]). A constant story height of 300 and a constant bay length of 400 are assumed for the sake simplicity. Three loading cases are considered: two distributed vertical loads p_1 and p_2 and a seismic action defined as transversal force linearly increasing by P_3 from the ground to the top floor (see Fig.4.11). Some mechanical properties are reported in Table 4.2, and the load domain is defined by:

$$9\mu \le p_1 \le 10\mu;\ 0\mu \le p_2 \le 5\mu;\ -500\mu \le P_3 \le 500\mu.$$

Table 4.3 presents the comparison of load multipliers for both limit and shakedown analysis of the series frames.

The load multipliers obtained by Casciaro and by CEPAO in agreement for the limit analysis for all frames and for the shakedown analysis for 3×4 frame. While the differences are respectively: -10,5%, -6,4% and -6,5% for 4×6 frame, 5×9 frame and 6×10 frame in the shakedown analysis.

Table 4.4 presents the load multipliers in the case of shakedown analysis for 4×6, 5×9, 6×10 frame, with the following assumption: the alternating plastic occurs in the sections A, B, C using the envelope of bending moment calculated by software SAP2000. Clearly, the load multipliers in the Table 4.4 are the *upper bounds*. The actual load multipliers cannot exceed these values. The differences between the results obtains by CEPAO and the above-mentioned values is about from 3,5% to 6,4% while those of Casciaro [14] are from 9,4% to 15,3%. It is useful to note that the differences of the value of the envelope of the bending moment between SAP2000 and CEPAO is due to the lumping of the uniformly distributed load at the central point and the two ends of each element in CEPAO.

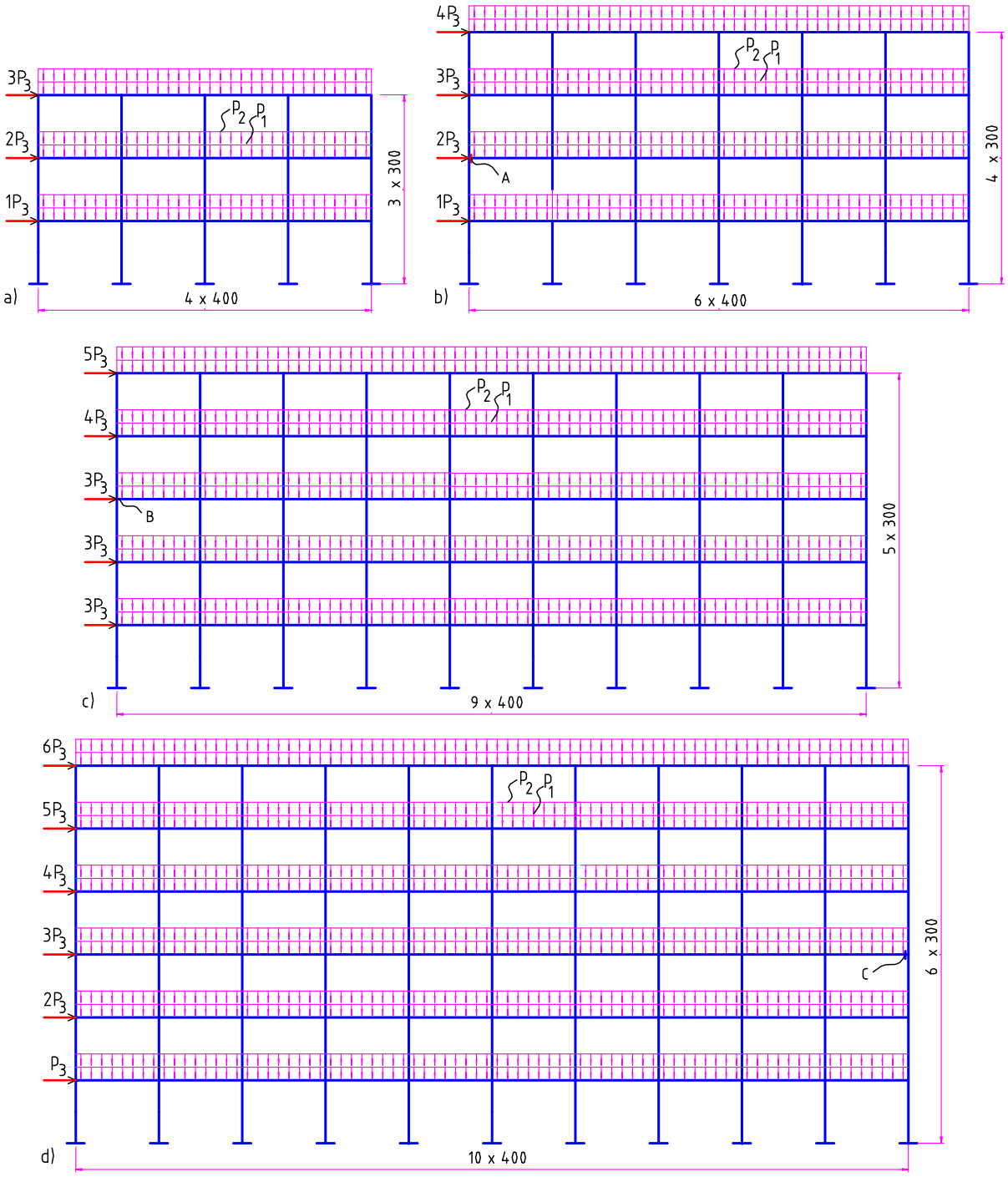

Fig.4.11. Example 4.2 - geometry and loads for the series frames
(a- 3x4 frame; b- 4x6 frame; c- 5x9 frame; d- 6x10 frame)

Table 4.2: Example 4.2 – Mechanical properties for the series of frames

	Young modulus (E)	Moment of inertia (I)	Plastic capacity (M_P)
Column	300000	540000	1800000
Beam	300000	67500	450000

Table 4.3: Example 4.2 – Comparison of load multipliers

Type of frame	Limit analysis			Shakedown analysis		
	Ref. [14]	CEPAO	Difference	Ref. [14]	CEPAO	Difference
3×4 frame	2.4612	2.4612	0.0%	2.0134	2.0102 (*)	0.0%
4×6 frame	1.8610	1.8610	0.0%	1.3993	1.2655 (**)	-10.5%
5×9 frame	1.2000	1.2000	0.0%	0.7533	0.7076 (**)	-6.4%
6×10 frame	1.1532	1.1532	0.0%	0.7209	0.6771 (**)	-6.5%

(*): incremental plasticity; (**): alternating plasticity at section A, B, C (see Fig.4.11)

Table 4.4: Example 4.2 –Some upper bound of load multipliers

Sections	Envelope of bending moment		Plastic capacity	Load Multiplier
	M^+	M^-	(M_p)	$=2M_p/(M^+ + M^-)$
Section A (Fig.4.11b)	282717	477057	450000	1.1846
Section B (Fig.4.11c)	563240	757155	450000	0.6816
Section C (Fig.4.11d)	591835	785758	450000	0.6533

4.6. Conclusions

It appears that the canonical formulas in the both limit and shakedown analysis using linear programming for 3-D steel frames may be reduced by a special change of the variables and by a natural choice of the initial basic matrix used in the simplex algorithm. The distribution of the internal forces may be directly calculated by the application of duality aspects in the linear programming technique. This allows to avoid expensive static analysis of the primal problem. The above mentioned techniques are very suitable for automatic computation. By consequence, they were completely implemented in CEPAO package. By the way, the problem of ultimate strengths of the large-scale 3-D steel frames under fix or repeated loading, in the sense of respectively limit and shakedown analysis, can be solved now by the CEPAO package in an automatic manner look like any finite element algorithm devoted to 3-D frame structures. This chapter shows also that the simplex technique still is a necessary tool in the automatic plastic analysis of 3-D steel frameworks after a less eventful period of the application of linear programming in the analysis of frame structures.

Chapter **5**

Limit and shakedown design of 3-D steel frames by linear programming

In Chapter 4, the number of *variables* in both limit and shakedown *analysis* by *kinematic* approach using linear programming are considerably reduced. In duality, in this chapter, the number of *constraints* in both limit and shakedown *design* by *static* approach using linear programming are strongly reduces. Two techniques are proposed: the *fixed- push* and the *standard-transformation* technique, where the second technique was dealt with by Nguyen-Dang [117] for 2-D bending frames. The mentioned techniques lead to the *semi-direct* algorithm. The stiffness and stability constraint are not yet considered in the present work.

Keywords: *Limit design*; *Shakedown design*; *Plastic hinge; Space frames; Linear programming.*

5.1. Weight function

Let us consider a steel frame with the node layout has been selected and fixed. One strives to find the optimum selection of profile presented in the database. Generally, the member sizes of a frame are grouped by the technological condition. In each group, the members are made with the same profile. Because the plastic axial capacity is proportional to the area of the member, the weight (or the volume) of each group is proportional to the product of the plastic axial capacity and the total length (of group). Therefore, the objective function of the frame may be written as:

$$Z = \bar{\mathbf{n}}_{\mathrm{p}}^{\mathrm{T}} \bar{\mathbf{l}},$$

where $\bar{\mathbf{n}}_{\mathrm{p}}$, $\bar{\mathbf{l}}$ are, respectively, the vector of plastic axial capacity and the vector of group lengths.

The vector of plastic axial capacity of the critical sections ($\mathbf{n}_{\mathrm{p}}$) may be recovered from the vector $\bar{\mathbf{n}}_{\mathrm{p}}$ as follows:

$$\mathbf{n}_{\mathrm{p}} = \mathbf{L}\bar{\mathbf{n}}_{\mathrm{p}}, \tag{5.1}$$

with $\mathbf{L}$ is a Boolean matrix.

5.2. Limit design by static approach

Section 5.2.1 will briefly present the traditional algorithm. The difficulties of the latter, the idea of improvement and the detail formulation of a new algorithm with the reduction of constraints are described in Sections 5.2.2.

5.2.1. Direct algorithm (traditional algorithm)

The licit field of internal force (**s**) must satisfy the equilibrium condition and the plastic condition, so that the static approach to the limit design problem leads to the following formulation:

$$Min\ Z(\bar{\mathbf{n}}_p, \mathbf{s}) \equiv \bar{\mathbf{n}}_p^T \bar{\mathbf{l}} \tag{5.2}$$

subject to

$$\mathbf{B}^T\mathbf{s} = \mathbf{f}\ ; \tag{5.3}$$

$$\mathbf{N}_c^T\mathbf{s} \le \mathbf{n}_p\ , \tag{5.4}$$

where: **f** is the vector of the given load; $\mathbf{B}^T$ is the equilibrium matrix defined in Chapter 3. Eq.(5.4) is Eq.(4.9) when $\mathbf{s}_0 = \mathbf{n}_p$.

When the coefficients $a_1,...,a_6$ [in matrix $\mathbf{N}_c$ of Eq.(5.4)] are given in advance by the choice of the initial member size, the problem described by Eqs. (5.2-5.4) has a linear programming formulation. However, if this problem is only solved by unique iteration, mentioned coefficients in the input may be different from themselves in the output. Therefore, an iterative process shown on Fig.5.1 needs to be adopted. Because Eqs.(5.2-5.4) are directly solved, the algorithm is called the *direct* algorithm.

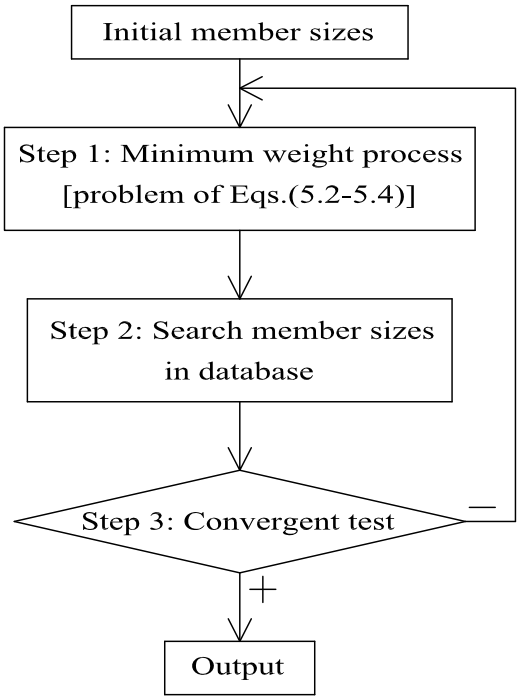

Fig.5.1. Direct algorithm

5.2.2. Semi-direct algorithm

As n_s is the number of the critical sections, n_m is the number of independent mechanisms (independent equilibrium equations). If the sixteen- facet polyhedron is used to indicate the plastic admissibility then the number of the constraints in Eqs.(5.3) and (5.4) equal (Fig.5.2):

$$n = n_m + 16n_s\ . \tag{5.5}$$

We observe that *n* is very large respect to a large-scale frame, it may become an obstacle in the computational procedure. To reduce the value *n*, *fixed-push* technique and *standard-*

transformation technique are respectively presented in the following (Sections 5.2.2.1 and 5.2.2.2). It leads to the *semi-direct* algorithm that is described in Section 5.2.2.3.

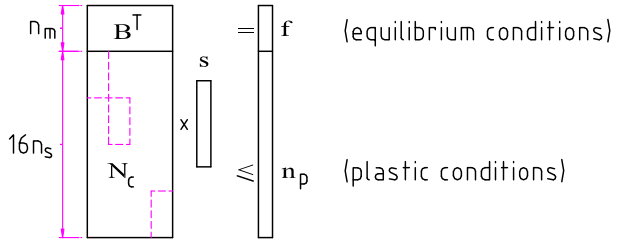

Fig.5.2.The constraints in the plastic design problem using static approach

5.2.2.1. Fixed-push technique

With the direct algorithm (Fig.5.1), the initial structure is successively improved during the iteration procedure. Consider now a structure at any time of the above procedure, two parallel operations are imagined:

1. Optimizing this frame by Eqs.(5.2-5.4), one has the distribution of the internal force, **s**, in the output. It may be decomposed into two parts:

$$\mathbf{s}^{\mathrm{T}} = [\mathbf{s}_{\mathrm{m}}^{\mathrm{T}} \quad \mathbf{s}_{\mathrm{n}}^{\mathrm{T}}],$$

where $\mathbf{s}_{\mathrm{m}}$ collects the bending moments and $\mathbf{s}_{\mathrm{n}}$ indicates the axial forces.

2. Analyzing the same structure by the limit analysis algorithm presented in Chapter 4. With the primal-dual technique (Section 4.2.3 in Chapter 4), one obtains other licit field of internal force:

$$\mathbf{s}'^{\mathrm{T}} = [\mathbf{s}_{\mathrm{m}}'^{\mathrm{T}} \quad \mathbf{s}_{\mathrm{n}}'^{\mathrm{T}}].$$

We may agree that: (1) the difference between the structures in two successive iterations of the design procedure (Fig.5.1) is progressively reduced; (2) the axial force is less sensible (in comparison with the bending moments) with the variation of the member size. Therefore, one may believe that:

$$\mathbf{s}_{\mathrm{n}} \approx \mathbf{s}_{\mathrm{n}}'.$$

Based on this observation, the following assumption is made: during each iteration of the design procedure (Fig.5.1), the axial force is considered as a *fixed* quantity:

$$\mathbf{s}_{\mathrm{n}} = \mathbf{s}_{\mathrm{n}}'. \tag{5.6}$$

In the other word, the axial force is not yet the variables in the simplex process, it is approximated in advance by Eq.(5.6). With the supplementary condition of Eq.(5.6), the constraints of the problem of Eqs.(5.2-5.4) are modified as follows.

Firstly, at the i^{th} critical section, if the axial force (N'^i) is given in advance, the plastic admissibility of sixteen-facet polyhedron becomes a quadrilateral that may be arranged as follows (Fig.5.3):

$$\begin{bmatrix} a_{2(5)}^i & a_{3(6)}^i \\ -a_{2(5)}^i & a_{3(6)}^i \\ -a_{2(5)}^i & -a_{3(6)}^i \\ a_{2(5)}^i & -a_{3(6)}^i \end{bmatrix} \begin{bmatrix} M_y^i \\ M_z^i \end{bmatrix} \le \begin{bmatrix} N_p^i - a_{1(4)}^i \left| N'^i \right| \\ N_p^i - a_{1(4)}^i \left| N'^i \right| \\ N_p^i - a_{1(4)}^i \left| N'^i \right| \\ N_p^i - a_{1(4)}^i \left| N'^i \right| \end{bmatrix},$$

or, symbolically:

$$\begin{cases} \widetilde{\mathbf{N}}_{\mathrm{cm}}^{\mathrm{iT}}\mathbf{s}_{\mathrm{m}}^{\mathrm{i}} \le \mathbf{D}^{\mathrm{i}}N_{\mathrm{p}}^{\mathrm{i}} - \widetilde{\mathbf{N}}_{\mathrm{cn}}^{\mathrm{iT}}\left|N'^{i}\right| \\ -\widetilde{\mathbf{N}}_{\mathrm{cm}}^{\mathrm{iT}}\mathbf{s}_{\mathrm{m}}^{\mathrm{i}} \le \mathbf{D}^{\mathrm{i}}N_{\mathrm{p}}^{\mathrm{i}} - \widetilde{\mathbf{N}}_{\mathrm{cn}}^{\mathrm{iT}}\left|N'^{i}\right| \end{cases}; \tag{5.7}$$

where:

$$\widetilde{\mathbf{N}}_{\mathrm{cm}}^{\mathrm{iT}} = \begin{bmatrix} a_{2(5)}^{i} & a_{3(6)}^{i} \\ -a_{2(5)}^{i} & a_{3(6)}^{i} \end{bmatrix};$$

$$\mathbf{D}^{\mathrm{iT}} = [1 \quad 1];$$

$$\widetilde{\mathbf{N}}_{\mathrm{cn}}^{\mathrm{i}} = [a_{1(4)}^{i} \quad a_{1(4)}^{i}].$$

Eq.(5.7) may be written for the whole structure as:

$$\begin{cases} \widetilde{\mathbf{N}}_{\mathrm{cm}}^{\mathrm{T}}\mathbf{s}_{\mathrm{m}} \le \mathbf{D}\mathbf{n}_{\mathrm{p}} - \widetilde{\mathbf{N}}_{\mathrm{cn}}^{\mathrm{T}}\widetilde{\mathbf{s}}_{\mathrm{n}}' \\ -\widetilde{\mathbf{N}}_{\mathrm{cm}}^{\mathrm{T}}\mathbf{s}_{\mathrm{m}} \le \mathbf{D}\mathbf{n}_{\mathrm{p}} - \widetilde{\mathbf{N}}_{\mathrm{cn}}^{\mathrm{T}}\widetilde{\mathbf{s}}_{\mathrm{n}}' \end{cases}; \tag{5.8}$$

with:

$$\widetilde{\mathbf{N}}_{\mathrm{cm}}^{\mathrm{T}} = \begin{bmatrix} \widetilde{\mathbf{N}}_{\mathrm{cm}}^{1\mathrm{T}} & & & \\ & \widetilde{\mathbf{N}}_{\mathrm{cm}}^{2\mathrm{T}} & & \\ & & \cdots & \\ & & & \widetilde{\mathbf{N}}_{\mathrm{cm}}^{\mathrm{n_s T}} \end{bmatrix};$$

$$\mathbf{D} = \begin{bmatrix} \mathbf{D}^{1} & & & \\ & \mathbf{D}^{2} & & \\ & & \cdots & \\ & & & \mathbf{D}^{n_s} \end{bmatrix};$$

$$\widetilde{\mathbf{N}}_{\mathrm{cn}}^{\mathrm{T}} = \begin{bmatrix} \widetilde{\mathbf{N}}_{\mathrm{cn}}^{1\mathrm{T}} & & & \\ & \widetilde{\mathbf{N}}_{\mathrm{cn}}^{2\mathrm{T}} & & \\ & & \cdots & \\ & & & \widetilde{\mathbf{N}}_{\mathrm{cn}}^{\mathrm{n_s T}} \end{bmatrix};$$

$$\widetilde{\mathbf{s}}_{\mathrm{n}}'^{\mathrm{T}} = \left[\left|N'^{1}\right|, \left|N'^{2}\right|, \cdots, \left|N'^{n_s}\right|\right].$$

Secondly, the equilibrium relation of Eq.(5.3) is rewritten as:

$$\mathbf{B}_{\mathrm{m}}^{\mathrm{T}}\mathbf{s}_{\mathrm{m}} = \mathbf{f} - \mathbf{B}_{\mathrm{n}}^{\mathrm{T}}\mathbf{s}_{\mathrm{n}}'. \tag{5.9}$$

Because $\mathbf{s}_{\mathrm{n}}'$ is a subset of a licit field of internal force, certain equations in the system of Eq.(5.9) are auto-satisfied. Therefore, Eq.(5.3) contains n_m independent equations (independent mechanisms) but Eq.(5.9) contains only $\bar{n}_m$ independent equations, $\bar{n}_m \le n_m$.

Let us note that the form Eq.(5.8) may be applied to other yield surface, for example with the yield surface of eight-facet polyhedron. The fixed-push technique is illustrated on Fig.5.3.

5.2.2.2. Standard-transformation technique

The simplex method requires that all variables must be non-negative. To make the best of this, the following change of variables is adopted:

$$\mathbf{s}_m^* = \tilde{\mathbf{N}}_{cm}^T \mathbf{s}_m + \mathbf{D}\mathbf{n}_p - \mathbf{N}_{cn}^T \tilde{\mathbf{s}}_n' . \tag{5.10}$$

Since the matrix $\tilde{\mathbf{N}}_{cm}^T$ is always non-singular, drawing $\mathbf{s}_m$ from Eq. (5.10), one obtains:

$$\mathbf{s}_m = \left(\tilde{\mathbf{N}}_{cm}^T\right)^{-1}\left(\mathbf{s}_m^* - \mathbf{D}\mathbf{n}_p + \mathbf{N}_{cn}^T \tilde{\mathbf{s}}_n'\right). \tag{5.11}$$

Using the value of $\mathbf{s}_m$ from Eq. (5.11), the system (5.8) becomes:

$$\begin{cases} \mathbf{s}_m^* \le 2\mathbf{D}\mathbf{n}_p - 2\tilde{\mathbf{N}}_{cn}^T \tilde{\mathbf{s}}_n' \\ \mathbf{s}_m^* \ge 0 \end{cases}. \tag{5.12}$$

The inequalities $\mathbf{s}_m^* \ge 0$ in Eq.(5.12) are self-satisfying in the simplex process. Therefore, the plastic admissibility of Eq.(5.4) is reduced to $2n_s$ inequalities:

$$-\mathbf{s}_m^* + 2\mathbf{D}\mathbf{n}_p \ge 2\tilde{\mathbf{N}}_{cn}^T \tilde{\mathbf{s}}_n' . \tag{5.13}$$

Let us return to the equilibrium relation, substituting Eq.(5.11) in Eq.(5.9), one obtains:

$$\mathbf{B}_m^T \tilde{\mathbf{N}}_{cm}^{-T} \mathbf{s}_m^* - \mathbf{B}_m^T \tilde{\mathbf{N}}_{cm}^{-T} \mathbf{D}\mathbf{n}_p = \mathbf{f} - \mathbf{B}_n^T \mathbf{s}_n' - \mathbf{B}_m^T \tilde{\mathbf{N}}_{cm}^{-T} \tilde{\mathbf{N}}_{cn}^T \tilde{\mathbf{s}}_n' . \tag{5.14}$$

The change of variables the so-called standard-transformation may be also illustrated on Fig.5.3.

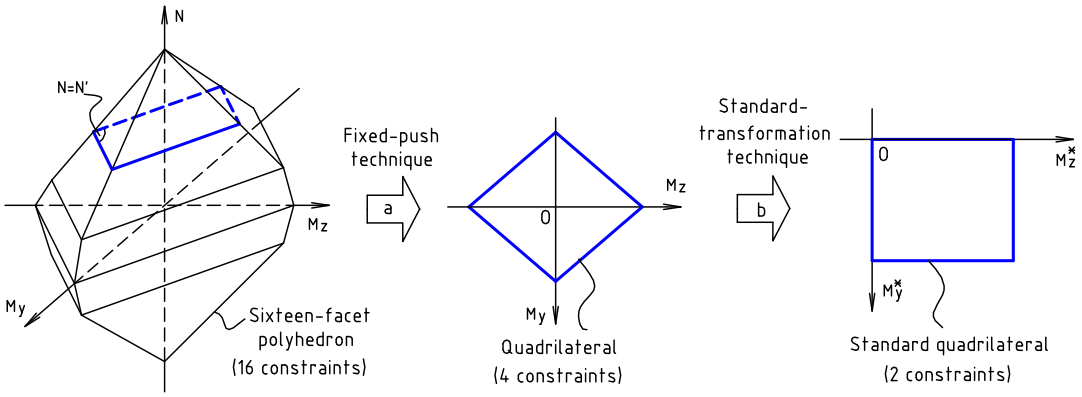

Fig .5.3. Fixed-push and Standard-transformation techniques

5.2.2.3. Reduced formulas

With the plastic condition of Eq.(5.13) and the equilibrium equation (5.14), taking into account Eq.(5.1), the problem of Eqs.(5.2-5.4) is reduced to the standard form of the simplex method with fewer constraints:

$$Min\ Z = \mathbf{c}^T \mathbf{x} \left| \begin{matrix} \mathbf{W}\mathbf{x} = \mathbf{b} \\ \mathbf{x} \ge \mathbf{0} \end{matrix} \right. , \tag{5.15}$$

where:

$$\mathbf{x}^T = [\mathbf{s}_m^* \quad \bar{\mathbf{n}}_p \quad \mathbf{P}^T \quad \mathbf{R}^T \quad \mathbf{Q}^T];$$

$$\mathbf{c}^T = [\mathbf{0}^T \quad \bar{\mathbf{l}}^T \quad \mathbf{0}^T \quad \mathbf{0}^T \quad \mathbf{0}^T];$$

$$\mathbf{b}^T = [2\tilde{\mathbf{N}}_{cn}^T \tilde{\mathbf{s}}_n' \qquad \mathbf{f} - \mathbf{B}_n^T \mathbf{s}_n' - \mathbf{B}_m^T \tilde{\mathbf{N}}_{cm}^{-T} \tilde{\mathbf{N}}_{cn}^T \tilde{\mathbf{s}}_n'];$$

$$\mathbf{W} = \begin{bmatrix} -\mathbf{E}_1 & 2\mathbf{D}\mathbf{L} & -\mathbf{E}_1 & \mathbf{E}_1 & \mathbf{0} \\ \mathbf{B}_m^T \tilde{\mathbf{N}}_{cm}^{-T} & -\mathbf{B}_m^T \tilde{\mathbf{N}}_{cm}^{-T} \mathbf{D}\mathbf{L} & \mathbf{0} & \mathbf{0} & \mathbf{E}_2 \end{bmatrix} \begin{matrix} 2n_s \\ \bar{n}_m \end{matrix};$$

$$\begin{matrix} 2n_s & n_g & 2n_s & 2n_s & \bar{n}_m \end{matrix}$$

where **P** is the slack variables; **R** and **Q** are the artificial variables; $\mathbf{E}_1$, $\mathbf{E}_2$ indicate the unity matrices; n_g is the number of groups of member sizes (technology condition).

The initial basic matrix of the simplex method is evidently chosen as:

$$\mathbf{X}_0 = \begin{bmatrix} \mathbf{E}_1 & \\ & \mathbf{E}_2 \end{bmatrix}.$$

From aforementioned discussions, the direct algorithm (Fig.5.1) for the limit plastic design may be modified into another shown on Fig.5.4, so-called the *semi-direct* algorithm.

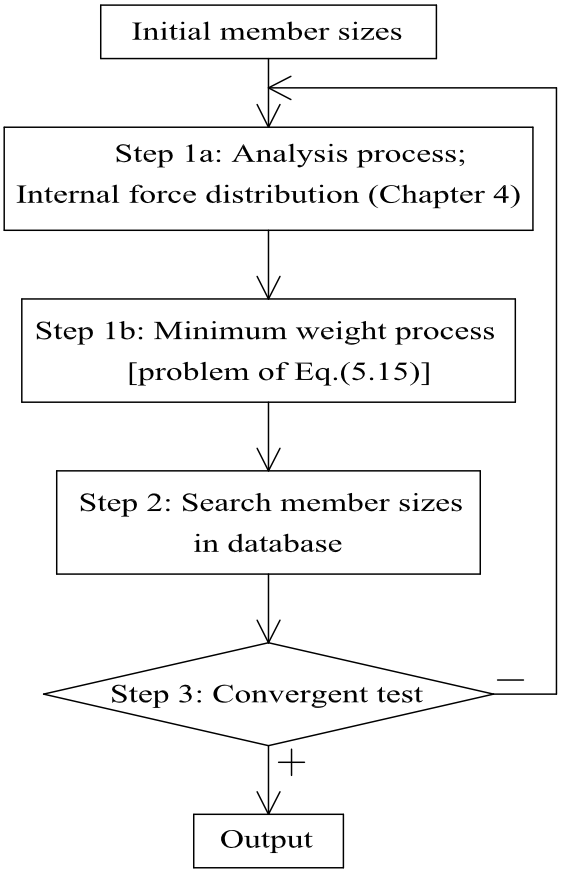

Fig.5.4. Semi-direct algorithm

5.3. Shakedown design by static approach

The form of this section is similar with which of Section 5.2, but the formulation devotes to the shakedown design problem.

5.3.1. Direct algorithm

The residual interne force distribution ($\boldsymbol{\rho}$) must satisfy the self-equilibrium equation and the plastic condition, so that the static approach to the shakedown design problem leads to the following formulation:

$$Min\ Z(\bar{\mathbf{n}}_p, \boldsymbol{\rho}) \equiv \bar{\mathbf{n}}_p^T \bar{\mathbf{l}} \tag{5.16}$$

subject to

$$\mathbf{B}^T \boldsymbol{\rho} = \mathbf{0}, \tag{5.17}$$

$$\mathbf{N}_c^T (\mathbf{s}_e + \boldsymbol{\rho}) \le \mathbf{n}_p, \tag{5.18}$$

where $\mathbf{s}_e$ is the envelope of the elastic internal forces of the considered loading domain. It involves two extreme values, positive ($\mathbf{s}_e^{\max}$) and negative ($\mathbf{s}_e^{\min}$).

The direct algorithm for the shakedown design is similar to the Fig.1 except the shakedown design requires preliminary calculation of elastic response and the Eqs.(5.2-5.4) are replaced by Eqs.(5.16-5.18). It is not necessary to be presented herein.

5.3.2. Semi-direct algorithm

The number of constraints in the Eqs.(5.17) and (5.18) is the same with which of Eqs.(5.3) and (5.4), it is together given by Eq.(5.5). In the following, as the limit design problem, fixed-push technique and standard-transformation technique for the shakedown design problem are described. To avoid the repeat of the arguments, herein we present only the necessary formulas for the case of shakedown design.

5.3.2.1. Fixed-push technique

The distribution of residual axial forces ($\boldsymbol{\rho}_{\mathrm{n}}$) is prescribed in advance by $\boldsymbol{\rho}'_{\mathrm{n}}$ that is given by primal-dual technique in shakedown analysis problem (Chapter 4). At the i$^{\text{th}}$ critical section, the system of inequalities (5.18) for the case of shakedown design becomes now:

$$\begin{cases} \widetilde{\mathbf{N}}_{\mathrm{cm}}^{\mathrm{iT}}\boldsymbol{\rho}_{\mathrm{m}}^{\mathrm{i}} \le \mathbf{D}^{\mathrm{i}} N_{\mathrm{p}}^{\mathrm{i}} - \widetilde{\mathbf{N}}_{\mathrm{cn}}^{\mathrm{iT}} \overline{N}^{i} - \bar{\mathbf{s}}_{+\mathrm{em}}^{\mathrm{i}} \\ -\widetilde{\mathbf{N}}_{\mathrm{cm}}^{\mathrm{iT}}\boldsymbol{\rho}_{\mathrm{m}}^{\mathrm{i}} \le \mathbf{D}^{\mathrm{i}} N_{\mathrm{p}}^{\mathrm{i}} - \widetilde{\mathbf{N}}_{\mathrm{cn}}^{\mathrm{iT}} \overline{N}^{i} - \bar{\mathbf{s}}_{-\mathrm{em}}^{\mathrm{i}} \end{cases}, \tag{5.19}$$

where

$$\overline{N}^{i} = \max\left(\left\{-\rho'^{i} - N_{-e}^{i}\right|, \left|\rho'^{i} + N_{-e}^{i}\right|\right);$$

$$\bar{\mathbf{s}}_{+\mathrm{em}}^{\mathrm{i}} = \begin{bmatrix} a_{2(5)}^{i} M_{+ye}^{i} + a_{3(6)}^{i} M_{+ze}^{i} \\ a_{2(5)}^{i} M_{-ye}^{i} + a_{3(6)}^{i} M_{+ze}^{i} \end{bmatrix};$$

$$\bar{\mathbf{s}}_{-\mathrm{em}}^{\mathrm{i}} = \begin{bmatrix} a_{2(5)}^{i} M_{-ye}^{i} + a_{3(6)}^{i} M_{-ze}^{i} \\ a_{2(5)}^{i} M_{+ye}^{i} + a_{3(6)}^{i} M_{-ze}^{i} \end{bmatrix};$$

$$N_{+e}, M_{+ye}, M_{+ze} \in \mathbf{s}_e^{\max};$$

$$N_{-e}, M_{-ye}, M_{-ze} \in \mathbf{s}_e^{\min}.$$

For the whole structure, Eq.(5.19) may be rewritten:

$$\begin{cases} \widetilde{\mathbf{N}}_{\mathrm{cm}}^{\mathrm{T}}\boldsymbol{\rho}_{\mathrm{m}} \le \mathbf{D}\mathbf{n}_{\mathrm{p}} - \widetilde{\mathbf{N}}_{\mathrm{cn}}^{\mathrm{T}} \bar{\mathbf{s}}_{\mathrm{n}} - \bar{\mathbf{s}}_{+\mathrm{em}} \\ -\widetilde{\mathbf{N}}_{\mathrm{cm}}^{\mathrm{T}}\boldsymbol{\rho}_{\mathrm{m}} \le \mathbf{D}\mathbf{n}_{\mathrm{p}} - \widetilde{\mathbf{N}}_{\mathrm{cn}}^{\mathrm{T}} \bar{\mathbf{s}}_{\mathrm{n}} - \bar{\mathbf{s}}_{-\mathrm{em}} \end{cases}, \tag{5.20}$$

where:

$\widetilde{\mathbf{N}}_{\mathrm{cm}}^{\mathrm{T}}$, $\widetilde{\mathbf{N}}_{\mathrm{cn}}^{\mathrm{T}}$, $\mathbf{D}$ have been defined above (see Section 5.2.2.1);

$$\bar{\mathbf{s}}_{\mathrm{n}}^{\mathrm{T}} = [\overline{N}^{1}, \overline{N}^{2}, ..., \overline{N}^{n_s}];$$

$$\bar{\mathbf{s}}_{+\mathrm{em}}^{\mathrm{T}} = [\bar{\mathbf{s}}_{+\mathrm{em}}^{1}, \bar{\mathbf{s}}_{+\mathrm{em}}^{2}, ..., \bar{\mathbf{s}}_{+\mathrm{em}}^{\mathrm{n_s}}];$$

$$\bar{\mathbf{s}}_{-\mathrm{em}}^{\mathrm{T}} = [\bar{\mathbf{s}}_{-\mathrm{em}}^{1}, \bar{\mathbf{s}}_{-\mathrm{em}}^{2}, ..., \bar{\mathbf{s}}_{-\mathrm{em}}^{\mathrm{n_s}}].$$

5.3.2.2. Standard-transformation technique

The following change of variables is adopted:

$$\boldsymbol{\rho}_{\mathrm{m}}^{*} = \widetilde{\mathbf{N}}_{\mathrm{cm}}^{\mathrm{T}}\boldsymbol{\rho}_{\mathrm{m}} + \mathbf{D}\mathbf{n}_{\mathrm{p}} - \widetilde{\mathbf{N}}_{\mathrm{cn}}^{\mathrm{T}}\bar{\mathbf{s}}_{\mathrm{n}} - \bar{\mathbf{s}}_{-\mathrm{em}}.$$

The system of Eq.(5.19) becomes then:

$$\begin{cases} \boldsymbol{\rho}_{\mathrm{m}}^{*} \le 2\mathbf{D}\mathbf{n}_{\mathrm{p}} - 2\widetilde{\mathbf{N}}_{\mathrm{cn}}^{\mathrm{T}}\bar{\mathbf{s}}_{\mathrm{n}} - \bar{\mathbf{s}}_{+\mathrm{em}} - \bar{\mathbf{s}}_{-\mathrm{em}} \\ \boldsymbol{\rho}_{\mathrm{m}}^{*} \ge 0 \end{cases}.$$

With new mentioned variables, the self-equilibrium equation of Eq.(5.17) may be written:

$$\mathbf{B}_{\mathrm{m}}^{\mathrm{T}}\widetilde{\mathbf{N}}_{\mathrm{cm}}^{-\mathrm{T}}\boldsymbol{\rho}_{\mathrm{m}}^{*} - \mathbf{B}_{\mathrm{m}}^{\mathrm{T}}\widetilde{\mathbf{N}}_{\mathrm{cm}}^{-\mathrm{T}}\mathbf{D}\mathbf{n}_{\mathrm{p}} = -\mathbf{B}_{\mathrm{n}}^{\mathrm{T}}\boldsymbol{\rho}_{\mathrm{n}}' - \mathbf{B}_{\mathrm{m}}^{\mathrm{T}}\widetilde{\mathbf{N}}_{\mathrm{cm}}^{-\mathrm{T}}\widetilde{\mathbf{N}}_{\mathrm{cn}}^{\mathrm{T}}\bar{\mathbf{s}}_{\mathrm{n}} - \mathbf{B}_{\mathrm{m}}^{\mathrm{T}}\widetilde{\mathbf{N}}_{\mathrm{cm}}^{-\mathrm{T}}\bar{\mathbf{s}}_{\text{-em}}.$$

5.3.2.3. Reduced formulas

The formulation applied to the simplex algorithm of the shakedown design is similar to the Eq.(5.15) in limit design, with the following vectors and matrices:

$$\mathbf{x}^{\mathrm{T}} = [\boldsymbol{\rho}_{\mathrm{m}}^{*} \quad \bar{\mathbf{n}}_{\mathrm{p}} \quad \mathbf{P}^{\mathrm{T}} \quad \mathbf{R}^{\mathrm{T}} \quad \mathbf{Q}^{\mathrm{T}}];$$

$$\mathbf{c}^{\mathrm{T}} = [\mathbf{0}^{\mathrm{T}} \quad \bar{\mathbf{l}}^{\mathrm{T}} \quad \mathbf{0}^{\mathrm{T}} \quad \mathbf{0}^{\mathrm{T}} \quad \mathbf{0}^{\mathrm{T}}];$$

$$\mathbf{b} = \begin{bmatrix} 2\widetilde{\mathbf{N}}_{\mathrm{cn}}^{\mathrm{T}}\bar{N} + \bar{\mathbf{s}}_{+\mathrm{em}} + \bar{\mathbf{s}}_{\text{-em}} \\ -\mathbf{B}_{\mathrm{n}}^{\mathrm{T}}\boldsymbol{\rho}_{\mathrm{n}} - \mathbf{B}_{\mathrm{m}}^{\mathrm{T}}\widetilde{\mathbf{N}}_{\mathrm{cm}}^{-\mathrm{T}}\widetilde{\mathbf{N}}_{\mathrm{cn}}^{\mathrm{T}}\bar{\mathbf{s}}_{\mathrm{n}} - \mathbf{B}_{\mathrm{m}}^{\mathrm{T}}\widetilde{\mathbf{N}}_{\mathrm{cm}}^{-\mathrm{T}}\bar{\mathbf{s}}_{\text{-em}} \end{bmatrix};$$

$$\mathbf{W} = \begin{bmatrix} -\mathbf{E}_1 & \mathbf{2DL} & -\mathbf{E}_1 & \mathbf{E}_1 & \mathbf{0} \\ \mathbf{B}_{\mathrm{m}}^{\mathrm{T}}\widetilde{\mathbf{N}}_{\mathrm{cm}}^{-\mathrm{T}} & -\mathbf{B}_{\mathrm{m}}^{\mathrm{T}}\widetilde{\mathbf{N}}_{\mathrm{cm}}^{-\mathrm{T}}\mathbf{DL} & \mathbf{0} & \mathbf{0} & \mathbf{E}_2 \\ 2n_s & n_g & 2n_s & 2n_s & \bar{n}_m \end{bmatrix} \begin{matrix} 2n_s \\ \bar{n}_m \end{matrix};$$

$$\mathbf{X}_0 = \begin{bmatrix} \mathbf{E}_1 & \\ & \mathbf{E}_2 \end{bmatrix}.$$

We observe that the matrix of constraints, **W**, is identified with the case of limit design, it is an advantage to implement in the computer program.

Consequently, similar to the case of limit design (Fig.5.4), the semi-direct algorithm for shakedown design problem is easy to be outlined. It does not need to be presented herein.

5.4. Advantage of semi-direct algorithm

Let us recall that both limit and shakedown analysis of 3-D steel frame by linear programming technique contains ($3n_s$+1) constraints, it indicates the licit mechanism (see Eq.(4.5) or (4.17)). Then, instead of a problem with ($n_m + 16n_s$) constraints (step 1 on Fig.5.1), one solve respectively an analysis problem of ($3n_s$ +1) constraints (step 1a on Fig.5.4) and a design problem with ($\bar{n}_m + 2n_s$) constraints (step 1b on Fig.5.4). That leads to a considerable reduction of the memory and the computational time. Indeed, to solve a rigid-plastic problem by linear programming technique, the following phases are needed:

- *Phase 1*: Building the necessary matrix for the simplex technique: the vector of second member (**b**); the matrix of constraint (**W**); basic matrix ($\mathbf{X}_0$).

- *Phase 2*: Realizing the simplex process;

- *Phase 3*: Calculating the necessary quantity (load factor, internal force, etc.) from the output in the convergence of the simplex algorithm.

On the point of view of quantity, almost mathematical operation belong Phase 2, because it is an iterative procedure. Whereas the number of the constraints (number of row of the matrix

of constraints) is the dimension of the basic matrix that strongly influences the memory and the computational time in the simplex method. Therefore, in some measure, the reduction of the basic matrix size of simplex technique may represent the reduction of the whole algorithms for rigid-plastic problem by linear programming. With the *semi-direct* technique, the reduction of the basic matrix size is:

$$r = \frac{(n_m + 16n_s)^2}{(3n_s + 1)^2 + (\overline{n}_m + 2n_s)^2} \quad . \tag{5.21}$$

The value r depends on each structure, but one may observe that it is signification. That will be affirmed in the numerical examples.

5.5. Numerical examples and discussions

The examples in this section aim to point out two messages: (1) the reduction of the computational time in the plastic design problem allowing the large-scale 3-D frames may be carried out; (2) although the stiffness and stability constraint are not yet considered but the member configurations given in the output may be the interesting references for engineers.

Two 3-D frames that have been considered in Chapter 4 are examined in this section:

Example 5.1 – Limit minimum weight: A twenty-story space frame of which the dimensions and the design variables are shown in Fig.5.5. The yield strength of all members is 344.8 MPa and Young'modulus is 200 GPa. Uniform floor pressure of 4.8μ kN/m2; wind loads =0.96μ kN/m2, acting in the Y direction. The uniformly distributed loads are lumped at the joints of frames.

Example 5.2 – Shakedown minimum weight: Fig.5.6 shows the dimension and the member size group of six-story space frame. The yield strength of all members is 250 MPa and Young'modulus is 206 GPa. Uniform floor pressure of $4.8\mu_1$ kN/m2; wind loads are simulated by point loads of $26.7\mu_2$ kN in the Y-direction at every beam-column joint. With $0 \le \mu_1 \le 1$ and $-1 \le \mu_2 \le 1$, that define the loading domain.

The initial configurations of frames in the design process (Tables. 5.1 and 5.2) were considered in Chapter 4 and in various references [28, 35, 71, 81, 88, 89]. The results of both limit and shakedown analysis of initial frames given by CEPAO were presented on Table 4.1. Some values that concern the rigid-plastic design are quoted herein: Load factor of limit analysis of example 5.1 equal 1.698; whereas shakedown analysis gives the load factor 1.670 for example 5.2. For the sake of comparison the initial configuration with the optimal configuration, the mentioned number (μ=1.698 and 1.670) are considered as the safely factor in the corresponding design problems (see Tables 5.1 and 5.2).

The mentioned choices of initial configuration and safely factors aim to make the relation with the results available from the literature. In principle, any initial member size and any safely factor may be used.

The results of the optimal problem are shown on Tables 5.1 and 5.2. Some discussions are pointed out:

- The optimal solution is obtained after a few iterations.

- The mathematical operations are powerfully reduced against the initial formulation, about 15 times (Table 5.3).

- After each optimal process (step 1b on Fig.5.4, i^{th} iteration) the total weight is considerable reduced while the safe factor given by the next analysis process (step 1a on Fig.5.4, $i+1^{th}$ iteration) is not always violated (Tables 5.1 and 5.2). Finally, the convergence is reached.

So, semi-direct algorithm not only reduces the cost of computation but also makes an auto-controlled procedure.

- In principle, the optimal configurations given in the output cannot use in practice without the verification by the effective standards, specially, the *stiffness* and *stability* requirements. The latter are a subject of the next works. However, for instance, the results given by proposed technique may be interesting references for engineers working on design of steel frame. The engineers have an extra selection among their solutions. For example, on the point of view of global behaviour, the optimal configuration of six-story frame (Table 5.2) is a rational frame. Both initial and optimal configuration of six-story frame are analyzed by CEPAO with various models, the results are shown on Table 5.4, Figs. 5.7 and 5.8. With the optimal configuration, although the load factor and the ductile degree are little less than which of the initial member size but the weigh is considerably reduced. Based on this optimal member size, with some modifies if necessary, one may obtain the economized frames that responds the safe requirements. The elastic-plastic analysis (see Table 5.4, Figs. 5.7 and 5.8) will be presented in Chapter 6.

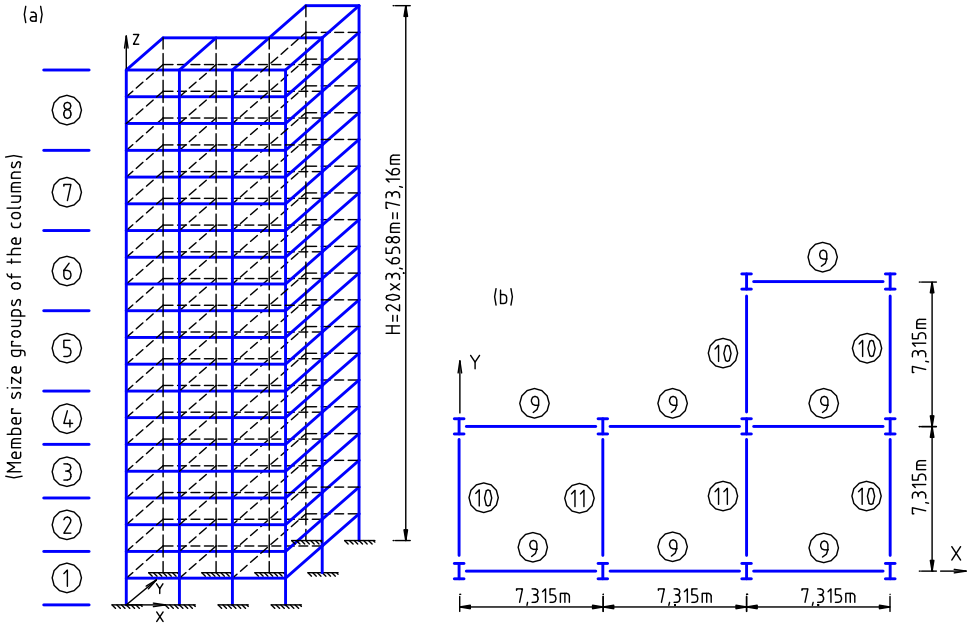

Fig.5.5. Example 5.1- Twenty story space frame (a- perspective view; b- plan view)

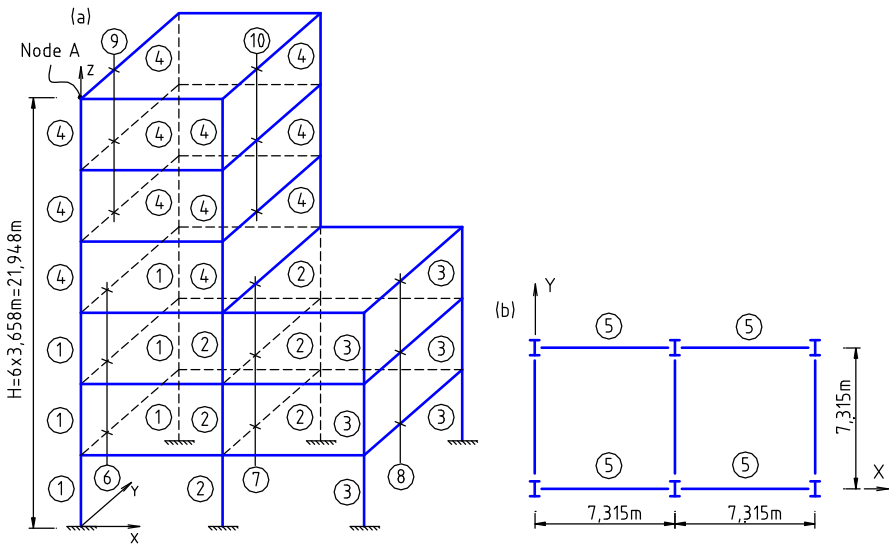

Fig.5.6. Example 5.2- Six-story space frame (a – perspective view, b- plan view)

Table 5.1: Member sizes, total weight and safely factor of twenty-story space frame

Design variable	Initial	First iteration	Second iteration (optimal)
1	W14x176	W40x215	W40x183
2	W14x159	W33x152	W40x149
3	W14x145	W36x135	W33x130
4	W14x132	W30x116	W30x99
5	W12x106	W12x106	W12x96
6	W12x87	W12x79	W18x71
7	W10x60	W12x53	W16x45
8	W8x31	W16x31	W12x26
9	W12x26	W12x21	W10x12
10	W16x36	W16x36	W16x31
11	W21x57	W24x55	W24x55
Weight (kN)	2089.3	1984.5	1695.6
Safely factor	1.698	1.868	1.699

Table 5.2: Member sizes, total weight and safely factor of six-story space frame

Design variable	Iteration					
	0 (initial)	1	2	3	4	5 (optimal)
1	W12X87	W16X89	W16X67	W16X67	W18X65	W21X62
2	W12X120	W21X101	W24X76	W24X76	W24X76	W24X76
3	W12X87	W24X55	W18X55	W21X44	W21X44	W21X44
4	W10X60	W18X60	W18X40	W16X40	W16X40	W16X40
5	W12X26	W12X21	W12X14	W12X14	W12X14	W12X14
6	W12X53	W18X60	W18X50	W18X50	W18X50	W18X50
7	W12X87	W14X61	W18X46	W21X44	W18X50	W18X50
8	W12X53	W14X48	W12X21	W12X19	W12X19	W12X19
9	W12X53	W14X43	W14X30	W16X26	W16X26	W16X26
10	W12X87	W18X45	W18X35	W16X31	W16X26	W16X26
Weight (kN)	295.2	244.1	178.0	170.8	170.4	169.4
Safely factor	1.670	2.283	1.785	1.784	1.767	1.754

Table 5.3: Comparison of basic matrix size in the simplex method

	Proposed technique (analysis + design)	Initial formulation	Reduced mathematical operation (Eq.(5.21))
twenty-story frame	(2761 x 2761) + (3040 x 3040)	(16380 x 16380)	15.9 times
six-story frame	(379 x 379) + (432 x 432)	(2259 x 2259)	15.5 times

Table 5.4: Load factors given by CEPAO for initial and optimal configuration of six-story frame

Model	Initial member size (Table 2) (weight = 295.2 kN)	Optimal member size (Table 2) (weight = 169.4 kN)
Elastic-plastic first order	2.489	2.253
Elastic-plastic second order	2.033	2.022
Limit analysis	2.412	2.215
Shakedown analysis	1.670	1.754

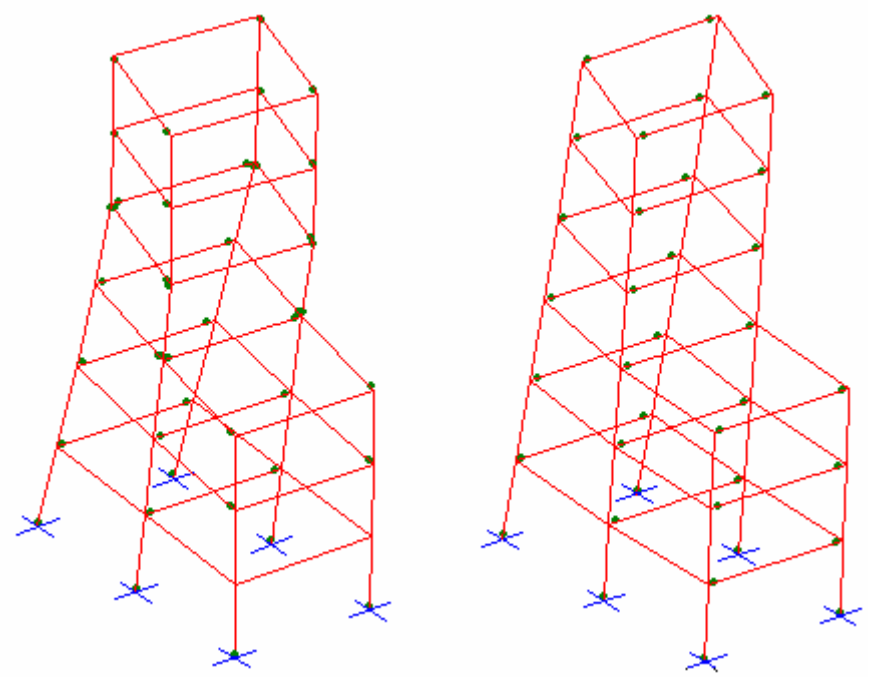

Initial member size Optimal member size

a) Elastic-plastic analysis, first-order analysis

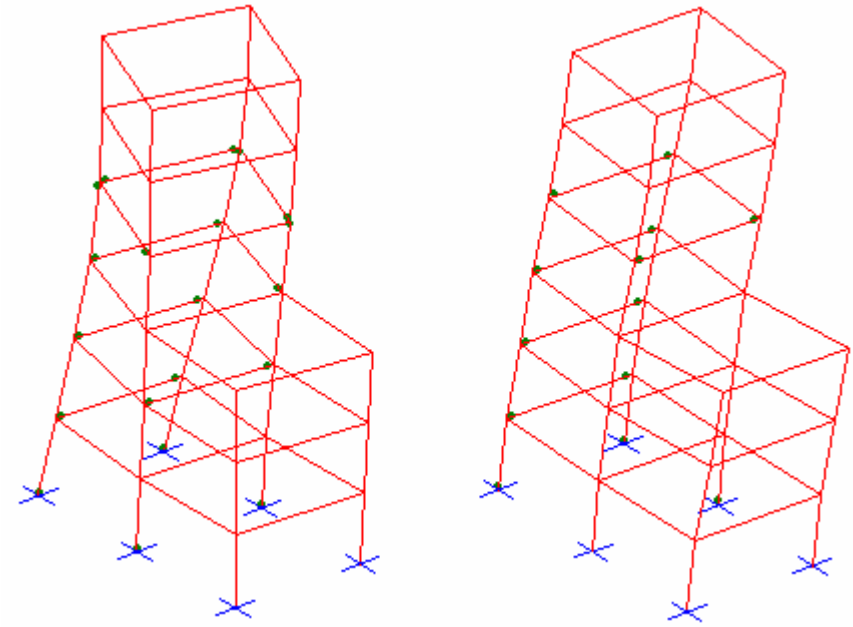

Initial member size Optimal member size

b) Elastic-plastic analysis, second-order analysis

Fig.5.7. Deformation at limit state of six-story frame

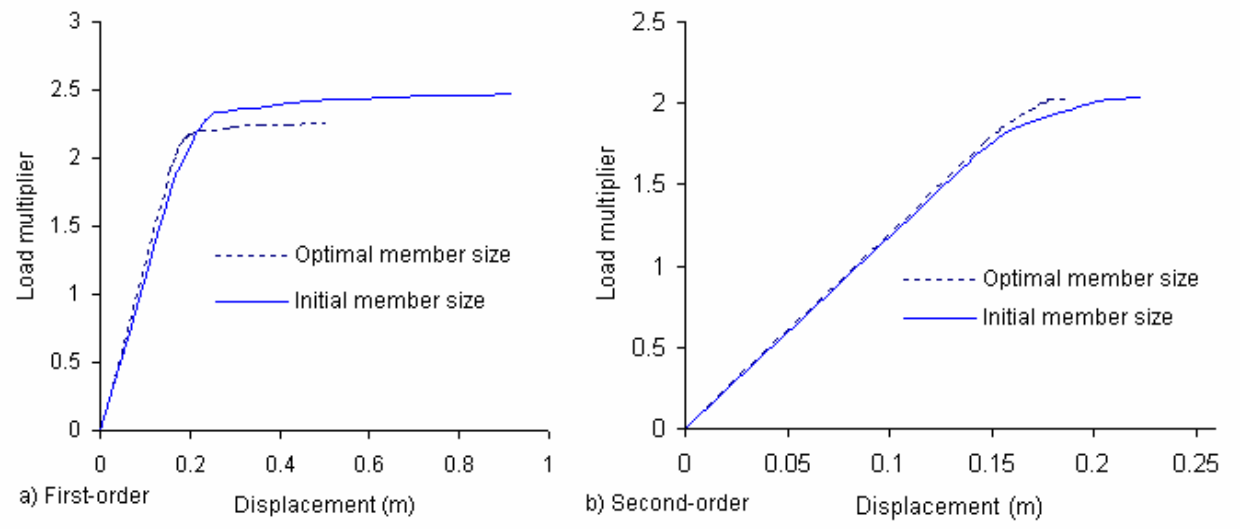

Fig.5.8. Load-deflection in Y direction results at point A of six-story frame (Fig.5.6)

5.6. Conclusions

It appears that in the proposed algorithm – the so-called *semi-direct* algorithm, the dimension of basic matrix in the simplex method is considerably reduced, about 15 times. This feature is due to the following techniques: *fixed- push* and *standard-transformation*. The first technique makes the best of the *primal-dual* technique in rigid-plastic analysis problem (Chapter 4), while the second technique makes the best of a permanent requirement of the simplex method (all variables must be non-negative). By semi-direct algorithm, the linear programming technique may now apply in the limit and shakedown design of the large-scale 3-D steel frames. How to take into account the stiffness and stability constraints is the objective of the next works. On the practical aspect, with any initial member size, under limit or shakedown constraints the proposed algorithm gives an optimal configuration that may be interesting references for engineers working on design of steel frames.

Chapter **6**

Second-order plastic-hinge analysis of 3-D steel frames including strain hardening effects

The geometric nonlinearity is taken into account when the equilibrium and kinematic relationships are written with respect to the deformed configuration of structures. The conventional second-order approach is a simple case of the geometric nonlinearity analysis. It is widely adopted for building frames. The conventional second-order analysis takes into account the secondary bending moment which arise as the result of the axial force applying on the lateral displacement of the member. The lateral displacement of the member may be divided into two parts: relative displacement to its chord (Fig.6.0a) and relative displacement of two ends (Fig.6.0b). In short, conventional second-order/P-delta approach is the geometric linearity adding the P-δ and P- Δ effects.

During the last 10 years, many researchers focus on the second-order plastic-hinge analysis of 3-D steel frames under the subject of "the nonlinear advanced analysis of steel frames", e.g. Liew (2000, 2001)[88, 89], Kim (2001, 2002, 2003, 2006)[81, 79, 80, 78], Choi (2002)[27], Landesmann (2005)[85], Cuong (2006)[35], among many others. These researches aim to model one physical member by one element while the complex behaviours may be taken into account (e.g. distributed plasticity, initial imperfections). However, the strain hardening is not adequately highlighted in this direction.

For a long time ago, the general physical relation for plastic hinges taking into account strain hardening were discussed, e.g. in Maier (1973, 1976)[98, 100]. However, they are the general formulation; to apply for the practical engineering, the more detail researches are needed.

In the recent years, the practical models that consider the strain hardening behaviour of steel fames have been developed by Davies (2002, 2006)[36, 37] and Byfiled (2005)[10]. However, it is only applicable for the case of 2-D bending steel frames.

This chapter propose a new algorithm for the second-order plastic-hinge analysis of 3-D steel frames accounting strain hardening behaviour.

Keywords: *Strain hardening*; *Plastic-hinge*; *Second-order; Steel frames.*

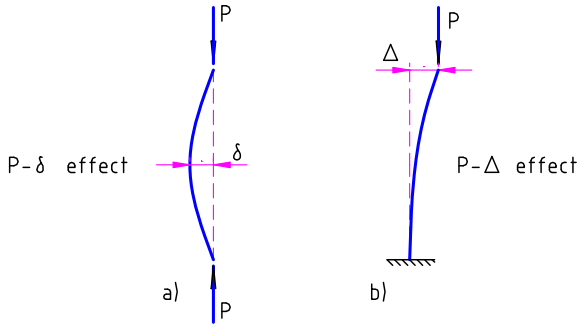

Fig.6.0. P-delta effect

6.1. Modelling of plastic-hinge accounting strain hardening

Section 3.1 of Chapter 3 presents the constitutive law at 3-D plastic-hinges with the elastic-perfectly plastic material hypothesis. This section enlarges this relation to consider strain hardening effects.

6.1.1. Strain hardening rule

When the strain hardening is taken into account in elastic-plastic analysis, the diagram $\sigma - \varepsilon$ shown on Fig.6.1a is generally adopted. In principle, from this diagram, one may deduce a yield surface that is written in the space of internal forces (axial force and bending moments). However, the obtained yield surface may be too complicated and not suitable for global plastic-hinge analysis. For the practical purpose, an isotropic strain hardening rule is proposed as below:

$$\Phi = \phi - H\bar{\varepsilon}^p \le 0 \text{ if } \bar{\varepsilon}^p = 0; \tag{6.1a}$$

$$\Phi = \phi - H\bar{\varepsilon}^p = 0 \text{ if } 0 < \bar{\varepsilon}^p \le \bar{\varepsilon}_l^p; \tag{6.1b}$$

$$\Phi = \phi - H\bar{\varepsilon}_l^p = 0 \text{ if } \bar{\varepsilon}^p > \bar{\varepsilon}_l^p; \tag{6.1c}$$

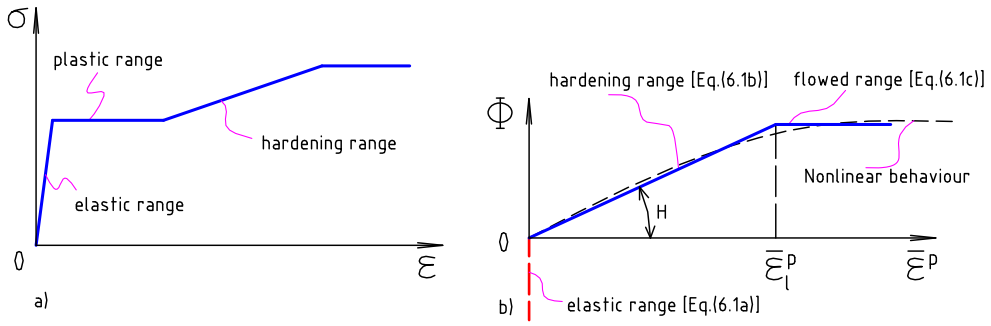

Fig.6.1. Hardening rule

In Eqs.(6.1), ϕ is the Orbison's yield surface [see Eq.(3.1)]. H is called the strain hardening modulus (or plastic modulus), it is considered as a constant (linear hardening low); $\bar{\varepsilon}^p$ is the effective strain that is defined below; $\bar{\varepsilon}_l^p$ is the limit effective strain.

Eqs.(6.1) describe, respectively, the elastic range, the hardening range, and the flowed range (Fig.6.1b). It shows that a nonlinear hardening rule is approximated by bi-linear procedures [Eqs.(6.1b) and (6.1c)]. In the space of internal forces, Φ and ϕ have the same shape, i.e. Φ is an expansion of ϕ.

With a 3-D plastic-hinge, the plastic deformations are described by three components: Δ^p, θ_y^p, θ_z^p; they are plastic axial displacement and two net plastic rotations with respect to y and z axes. The effective strain may be intuitively defined as follows:

$$\bar{\varepsilon}^p = \frac{\left|\Delta^p\right|}{l} + \frac{\left|\theta_y^p\right| h}{2l} + \frac{\left|\theta_z^p\right| b}{2l}, \tag{6.2}$$

in which: h and b are, respectively, the depth and the wide of the section; l is the length of the element.

How to determine the limit effective strain ($\bar{\varepsilon}_l^p$) and the strain hardening modulus (H) is described in Section 6.3.

6.1.2. Incremental deformation-force relation

With the yield surface given by Eq.(6.1), Eq.(3.8) is rewritten as:

$$d\Phi = \frac{\partial \Phi}{\partial N} dN + \frac{\partial \Phi}{\partial M_y} dM_y + \frac{\partial \Phi}{\partial M_z} dM_z - H d\bar{\varepsilon}^p = 0 . \tag{6.3}$$

From Eqs.(3.5) and (6.2), one has:

$$d\bar{\varepsilon}^p = \frac{1}{l}[1 \quad h/2 \quad b/2] \begin{Bmatrix} \left|\partial \Phi / \partial N\right| \\ \left|\partial \Phi / \partial M_y\right| \\ \left|\partial \Phi / \partial M_z\right| \end{Bmatrix} d\lambda . \tag{6.4}$$

Substituting Eq.(6.4) in Eq.(6.3), one obtains the incremental deformation–force relation:

$$[dN \; dM_y \; dM_z] \begin{Bmatrix} \partial \Phi / \partial N \\ \partial \Phi / \partial M_y \\ \partial \Phi / \partial M_z \end{Bmatrix} - H \frac{1}{l} [1 \quad h/2 \quad b/2] \begin{Bmatrix} \left|\partial \Phi / \partial N\right| \\ \left|\partial \Phi / \partial M_y\right| \\ \left|\partial \Phi / \partial M_z\right| \end{Bmatrix} d\lambda = 0 . \tag{6.5}$$

Eq.(6.5) is suitable to build-up the elastic-plastic constitutive relation for whole structure that is mentioned below (Section 6.2).

6.2. Global plastic-hinge analysis formulation

In comparison with linear elastic analysis, the second-order plastic-hinge analysis must be modified to treat the present of plastic-hinges and of P-delta effect. In the following, an algorithm for global plastic-hinge analysis is presented.

6.2.1. Elastic-plastic constitutive equation

Let $\Delta \mathbf{e}_C$ and $\Delta \mathbf{e}_R$ be the vectors of increment of net displacement at the yielded sections (plastic hinges), and at the elastic sections, respectively. Elastic constitutive equation [the Hooke's law – Eq.(3.23)] for the structure may be written as:

$$\begin{bmatrix} \Delta \mathbf{s}_R \\ \Delta \mathbf{s}_C \end{bmatrix} = \begin{bmatrix} \mathbf{D}_{RR} & \mathbf{D}_{RC} \\ \mathbf{D}_{RC}^T & \mathbf{D}_{CC} \end{bmatrix} \begin{bmatrix} \Delta \mathbf{e}_R - \mathbf{0} \\ \Delta \mathbf{e}_C - \Delta \mathbf{e}_C^p \end{bmatrix}, \tag{6.6}$$

in which, $\Delta \mathbf{e}_C^p$ are the plastic parts of the incremental net displacement at plastic hinges; $\Delta \mathbf{s}_R$ and $\Delta \mathbf{s}_C$ are, respectively, the vectors of incremental internal forces at elastic sections and plastic-hinges. $\mathbf{D}$ is the elastic stiffness matrix of the frame given by Eq.(3.24) but the $\mathbf{D}_k$ is modified to include the $P-\delta$ effect:

$$\mathbf{D}_k = \frac{1}{l}\begin{bmatrix} 2EA & 0 & 0 & 0 & 0 & 0 \\ 0 & S_1 EI_y & 0 & 0 & -S_2 EI_y & 0 \\ 0 & 0 & S_3 EI_z & 0 & 0 & -S_4 EI_z \\ 0 & 0 & 0 & 2EA & 0 & 0 \\ 0 & -S_2 EI_y & 0 & 0 & S_1 EI_y & 0 \\ 0 & 0 & -S_4 EI_z & 0 & 0 & S_3 EI_z \end{bmatrix}$$

where E is the Young'modulus; A, I_y, I_z are, respectively, the area, the moment of inertias of the cross-section with respect to y and z axes respectively; l is the length of the considered element; S_1, S_2, S_3, S_4 are the stability functions with respect to y and z axes. The formulas of these functions may be found in various texts among references (e.g. Chen (1996)[19]):

$$S_{1(3)} = \begin{cases} \dfrac{\rho_{y(z)} l \sin(\rho_{y(z)} l\ ) - (\rho_{y(z)} l)^2 \cos(\rho_{y(z)} l)}{2 - 2\cos(\rho_{y(z)} l) - \rho_{y(z)} l \sin(\rho_{y(z)} l)} & \text{for} \quad N \le 0 \\ \dfrac{(\rho_{y(z)} l)^2 \cosh(\rho_{y(z)} l) - \rho_{y(z)} l \sinh(\rho_{y(z)} l)}{2 - 2\cosh(\rho_{y(z)} l) + \rho_{y(z)} l \sinh(\rho_{y(z)} l)} & \text{for} \quad N > 0 \end{cases}; \tag{6.7a}$$

$$S_{2(4)} = \begin{cases} \dfrac{(\rho_{y(z)} l)^2 - \rho_{y(z)} l \sin(\rho_{y(z)} l)}{2 - 2\cos(\rho_{y(z)} l) - \rho_{y(z)} l \sin(\rho_{y(z)} l)} & \text{for} \quad N \le 0 \\ \dfrac{\rho_{y(z)} l \sinh(\rho_{y(z)} l) - (\rho_{y(z)} l)^2}{2 - 2\cosh(\rho_{y(z)} l) + \rho_{y(z)} l \sinh(\rho_{y(z)} l)} & \text{for} \quad N > 0 \end{cases}; \tag{6.7b}$$

where $\rho_{y(z)} = \sqrt{N / EI_{y(z)}}$, N is the axial force, taken as positive in tension.

In fact, Eqs. (6.7a) and (6.7b) are indeterminate when the axial force is zero. To circumvent this problem, in the case of $-1.0 \le \xi \le 1.0$, the following approximation of the stability functions are used (see Chen (1996)[19]):

$$S_{1(3)} = 4 + \frac{2\pi^2 \xi_{y(z)}}{15} - \frac{(0.01\xi_{y(z)} + 0.543)\xi_{y(z)}^2}{4 + \xi_{y(z)}} - \frac{(0.004\xi_{y(z)} + 0.285)\xi_{y(z)}^2}{8.183 + \xi_{y(z)}};$$

$$S_{2(4)} = 2 - \frac{\pi^2 \xi_{y(z)}}{30} + \frac{(0.01\xi_{y(z)} + 0.543)\xi_{y(z)}^2}{4 + \xi_{y(z)}} - \frac{(0.004\xi_{y(z)} + 0.285)\xi_{y(z)}^2}{8.183 + \xi_{y(z)}}.$$

where $\xi_{y(z)} = N / (\pi^2 EI_{y(z)} l^2)$. In some research (e.g. Kim (2002)[79]), the above approximations are used in the case of $-2.0 \le \xi \le 2.0$.

Clearly, in the first order analysis, $S_1 = S_3 = 4; S_2 = S_4 = 2$.

Return now the physical relation at plastic hinges, under form of matrix, Eqs.(3.6) and (6.5) may be written, respectively:

$$\Delta \mathbf{e}_C^p = \mathbf{N}_C \Delta\boldsymbol{\lambda}, \tag{6.8}$$

$$\mathbf{N}_C^T \Delta \mathbf{s}_C - H\mathbf{F}\mathbf{N}'_C \Delta\lambda = 0. \tag{6.9}$$

In Eqs.(6.8) and (6.9), $\mathbf{N}_C$ is a gradient matrix of the yield surface Φ; $\mathbf{N}'_C$ contains the absolute value of gradient of the yield surface [see Eq.(6.5)]. And

$$\mathbf{F} = \sum_i \mathbf{F}_i,$$

with

$$\mathbf{F}_i = \frac{1}{l_i}[1 \quad h_i/2 \quad b_i/2].$$

Using (6.7), (6.8) and (6.9), the plastic deformation magnitude may be deduced:

$$\begin{bmatrix} \mathbf{0} \\ \Delta\boldsymbol{\lambda} \end{bmatrix} = \begin{bmatrix} \mathbf{0} & \mathbf{0} \\ \mathbf{R}_1 & \mathbf{R}_2 \end{bmatrix} \begin{bmatrix} \Delta\mathbf{e}_R \\ \Delta\mathbf{e}_C \end{bmatrix}. \tag{6.10}$$

with

$$\mathbf{R}_1 = (\mathbf{N}_C^T \mathbf{D}_{CC} \mathbf{N}_C + H\mathbf{F}\mathbf{N}_C')^{-1} \mathbf{N}_C^T \mathbf{D}_{RC}^T ,$$

$$\mathbf{R}_2 = (\mathbf{N}_C^T \mathbf{D}_{CC} \mathbf{N}_C + H\mathbf{F}\mathbf{N}_C')^{-1} \mathbf{N}_C^T \mathbf{D}_{CC} .$$

Eq. (6.8) may be rewritten in the following form:

$$\begin{bmatrix} \mathbf{0} \\ \Delta\mathbf{e}_C^p \end{bmatrix} = \begin{bmatrix} \mathbf{0} & \mathbf{0} \\ \mathbf{0} & \mathbf{N}_C \end{bmatrix} \begin{bmatrix} \mathbf{0} \\ \Delta\boldsymbol{\lambda} \end{bmatrix}. \tag{6.11}$$

Substituting (6.10) in (6.11), one obtains:

$$\begin{bmatrix} 0 \\ \Delta\mathbf{e}_C^p \end{bmatrix} = \begin{bmatrix} \mathbf{0} & \mathbf{0} \\ \mathbf{N}_C\mathbf{R}_1 & \mathbf{N}_C\mathbf{R}_2 \end{bmatrix} \begin{bmatrix} \Delta\mathbf{e}_R \\ \Delta\mathbf{e}_C \end{bmatrix}. \tag{6.12}$$

From (6.7) and (6.12), one finally obtains the *elastic-plastic constitutive relation*:

$$\begin{bmatrix} \Delta\mathbf{s}_R \\ \Delta\mathbf{s}_C \end{bmatrix} = \begin{bmatrix} \mathbf{D}_{RR} - \mathbf{D}_{RC}\mathbf{N}_C\mathbf{R}_1 & \mathbf{D}_{RC} - \mathbf{D}_{RC}\mathbf{N}_C\mathbf{R}_2 \\ \mathbf{D}_{RC}^T - \mathbf{D}_{CC}\mathbf{N}_C\mathbf{R}_1 & \mathbf{D}_{CC} - \mathbf{D}_{CC}\mathbf{N}_C\mathbf{R}_2 \end{bmatrix} \begin{bmatrix} \Delta\mathbf{e}_R \\ \Delta\mathbf{e}_C \end{bmatrix}. \tag{6.13}$$

6.2.2. Elastic-plastic stiffness matrix

Due to the decomposition (6.6), the compatibility relation (3.18) and equilibrium relation (3.20) (under form of increment) may be rearranged as:

$$\begin{bmatrix} \Delta\mathbf{e}_R \\ \Delta\mathbf{e}_C \end{bmatrix} = \begin{bmatrix} \mathbf{B}_R \\ \mathbf{B}_C \end{bmatrix} \Delta\mathbf{d} , \tag{6.14}$$

$$\Delta\mathbf{f} = [\mathbf{B}_R^T \quad \mathbf{B}_C^T] \begin{bmatrix} \Delta\mathbf{s}_R \\ \Delta\mathbf{s}_C \end{bmatrix}. \tag{6.15}$$

The Eqs.(6.13), (6.14) and (6.15) may be rewritten as:

$$\Delta\mathbf{s} = \overline{\mathbf{D}}\Delta\mathbf{e} ; \tag{6.16}$$

$$\Delta\mathbf{e} = \overline{\mathbf{B}}\Delta\mathbf{d} ; \tag{6.17}$$

$$\Delta\mathbf{f} = \overline{\mathbf{B}}^T\Delta\mathbf{s} . \tag{6.18}$$

From Eqs.(6.16), (6.17) and (6.18), one obtains:

$$\Delta\mathbf{d} = \mathbf{K}^{-1}\Delta\mathbf{f} , \tag{6.19}$$

where $\mathbf{K} = \overline{\mathbf{B}}^T\overline{\mathbf{D}}\overline{\mathbf{B}}$

is the elastic-plastic stiffness matrix of the frame.

6.2.3. Taking into account $P-\Delta$ effect

When the relative lateral displacement of the two ends of the member is considered, an additional axial force and shear force will be induced in the member ends (Fig.6.2). The relation between those additional forces with the vector of displacement of the frame may be written as:

$$\mathbf{s}^s = \mathbf{U}\mathbf{d} . \tag{6.20}$$

In Eq.(6.20),

$$\mathbf{s}^s = \sum_k \mathbf{s}_k^s \ ; \mathbf{U} = \sum_k \mathbf{H}_k\mathbf{T}_k ,$$

with $\mathbf{s}_k^s$ is secondary force (additional force) on k^{th} element:

$$\mathbf{s}_{\mathrm{k}}^{\mathrm{sT}} = [N_A^s \quad Q_{yA}^s \quad Q_{zA}^s \quad N_B^s \quad Q_{yB}^s \quad Q_{zB}^s] .$$

and

$$\mathbf{H}_{\mathrm{k}} = \begin{bmatrix} 0 & b & a & 0 & 0 & 0 & -b & -a & 0 & 0 & 0 \\ 0 & c & 0 & 0 & 0 & 0 & -c & 0 & 0 & 0 & 0 \\ 0 & 0 & c & 0 & 0 & 0 & 0 & -c & 0 & 0 & 0 \\ 0 & -b & -a & 0 & 0 & 0 & b & a & 0 & 0 & 0 \\ 0 & d & 0 & 0 & 0 & 0 & -d & 0 & 0 & 0 & 0 \\ 0 & 0 & d & 0 & 0 & 0 & 0 & -d & 0 & 0 & 0 \end{bmatrix},$$

where:

$$a = \frac{M_{yA} - M_{yB}}{l^2}; b = \frac{M_{zA} - M_{zB}}{l^2}; c = \frac{N_A}{l}; d = \frac{N_B}{l} .$$

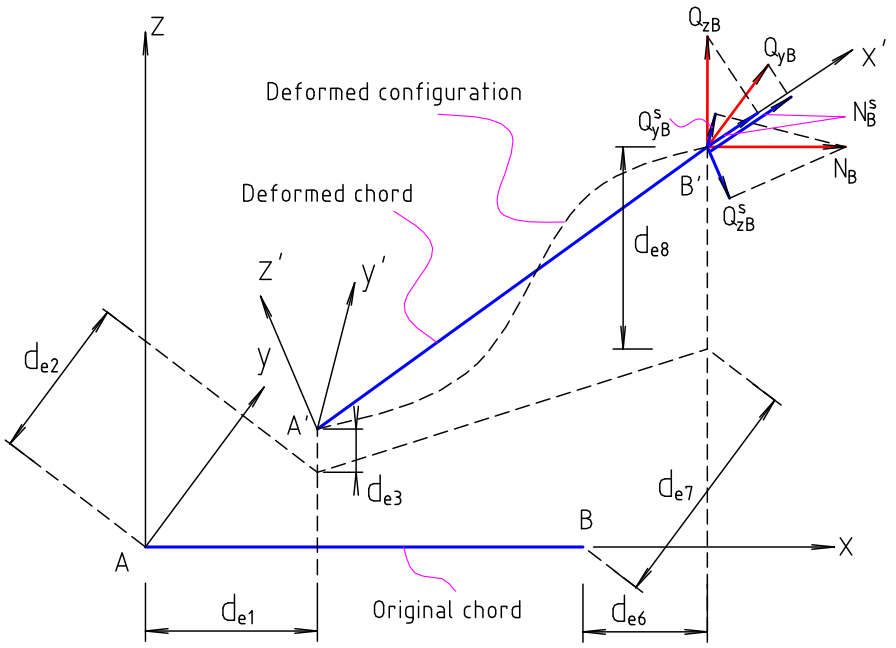

Fig.6.2. Additional forces at and B of considered element

From Eq.(6.20), one obtains the increment of secondary force as follows:

$$\Delta\mathbf{s}^{\mathrm{s}} = \Delta\mathbf{U}\mathbf{d} + \mathbf{U}\Delta\mathbf{d} + \Delta\mathbf{U}\Delta\mathbf{d} .$$

We can calculate the vector of increment of external force that is equilibrium with the additional forces:

$$\Delta\mathbf{f}^{\mathrm{s}} = \mathbf{B}^{\mathrm{sT}}\Delta\mathbf{s}^{\mathrm{s}} = \mathbf{B}^{\mathrm{sT}}\mathbf{U}\Delta\mathbf{d} + \mathbf{B}^{\mathrm{sT}}\Delta\mathbf{U}(\mathbf{d} + \Delta\mathbf{d}) , \tag{6.21}$$

where

$$\mathbf{B}^s = \sum_k \mathbf{T}_k .$$

Using Eqs.(6.19) and (6.21), the nonlinear relation between the increment of external forces and the increment of displacements is written as:

$$\Delta\mathbf{f} = (\overline{\mathbf{K}} + \mathbf{K}^s)\Delta\mathbf{d} + \mathbf{V} , \tag{6.22}$$

with

$$\mathbf{K}^{\mathrm{s}} = \mathbf{B}^{\mathrm{sT}}\mathbf{U} ,$$

and

$$\mathbf{V} = \mathbf{B}^{\mathrm{sT}}\Delta\mathbf{U}(\mathbf{d} + \Delta\mathbf{d}) .$$

6.2.4. Global solution procedure

Through the above formulation one observes that the material nonlinearity is completely taken into account by elastic-plastic constitutive matrix [see Eq.(6.13)]. Unless the elastic constitutive matrix is replaced by the elastic-plastic constitutive matrix, all procedures are identical to any global elastic analysis procedures. In present work, Eq.(6.22) is solved by Newton-Raphson method. The elastic-plastic constitutive matrix is updated once a plastic-hinge occurs. At plastic hinges, where the effective strain reached the limit value ($\bar{\varepsilon}_l^p$), the strain hardening modulus (H) needs to be vanished.

6.3. Limit effective strain and strain hardening modulus

6.3.1. Stress-hardened and limit effective strain

Some interesting results on the strain hardening behaviour for 2-D bending beams are presented in Byfileld (2005)[10]. In this reference, a simple beam under variable loading types has been examined, the required end-rotation to achieve the value $1.0M_p$, $1.10M_p$, $1.15M_p$ are evaluated, it is rewritten in the present work by Table 6.1. To exceed plastic moment (M_{py}) the normal stress on the section must surpass the yield strength (f_y). The augmentation of stress against yield strength is called stress-hardened. To extend to the 3-D plastic hinges, *the bending moment-hardened* and *the required rotation* notions are needed to be changed into *the stress-hardened* and *the required strain* notions. For this purpose, the stress-hardened at the limit state is assumed be linear distribution, as the show of Fig.6.3.

Table 6.1: Required rotation (mrad) to achieve $1.00\,M_p$, $1.10\,M_p$, $1.15\,M_p$ [10]

Grade		l/h =10			l/h =20			l/h =30			l/h =40			l/h =50			l/h =60		
		1PL	UDL	2PL	1PL	UDL	2PL	1PL	UDL	2PL	1PL	UDL	2PL	1PL	UDL	2PL	1PL	UDL	2PL(*)
S275	$1.00\,M_p$	9.6	18.8	28.3	19	37.5	56.5	28.6	56.5	84.6	32.8	75.4	112.9	47.8	94.1	141.2	57.4	113.1	169.5
S275	$1.10\,M_p$	21.6	58.3	82.9	43.3	116.6	165.5	65.1	175.1	248.7	86.7	233.4	331.4	108.4	291.6	414.5	130	349.9	497.2
S275	$1.15\,M_p$	30.9	81.3	108.4	61.8	162.5	216.6	92.7	243.8	325	123.7	325.2	433.4	154.5	406.3	541.6	185.5	487.6	650
S355	$1.00\,M_p$	11.3	23.6	44	22.9	47.1	88	34.2	70.7	131.8	45.7	94.4	175.8	57.1	118	219.7	68.6	141.5	263.7
S355	$1.10\,M_p$	27.4	74.7	106.6	54.8	149.4	213.3	82.2	224.1	319.9	109.8	298.8	426.6	137.2	373.3	533.2	164.6	448	639.8
S355	$1.15\,M_p$	39.4	104.4	139.5	78.7	208.7	278.9	118.2	313.1	418.5	157.6	417.5	558	196.9	521.9	697.4	236.3	626.2	836.9

(*): 1PL=Single point load case; UDL: Uniformly distributed load case; 2PL: Two point load case [10].

Considering the case of bending about y axes (major-axes), we examine separately three states of stress as shown in Fig.6.4. Plastic moment M_{py}, elastic moment M_{ey} and moment-hardened M_{hy} are respectively equilibrium with those states of stress. One has the following relations:

$$M_{py} = 1.15 M_{ey}, \tag{6.23}$$

$$M_{hy} = (\sigma_h / f_y) M_{ey}. \tag{6.24}$$

The value 1.15 in Eq.(6.23) is well agreed with I-shaped sections (see Massonnet (1976)[106]). From Eqs.(6.23) and (6.24), one obtains:

$$M_{py} + M_{hy} = [1 + 0.869(\sigma_h / f_y)] M_{py}.$$

In present work, the value $1.15M_{py}$ is considered as the limit state, one obtains:

$$1 + 0.869\sigma_h / f_y = 1.15,$$

or:

$$\sigma_h = 0.173 f_y . \tag{6.25}$$

It shows that instead of moment-hardened $0.15M_{py}$, one may use stress- hardened σ_h=$0.173f_y$.

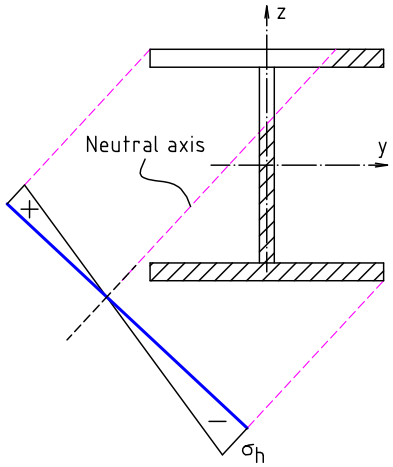

Fig.6.3. Assumption of stress-hardened distribution

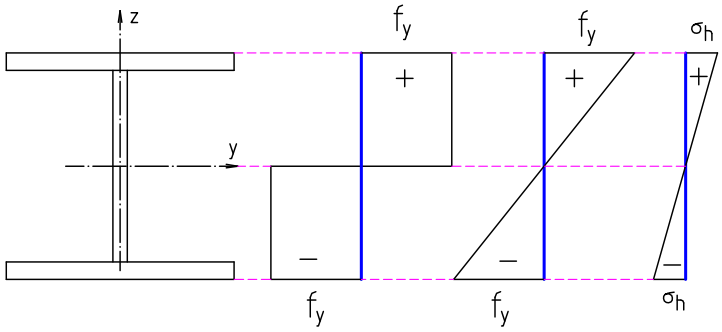

Fig.6.4. Stress distribution in the case of bending about y axes

We convert the required rotation into required effective strain. In the plastic-hinge analysis, the end-rotation to achieve $1.0M_p$ clearly is the limit of elastic end-rotation, $\bar{\varepsilon}_{y,e}^{end}$. Therefore, the required plastic rotation to achieve $1.15M_{py}$ is calculated by:

$$\theta_y^{p,end} = \theta_{y,1.15}^{end} - \theta_{y,e}^{end} .$$

Based on the geometric relations of the considered beams in Byfiled (2005)[10], one may take the plastic rotation at plastic hinges (in middle of beams) are twice as the plastic end-rotations:

$$\theta_y^p = 2\theta_y^{p,end} .$$

If the notion of the effective strain is adopted, the requirement of plastic rotation may be transferred to the requirement of the effective strain. In the case of 2-D bending, from Eq.(6.2), the required effective strain to reach $1.15M_p$ is:

$$\bar{\varepsilon}_{yl}^p = \frac{|\theta_y^p| h}{2l} . \tag{6.26}$$

This is the limit effective strain. We note from the data on Table 6.1 that the required end-rotation increases linearly with *l/h* ratio. In other words, the ratio $\theta_y^p h / l$ only depends on the

grade of steel and the type of load. Consequently, the limit effective strain ($\bar{\varepsilon}_{yl}^{p}$) may be shown on Table 6.2, independent with the depth-to-span ratio.

With a section under axial force and bi-bending moments (3-D plastic hinge), the state of stress is still uniaxial. One supposes that in both 2-D and 3-D plastic hinges, when the effective strain reached the values given on Table 6.2 the maximum stress-hardened achieves $0.173f_y$. They are the limit effective strain ($\bar{\varepsilon}_{l}^{p}$) and the limit stress-hardened (σ_h).

Table 6.2: Value $\bar{\varepsilon}_{yl}^{p}$ (x10^{-2})

Grade	Load (*)		
	1PL	UDL	2PL
S275	0.213	0.625	0.801
S355	0.281	0.808	0.955

(*): see Table 6.1.

6.3.2. Strain hardening modulus

At the limit state, with each location of the neutral axis, the distribution of stress over the section may be determined (Fig.6.5a). By consequence, one obtains the corresponding internal forces by equilibrium equations (Fig.6.5b). The internal forces are described by a point so-called limit point force as the show of Fig.6.5b. With variable location of neutral axis, one has the locus of the limit point forces that constitutes a bounding surface (Φ'). However, this bounding surface (Φ') is not the same shape with the yield surface ($\phi = 0$). It does not agree with the hardening rule given by Eq.(6.1) where the hardening is modelled by the *expansion* of the yield surface. Therefore, it needs to find a surface Φ (the same shape with ϕ) that approximates to Φ'. The following limit surface is proposed (Fig.6.5b):

$$\Phi = \phi - 0.3225 = 0\,. \tag{6.27}$$

This limit surface corresponds exactly to the case of bending about y axes, i.e.: $n = m_z = 0$, $m_y = 1.15$ (point A on Fig.6.5b). Furthermore, it may be verified that almost limit point forces locates the outside of the limit surface. For example, one verifies two particular cases:

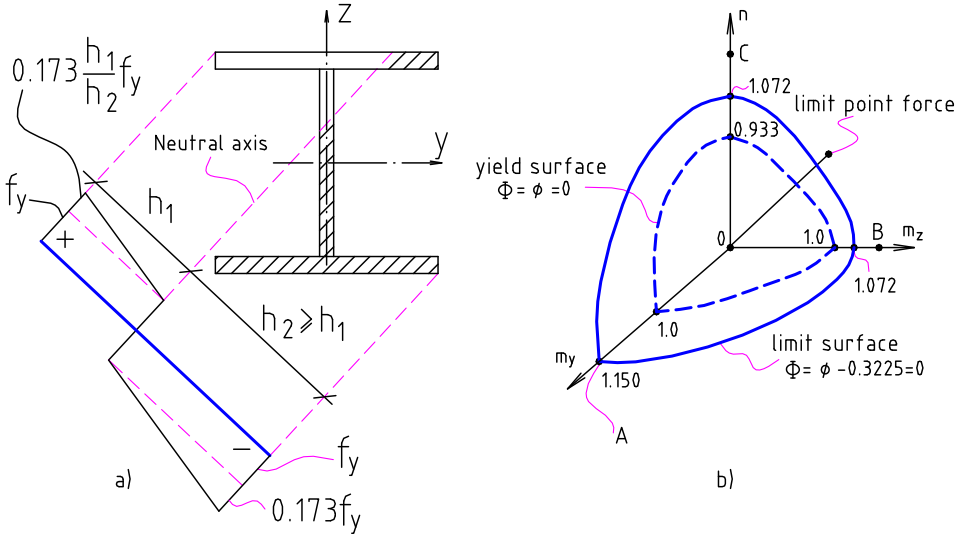

Fig.6.5. a) Limit state of tress; b) Limit point force, yield surface and limit surface

-Bending about z axes: Under bending about z axes the I-shaped sections may be considered as the rectangular sections (Fig.6.6). Similar to the case of bending about y axes, we have the following relations:

$$M_{pz} = 1.50 M_{ez}\,, \tag{6.28}$$

$$M_{hz} = (\sigma_h / f_y) M_{ez}\,. \tag{6.29}$$

The value 1.50 in Eq.(6.28) is deduced for rectangular sections.

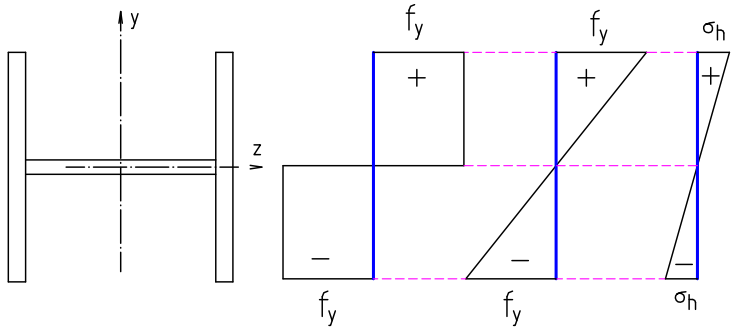

Fig.6.6. Bending about z axes

From Eqs.(6.25), (6.28) and (6.29), one has:

$$M_{pz} + M_{hz} = 1.12 M_{pz}\,,$$

its position is the outside of the limit surface (point B on Fig.6.5b).

- *Compression (or tension)*: It is simple to obtain:

$$N_p + N_h = 1.730 N_p\,,$$

it also locates at the outer space of the limit surface (point C on Fig.6.5b).

From Eqs.(6.1c), (6.27) one obtains the strain hardening modulus:

$$H = 0.3225 / \bar{\varepsilon}_l^p\,, \tag{6.30}$$

with the limit effective strain given on Table 6.2.

6.4. Numerical examples and discussions

In this section, five examples are examined. In which, two 3-D steel frames considered in Chapter 4 [examples 4.1 (Fig.4.6) and 4.2 (Fig.4.7)]; they are renamed, respectively, by frame 6.1 (six-story) and frame 6.2 (twenty-story). Example 6.3 shown on Fig.6.7 that was analyzed by Orbison (1982)[126]. Examples 6.4 and 6.5 are respectively reported on Figs.6.8 and 6.9.

Tow aims are underlined: (1) evaluate the techniques in this chapter in comparison with various available results in the literatures; (2) comparison the load multiplier given by the step-by-step method and of the direct methods.

Concerning the strain hardening parameters, one determines the value of $\bar{\varepsilon}_l^p$ and H for each example. Grade of steel S275 and S355 may be assigned to the frame 6.1 and frame 6.2, respectively. From Table 6.2, one has: $\bar{\varepsilon}_l^p = 0.213x10^{-2}$ for frame 6.1 and $\bar{\varepsilon}_l^p = 0.281x10^{-2}$ for frame 2. From Eq.(6.30), one obtains: $H = 151.41$ for frame 6.1 and $H = 114.77$ for frame 6.2.

Different models have been adopted by some researches to capture the both material inelasticity and geometric nonlinearity [28, 35, 71, 81, 88, 89]. Although the used models are different but the value of load ratios are well accordant (see Table 6.3).

In Chiorean (2005)[28], the Ramberg-Osgood shape parameter ($a=1; n=30$) are used for both frame 6.1 and frame 6.2 to take into account the hardening effect that makes increasing the load factor by 6.3% for frame 6.1 and 5.7% for frame 6.2. With CEPAO, when the strain hardening is taken into account, the ultimate strength of the frames increases by 5.7% and 2.6% for frame 6.1 and frame 6.2, respectively. Clearly, the hardening effect decreases when the second-order effect is dominant (frame 6.2).

Table 6.3: Load multiplier

Author	Model	Load multiplier	
		Frame 6.1	Frame 6.2
Liew JYR- 2000 [88]	Plastic hinge	2.010	-
Kim SE -2001[81]	Plastic hinge	2.066	-
Cuong NH - 2006 [35]	Fiber plastic hinge	2.040	1.003
Liew JYR- 2001 [89]	Plastic hinge	-	1.031
Jiang XM - 2002 [71]	Fiber element	-	1.000
Chiorean CG-2005 [28]	Distributed plasticity, n = 300 (hardening ignored)	1.998	1.005
	Distributed plasticity, n = 30 (hardening considered)	*2.124*	*1.062*
Present work -CEPAO	Plastic hinge, hardening ignored	2.033	1.024
	Plastic hinge, hardening considered	*2.149*	*1.051*

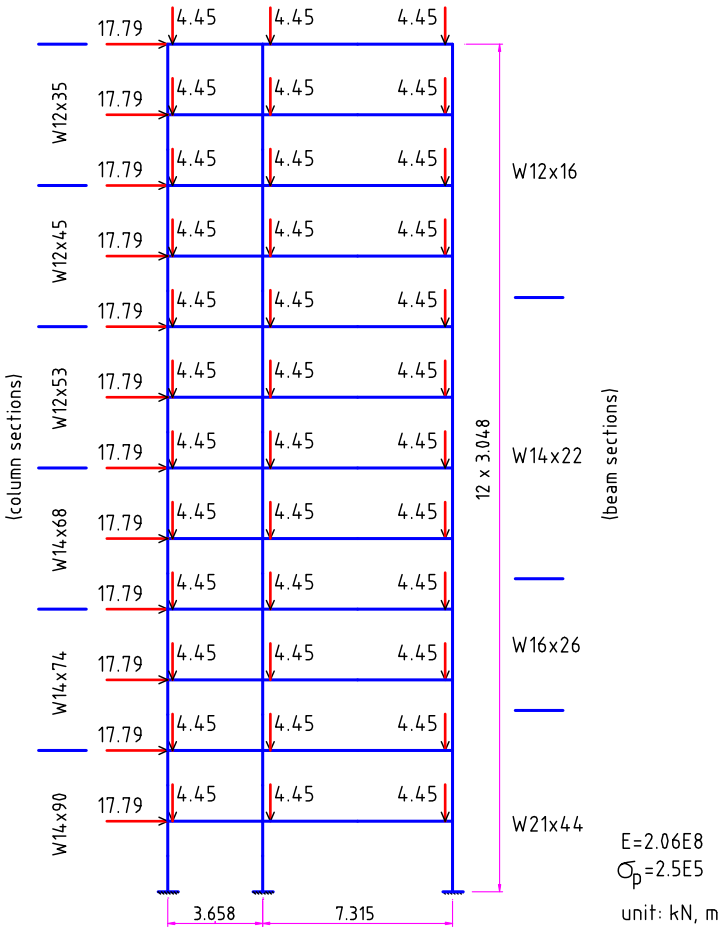

Fig.6.7. Twelve-story frame (frame 6.3)

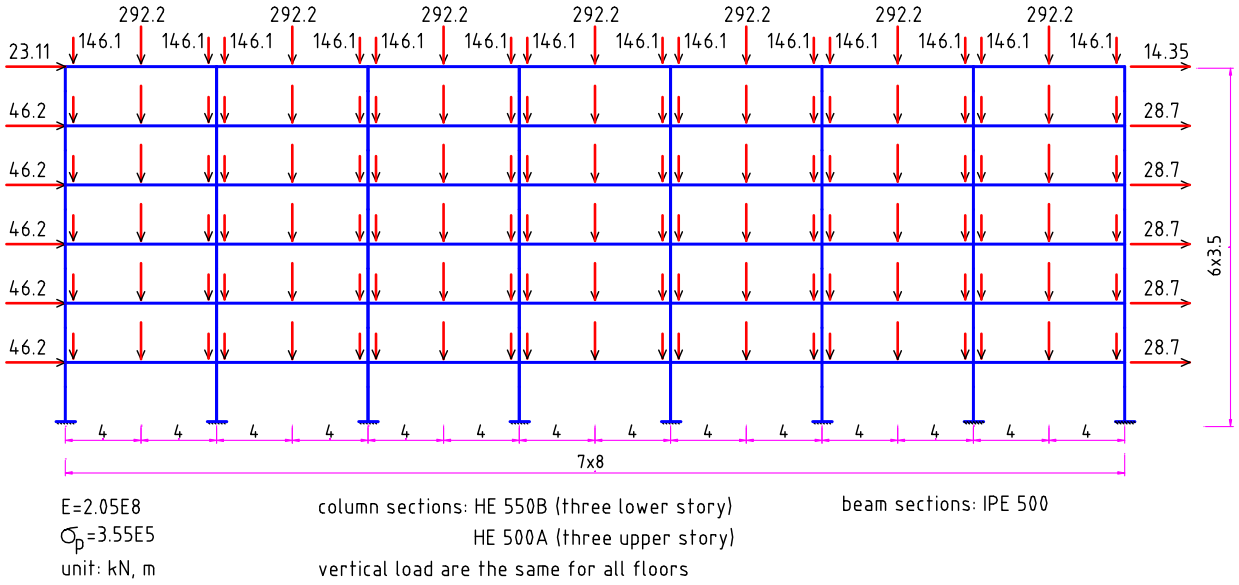

Fig.6.8. Six-story seven-bay frame (frame 6.4)

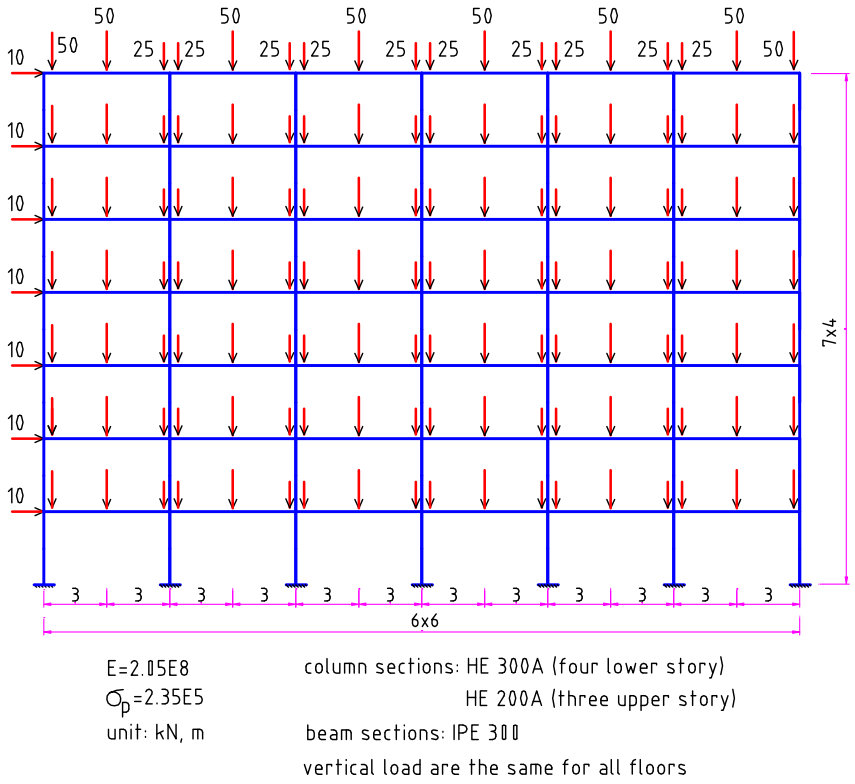

Fig.6.9. Seven-story six-bay frame (frame 6.5)

Figures 6.10 and 6.12 show the load-deflection relation results at a referential node. Figure 6.11 reports the deformation at limit state and distribution of plastic-hinge of frame 6.1. The behaviours of these frames by various type of analysis are outlined on Fig.6.13.

Figures 6.14 - 6.18 show the collapse mechanisms and corresponding load multipliers of the frames by the direct method and by the step-by-step method. Herein (Fig.6.13 -Fig.6.18), the strain hardening behaviours are ignored. It appears that an expectable coincidence of results calculated by direct method and step-by-step method. That allow to deduce: the good convergence between the dual methods in the CEPAO (kinematic and static method); and the good correlation between the Orbison'yield surface and this in AISC-LRFD. This statement will be confirmed again in Chapter 8.

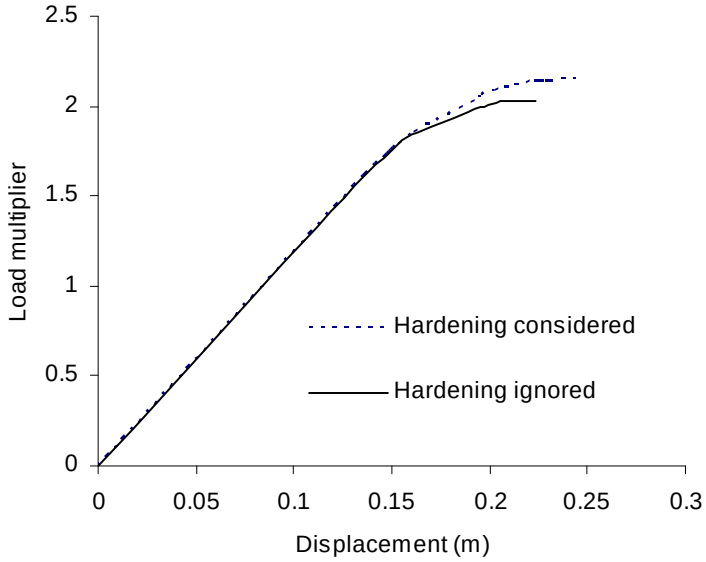

Fig.6.10. Frame 6.1- Load-deflection results at node A in Y direction (Fig.4.6) given by CEPAO

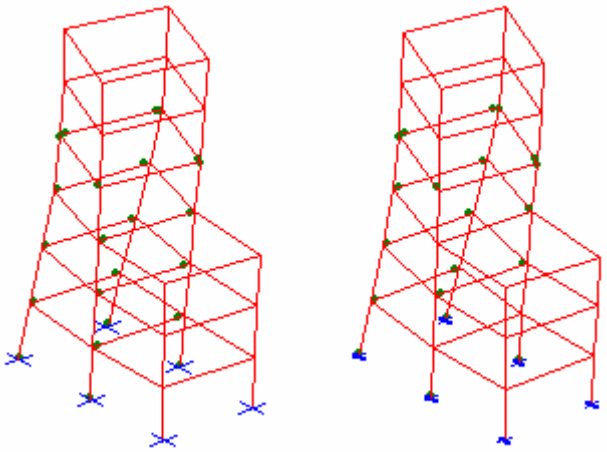

Hardening considered Hardening ignored

Fig.6.11. Frame 6.1 – Deformation at limit state and distribution of plastic-hinges

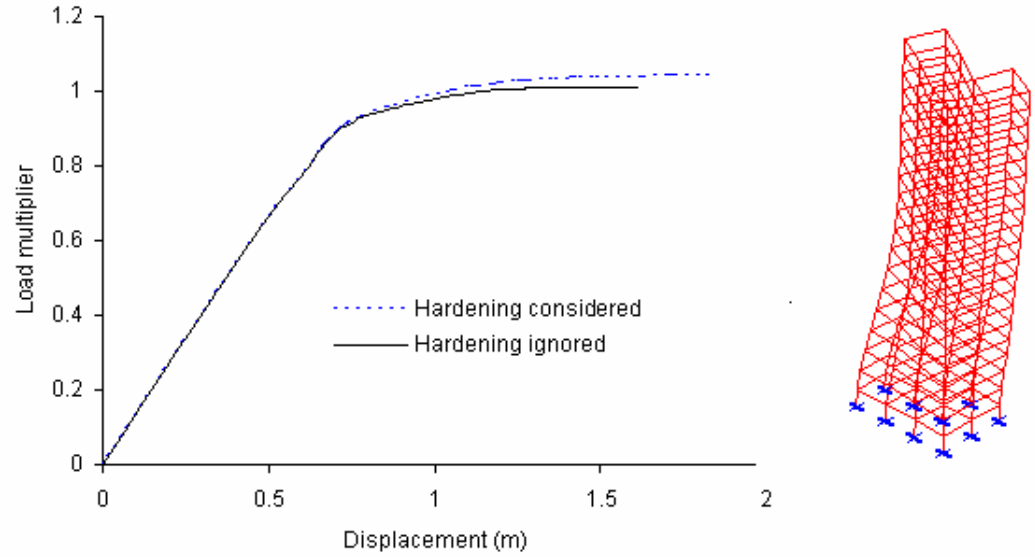

Fig.6.12. Frame 6.2-Load-deflection results at node A in Y direction (Fig.4.7) given by CEPAO

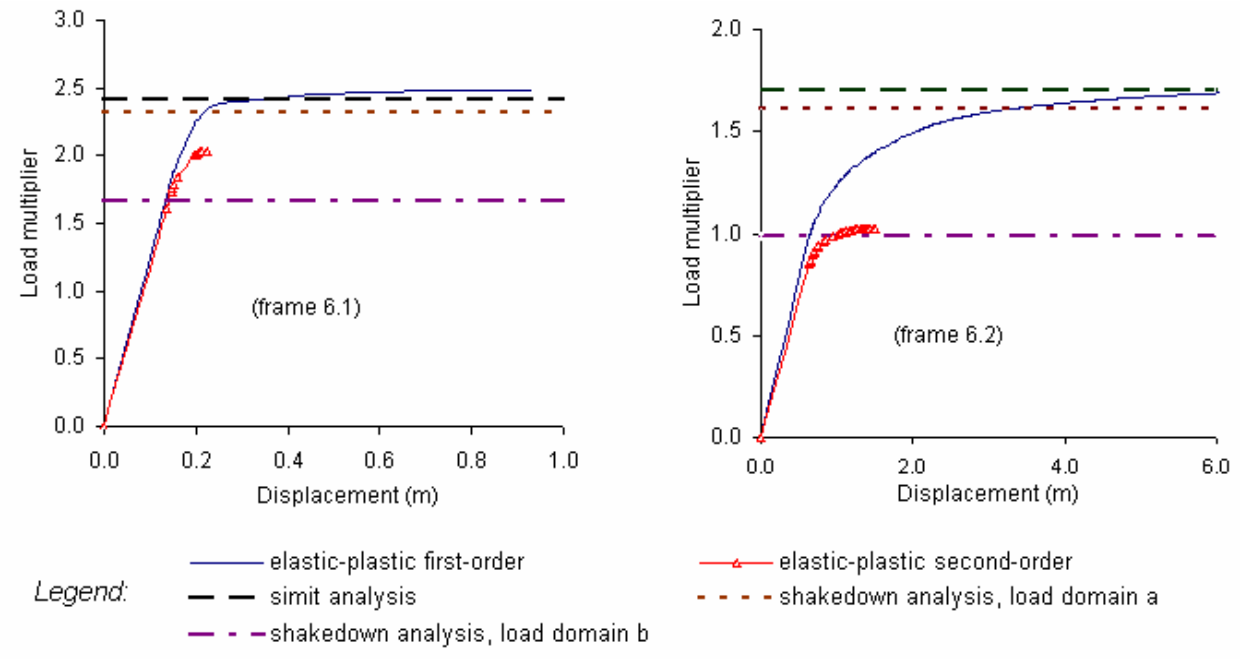

Fig.6.13. Load-deflection results at point A (Figs. 4.6 and 4.7) given by CEPAO

Direct method (load multiplier = **2.412**) Step-by-step method method (load multiplier = **2.489**)

Fig.6.14. Frame 6.1-collapse mechanism

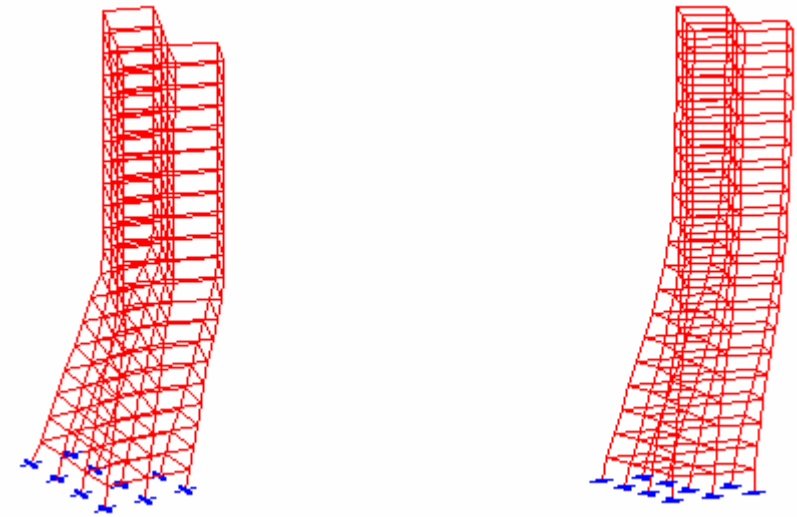

Direct method (load multiplier = **1.698**) Step-by-step method (load multiplier = **1.689**)

Fig.6.15. Frame 6.2-collapse mechanism

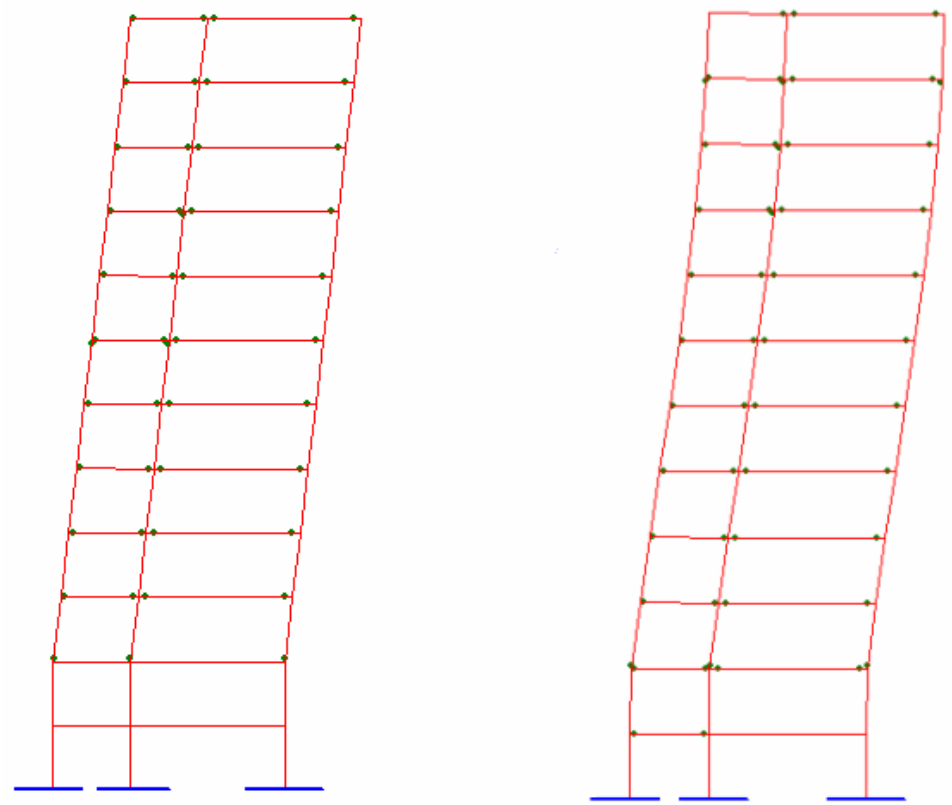

Direct method (load multiplier = **2.126**) Step-by-step method (load multiplier = **2.175**)

Fig.6.16. Frame 6.3-collapse mechanism

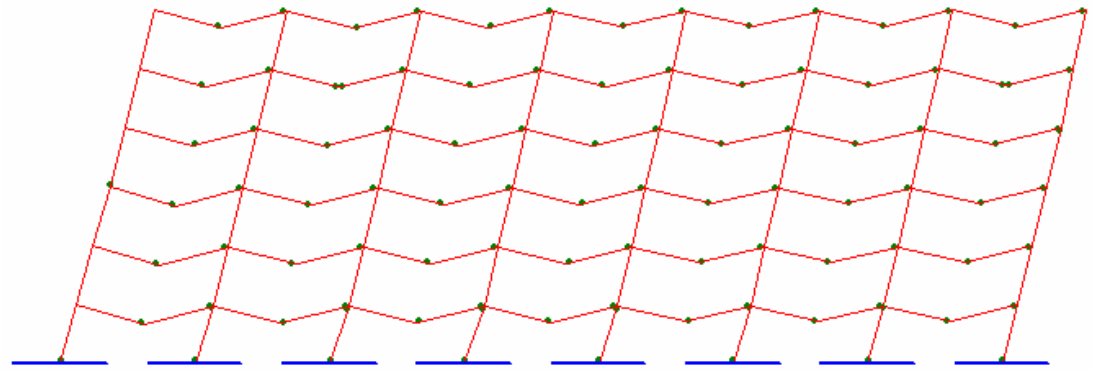

Fig.6.17a. Frame 6.4-collapse mechanism given by the direct method (load multiplier = **2.469**)

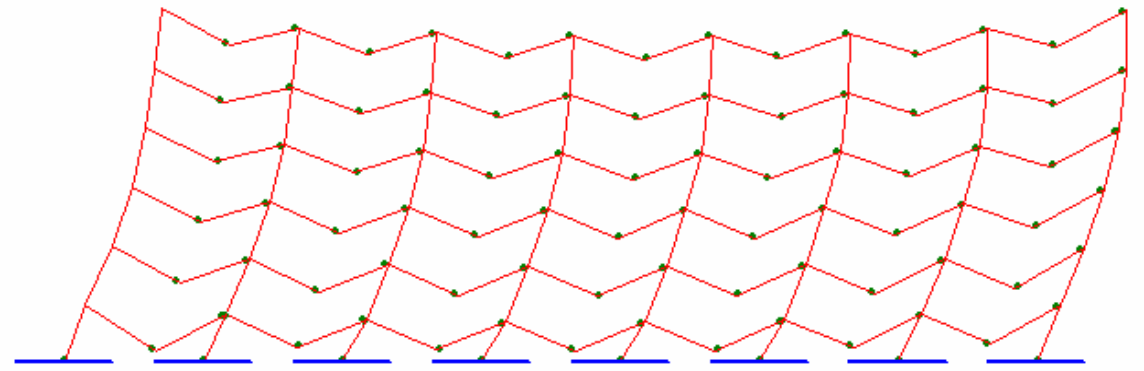

Fig.6.17b. Frame 6.4-collapse mechanism given by the step-by-step method (load multiplier = **2.402**)

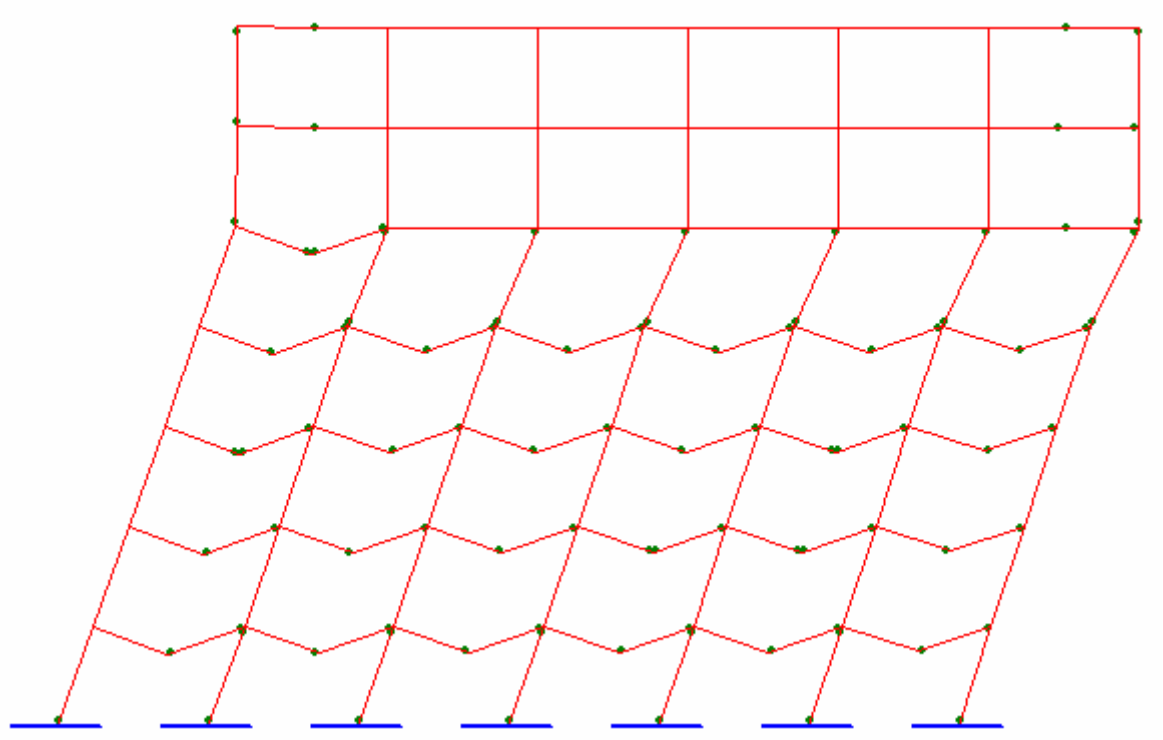

Fig.6.18a. Frame 6.5-collapse mechanism given by the direct method (load multiplier = **2.226**)

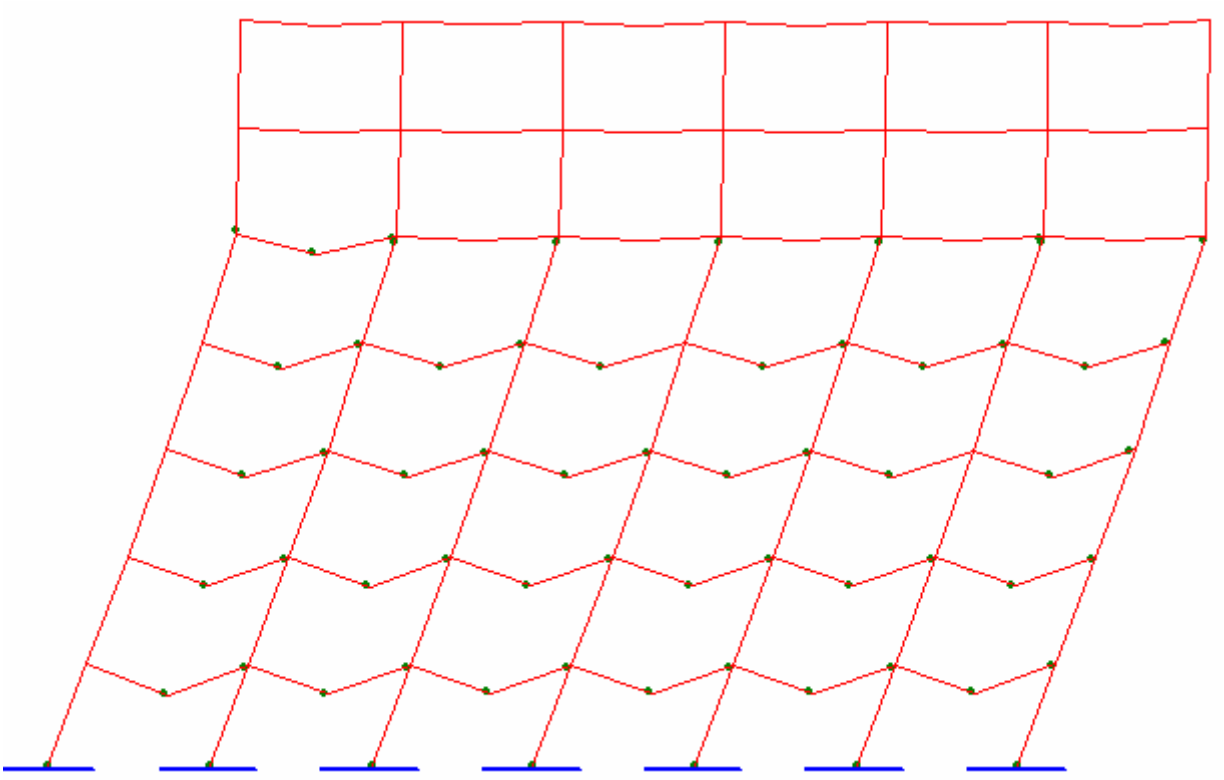

Fig.6.18b. Frame 6.5-collapse mechanism given by the step-by-step method (load multiplier = **2.264**)

6.5. Conclusions

The proposed algorithm allows take into account the strain hardening effects in the plastic-hinge analysis of 3-D steel frames. It appears that the plastic hinge analysis procedure is

identical to the elastic analysis procedure unless only elastic physical matrix is replaced by elastic-plastic physical matrix. This is an advantage when developing the multi-functions computer program, as CEPAO package. The values of the hardening parameters are reliable because it is based on the recent research on the hardening behaviours of steel structures. Through the numerical examples, a good agreement between our results and other benchmark results from the literature is obtained, it allows us demonstrate the achievement of the present model. This work may be considered as a contribution in the structural system approach to design of steel frames (see Chen (2008)[25]).

Chapter 7

Local buckling check according to Eurocode-3 for plastic-hinge analysis of 3-D steel frames

With an I or H-shaped section, local buckling may occur in outstanding flanges or webs under compressed stress. At the plastic-hinge with a large rotation, cross-sections are in at risk of local buckling, even with rolled sections that are generally considered as compact sections (see Massonnet (1976)[106]). Therefore, local buckling needs be taken into account in the analysis and design procedure of structures, especially, with the plastic design. There are two directions for the consideration of local buckling, either by plastic- zone analysis or by the application of Standards. The first direction leads to an increase in computation time. A way of the last direction is presented in Kim (2003)[80], in which practical equations of Load and Resistance Factor Design specification of American Institute of Steel construction are applied. Aside from this research, almost all plastic-hinge analysis assumes that all sections are compact, and local buckling will be examined last in the design procedure.

The local buckling phenomenon of the steel frames is considered in Eurocode-3 [46] by the concept of classification of cross-section. The classification of cross-sections depends on the width-to-thickness ratio of parts subject to compression. It is only achieved when the stress distribution on cross-sections is determined. However, we observe that engineers still need an efficient way to determine the position of the neutral axis of a yielded I or H-shaped section (in space behaviour). Furthermore, the local buckling needs to be automatically verified throughout the process of global analysis of structures.

This chapter present an algorithm for determination of the stress distribution at a plastic-hinge with the special behaviour such a way that the concept of classification of cross-section in Eurocode-3 is directly applied.

Keywords: *Local buckling*; *Plastic-hinge*; *Space frames.*

7.1. Conception of local buckling in Eurocode-3

Based on local buckling resistance, Eurocode-3 [46] provides a classification for beams and columns in four classes:

- Class 1 cross-section permits the formation of a plastic hinge with the rotation capacity required from plastic analysis;

- Class 2 cross-section allows the development of a plastic hinge but with limited rotation;

- Class 3 cross-section where local buckling is liable to prevent development of plastic moment resistance;

- Class 4 cross-section where local buckling will occur before the attainment of yield stress in one or more parts of the cross-section.

The classification of a cross-section depends on the width-to-thickness ratio of parts subject to compression. Table 7.1 presents the limited width-to-thickness ratios for compression parts (outstand flanges or webs) in which stress distribution is shown on Fig.7.1.

Table 7.1: Classification of cross-section

Class	Web		Flange
1	$d/t_w \le 396\varepsilon/(13\alpha-1)$	when $\alpha > 0.5$	$b_0/t_f \le 9\varepsilon/\alpha$
	$d/t_w \le 36\varepsilon/\alpha$	when $\alpha \le 0.5$	
2	$d/t_w \le 456\varepsilon/(13\alpha-1)$	when $\alpha > 0.5$	$b_0/t_f \le 10\varepsilon/\alpha$
	$d/t_w \le 41{,}5\varepsilon/\alpha$	when $\alpha \le 0.5$	
3	$d/t_w \le 42\varepsilon/(0{,}67+0.33\psi)$	when $\psi > -1$	$b_0/t_f \le 21\varepsilon\sqrt{0{,}57-0{,}21\psi+0{,}07\psi^2}$ when $-3 \le \psi \le 1$
	$d/t_w \le 62\varepsilon(1-\psi)\sqrt{-\psi}$	when $\psi \le -1$	
4	A parts which fails to satisfy the limit for Class 3 should be taken as Class 4		

Remarks: $\varepsilon = \sqrt{235/f_y}$, $d, b_0, t_f, t_w, \alpha, \psi$ are indicated in Figs.7.1 and 7.2.

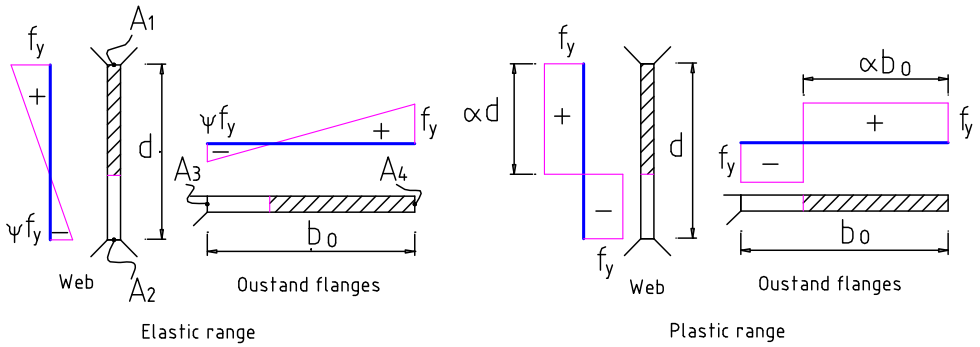

Fig.7.1. Stress distribution on outstand flanges and web

When a local buckling check is taken into account, the procedure for analysis of a steel frame includes four steps as follows:

1. Selecting member sizes for the structure and assuming that all cross-sections have Class 1.

2. Analyzing the structure by the plastic-hinge method and determining the internal forces at the cross-sections.

3. Determining stress distribution at the cross-sections.

4. Classifying cross-sections; and checking local buckling based on the cross-section requirements for plastic global analysis.

Step 3 and Step 4 may be realized at any time of the analysis procedure as long as internal forces at cross-sections are computed. In Sections 7.2 and 7.3, Step 3 and Step 4 will be described in detail, respectively.

7.2. Stress distribution over a cross-section

In principle, the stress distribution over a cross-section may be deduced from equilibrium and compatibility conditions. However, the problem becomes complicated due to the inherent

form of I or H-shaped sections and the inelastic properties of the material. Therefore, it is interesting to establish a simple and clear algorithm for this problem.

7.2.1. At yielded sections (plastic-hinges)

7.2.1.1. Plastic-hinge concept

Under the combined effects of axial force and bending moments, only the normal stress is effected on the cross-section. The plastic-hinge concept indicates that a cross-section is fully yielded by compression ($-f_y$) or tension (f_y) separated by a neutral line. In the global plastic analysis of structure, the plastic-hinge is assumed to be resulted when the force point reaches the yield surface: $\Phi(N, M_y, M_z) = 0$. In the present work, *passive* plastic-hinges define the plastic-hinges without plastic deformation. Conversely, one has the *active* plastic-hinges.

7.2.1.2. Assumptions

In Eurocode-3's guidance, stress distributions over sections are simplified (see Fig.7.1); it does not include all possibilities of locations of the neutral axis of a section in space behaviour. Moreover, it is complicated to determine the "real" stress state over sections. Therefore, the following assumptions are made in the present work.

1- The neutral axis is a straight line, it divides the cross-section into two parts, one is in compression and other is in traction.

2- The cross-section is idealized as a section composed of three rectangular strips (Fig.7.2a).

3- The area of the compressed zone and the tensional zone are approximated as shown in Fig.7.2b.

4- The bending moment with respect to the weak axis, M_z, is only supported by two flanges.

5- Residual stress is neglected.

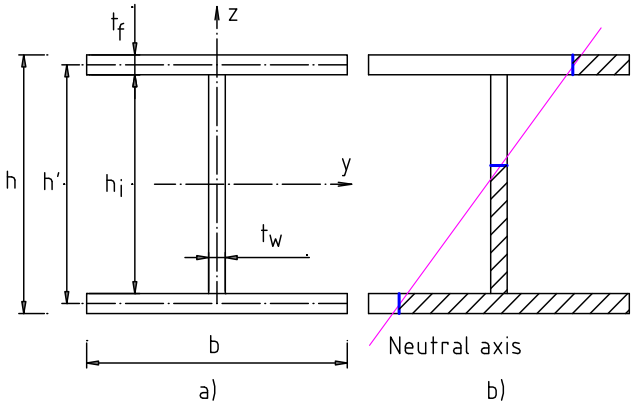

Fig.7.2. Simplified shape and simplified stress distribution

7.2.1.3. Formulation

Since the neutral axis is a straight line, its position may be determined by two geometry parameters. In principle, the distribution of the stress on the cross-section must satisfy three equilibrium conditions according to N, M_y, M_z. However, one equilibrium equation among them is constrained by $\Phi(N,M_y,M_z)=0$. Therefore, two necessary parameters to locate the position of neutral axis are determined by two suitable equilibrium equations. A way to find the formulas is summarized as follows:

- First, grouping the location of the neutral axis and writing the corresponding equilibrium equations (equilibrium between the stress and internal forces), they are reported in Table 7.2. The description of the location of neutral axis is abbreviated to: NA1 or NA2 or NA3.

Table 7.2: Location of neutral axis (NA) and corresponding equilibrium equations

Location of NA	Notation	Unknowns	Equilibrium equations	
NA passes through two flanges (Fig.7.3a)	NA1	b_1, b_2	$\|M_y\| = f_y t_f (b_1 - b_2) h'$	(a1)
			$\|M_z\| = f_y t_f [b_1 (b - b_1) + b_2 (b - b_2)]$	(a2)
			$\|N\| = f_y [2 t_f (b - b_1 - b_2) + h_i t_w]$	(a3)
NA passes through the web and a flange (Fig.7.3b)	NA2	b_1, z_1	$\|M_z\| = f_y t_f b_1 (b - b_1)$	(b1)
			$\|N\| = f_y (2 z_1 t_w + 2 b_1 t_f)$	(b2)
			$\|M_y\| = f_y [h' t_f (b - b_1) + (h_i^2 / 4 - z_1^2) t_w]$	(b3)
NA passes through the web and two flanges (Fig.7.3c)	NA3	b_1, b_2	$\|M_z\| = f_y t_f [b_1 (b - b_1) + b_2 (b - b_2)]$	(c1)
			$\|N\| = f_y [h' t_w (b_1 - b_2) / (b - b_1 - b_2) + 2 (b_1 - b_2) t_f]$	(c2)
			$\|M_y\| = f_y [h' t_f (b - b_1 - b_2) + (h_i^2 / 4 - z_1^2) t_w]$	(c3)

Note: with NA1, b_2 may be disappeared; with NA2, b_1 or z_1 may be disappeared.

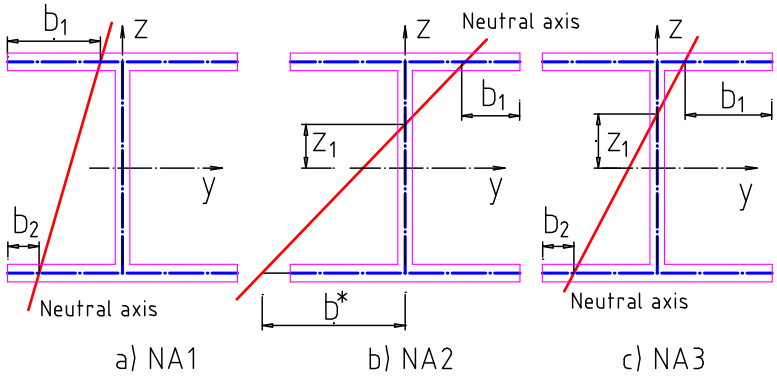

Fig.7.3. Location of the neutral axis

- Next, let us introduce the following non-negative parameters in accordance with the given dimensions of the profile (Fig.7.2a) and the given internal forces.

$$c_y = \frac{|M_y|}{f_y h'(b/2) t_f};$$

$$c_z = \frac{|M_z|}{f_y (b^2/4) t_f};$$

$$c_n = \frac{|N|}{f_y h_i t_w};$$

$$\beta = h'/h_i;$$

$$\gamma = \frac{b t_f}{h_i t_w}.$$

- Finally, the equilibrium equations are solved, taking into account the existential solution condition, we obtain the following results:

Case 1:

If

$$\begin{cases} c_y \le 1 \\ 2c_y \le c_y^2 + c_z \le 2 \end{cases}. \tag{7.1a}$$

then the NA1 is accorded, and:

$$\begin{cases} b_1 = \dfrac{b}{2}\left(1 + \dfrac{c_y}{2} - \sqrt{1 - \dfrac{c_z}{2} - \dfrac{c_y^2}{4}}\right) \\ b_2 = \dfrac{b}{2}\left(1 - \dfrac{c_y}{2} - \sqrt{1 - \dfrac{c_z}{2} - \dfrac{c_y^2}{4}}\right) \end{cases}. \tag{7.1b}$$

Case 2:

If

$$\begin{cases} c_z \le 1 \\ \dfrac{\sqrt{1-c_z}\,(c_n + \beta) + c_n - \beta}{c_z} \ge \gamma \end{cases}, \tag{7.2a}$$

then the NA2 is agreed, and:

$$\begin{cases} b_1 = \dfrac{b}{2}\left(1 - \sqrt{1 - c_z}\right) \\ z_1 = \dfrac{h_i}{2}\left[c_n - (1 - \sqrt{1 - c_z})\gamma\right] \end{cases}. \tag{7.2b}$$

Case 3:

If the both conditions (7.1a) and (7.2a) are not satisfied, the NA3 is adopted, and:

$$\begin{cases} b_1 = \dfrac{b}{2}\left(1 - \sqrt{1 - c_z + \xi c_z}\right) \\ b_2 = \dfrac{b}{2}\left(1 - \sqrt{1 - \xi c_z}\right) \\ z_1 = \dfrac{h_i}{2}\dfrac{(\sqrt{1 - \xi c_z} - \sqrt{1 - c_z + \xi c_z})}{(\sqrt{1 - \xi c_z} + \sqrt{1 - c_z + \xi c_z})}\beta \end{cases}. \tag{7.3a}$$

with:

$$\xi = \frac{1}{2}\left\{1 - \sqrt{1 - \frac{1}{c_z^2}\left[(x^2 - 2 + c_z)^2 + 4c_z - 4\right]}\right\}, \tag{7.3b}$$

while x must satisfy the following equation:

$$\gamma^2 x^4 + 2\beta\gamma x^3 + (c_n^2 + \beta^2 - 4\gamma^2 + 2\gamma^2 c_z)x^2 + (4\beta\gamma c_z - 8\beta\gamma)x + 2\beta^2 c_z - 4\beta^2 = 0. \tag{7.3c}$$

Eq. (7.3c) may be solved by the Newton-Raphson iteration; it becomes better with the following bounds:

$$\begin{cases} \sqrt{2 - c_z} \le x \le \sqrt{2}\sqrt{2 - c_z} \text{ when } c_z \ge 1 \\ \sqrt{2(\sqrt{1 - c_z} + 1) - c_z} \le x \le \sqrt{2}\sqrt{2 - c_z} \text{ when } c_z < 1 \end{cases}. \tag{7.3d}$$

Remark: *The derivation of Eq.(7.1a) to Eq.(7.3d)*

- Without losing generality, we assume that $b_1 \geq b_2$ (Figs.7.3a and 7.3c). If $\alpha_z > 2$ then one takes $\alpha_z = 2$, it agrees with fourth assumption that is above mentioned.

- The values b_1 and b_2 in Eq.(7.1b) are the solution of the system of Eqs.(a1) and (a2) in Table 7.2, while Eq.(7.1a) is obtained by the condition of $0 \leq b_2 \leq b_1 \leq b/2$.

- Solving the system of Eqs.(b1) and (b2) in Table 7.2 one obtains the values b_1 and z_1 in Eq.(7.2b). Eq.(7.2a) is deduced from the condition of $b^* \geq b/2$, with b^* (Fig.7.3b) is calculated by the geometric relation with b_1 and z_1:

$$b^* = (b/2 - b_1)(h'/2 + z_1)/(h'/2 - z_1).$$

- The bending moment M_z may be decomposed into two parts ξM_z and $(1-\xi)M_z$, each part is supported by each flange. By Consequence, Eq.(c1) in Table 7.2 is equivalent to the following system:

$$\begin{cases} b(b-b_2) f_y t_f = \xi M_z \\ b(b-b_1) f_y t_f = (1-\xi) M_z \end{cases},$$

it gives the values b_1 and b_2 in Eq.(7.3a). Substituting the values b_1 and b_2 in the geometric relation of (Fig.7.3c)

$$z_1 = \frac{1}{2} h' \frac{b_1 - b_2}{b - (b_1 + b_2)},$$

one obtains value z_1 in Eq.(7.3a).

The value ξ in Eq.(7.3b) obtained by the following put:

$$x = \sqrt{1 - \xi c_z} + \sqrt{1 - c_z + \xi c_z}.$$

Writing b_1 and b_2 in Eq.(7.3b) under formulation of x and substituting then in Eq.(c2) (Table 7.2), one obtains Eq.(7.3c). Because $b_1 \geq b_2$, one has $0 \leq \xi \leq 1/2$, it leads to Eq.(7.3d).

If the value of x obtained by (7.3c) violates the condition (7.3d) the real value ξ in Eq. (7.3b) is then not found. This statement may be due to the force point exceeding the "real" yield surface with a considerable amount. We can say that it very rarely occurs with the practical yield surfaces.

7.2.1.4. Particular cases

There are two particular cases of the location of the neutral axis as the shown in Fig.7.4; they are noted by NA4 and NA5. Those cases rarely happen with the steel frames in practice, and they are not indicated in Eurocode-3. In the following, some treatments of the cases are proposed.

NA4 is a particular case of NA1 when $b_2 \geq (b - t_w)/2$, with b_2 is determined by Eq.(7.1b). To apply the classification of the rule of cross-sections in Eurocode-3, one considers that the whole web is in compression if N is compression and $c_n \geq 0.5$ (Table 7.3). Contrarily, the web is in traction (no local buckling).

NA5 is the particular case of NA2 when $b_1 = 0$ and $z_1 > h_i/2$, with b_1 and z_1 are calculated by Eq.(7.2b). In the case where N is compression, there is always a flange is in compression. Contrarily (N is traction), the following rule may be adopted (Table 7.3): (1) If $c_y \geq 1.5$ then one

flange is in compression and other is in traction. (2) When c_y<1.5 the whole section is in traction (no local buckling).

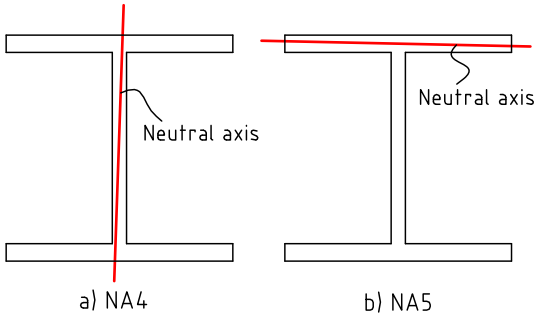

Fig.7.4. Particular cases of the location of neutral axis

7.2.1.5. Coefficient α (see Fig.7.1)

Table 7.3 presents the values of this coefficient according to the stress distribution at the plastic-hinges. The coefficient α is used to classify the cross-sections (see Section 4).

Table 7.3: Coefficient α (see Figs.7.1 and 7.3)

Location of NA	Flange	Web
NA1	$\alpha = 1$ if $N > 0$ $\alpha = b_1 / b_0$ if $N \le 0$	$\alpha = 1$ if $N > 0$ $\alpha = 0$ if $N \le 0$
NA2	$\alpha = 1$	$\alpha = (d/2 + z_1)/d$ if $N > 0$ $\alpha = (d/2 - z_1)/d$ if $N \le 0$
NA3	$\alpha = 1$	$\alpha = (d/2 + z_1)/d$ if $N > 0$ $\alpha = (d/2 - z_1)/d$ if $N \le 0$
NA4	$\alpha = 1$	$\alpha = 1$ if $N > 0$ and $c_n \ge 0.5$ $\alpha = 0$ if $N \le 0$ or $c_n < 0.5$
NA5	$\alpha = 1$ if $N > 0$ or $c_y < 1.5$ $\alpha = 0$ if $N \le 0$ and $c_y \ge 1.5$	$\alpha = 1$ if $N > 0$ $\alpha = 0$ if $N \le 0$

Note: $N > 0$: compression; $N < 0$: tension; take $\alpha = 1$ if $\alpha > 1$.

7.2.1.6. Verification

The mentioned formulas are completely deduced by analytic way. However, they are only considered as "exact" solutions when a "real" yield surface is used. Unfortunately, most yield surfaces for an I-shaped section (in space behaviour) are established by the approximate way (see Chen (1977)[20]). Therefore, a post-process of verification is then necessary. From the location of NA obtained by proposed formulas, the axial force and two bending moments ($\overline{N}, \overline{M}_y, \overline{M}_z$), the absolute values, may be determined by three corresponding equilibrium equations (Table 7.2). The following coefficient:

$$\zeta = \frac{\left| \sqrt{N^2 + M_y^2 + M_z^2} - \sqrt{\overline{N}^2 + \overline{M}_y^2 + \overline{M}_z^2} \right|}{\sqrt{N^2 + M_y^2 + M_z^2}} \qquad (7.4)$$

permits to evaluate the degree of precision of the solution. The value of this coefficient need be reported in the output so that the exceptional cases are eliminated. Analysis on a large number of plastic-hinges will highlight this coefficient.

In two particular cases (NA4 and NA5), Eqs.(a3) and (b3) in Table 7.2 are not valid. Therefore, in the case of NA4 (or NA5), N (or M_y) and $\overline{N}$ (or $\overline{M}_y$) in Eq.(7.4) are ignored.

7.2.2. At elastic sections

Since the residual stress is ignored, cross-sections work in the elastic range when their internal forces are limited by the elastic surface:

$$\phi_e = \frac{|N|}{A} + \frac{|M_y|}{I_y}\frac{h}{2} + \frac{|M_z|}{I_z}\frac{b}{2} - f_y = 0,$$

in which, A, I_y, I_z are the area, and the moment of inertia of the cross-section, respectively.

The coefficient ψ (Table 7.1 and Fig.7.1) may be deduced from the elastic stress at the points A1, A2, A3, A4 (Fig.7.1). The elastic stress state is easily determined; it does not need to be presented herein.

7.2.3. At elasto-plastic sections

This kind of section is indicated by the force point that is bounded by the elastic surface and the yield surface (i.e. ϕ_e>0 and Φ<0). It is complicated to determinate the "exact" position of the neutral axis in this case. Moreover, Eurocode-3 only gives two types of stress distribution: elastic and plastic. Therefore, the position of the neutral axis in this case may be approximately determined as the yielded cross-sections (plastic-hinges) with a modified value of the internal forces: κN, κM_y, κM_z. In which, κ is a coefficient such that: $\Phi(\kappa N, \kappa M_y, \kappa M_z)$=0, it shows that $\kappa > 1$. Thus, instead of considering the sections under N, M_y, M_z, we examine the sections subjected to κN, κM_y, κM_z.

To discuss above way, one may agree two following remarks: (1) if a section is compact under κN, κM_y, κM_z then it is compact under N, M_y, M_z; (2) if a section is non-compact under κN, κM_y, κM_z then it is either compact or non-compact under N, M_y, M_z. Therefore, the proposed way is strict right in the case where the sections are compact under κN, κM_y, κM_z. In the other case, if the sections are non-compact under κN, κM_y, κM_z, the way reserves some securities. Let us note that the internal force state of κN, κM_y, κM_z is a *fictive state* for examination the real state (N, M_y, M_z). In fact, from the elasto-plastic state to the plastic state of sections, the components of internal force changes non-proportionately.

7.3. Classification of cross-sections and local buckling check

7.3.1. Classification of cross-sections

With the parameter α for yielded and elasto-plastic sections (see *Section 7.2.1.5* and *Section 7.2.3*) or the parameter Ψ for elastic sections (see *Section 7.2.2*), cross-sections are classified by Table 7.1. Class 1 or Class 2 or no class are three possibilities for yielded and elasto-plastic sections while elastic sections have Class 3 or Class 4.

7.3.2. Local buckling check

Applying the cross-section required for plastic global analysis in Eurocode-3 [46], the following rule may be adopted:

- Cross-sections in which the active plastic hinge occurs must be Class 1.

- At the passive plastic-hinge and the elasto-plastic sections, only Class 1 or Class 2 is allowed.

- Cross-sections working in the elastic range must be Class 3.

When above requirements are satisfied, the sections resist the local buckling phenomenon. Conversely, the sections are in the *risk of local buckling*.

7.4. Numerical examples and discussions

The proposed rule for local buckling detection was implemented in CEPAO computer program. Second-order plastic-hinge analysis for two 3-D steel frames (six-story and twenty-story frames) is chosen to illustrate the technique. The local buckling check is realized throughout the computation time.

Frame 7.1 – Six-story space frame (Fig.7.5): It is the example 4.1 but the member sizes and the loading cases are varied (Table 7.4). There are two loading cases: (1) Uniform floor pressure of 4.8 kN/m2; wind loads are simulated by point loads of 26.7 kN in the Y-direction at every beam-column joint; (2) Four nodal load of 25 kN with negative x direction that apply at the four nodes of the highest level of the frame. Three cases are examined: Frame-7.1a: configuration of member size 1 subjects the loading case 1; Frame-7.1b: configuration of member size 2 supports the loading case 1; Frame-7.1c: configuration of member size 1 with the loading case 2. In which, the frame-7.1a were analysed in precedent chapters.

Frame-7.2 – Twenty-story space frame shown on Fig.4.7 (example 4.2) is analyzed by the elastic-plastic second-order subroutine under checking the risk of local buckling.

Table 7.4: Frame 7.1 – Configuration of member size

Configuration	Group of member size (Fig.7.5)				
	1	2	3	4	5
1	W12x87	W12x120	W10x60	W12x26	W12x53
2	W18x86	W12x120	W10x60	W12x26	W12x53

Some following points are discussed:

- *Load factor at limit state*: In Chapter 6, it appears that load ratios according to the second-order plastic-hinge analysis given by CEPAO are in agreement with other benchmarks results available from the literature (see Table 6.3). It shows that the data for the process of local buckling checks are objective data and practical data. The distribution of plastic-hinges of frame-7.1 is reported on Fig.7.6 while the load-deflection result at referent nodes is reported on Fig.7.7. There is no space behaviour in the frame-7.1c.

- *Local buckling detection*: It is realized after each computational step. In Frames 7.1a, 7.1c and 2, all sections satisfy the cross-section requirements for plastic global analysis. It is in agreement with other research in which the compact sections are assumed. Table 7.5 details the necessary information of local buckling check for the active plastic-hinges at the limit state of Frame-7.1a. The particular location of neutral axis (NA4) happens at the plastic hinges in the frame-1c (Table 7.6). In the other context, at the section 7 of the frame-7.1b (Fig. 7.6b), the risk of local buckling happens at the web of the section when the load factor reached 2.13 while plastic-hinge has been already formed with a load factor of 2.08. During the force point moves on the yield surface, the neutral axis transfers on the cross-section leading to the risk of local buckling in the web. Developments of this process are described in Table 7.7 and Fig.7.9. It shows the degree of refinement of present analysis.

- *Position of the neutral axis*: The value of the coefficient ζ [see Eq. (7.4)] of 103 active plastic-hinges (both two frames) is summarized on the Table 7.8. This points out: (1) the Orbison's yield surface (Eq.(3.1)) is in good correlation with the "actual" yield surface; (2)

stress distributions at the plastic-hinges obtained by proposed technique may be applied in practice with high-level of reliability.

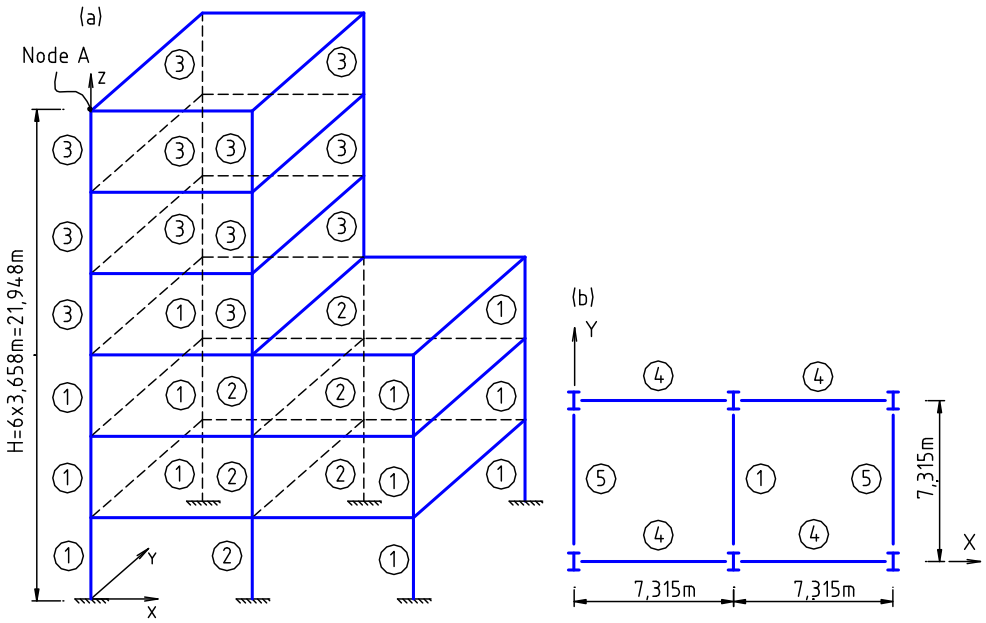

Fig.7.5. Frame-1: Six-story space frame (a – perspective view, b- plan view)

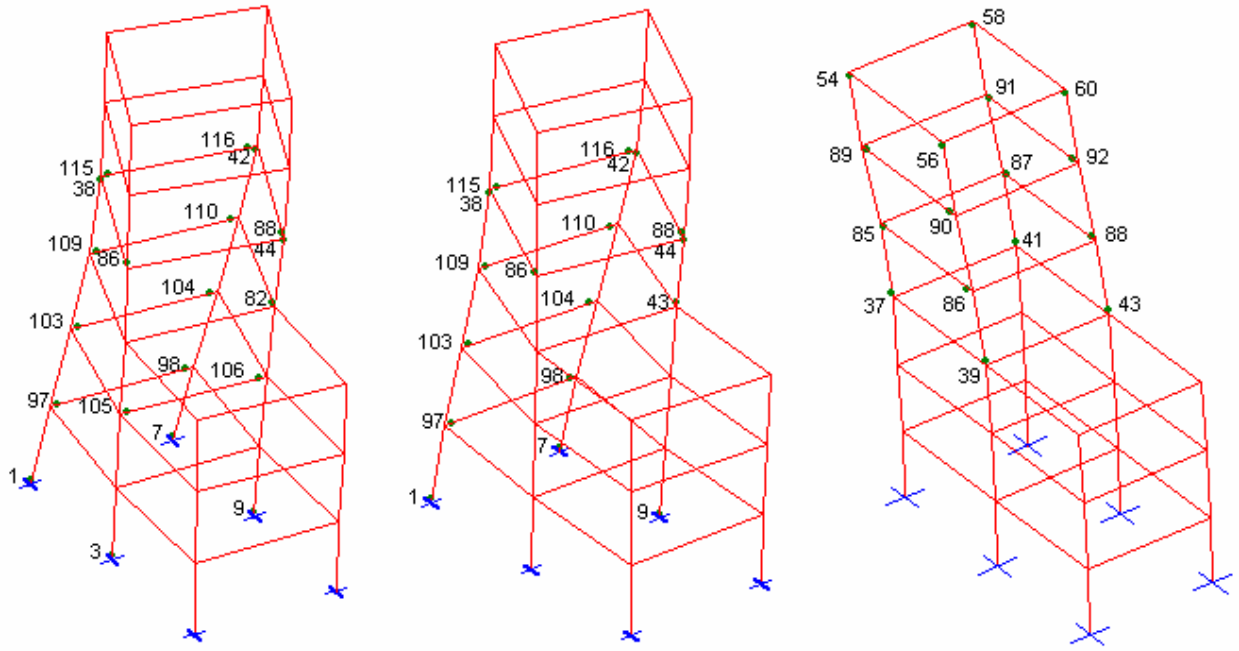

a) Frame-7.1a (load factor = 2.033) b) Frame-7.1b (load factor = 2.254) c) Frame-7.1c (load factor = 2.161)

Fig.7.6. Frame-7.1: Deformation and distribution of plastic-hinges at the limit state

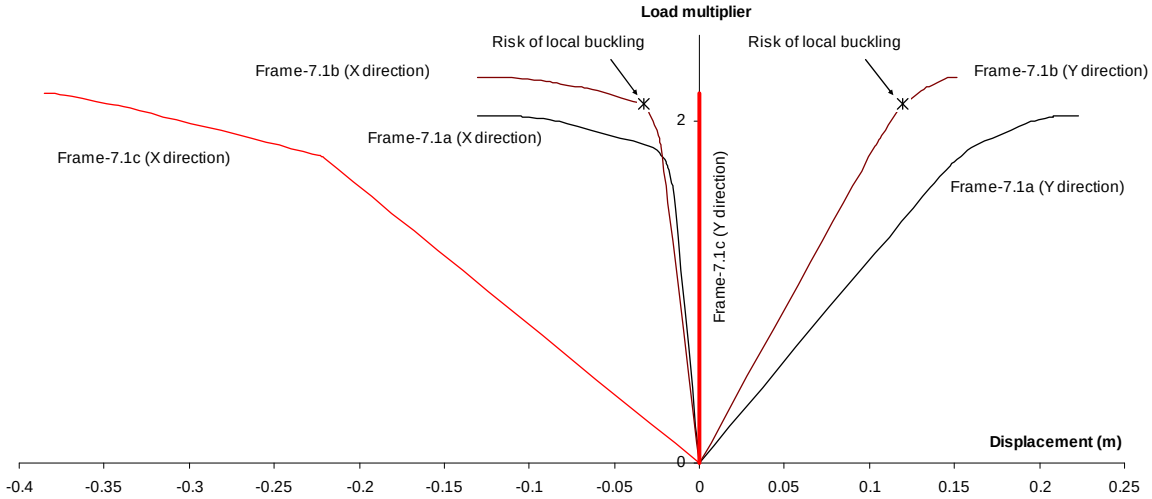

Fig.7.7. Frame-7.1: Load-deflection results at node A (Fig.7.5) given by CEPAO

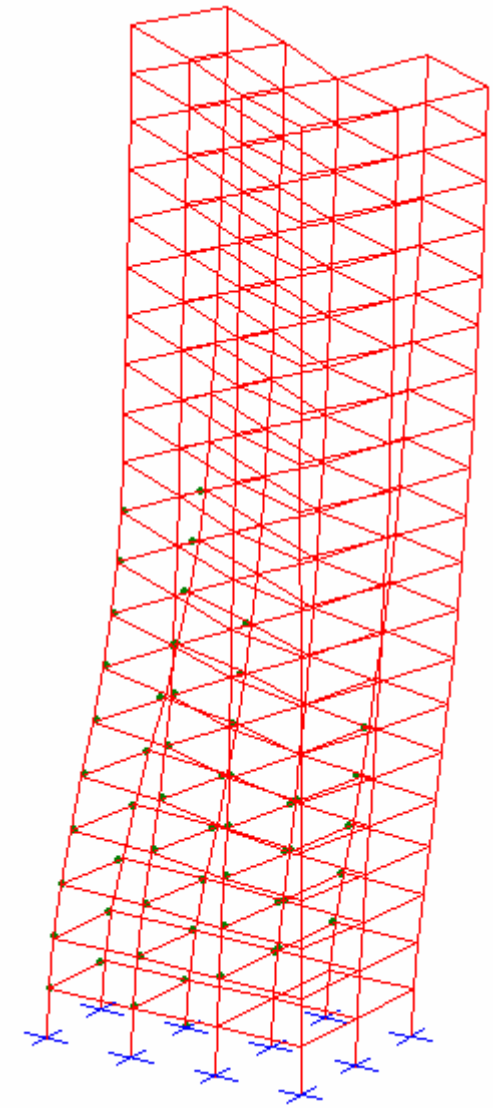

Fig.7.8. Frame-7.2: Deformation and distribution of plastic-hinges at the limit state (load multiplier = 1.024)

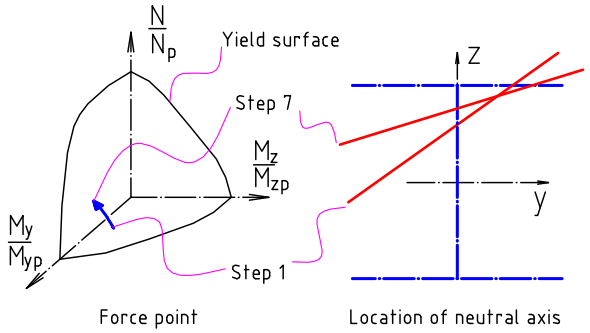

Fig.7.9. Frame-7.1b: behaviour of section 7 (Fig.7.6b indicates the section 7)

Table 7.5: Frame-7.1a: Local buckling check for the active plastic-hinges at the limit state (load factor = 2.032)

Section		Given forces			Location of neutral axis				Verified-forces				Width to thickness ratios (limit and real)of the web and compressed outstand flange			
S*	P**	N	M_y	M_z	NA	b_1	b_2	z_1	$\overline{N}$	$\overline{M}_y$	$\overline{M}_z$	ς	$[d/t_w]$	d/t_w	$[b/t_f]$	b/t_f
		(kN)	(kNm)	(kNm)		(mm)	(mm)	(mm)	(kN)	(kNm)	(kNm)	(%)				
1	1	485.59	528.56	-4.65	NA2	2.96	-	69.48	485.59	514.12	4.65	1.47	41.91	18.84	8.73	6.43
3	2	539.54	662.91	-97.36	NA3	38.71	10.72	16.19	538.99	649.56	97.36	1.23	60.44	13.71	8.73	4.72
7	1	1081.82	463.86	6.06	NA2	3.87	-	159.08	1081.82	465.81	6.06	0.07	31.99	18.84	8.73	6.43
9	2	1820.08	565.43	102.55	NA2	57.03	-	113.20	1820.08	576.80	102.55	0.18	33.49	13.71	8.73	4.72
38	3	295.75	-282.76	25.31	NA2	25.37	-	14.26	295.75	275.52	25.31	1.21	59.71	18.64	8.73	6.34
42	3	488.98	-267.85	-30.10	NA2	30.92	-	41.40	488.98	265.65	30.10	0.19	46.83	18.64	8.73	6.34
44	3	603.97	-224.60	-65.58	NA3	62.16	12.80	33.09	603.96	221.07	65.58	0.19	50.14	18.64	8.73	6.34
86	4	-12.41	75.24	29.16	NA3	54.84	53.83	2.68	12.66	71.62	29.16	4.02	71.20	47.34	8.73	7.38
88	4	13.29	-80.55	28.09	NA3	51.23	50.08	2.73	13.55	76.98	28.09	3.80	68.20	47.34	8.73	7.38
97	5	11.44	317.71	4.94	NA3	3.28	2.10	0.69	11.59	306.57	4.94	3.50	69.35	28.05	8.73	7.37
98	5	11.44	-317.67	-5.01	NA3	3.32	2.15	0.69	11.59	306.48	5.01	3.52	69.35	28.05	8.73	7.37
103	5	25.09	313.83	10.47	NA3	7.07	4.51	1.54	25.43	299.98	10.47	4.37	68.79	28.05	8.73	7.37
104	5	25.09	-313.96	-10.38	NA3	7.02	4.46	1.54	25.43	300.09	10.38	4.37	68.79	28.05	8.73	7.37
105	1	29.06	536.97	14.11	NA3	5.61	3.43	1.08	29.56	520.62	14.11	3.03	69.09	18.84	8.73	6.43
106	1	29.06	-536.94	-14.18	NA3	5.63	3.45	1.08	29.56	520.55	14.18	3.04	69.09	18.84	8.73	6.43
109	5	25.51	305.69	17.65	NA3	11.20	8.63	1.60	25.87	291.20	17.65	4.68	68.75	28.05	8.73	7.37
110	5	25.51	-305.53	-17.79	NA3	11.28	8.70	1.60	25.87	291.03	17.79	4.68	68.75	28.05	8.73	7.37
115	5	18.07	287.60	29.04	NA3	17.67	15.87	1.19	18.33	276.62	29.04	3.76	69.02	28.05	8.73	7.37
116	5	18.07	-287.79	-28.96	NA3	17.62	15.82	1.19	18.33	276.72	28.96	3.78	69.02	28.05	8.73	7.37

Remarks: (*): S= Section (see Fig.7.6a), (**): P=Profile (see Table 7.4);
$[d/t_w]$ and $[b_0/t_f]$ are the limited ratios.

Table 7.6: Frame-1c: Local buckling check for the active plastic-hinges at the limit state (load factor = 2.161)

Section		Given forces			Location of neutral axis				Verified-forces				Width to thickness ratios (limit and real)of the web and compressed outstand flange			
S*	P**	N	M_y	M_z	NA	b_1	b_2	z_1	$\overline{N}$	$\overline{M}_y$	$\overline{M}_z$	ς	$[d/t_w]$	d/t_w	$[b/t_f]$	b/t_f
		(kN)	(kNm)	(kNm)		(mm)	(mm)	(mm)	(kN)	(kNm)	kNm)	(%)				
39	3	-121.54	0.00	-143.55	NA4	128.00	128.00	-	-	0.00	141.72	0.16	Infinit	18.64	8.73	6.34
43	3	-121.54	0.00	-143.55	NA4	128.00	128.00	-	-	0.00	141.72	0.16	Infinit	18.64	8.73	6.34
54	3	40.61	0.00	143.62	NA4	128.00	128.00	-	-	0.00	141.72	0.16	Infinit	18.64	8.73	6.34
56	3	-37.93	0.00	143.62	NA4	128.00	128.00	-	-	0.00	141.72	0.16	Infinit	18.64	8.73	6.34
58	3	40.61	0.00	143.62	NA4	128.00	128.00	-	-	0.00	141.72	0.16	Infinit	18.64	8.73	6.34
60	3	-37.93	0.00	143.62	NA4	128.00	128.00	-	-	0.00	141.72	0.16	Infinit	18.64	8.73	6.34
85	4	-0.21	-152.95	0.00	NA2	0.00	0.00	0.07	0.21	150.77	0.00	1.43	69.84	47.34	8.73	7.38
86	4	-0.21	152.95	0.00	NA2	0.00	0.00	0.07	0.21	150.77	0.00	1.43	69.84	47.34	8.73	7.38
87	4	-0.21	-152.95	0.00	NA2	0.00	0.00	0.07	0.21	150.77	0.00	1.43	69.84	47.34	8.73	7.38
88	4	-0.21	152.95	0.00	NA2	0.00	0.00	0.07	0.21	150.77	0.00	1.43	69.84	47.34	8.73	7.38
89	4	-1.89	-152.95	0.00	NA2	0.00	0.00	0.65	1.89	150.77	0.00	1.43	70.14	47.34	8.73	7.38
90	4	-1.89	152.95	0.00	NA2	0.00	0.00	0.65	1.89	150.77	0.00	1.43	70.14	47.34	8.73	7.38
91	4	-1.89	-152.95	0.00	NA2	0.00	0.00	0.65	1.89	150.77	0.00	1.43	70.14	47.34	8.73	7.38
92	4	-1.89	152.95	0.00	NA2	0.00	0.00	0.65	1.89	150.77	0.00	1.43	70.14	47.34	8.73	7.38

Remarks: (*): S= Section (see Fig.7.6c), (**): P=Profile (see Table 7.4);
$[d/t_w]$ and $[b_0/t_f]$ are the limited ratios.

Table 7.7: Frame-7.1b – Developments at the section 7 from plastic-hinge occurs to the risk of local buckling

Step	load factor	Given forces			Location of the neutral axis				Verified-forces				Width-to-thickness ratios the web	
		N (kN)	M_y (kNm)	M_z (kNm)	NA	b_1 (mm)	b_2 (mm)	z_1 (mm)	$\overline{N}$ (kN)	$\overline{M}_y$ (kNm)	$\overline{M}_z$ (kNm)	ς (%)	$[d/t_w]$	d/t_w
1	2.080	1170.12	634.17	10.52	NA2	7.83	-	179.24	1170.12	642.61	10.52	0.30	34.24	33.43
2	2.089	1173.99	633.55	10.34	NA2	7.70	-	180.09	1173.99	641.97	10.34	0.30	34.15	33.43
3	2.097	1177.23	633.03	10.19	NA2	7.58	-	180.82	1177.23	641.44	10.19	0.30	34.08	33.43
4	2.103	1179.14	633.11	9.12	NA2	6.77	-	182.43	1179.14	641.42	9.12	0.30	33.93	33.43
5	2.109	1180.93	633.18	8.02	NA2	5.93	-	184.07	1180.93	641.43	8.02	0.29	33.77	33.43
6	2.116	1182.96	633.23	6.69	NA2	4.93	-	186.01	1182.96	641.43	6.69	0.29	33.59	33.43
7	2.130	1186.42	633.14	4.62	NA2	3.39	-	189.05	1186.42	641.33	4.62	0.29	**33.31**	**33.43**(*)

(*) Risk of local buckling; $[d/t_w]$ is the limited ratio; position of the section 7 is indicated on Fig.7.6b.

Table 7.8: Evaluation of coefficient ζ for 103 active plastic- hinges

ζ (%)	$0 \le \xi \le 1$	$1 < \zeta \le 2$	$2 < \zeta \le 3$	$3 < \zeta \le 4$	$4 < \zeta \le 4{,}68$
Number of case	16 (=15.53%)	39 (=37.86%)	19 (=18.45%)	17 (=16.51%)	12 (=11.65%)

7.5. Conclusions

Proposed technique may be installed in any plastic global analysis procedure, such as elastic-plastic analysis by the step-by-step method or by the rigid-plastic analysis by mathematical programming. The risk of local buckling at critical sections is eliminated according to Eurocode-3's requirements. The present of this subroutine does not influence other results (e.g. multiplier load), it only points out confident signs about local buckling, and the final decision belongs to the engineers (e.g. add a stiffener or change the member size). The robustness of this algorithm is proved by numerical computations. While respecting the rule of Eurocod-3, it is then an efficient implementation of local buckling detection into automatic computer code.

Chapter **8**

Plastic-hinge analysis of semi-rigid frames

The terminology *semi-rigid frame* is used to underline that the behaviours of connexions/joints are taken into account. In the traditional analysis, rigid or pinned connexions is adopted, they are the extreme cases of the semi-rigid behaviour. Obviously, the connexion behaviours influence to the frame responses, such as displacements, internal force distributions. Therefore, beside member size, we have another parameter to vary our structural solutions. By consequence, we may obtain economical benefits from the utilization of semi-rigid joints (see Jaspart (1991)[68], Colson (1992)[34], Guisse (1993)[57]).

The first investigation into semi-rigid connexions of steel frames was dealt with ninety years ago. A useful history of the domain may be found in the state-of-the-art report by Jones (1983)[73]. During the last twenty years, the studies on the semi-rigid frames occupy an important position of the building steel research domain. A large number of authors have been devoted their efforts to this direction, e.g. Chen (1989, 1991, 1996)[23, 24, 19], Kishi (1990)[82], Bjorhovde (1990)[8], Maquoi (1991, 1992)[105, 104], Jaspart (1991, 1997, 1998, 2000, 2008)[68, 70, 66, 69, 67], Kim (2001)[77], Cabrero (2005, 2007)[11, 12], among many others. On the research point of view, there are two principal fields: (1) Modelling of connexions into forces-net displacements relationships; (2) Global analysis of frames including the semi-rigid connexions.

This chapter concerns the second field where we present how CEPAO takes into account the effects of connexions in the global plastic-hinge analysis of steel frames. Various semi-rigid frames are analyzed by CEPAO; the results are compared with other researches.

Keywords: *Semi-rigid frames*; *Plastic-hinge analysis*.

8.1. Practical modelling of connexions

On the one hand, in comparison with other components, the bending moment is dominant in beam-to-column connexions. On the other hand, according to actual forms of beam-to-column joints, the rotational stiffness is the most weak compared with axial and shear stiffness. Therefore, among all deformation components of joints, the rotational deformation is the most important (Fig.8.1.a). By consequence, the behaviour of connexions is generally described by the moment-rotation relationship (Fig.8.1b). Both experiment and numerical simulation demonstrates that this relationship is nonlinear with the slope depends on the actual form of assemblages (see Jaspart (1991)[68], Chen (1991)[24]). For the practical purpose, a lot of simple expressions have been proposed to approximate actual moment-rotation curves. In the plastic global analysis, the elastic-perfectly plastic modelling is widely adopted (Fig.8.1c) (see Jaspart (2000)[69]). Two necessary parameters for this modelling are the *connexion initial*

stiffness (R) and the *ultimate moment capacity* ($M_{j,p}$). These parameters of various connexion types have been introduced in Standards (e.g. Eurocode-3 Part 1-8 [454]).

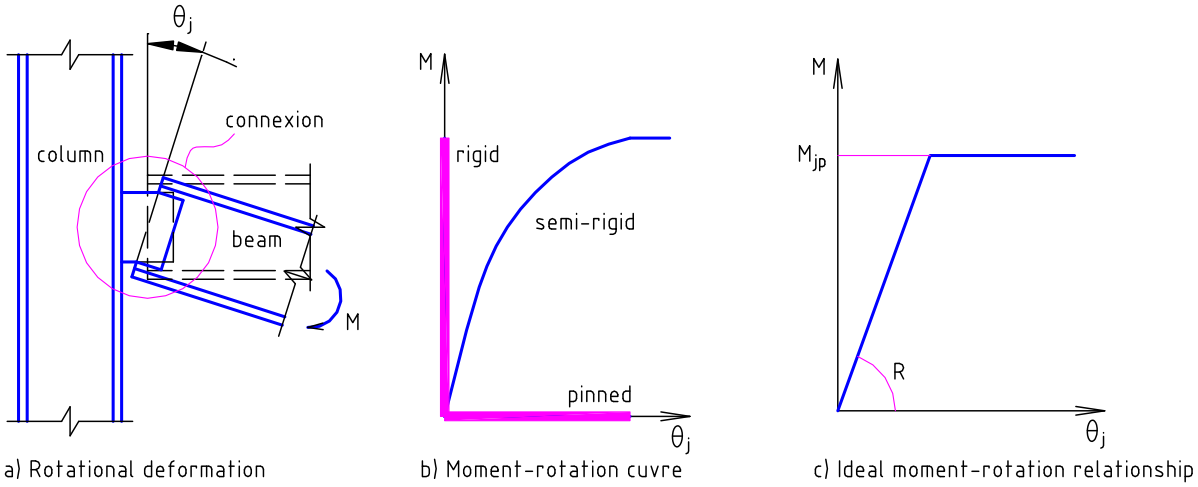

Fig.8.1. Modelling of beam-to-column connexions

8.2. Effects of semi-rigid connexions

This section deals with the taking into account effects of semi-rigid connexions in plastic-hinge analysis of steel frames. This question has been examined by many authors, e.g. Tin-Loi (1993, 1996)[145, 144], Xu (1993)[149], Kim (2001)[77], Hasan (2002)[58], Sekulović (2004)[138], Gizejowski (2006)[52], Kaveh (2006)[76], Liu (2008)[91], among others. Generally, the *spring-ends* are used to consider effects of initial stiffness while the *partial-yield surfaces* are adopted to examine the effects of ultimate strengths.

We suppose that axial and two rotational deformations of joints are considered (Fig.8.2a). Under effects of axial force and two bending moments, the joint behaviours may be modelled by a yield surface (Fig.8.2b). The behaviour shown on Fig.8.1c is a particular case of which in Fig.8.2. In the following, the effects of joints are taken into account in global plastic-hinge analysis using the connexion yield surface notion.

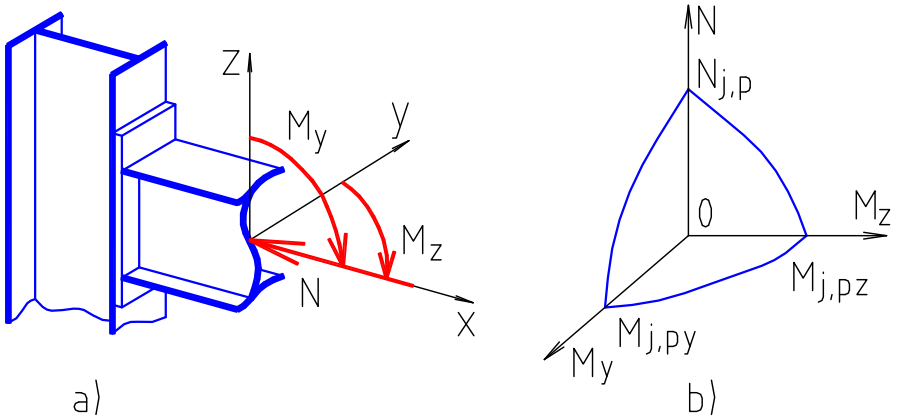

Fig.8.2. Yield surface of joints

8.2.1. Initial connexion stiffness effect

In the space, a connexion may be modelled as a three-directional spring (axial and two rotational directions) that is attached in corresponding end of beam-column elements, as the

show of Fig.8.3. With spring-ends, the physical relationship of beam-column elements [Eq.(3.22)] becomes Eq.(8.1):

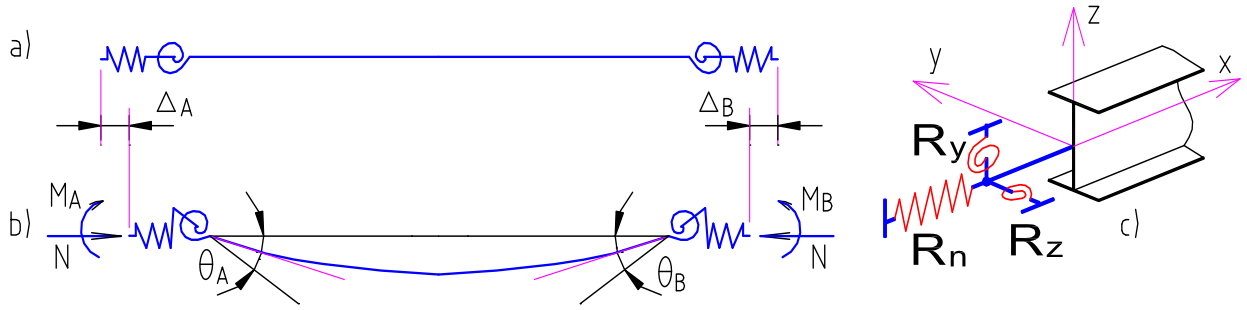

Fig.8.3. Beam-column element with spring-ends (a: initial configuration; b: deformed configuration; c: spring-ends)

$$\mathbf{D}_{\mathrm{k}}=\frac{1}{l}\begin{bmatrix} 2EA\left(\dfrac{R_{nA}}{R_{nA}+2EA/l}\right) & 0 & 0 & 0 & 0 & 0 \\ 0 & S_{1A}^{*}EI_y & 0 & 0 & -S_{2}^{*}EI_y & 0 \\ 0 & 0 & S_{3A}^{*}EI_z & 0 & 0 & -S_{4}^{*}EI_z \\ 0 & 0 & 0 & 2EA\left(\dfrac{R_{nB}}{R_{nB}+2EA/l}\right) & 0 & 0 \\ 0 & -S_{2}^{*}EI_y & 0 & 0 & S_{1B}^{*}EI_y & 0 \\ 0 & 0 & -S_{4}^{*}EI_z & 0 & 0 & S_{3B}^{*}EI_z \end{bmatrix}; \qquad (8.1)$$

with :

$$S_{1A}^{*}=\left(S_1+\frac{EI_yS_1^2}{lR_{yB}}-\frac{EI_yS_2^2}{lR_{yB}}\right)/R_y^{*}; \qquad (8.2a)$$

$$S_{1B}^{*}=\left(S_1+\frac{EI_yS_1^2}{lR_{yA}}-\frac{EI_yS_2^2}{lR_{yA}}\right)/R_y^{*}; \qquad (8.2b)$$

$$S_{3A}^{*}=\left(S_3+\frac{EI_zS_3^2}{lR_{zB}}-\frac{EI_zS_4^2}{lR_{zB}}\right)/R_z^{*}; \qquad (8.2c)$$

$$S_{3B}^{*}=\left(S_3+\frac{EI_zS_3^2}{lR_{zA}}-\frac{EI_zS_4^2}{lR_{zA}}\right)/R_z^{*}; \qquad (8.2d)$$

$$S_2^{*}=-S_2/R_y^{*}; \qquad (8.2e)$$

$$S_4^{*}=-S_4/R_z^{*}; \qquad (8.2f)$$

$$R_y^{*}=\left(1+\frac{EI_yS_1}{lR_{yA}}\right)\left(1+\frac{EI_yS_1}{lR_{yB}}\right)-\left(\frac{EI_y}{l}\right)^2\frac{S_2^2}{R_{yA}R_{yB}}; \qquad (8.2g)$$

$$R_z^{*}=\left(1+\frac{EI_zS_3}{lR_{zA}}\right)\left(1+\frac{EI_zS_3}{lR_{zB}}\right)-\left(\frac{EI_z}{l}\right)^2\frac{S_4^2}{R_{zA}R_{zB}}; \qquad (8.2h)$$

in Eqs. (8.1-8.2h): S_1, S_2, S_3, S_4 are the stability functions (Eqs. (6.7a) and (6.7b)); R_{yA}, R_{yB} are the stiffness in the Y-direction (strong axis) of spring A and B, respectively; R_{zA}, R_{zB} are the

stiffness in the Z-direction (weak axis) of spring A and B, respectively; R_{nA}, R_{nB} are the axial stiffness of spring A and B, respectively; normally, $R_{nA} = R_{nB} = \infty$.

8.2.2. Ultimate strength effect

Let $M_{j,py}, M_{j,pz}, N_{j,p}$ be respectively the plastic moment in Y-direction, the plastic moment in Z-direction and the squash load of connexions. As the cross-sections, in principle, we have yield surfaces for connexions:

$$\Phi_j(N/N_{j,p}, M_y/M_{j,py}, M_z/M_{j,pz}) = 0 .$$

The partial-yield surface ($\overline{\Phi}$) is the surface that envelope the intersection zone. The latter is constituted by the intersection between the cross-section yield surface and the joint yield surface (Fig.8.4a).

However, for the practical purpose, one may use the simple partial-yield surface. It is deduced from the cross-section yield surface but the plastic moments of sections (M_{py}, M_{pz}) are replaced by which of joints ($M_{j,py}, M_{j,pz}$) (Fig.8.4b).

$$\overline{\Phi} \equiv \Phi(N/N_p, M_y/M_{j,py}, M_z/M_{j,pz}) = 0$$

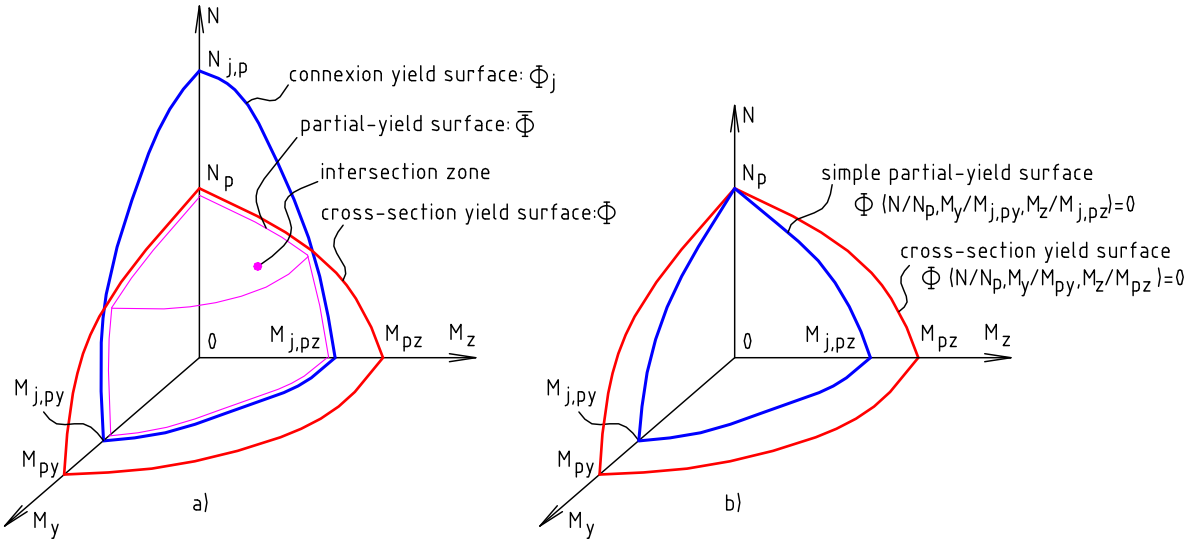

Fig.8.4. Partial-yield surface

8.2.3. Function objective including connexion cost

Clearly, there is a correlation between the properties (stiffness, strength) and the cost of connexions. Some authors were mathematized this relationship to take into account the connexion cost in optimization problems (e.g. Xu (1993)[149], Simões (1996)[139], Hayalioglu (2005)[59]). In present work, we utilise the cost function proposed by Simões (1996)[139]. According to this reference, the total weight (cost) of a member *i* including its connexions may have the following form:

$$Z_i = g_i + 0.2g_i - 0.8g_i\chi_i + 1.6g_i\chi_i^2 \qquad (8.3)$$

where g_i is the member weight, coefficient χ_i is the scale factor defined as:

$$\chi_i = 1/(1 + 3E_iI_{yi}/R_{yi}l_i) \qquad (8.4)$$

Where E_i, I_{yi}, l_i are respectively the Young'modulus, the inertia moment and the length of the member; R_{yi} is the initial stiffness of connexion about strong axis. It is evident that: $0 \le \chi \le 1$, in which $\chi = 0$ at the pinner-connexions and $\chi = 1$ at the rigid-connections. We observe in Eq.(8.4) that the cost of a steel member is increased by 20% if it has pinner-connection; and by 100% if its end-connection is fully rigid.

Coming back to the rigid-plastic design problem, but with the new objective function Eq.(8.4), for the plastic design problem, it is convenient to define the conventional length calculating by

$$\bar{l}_i = l_i + 0.2l_i - 0.8l_i\chi_i + 1.6l_i\chi_i^2 \tag{8.5}$$

It replace the actual length in the function objective of optimization problems (Eq.(5.1)).

8.3. Numerical examples and discussions

For instant, it seem that no available benchmark for 3-D semi-rigid frames in the open literature; the following examples are the planar frames. The aims of this section are: (1) comparing the results given by CEPAO with the other researches; (2) observing the behaviour of semi-rigid frames; (3) confirming again the good convergence between the direct method and the step-by-step method.

8.3.1. Example 8.1

Shakedown analysis of semi-rigid bending frames: These examples have been already analysis by Tin-Loi (1993)[145]. In this reference, the relation between the initial stiffness and the plastic moment of connexions are chosen according to the classification system that was proposed by Bjorhovde (1990)[8]. The relationship plastic moment-rotation of connexions is defined as:

$$M_{j,p} = (EI_y / \nu h)\theta_j \,, \tag{8.6}$$

where ν is a constant; h is the connecting beam depth. The graphical illustration of this behaviour is shown in Fig.8.5 where the ranges for rigid, semi-rigid and flexible behaviour are shown. Let s be the connexion strength, $s = M_{j,p}/M_p$ where M_p is the plastic moment of the beam. Intermediate values of plastic moment for given stiffness are interpolated in accordance with the dashed line (Fig.8.5). Some values of s and corresponding values of ν are shown on Table 8.1.

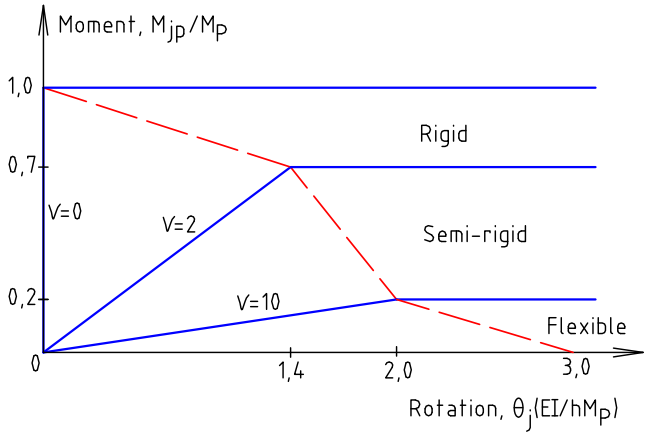

Fig.8.5. Moment – rotation relationship for connexions

Table 8.1: Relation between s and ν

s	0.1	0.2	0.3	0.4	0.5	0.6	0.7	0.8	0.9	1.0
ν	25.0000	10.0000	6.2667	4.4000	3.2800	2.5333	2.0000	1.1667	0.5185	0.0000

Note that the relation between R_{yA}, R_{yB} (Eqs.(8.2a) and (8.2b)) and ν is:

$$R_y = EI_y / \nu h .$$

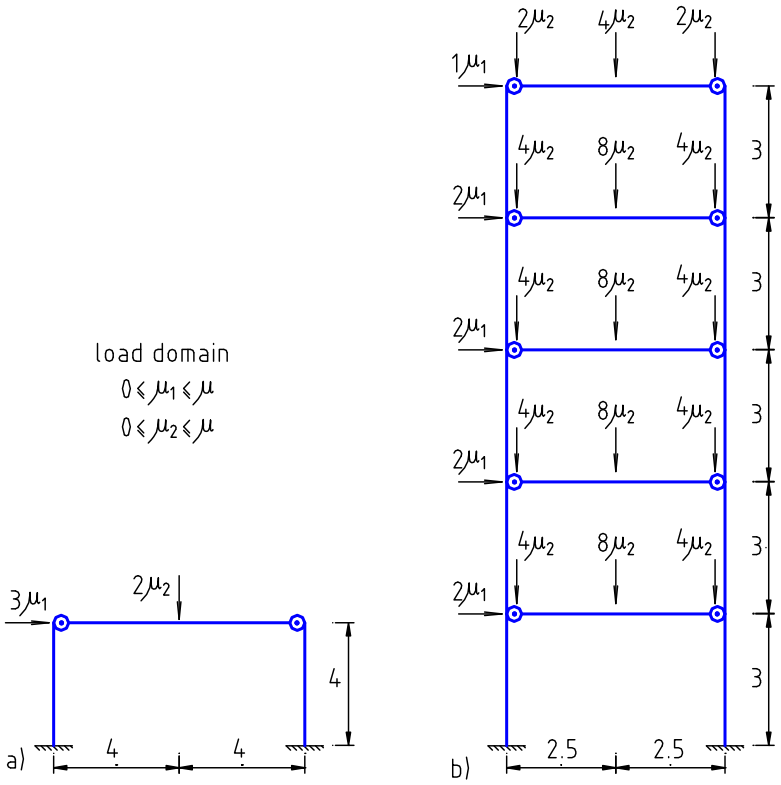

Fig.8.6. Example 8.1 – frame geometry and loading (a-frame 8.1a; b-frame 8.1b)

These examples aim to find the difference between shakedown and collapse limits for varying connection strengths. Two following mechanical and geometric data (in tonne and meter units) are examined:

Frame-8.1a: The frame geometry and loading are shown in the Fig.8.6a, the properties of all elements are: $E = 2.1\times10^{7}$; $I = 118.5\times10^{-6}$; $M_P = 20$; $h = 0.3$;

Frame-8.1b: The frame geometry and loading are shown in the Fig.8.6b, with the following properties: for the column: $E = 2.1\times10^{7}$; $I = 85.2\times10^{-6}$; $M_P = 10$; for the beams: $E = 2.1\times10^{7}$; $I = 118.5\times10^{-6}$; $M_P = 20$; $h = 0.3$.

Table 8.2 and Figs. 8.7a and 8.7b show that the results given by CEPAO are well agreement with which of Tin-Loi [145]. With the frame 8.1a, the alternating plasticity occurs in the shakedown analysis with connexion strength $s = 0.1$ and 0.2.

Table 8.2: Example 8.1 – Load Multipliers

Type of analyse	Connection strengths (s)									
	0.1	0.2	0.3	0.4	0.5	0.6	0.7	0.8	0.9	1.0
Frame 8.1a										
Collapse by Tin-loi	3.70	4.01	4.36	4.67	5.05	5.22	5.43	5.60	5.81	6.02
Collapse by CEPAO	3.67	4.00	4.33	4.67	5.00	5.20	5.40	5.60	5.80	6.00
Shakedown by Tin-Loi [145]	2.42	3.04	3.77	4.01	4.25	4.53	4.77	5.01	5.29	5.57
Shakedown by CEPAO	2.54	3.28	3.78	4.03	4.28	4.54	4.81	5.06	5.30	5.56
Frame 8.1b										
Collapse by Tin-Loi	0.53	0.80	1.02	1.14	1.25	1.34	1.42	1.49	1.49	1.49
Collapse by CEPAO	0.53	0.80	1.02	1.14	1.25	1.33	1.42	1.48	1.48	1.48
Shakedown by Tin-Loi [145]	0.50	0.71	0.91	1.00	1.12	1.18	1.25	1.31	1.35	1.35
Shakedown by CEPAO	0.50	0.71	0.91	1.01	1.12	1.19	1.26	1.32	1.35	1.35

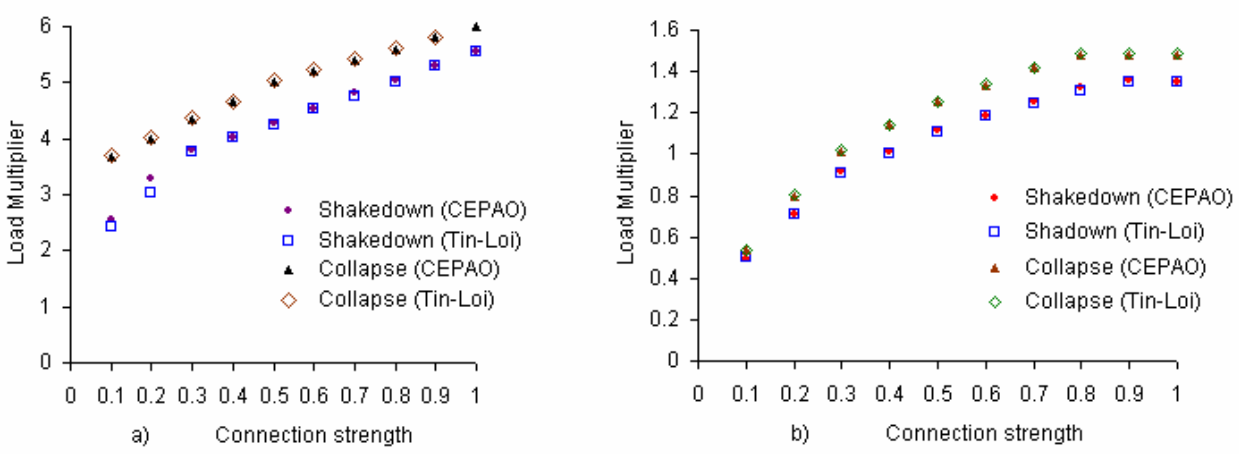

Fig.8.7. Example 8.1-Variation of load multiplier with connection strength
(a: frame-8.1a; b: frame-8.1b)

8.3.2. Example 8.2

Analysis and optimization for semi-rigid bending frame by CEPAO: A twenty- story three-bay semi-rigid frame with geometry and loading shown on the Fig.8.8 is analysed by CEPAO with the following studies: elastic analysis; first-order elastic-plastic analysis; second-order elastic-plastic analysis; rigid-plastic analysis; shakedown analysis; optimization-limit; optimization-shakedown. The ultimate strength-initial stiffness relationship of connexions are defined again by Fig.8.5.

Concerning loading domain, for shakedown problems, two cases are considered: a) $0 \le \mu_1 \le \mu$, $0 \le \mu_2 \le \mu$ and b) $-1 \le \mu_1 \le \mu$, $0 \le \mu_2 \le \mu$. For fixed or proportional loading obviously we must have: $\mu_1 = \mu_2 = \mu$;

For the optimal problem, forty different groups of elements are chosen as conception variables (Fig.8.8) and the load factor is fixed $\mu = 0.25$. The cost of semi-rigid connections are considered by the conventional length (Eq.(8.5)). In the optimal-shakedown problem, the results of the iterative process consisting of updating the inertia moments depending on the plastic capacity: $I_k/I_{max} = (M_{pk}/M_{pmax})^{1.4}$.

For the analysis problems, seven different groups of elements are considered (Table 8.3). Tables 8.4 and 8.5 and Figs.8.9 - 8.11 present some results, in which the units are kN and m.

Table 8.3: Example 8.2 – Profile used for analysis problems

Groups	1-5	6-10	11-15	16-20	21-25	26-30	31-35	36-40
Profile	IPE550	IPE500	IPE450	IPE330	HE600A	HE550A	HE450A	HE360

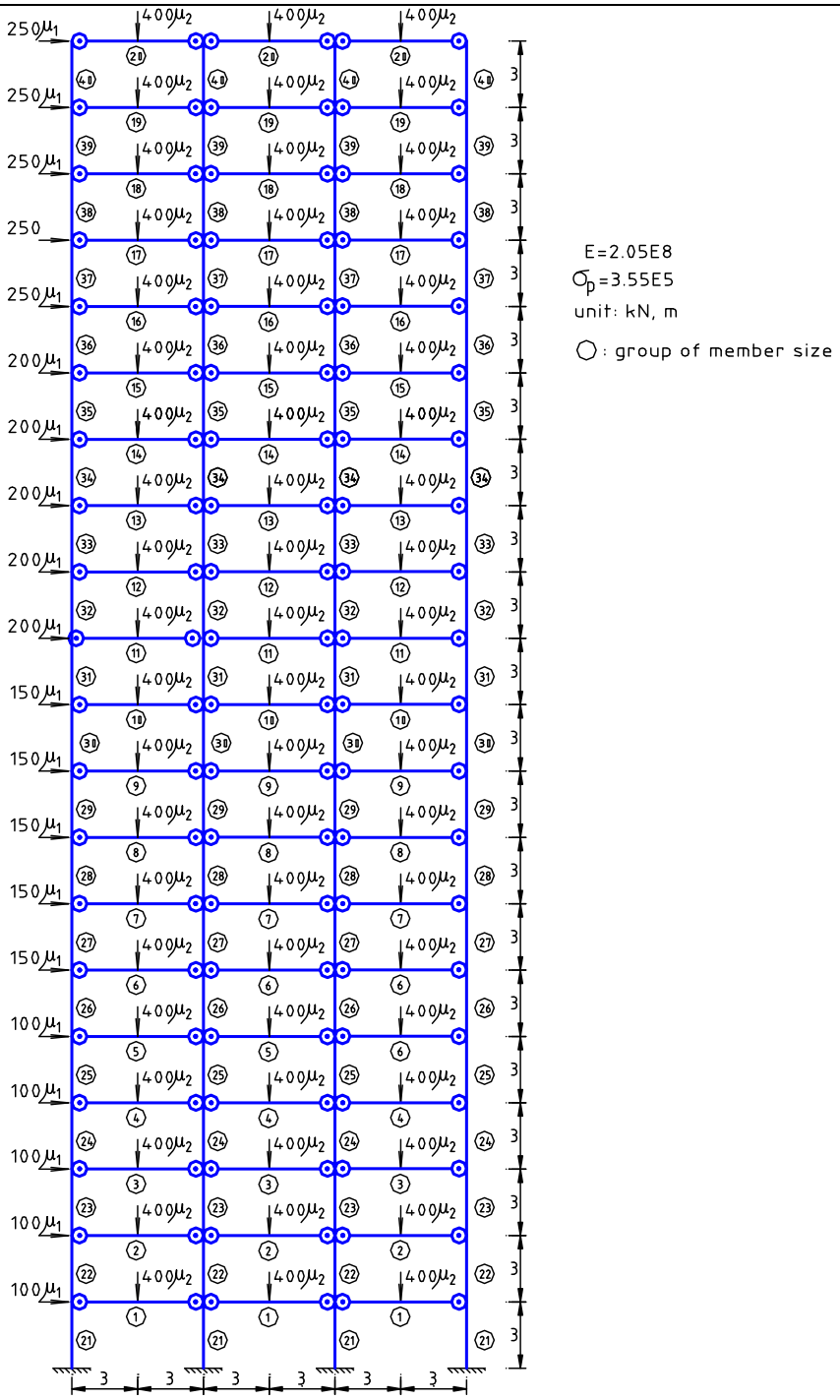

Fig.8.8. Example 8.2-frame geometry, group of element and loading

CEPAO has given a picture on the frame behaviour, some remarks are pointed out:

- The frame behaviours are regularly reflected by connexion properties (Figs.8.9 and 8.10a). There is a similar between Fig.8.5 and Fig.8.9.

- Table 8.4 shows that the load factors given by the direct method and the step-by-step method are exactly coincided. This has not completely obtained in space frames where some small differences exist. Because in the 2-D bending frames, two plastic conditions are the same in two methods (bending frame).

- In the case of small connection strengths or symmetric loading, the load multipliers determined by shakedown analysis are the smallest (alternating plasticity occurs). In the design problems, there exists a value of connection strength (s=0.7 in Fig.8.11b) corresponding to the minimum weight of the frame (including connections cost). Mentioned value depends on the *conventional length* (Eq.(8.5)). En fact, the latter depends on a lot of parameters: the material cost, the fabrication cost, etc.

Table 8.4: Example 8.2 – Load Multipliers of analysis problems

Type of analyse	Connection strengths									
	0.1	0.2	0.3	0.4	0.5	0.6	0.7	0.8	0.9	1.0
Rigid-Plastic	0.080	0.121	0.162	0.202	0.244	0.284	0.324	0.360	0.396	0.432
Elastic-plastic first order	0.080	0.121	0.162	0.202	0.244	0.284	0.324	0.360	0.396	0.432
Elastic-plastic second order	0.053	0.088	0.127	0.167	0.205	0.241	0.280	0.316	0.354	0.392
Shakedown, load domain (a)	0.065*	0.110	0.145	0.181	0.217	0.253	0.288	0.324	0.359	0.394
Shakedown, load domain (b)*	0.037	0.070	0.096	0.134	0.166	0.198	0.229	0.260	0.290	0.320

(*) alternating plastic occurs.

Table8.5. Example 8.2 – Results of optimal problems

Type of optimization	Connection strengths (s)						
	0.4	0.5	0.6	0.7	0.8	0.9	1.0
Theoretical weight (x10^6)							
Optimal – Limit (*)	0.280	0.242	0.215	0.196	0.180	0.168	0.158
Optimal – Shakedown (*)	0.315	0.260	0.230	0.208	0.192	0.192	0.169
Optimal – Limit (**)	0.408	0.385	0.378	0.378	0.383	0.393	0.405
Real weight (tonne) – after stability checks							
Optimal-Limit (*)	62.13	59.84	56.80	52.18	51.73	49.83	49.41
Optimal-Limit (**)	67.73	66.53	64.53	61.00	64.32	66.93	71.99

(*) member' weight considered, (**) member + semi-rigid connections' weight considered.

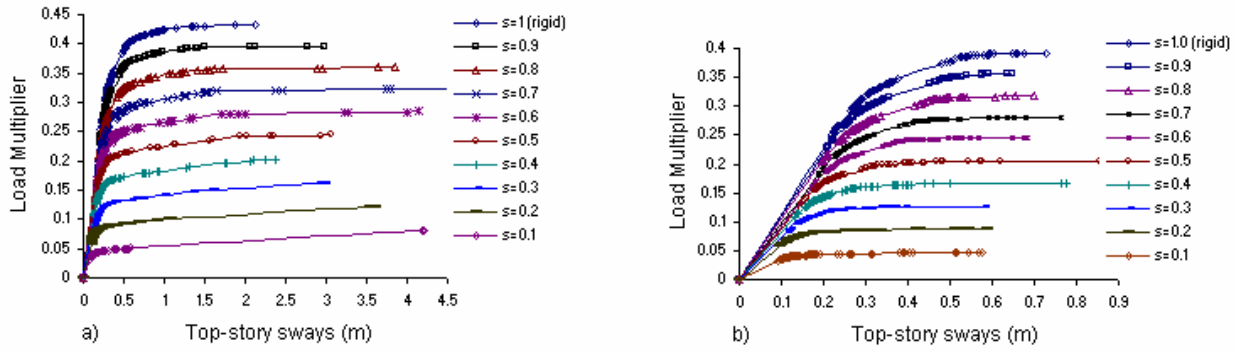

Fig.8.9. Example 8.2-Load-deflection result of step-by-step analysis (a – First-order; b – Second-order)

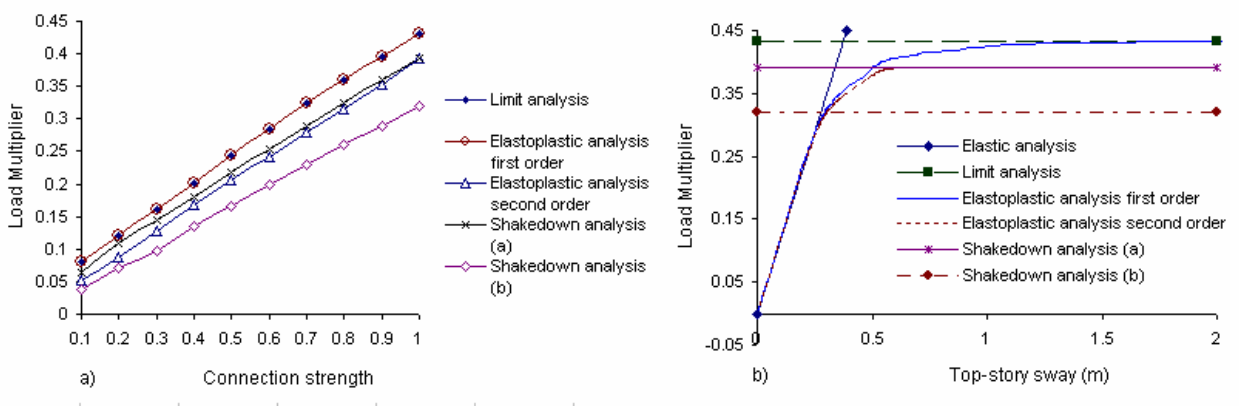

Fig.8.10. Example 8.2 (a- load multiplier; b- load-deflection result)

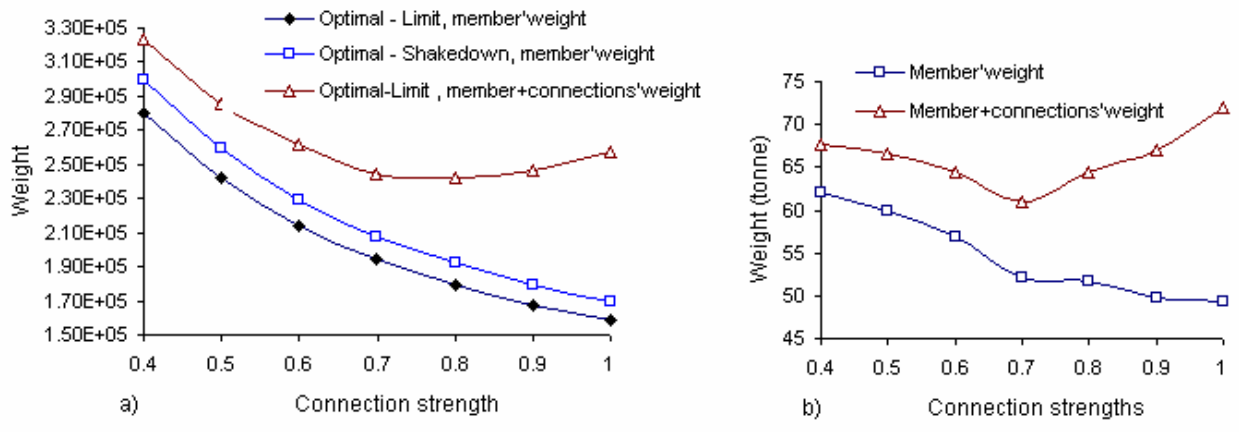

Fig.8.11. Example 8.2-Variation of weight according to connection strengths
(a -Theoretical weight; b-Real weight of optimal-limit)

8.3.3. Example 8.3: *Limit analysis of semi-rigid frames*: a series of semi-rigid frames have been already considered by Jaspart (1991)[68] (Chapter 9) using FINELG software. The frames are grouped into three classes B, C and D as the show of Figs.8.12-8.14. Figures 8.15-8.17 reports the loading types. With limit analysis that gives load multipliers, only the ultimate strengths of connexions are necessary, the joints initial stiffness are not used.

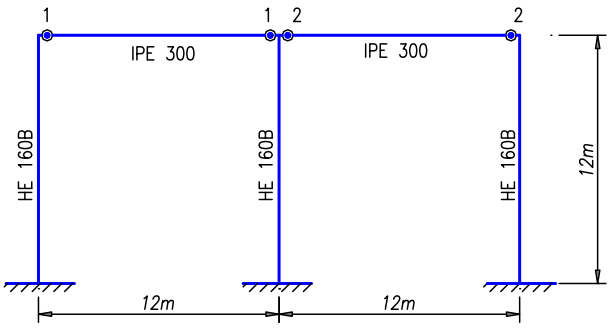

Fig.8.12. Example 8.3- structure of type B

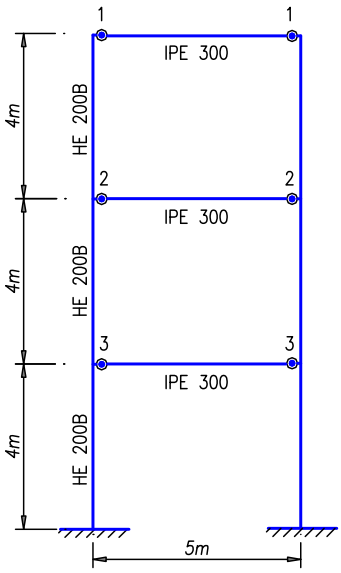

Fig.8.13. Example 8.3- structure of type C

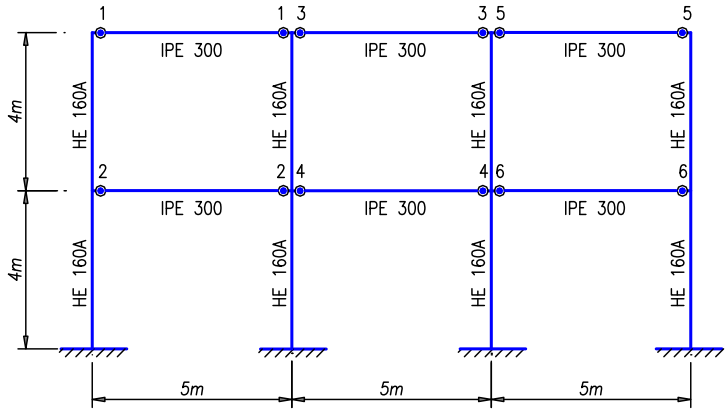

Fig.8.14. Example 8.3- structure of type D

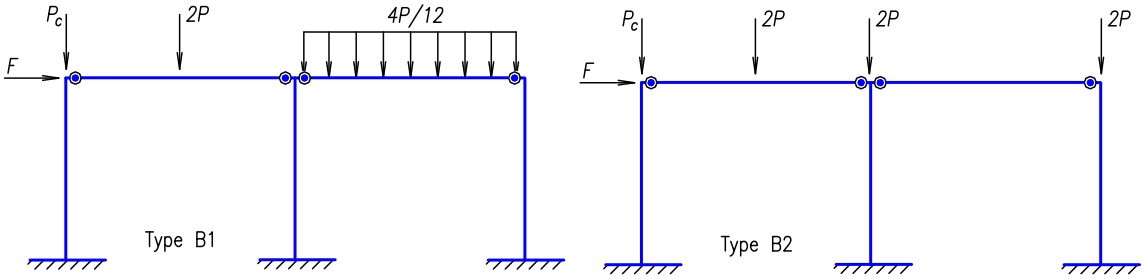

Fig.8.15. Example 8.3- loading for structure of type B

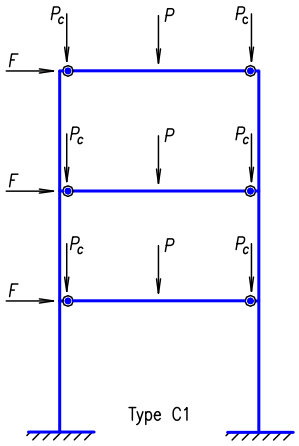

Fig.8.16. Example 8.3- loading for structure of type C

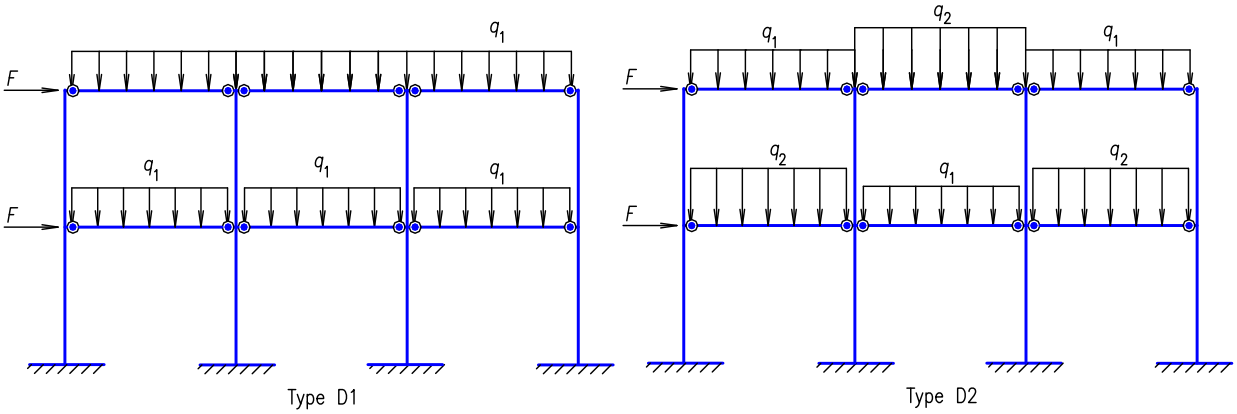

Fig.8.17. Example 8.3- loading for structure of type D

On the point of view of semi-rigid connexion research, the discussions were underlined in Jaspart (1991)[68], they are not rewritten herein. Tables 8.6-8.8 show the load multipliers given by FINELG and CEPAO. The mechanic collapses of the structures are respectively reported on Figures 8.18-8.20. The results of two programs are in agreement except the case of structures DP5 and DP6; it seems that the axial force effects are neglected in [68]. The results point out again the convergence between two methods in CEPAO.

Table 8.6: Example 8.3- load multiplier given by FINELG (Table 9.4 [68]) and CEPAO (structure B)

Structures	Loading (Fig.8.15)					Connexion-strength (Fig.8.12)		Load multipliers		
									CEPAO	
	Type	F(kN)	P(kN)	P_c(kN)	H/V	$M_{j,p1}$ (kNm)	$M_{j,p2}$ (kNm)	FINELG	Step-by-step method	Direct method
BP1	1	12.0	12.0	36.0	0.11	147.7	105.0	2.98	2.96	2.91
BP2	1	12.0	12.0	36.0	0.11	147.7	77.0	2.96	2.93	2.90
BP3	1	12.0	12.0	36.0	0.11	147.7	39.0	2.59	2.59	2.58
BP4	1	12.0	12.0	36.0	0.11	105.0	77.0	2.79	2.78	2.75
BP5	1	12.0	12.0	36.0	0.11	77.0	105.0	2.69	2.67	2.64
BP6	1	12.0	12.0	36.0	0.11	105.0	147.7	2.82	2.78	2.77
BP7	1	12.0	12.0	36.0	0.11	0.0	147.7	2.05	2.17	2.06
BP8	1	12.0	12.0	36.0	0.11	39.0	147.7	2.51	2.50	2.47
BP9	1	12.0	12.0	36.0	0.11	105.0	39.0	2.59	2.59	2.58
BP10	1	12.0	12.0	36.0	0.11	77.0	77.0	2.66	2.65	2.62
BP11	2	12.0	12.0	36.0	0.11	147.7	39.0	2.74	2.72	2.67
BP12	2	12.0	12.0	36.0	0.11	147.7	77.0	2.96	2.94	2.90
BP13	2	12.0	12.0	36.0	0.11	147.7	105.0	2.98	2.96	2.91
BP14	1	12.0	6.0	18.0	0.22	77.0	147.7	3.43	3.41	3.35

Table 8.7: Example 8.3- load multiplier given by FINELG (Table 9.5 [68])and CEPAO (structure C)

Structures	Loading (Fig.8.16)					Connexion-strength (Fig.8.13)	Load multipliers		
								CEPAO	
	Type	F(kN)	P(kN)	P_c(kN)	H/V	$M_{j,p1}=M_{j,p2}=M_{j,p3}$ (kNm)	FINELG	Step-by-step method	Direct method
CP1	1	10.0	100.0	50.0	0.05	25.0	1.35	1.32	1.31
CP 2	1	10.0	100.0	50.0	0.05	50.0	1.50	1.47	1.46
CP 3	1	10.0	100.0	50.0	0.05	75.0	1.65	1.61	1.60
CP 4	1	10.0	100.0	50.0	0.05	100.0	1.80	1.75	1.74
CP 5	1	10.0	100.0	50.0	0.05	125.0	1.96	1.90	1.88
CP 6	1	10.0	100.0	50.0	0.05	147.58	2.09	2.03	2.00
CP 7	1	2.0	100.0	50.0	0.05	100.0	1.98	1.98	1.97
CP 8	1	20.0	40.0	80.0	0.10	100.0	1.88	1.77	1.75

Table 8.8: Example 8.3- load multiplier given by FINELG (Table 9.6 [68])and CEPAO (structure D)

Structures	Loading (Fig.8.17)					Connexion-strength (Fig.8.14)	Load multipliers		
								CEPAO	
	Type	F(kN)	q_1 (kN/m)	q_2 (kN/m)	H/V	$M_{j,p1}=\ldots=M_{j,p6}$ (kNm)	FINELG	Step-by-step method	Direct method
DP1	1	5.0	40.0	-	0.0083	25.0	1.38	1.38	1.38
DP2	1	5.0	40.0	-	0.0083	37.5	1.48	1.48	1.47
DP3	1	5.0	40.0	-	0.0083	51.6	1.59	1.59	1.58
DP4	1	5.0	40.0	-	0.0083	120.0	1.89	1.87	1.85
DP5	1	25.0	20.0	-	0.083	120.0	2.30	*2.04*	*1.99*
DP6	2	20.0	20.0	40.0	0.222	120.0	2.14	*1.78*	*1.75*

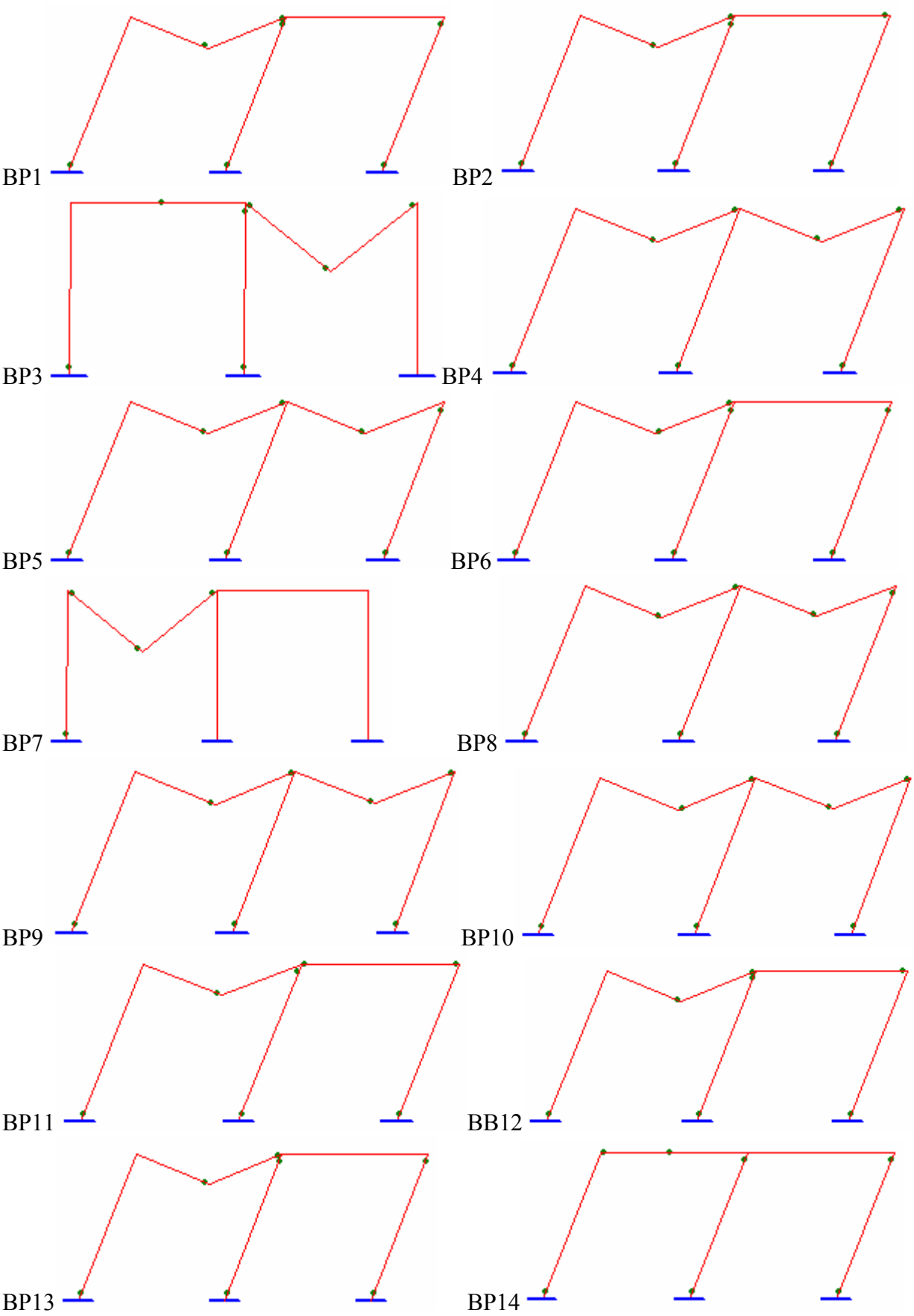

Fig.8.18. Example 8.3- collapse mechanic of structure B given by CEPAO (direct method)

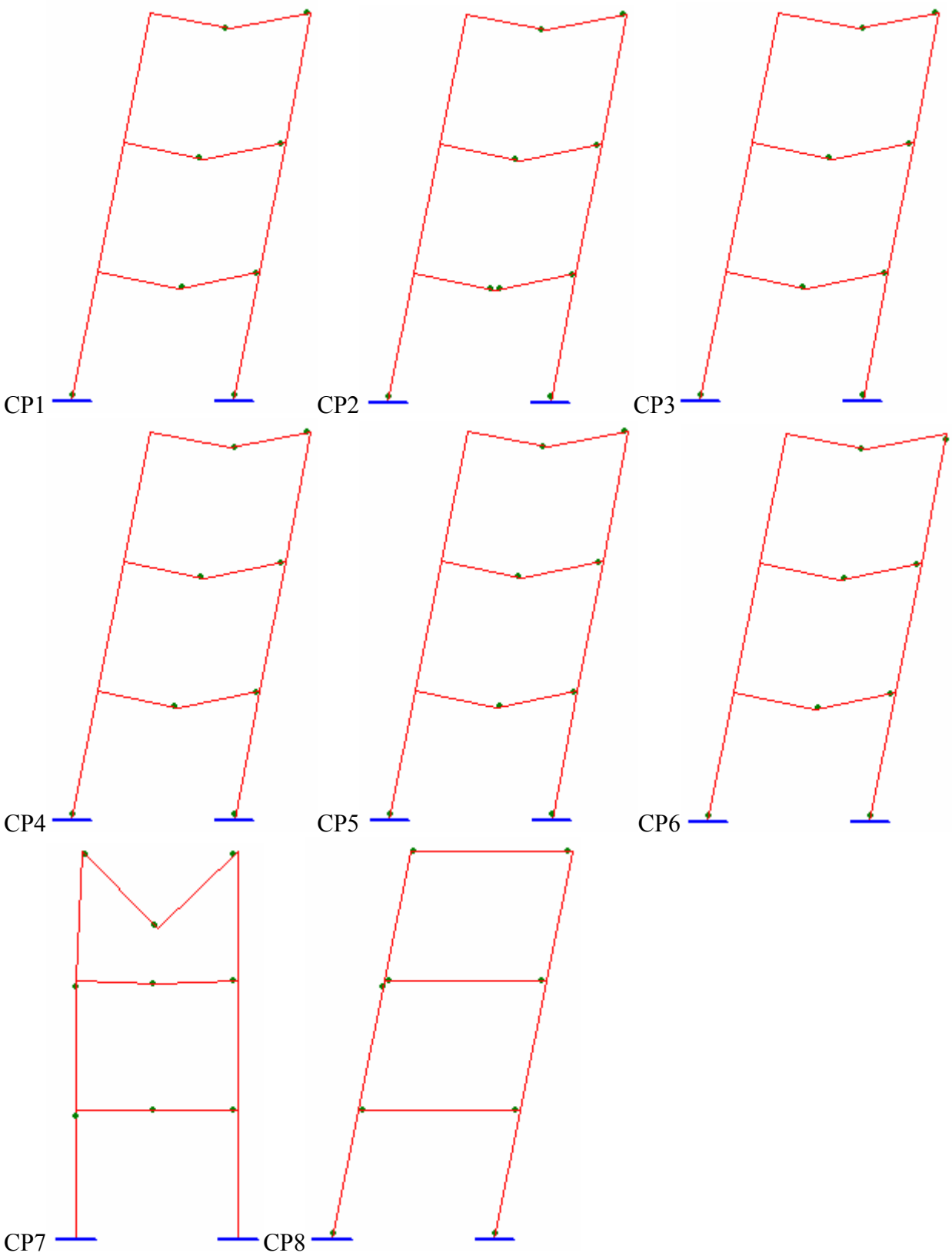

Fig.8.19. Example 8.3- collapse mechanic of structure C given by CEPAO (direct method)

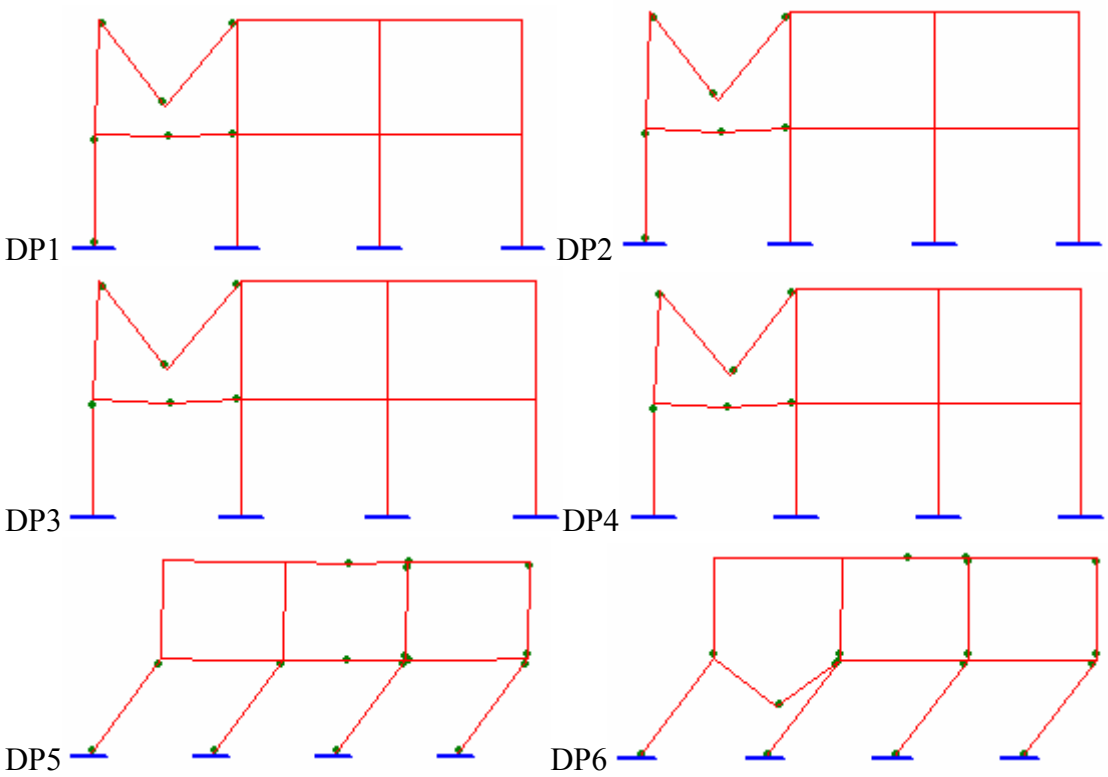

Fig.8.20. Example 8.3- collapse mechanic of structure D given by CEPAO (direct method)

8.4. Conclusion

This chapter demonstrates that the global plastic analysis with the plastic-hinge model is suitable to take into account the semi-rigid behaviour of connexions. The numerical examples show that CEPAO is a useful tool for analysis and optimization of semi-rigid steel frames.

Chapter 9

CEPAO package: application aspect

9.1. Introduction

The previous chapters have presented the algorithms for various approaches of plastic-hinge analysis and design of 3-D steel frames. They were completely implemented in CEPAO using FORTRAN language. Fig.9.1 shows the global organization of CEPAO package. As the any computer program, the organization may be divided into three principal parts: input data, "black box" and output data.

The "black box" is the treatment centre that transfers the input data into the output date. It is the kernel and was formulated in previous chapters for 3-D steel frames and in Nguyen-Dang (1984)[117] for the 2-D bending frames. Many techniques are utilized to improve the computer capability (time and/or storage); however, they are not presented in this thesis.

On the application aspect, the input and output systems are very important. In some measure, they show the automatic level of computer programs. Although the input and output systems are not the aim of this thesis but we strive to minimize burden to users. It is demonstrated in the following sections.

9.2. Input data

9.2.1. Discretization of frames

As the discussion in Chapter 3, the element used in CEPAO must satisfy the following condition: straight, prismatic (the area is constant), no load. Therefore, the distributed load must be lumped; with the global analysis, the uniform load applies on the beam may be divided into three concentrated load as the show of Fig.9.2. The frames are discretized by a node layout that are and only are the following positions (Fig.9.3): intersections of beam-to-column, under concentrated load and variation of sections (rare).

9.2.2. Input file (see Table 9.1)

9.3. Output data

In CEPAO, there are two types of output data: text file and graphic image. In principle, the text file may furnish all information during the computational procedure. However, the text file does not us give the intuitive views, without that we have difficult to giving the discussions. In the numerical examples of previous chapters, some graphics furnished by CEPAO have been presented. To have a systematic view, Fig.9.5 (the captions written in French) shows an example that is completely described by "graphic-language". This example was realized by the 2-D version of CEPAO. In these figures, the unit is not appeared, the number indicate the ratio between the quantities. This example also confirms that CEPAO is a package; we may find in these images almost "keywords" of framework plastic analysis domain.

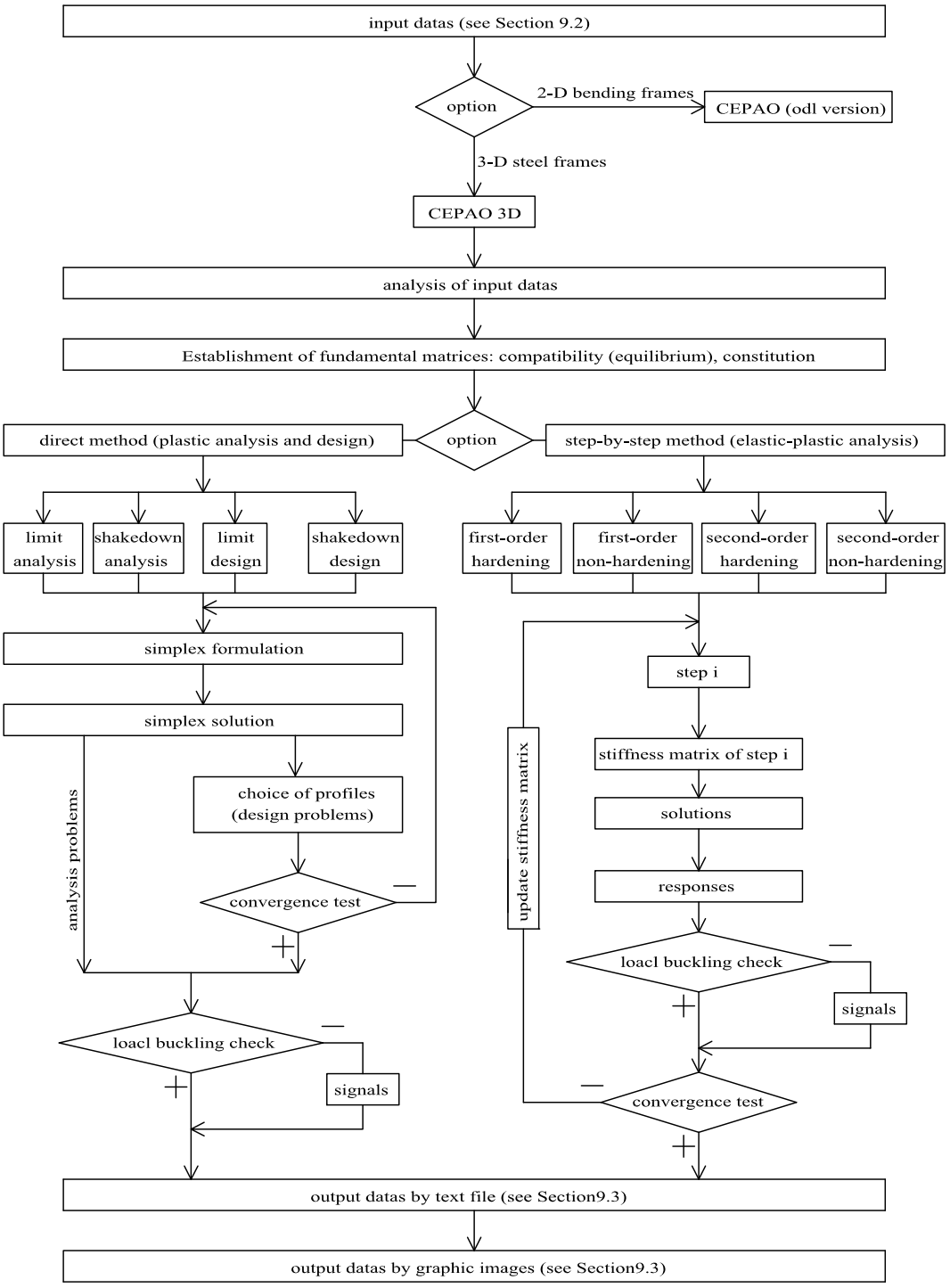

Fig.9.1. Global organization of CEPAO (version 2007)

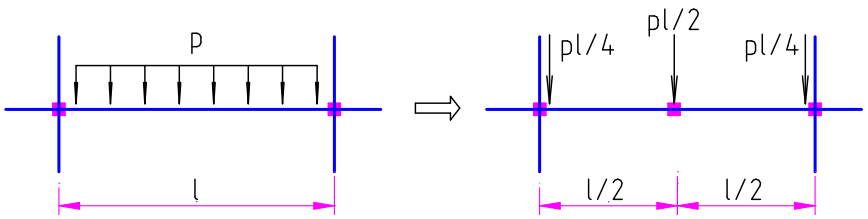

Fig.9.2. A simple method to lump the distributed load

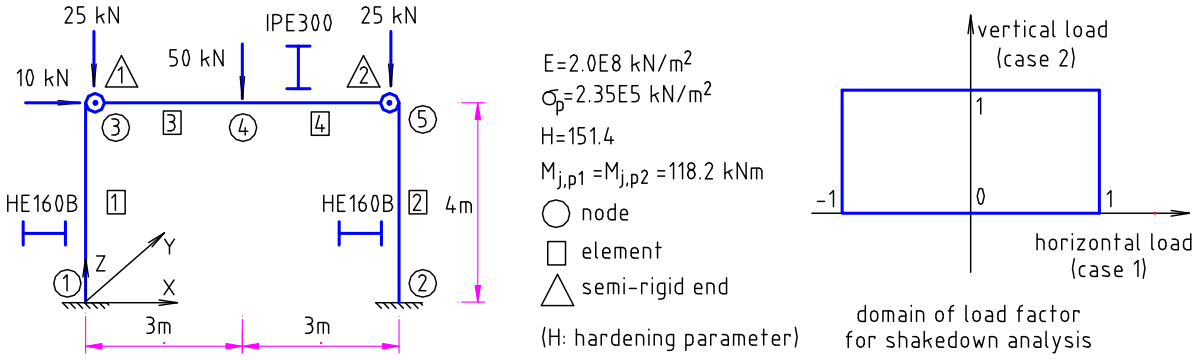

Fig.9.3. Discretization of frames

Table 9.1: Description of the input file

Bloc	Description	Data (to be inputted)	Example (Fig.9.3)
1	General definitions	-Type of frame: 2-D bending/3-D -Type of problem: analysis/design; -Type of method: limit/shakedown/first-order/second-order…	PLANNE/SPATIA ANALYS/OPTIMA LIMITE/ADAPTA/PASAPA/ PDELTA...
2	General information	-Number of: node, element, profile used, fixed node, loading case, load	5 4 2 2 2 4
3	Node information	-Co-ordinate (X, Y, Z)	0.0 0.0 0.0 6.0 0.0 0.0 0.0 0.0 4.0 3.0 0.0 4.0 6.0 0.0 4.0
4	Element information	-End-nodes; local axis definition (Fig.9.4); material referenced; semi-rigid information of its nodes (initial stiffness, ultimate strength).	1 3 1 1 1.0 1.0 1.0 1.0 2 5 1 1 1.0 1.0 1.0 1.0 3 4 3 2 0.8(*) 1.0 1.0 1.0 4 5 3 2 1.0 1.0 0.8 1.0
5	Material information	European /American profile (E/A); Its order in the database (see Tables 9.1 and 9.2); Young'modulus; yield strength; Hardening parameter.	E 56 2.0E8 2.35E5 151.4 E 53 2.0E8 2.35E5 151.4
6	Loading information	-Number of loads of the loading case 1 -Domain (for shakedown analysis) Node; direction; value of the loads (Fig.9.3). -Number of loads of the loading case 2 -Domain (for shakedown analysis) Node; direction; value of the loads	1 -1 1 3 1 10 3 0 1 3 3 -25; 4 3 -50; 5 3 -25
7	Bound condition	Fixed nodes	1 2

Remark: (*) $0.8=M_{j,p}/M_{p(IPE300)} = 118.2/147.7$.

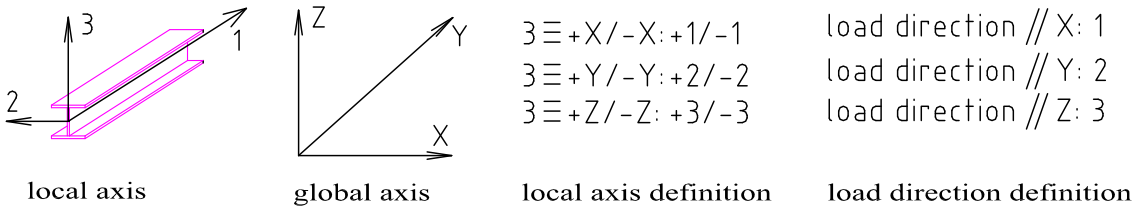

Fig.9.4. Convention of local axis and of load direction

Table 9.2: European profiles

Profile	Order	Profile	Order	Profile	Order	Profile	Order	Profile	Order
IPE 80 A	1	IPN 160	19	HE 300 AA	85	HE 900 A	209	HD 360 x 162	165
IPE 80	2	IPN 180	26	HE 300 A	104	HE 900 B	219	HD 360 x 179	176
IPE A 100	4	IPN 200	34	HE 300 B	131	HE 900 M	228	HD 360 x 196	186
IPE 100	5	IPN 220	41	HE 300 M	202	HE 900 x 391	242	HD 400 x 187	181
IPE A 120	7	IPN 240	47	HE 320 AA	87	HE 900 x 466	257	HD 400 x 216	195
IPE 120	8	IPN 260	51	HE 320 A	115	HE 1000 AA	196	HD 400 x 237	201
IPE A 140	9	IPN 280	59	HE 320 B	140	HE 1000 x 249	207	HD 400 x 262	212
IPE 140	13	IPN 300	67	HE 320 M	204	HE 1000 A	215	HD 400 x 287	218
IPE A 160	12	IPN 320	75	HE 340 AA	96	HE 1000 B	225	HD 400 x 314	224
IPE 160	17	IPN 340	82	HE 340 A	121	HE 1000 M	234	HD 400 x 347	233
IPE A 180	16	IPN 360	91	HE 340 B	145	HE 1000 x 393	243	HD 400 x 382	239
IPE 180	22	IPN 380	100	HE 340 M	206	HE 1000 x 415	247	HD 400 x 421	250
IPE O 180	25	IPN 400	111	HE 360 AA	99	HE 1000 x 438	252	HD 400 x 463	256
IPE A 200	21	IPN 450	130	HE 360 A	128	HE 1000 x 494	260	HD 400 x 509	262
IPE 200	28	IPN 500	149	HE 360 B	152	HE 1000 x 584	267	HD 400 x 551	265
IPE O 200	31	IPN 550	167	HE 360 M	208	HL 920 x 342	230	HD 400 x 592	270
IPE A 220	27	IPN 600	190	HE 400 AA	109	HL 920 x 365	236	HD 400 x 634	271
IPE 220	33	HE 100 AA	11	HE 400 A	138	HL 920 x 387	240	HD 400 x 677	274
IPE O 220	37	HE 100 A	18	HE 400 B	161	HL 920 x 417	249	HD 400 x 744	275
IPE A 240	32	HE 100 B	24	HE 400 M	210	HL 920 x 446	255	HD 400 x 818	278
IPE 240	39	HE 100 M	50	HE 450 AA	117	HL 920 x 488	259	HD 400 x 900	280
IPE O 240	43	HE 120 AA	15	HE 450 A	148	HL 920 x 534	263	HD 400 x 990	282
IPE A 270	40	HE 120 A	23	HE 450 B	168	HL 920 x 585	268	HD 400 x 1086	283
IPE 270	46	HE 120 B	35	HE 450 M	213	HL 920 x 653	273	HP 200 x 43	55
IPE O 270	52	HE 120 M	65	HE 500 AA	123	HL 920 x 784	277	HP 200 x 53	66
IPE A 300	48	HE 140 AA	20	HE 500 A	160	HL 920 x 967	281	HP 220 x 57	72
IPE 300	53	HE 140 A	30	HE 500 B	182	HL 1000 AA	221	HP 260 x 75	89
IPE O 300	61	HE 140 B	42	HE 500 M	214	HL 1000 A	227	HP 260 x 87	102
IPE A 330	57	HE 140 M	78	HE 550 AA	134	HL 1000 B	237	HP 305 x 79	95
IPE 330	60	HE 160 AA	29	HE 550 A	166	HL 1000 M	246	HP 305 x 88	103
IPE O 330	70	HE 160 A	38	HE 550 B	191	HL 1000 x 443	253	HP 305 x 95	114
IPE A 360	62	HE 160 B	56	HE 550 M	216	HL 1000 x 483	258	HP 305 x 110	127
IPE 360	71	HE 160 M	92	HE 600 AA	142	HL 1000 x 539	264	HP 305 x 126	139
IPE O 360	79	HE 180 AA	36	HE 600 A	175	HL 1000 x 554	266	HP 305 x 149	156
IPE A 400	73	HE 180 A	45	HE 600 B	193	HL 1000 x 591	269	HP 305 x 180	177
IPE 400	80	HE 180 B	64	HE 600 M	217	HL 1000 x 642	272	HP 305 x 186	180
IPE O 400	90	HE 180 M	106	HE 600 x 337	229	HL 1000 x 748	276	HP 305 x 223	197
IPE A 450	81	HE 200 AA	44	HE 600 x 399	244	HL 1000 x 883	279	HP 320 x 88	105
IPE 450	94	HE 200 A	54	HE 650 AA	147	HL 1100 A	231	HP 320 x 103	118
IPE O 450	110	HE 200 B	77	HE 650 A	184	HL 1100 B	241	HP 320 x 117	133
IPE A 500	97	HE 200 M	119	HE 650 B	199	HL 1100 M	251	HP 320 x 147	153
IPE 500	107	HE 220 AA	49	HE 650 M	220	HL 1100 R	261	HP 320 x 184	179
IPE O 500	124	HE 220 A	63	HE 650 x 343	232	HD 260 x 54.1	69	HP 360 x 84	101
IPE A 550	108	HE 220 B	86	HE 650 x 407	245	HD 260 x 68.2	84	HP 360 x 109	126
IPE 550	122	HE 220 M	132	HE 700 AA	157	HD 260 x 93.0	113	HP 360 x 133	143
IPE O 550	135	HE 240 AA	58	HE 700 A	192	HD 260 x 114	129	HP 360 x 152	158
IPE A 600	125	HE 240 A	74	HE 700 B	203	HD 260 x 142	151	HP 360 x 174	173
IPE 600	136	HE 240 B	98	HE 700 M	223	HD 260 x 172	171	HP 360 x 180	178
IPE O 600	159	HE 240 M	162	HE 700 x 352	235	HD 320 x 74.2	88	HP 400 x 122	137
IPE 750 x 137	146	HE 260 AA	68	HE 700 x 418	248	HD 320 x 97.6	116	HP 400 x 140	150
IPE 750 x 147	155	HE 260 A	83	HE 800 AA	169	HD 320 x 127	141	HP 400 x 158	163
IPE 750 x 173	172	HE 260 B	112	HE 800 A	198	HD 320 x 158	164	HP 400 x 176	174
IPE 750 x 196	187	HE 260 M	170	HE 800 B	211	HD 320 x 198	189	HP 400 x 194	185
IPN 80	3	HE 280 AA	76	HE 800 M	226	HD 320 x 245	205	HP 400 x 213	194
IPN 100	6	HE 280 A	93	HE 800 x 373	238	HD 320 x 300	222	HP 400 x 231	200
IPN 120	10	HE 280 B	120	HE 800 x 444	254	HD 360 x 134	144		
IPN 140	14	HE 280 M	183	HE 900 AA	188	HD 360 x 147	154		

Remark: the profiles are arranged according to their areas. The necessary parameters (geometric and mechanic) of all profile were installed in CEPAO.

Table 9.3: American profiles

Profile	Order	Profile	Order	Profile	Order	Profile	Order	Profile	Order
W4x13	5	W12x170	157	W14x53	64	W21x147	144	W33x152	148
W5x16	12	W12x19	19	W14x550	219	W21x166	154	W33x169	156
W5x19	18	W12x190	165	W14x605	221	W21x182	162	W36x135	138
W6x12	4	W12x21	22	W14x61	74	W21x201	170	W36x150	147
W6x15	9	W12x210	172	W14x665	223	W21x44	51	W36x160	153
W6x16	14	W12x22	26	W14x68	82	W21x50	61	W36x170	158
W6x20	21	W12x230	179	W14x730	224	W21x57	68	W36x182	163
W6x25	28	W12x26	30	W14x74	88	W21x62	76	W36x194	168
W6x9	1	W12x30	34	W14x82	94	W21x68	83	W36x210	171
W8x10	2	W12x35	42	W14x90	102	W21x73	87	W36x230	177
W8x13	6	W12x40	48	W14x99	109	W21x83	95	W36x245	182
W8x14	8	W12x45	52	W16x100	111	W21x93	103	W36x260	185
W8x15	11	W12x50	60	W16x26	31	W24x103	114	W36x280	191
W8x18	17	W12x53	63	W16x31	38	W24x104	115	W36x300	195
W8x21	23	W12x58	70	W16x36	43	W24x117	124	W36x328	199
W8x24	27	W12x65	77	W16x40	46	W24x131	134	W36x359	204
W8x28	33	W12x72	86	W16x45	54	W24x146	143	W36x393	209
W8x31	37	W12x79	93	W16x50	62	W24x162	152	W36x439	214
W8x35	41	W12x87	99	W16x57	69	W24x176	160	W36x527	218
W8x40	45	W12x96	106	W16x67	80	W24x192	166	W36x650	222
W8x48	56	W14x109	119	W16x77	91	W24x229	176	W40x149	146
W8x58	71	W14x120	128	W16x89	101	W24x279	190	W40x167	155
W8x67	79	W14x132	136	W18x106	117	W24x306	196	W40x183	164
W10x100	110	W14x145	142	W18x119	126	W24x335	201	W40x199	169
W10x112	121	W14x159	151	W18x130	133	W24x370	207	W40x211	174
W10x12	3	W14x176	161	W18x143	141	W24x55	67	W40x215	175
W10x15	10	W14x193	167	W18x158	150	W24x62	75	W40x235	181
W10x16	15	W14x211	173	W18x175	159	W24x68	84	W40x249	183
W10x17	16	W14x22	24	W18x35	40	W24x76	90	W40x264	187
W10x19	20	W14x233	180	W18x40	47	W24x84	96	W40x277	188
W10x22	25	W14x257	184	W18x41	49	W24x94	105	W40x278	189
W10x26	29	W14x26	32	W18x45	53	W27x102	113	W40x297	194
W10x30	36	W14x283	192	W18x46	55	W27x114	122	W40x324	198
W10x49	58	W14x30	35	W18x50	59	W27x129	131	W40x331	200
W10x54	65	W14x311	197	W18x55	66	W27x84	97	W40x362	205
W10x60	73	W14x34	39	W18x60	72	W27x94	104	W40x392	208
W10x68	81	W14x342	203	W18x65	78	W30x108	118	W40x397	210
W10x77	92	W14x370	206	W18x71	85	W30x116	123	W40x431	213
W10x88	100	W14x38	44	W18x76	89	W30x124	130	W40x503	217
W12x106	116	W14x398	211	W18x86	98	W30x132	137	W40x593	220
W12x120	127	W14x426	212	W18x97	107	W30x148	145	W44x230	178
W12x136	139	W14x43	50	W21x101	112	W30x99	108	W44x260	186
W12x14	7	W14x455	215	W21x111	120	W33x118	125	W44x290	193
W12x152	149	W14x48	57	W21x122	129	W33x130	132	W44x335	202
W12x16	13	W14x500	216	W21x132	135	W33x141	140		

Remark: the profiles are arranged according to their areas. The necessary parameters (geometric and mechanic) of all profile were installed in CEPAO.

Fig.9.5. Graphic images in the output of CEPAO for 2-D twenty-story frame (start)

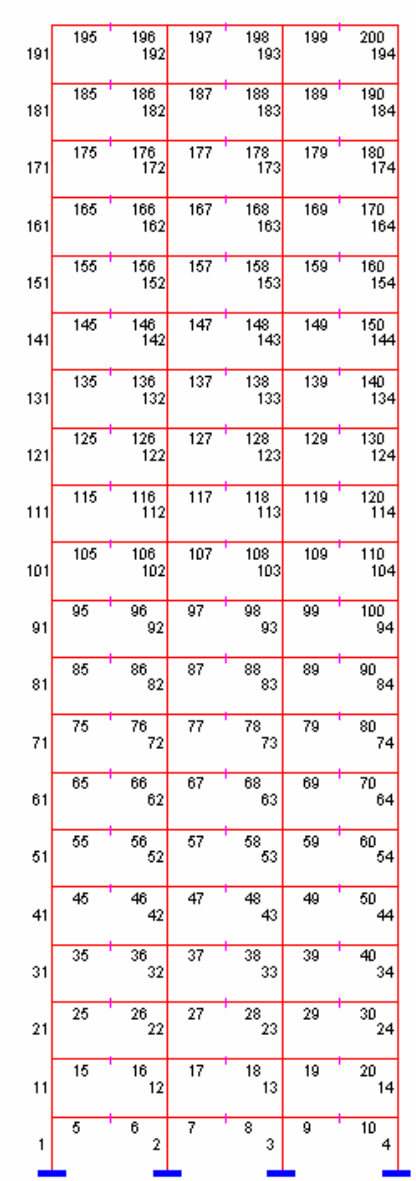

NUMEROTATION DES BARRES

CEPAO

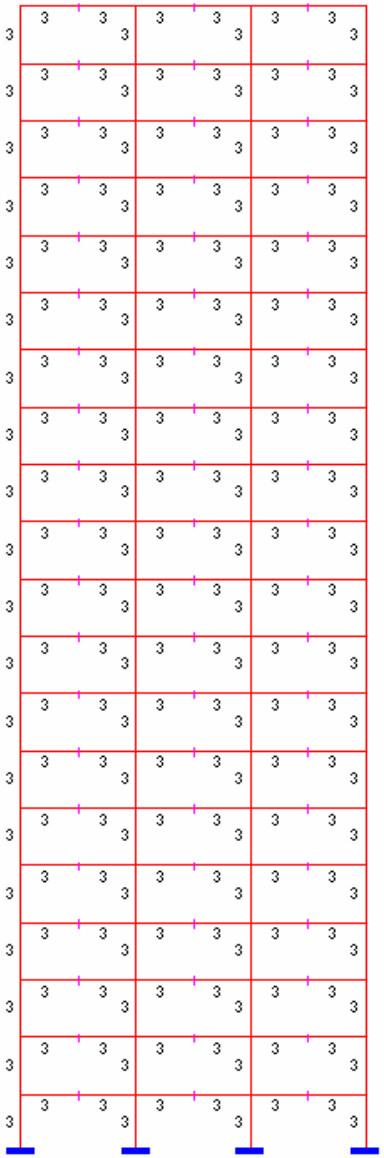

LONGUEURS DES BARRES

CEPAO

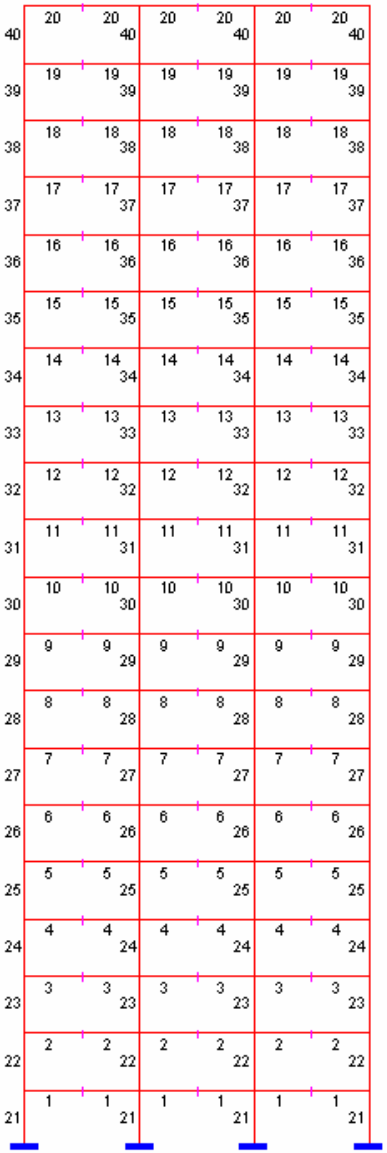

NUMEROTATION DES PORTEES

CEPAO

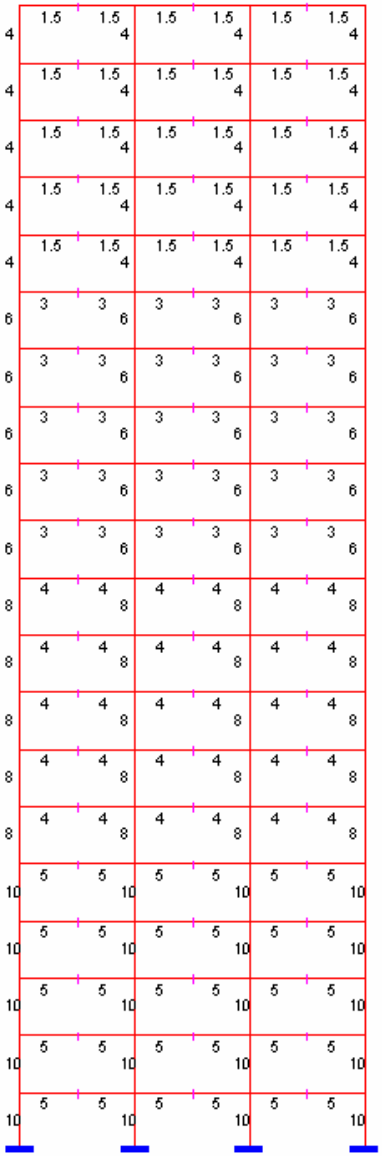

MOMENTS PLASTIQUES DONNES

CEPAO

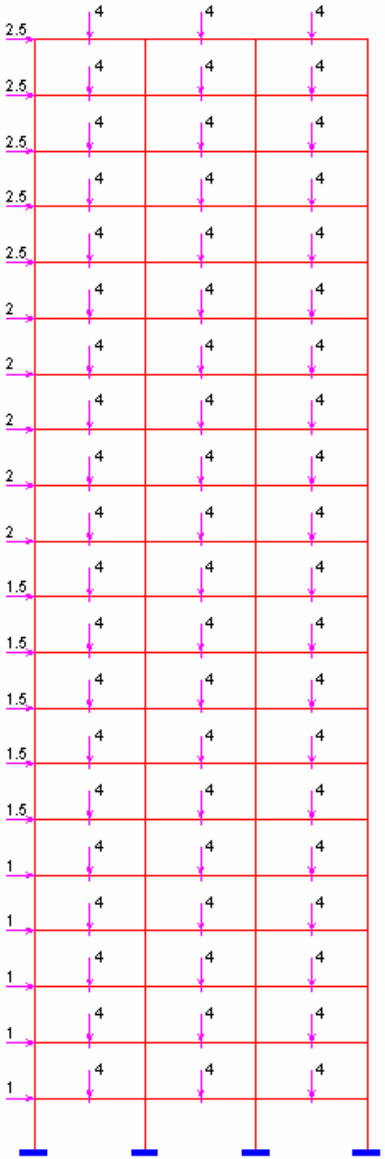

CAS DE CHARGES: 1

CEPAO ANALYSE - LIMITE

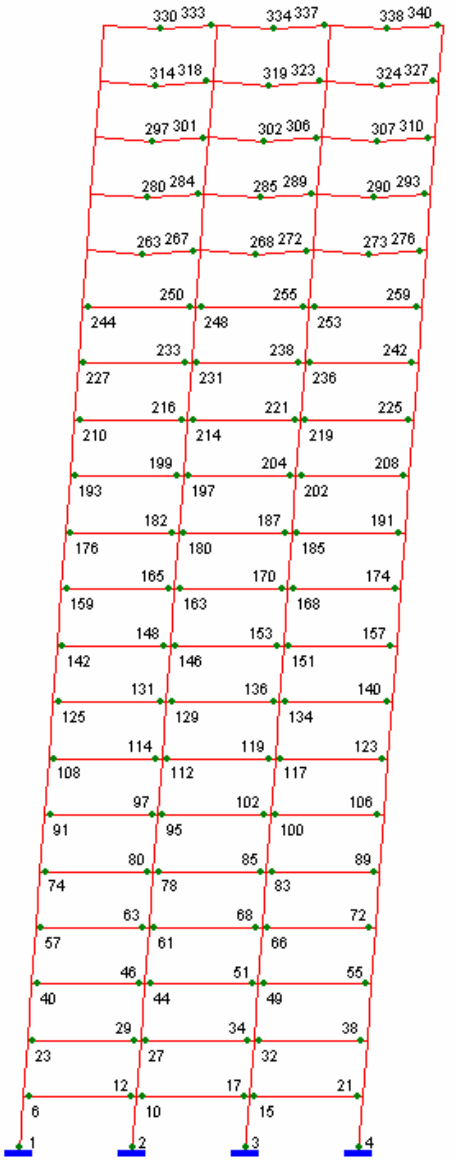

COEFFICIENT DE LA CHARGE LIMITE = 0.333

MECANISME REEL

CEPAO ANALYSE - LIMITE

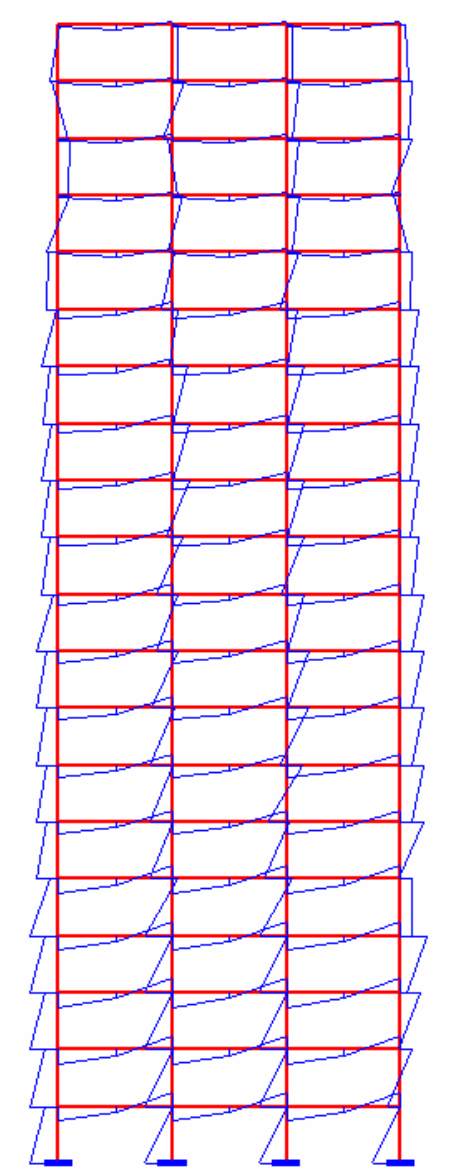

DIAGRAMME DE MOMENT FLECHISSANT

CEPAO ANALYSE - LIMITE

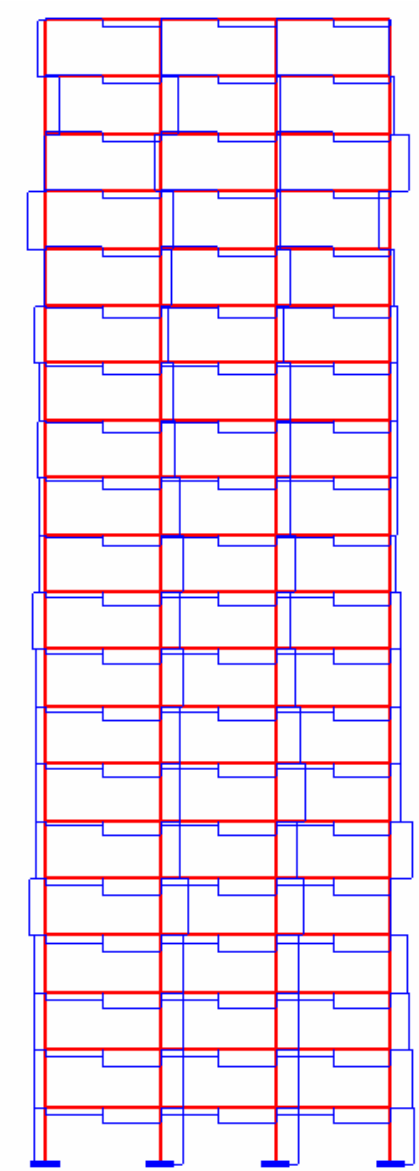

DIAGRAMME D'EFFORT TRANCHANT

CEPAO ANALYSE - LIMITE

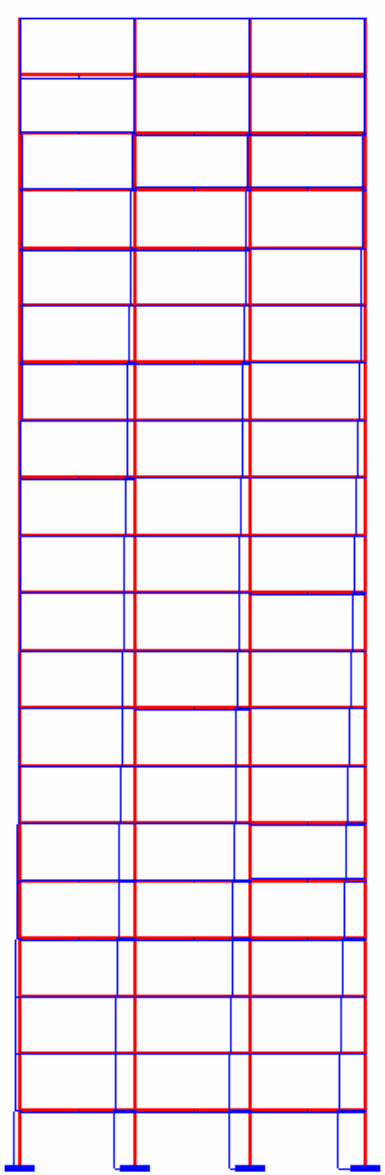

DIAGRAMME D'EFFORT NORMAL

CEPAO ANALYSE - LIMITE

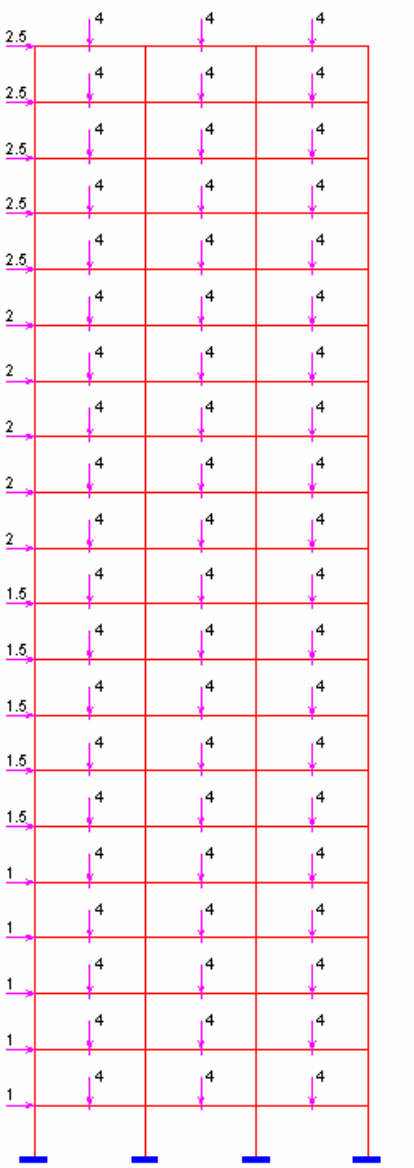

CAS DE CHARGES: 1

CEPAO ANALYSE - ELASTIQUE

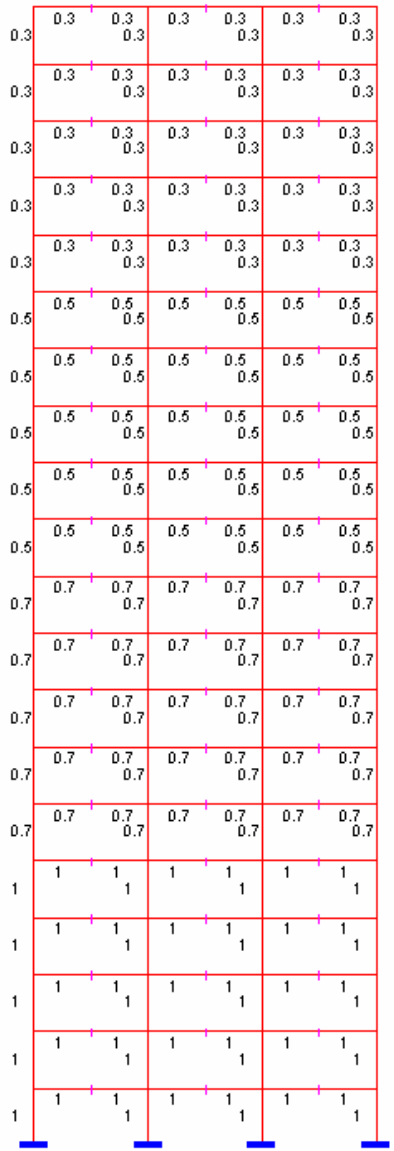

MOMENTS INERTIES DONNES

CEPAO ANALYSE - ELASTIQUE

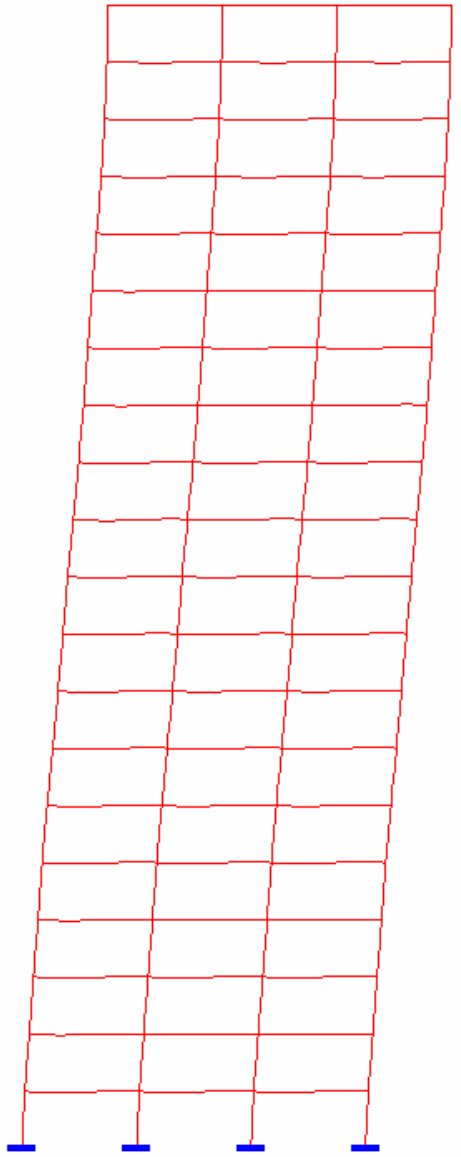

DEFORMATION

CEPAO ANALYSE - ELASTIQUE

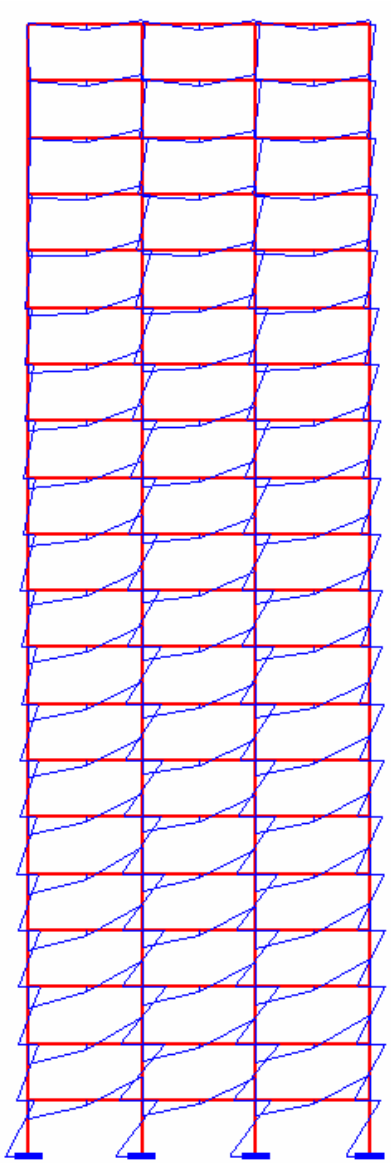

DIAGRAMME DE MOMENT FLECHISSANT

CEPAO ANALYSE - ELASTIQUE

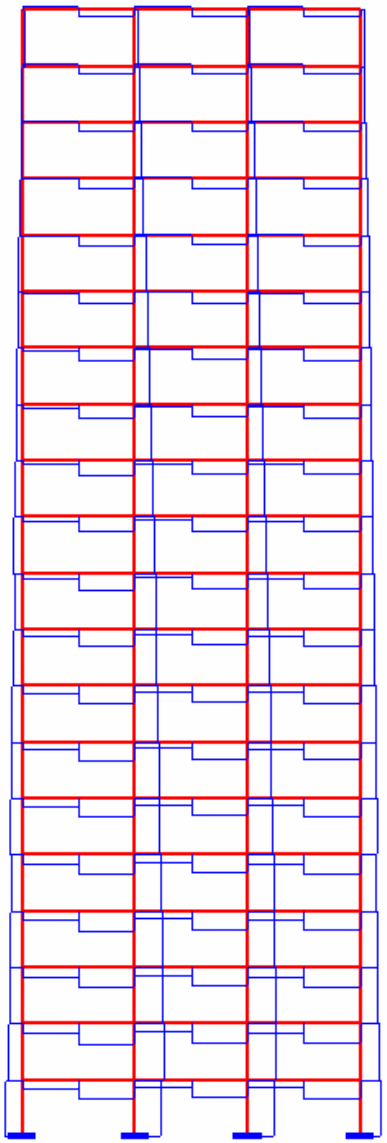

DIAGRAMME D'EFFORT TRANCHANT

CEPAO ANALYSE - ELASTIQUE

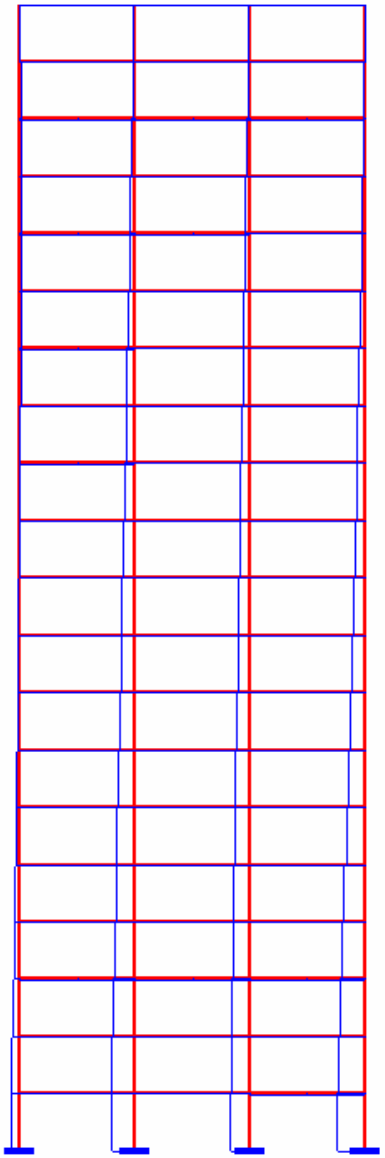

DIAGRAMME D'EFFORT NORMAL

CEPAO ANALYSE - ELASTIQUE

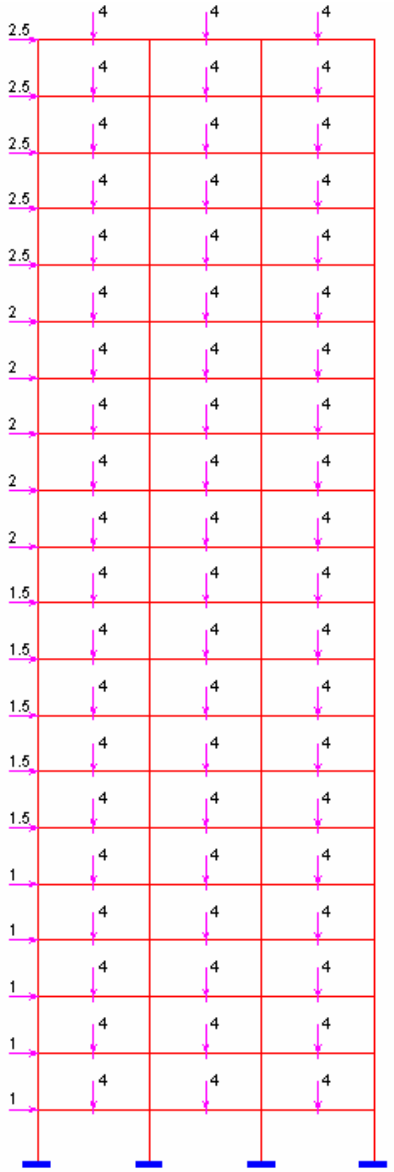

CAS DE CHARGES: 1

CEPAO ANALYSE - PAS A PAS

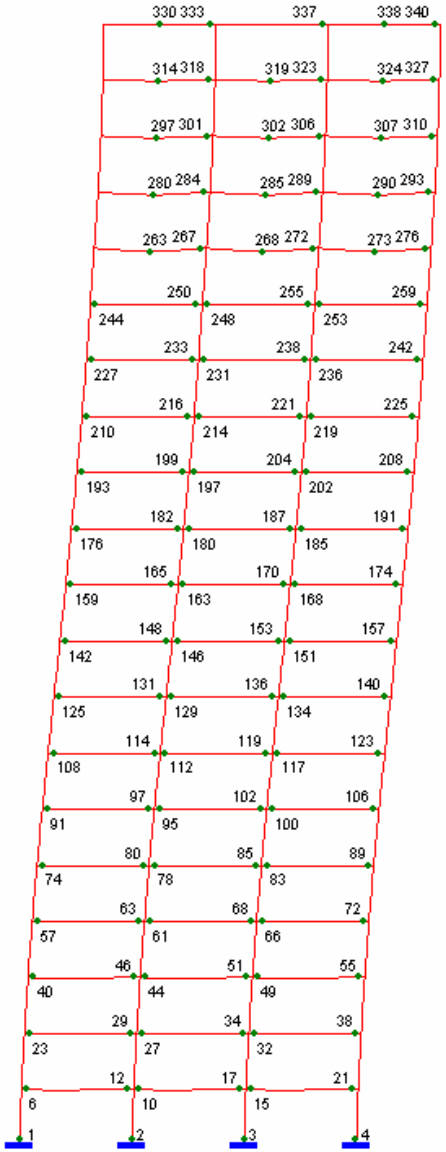

MULTIPLICATION DE LA CHARGE = 0.333

DEFORMATION JUSTE AVANT LA RUINE

CEPAO ANALYSE - PAS A PAS

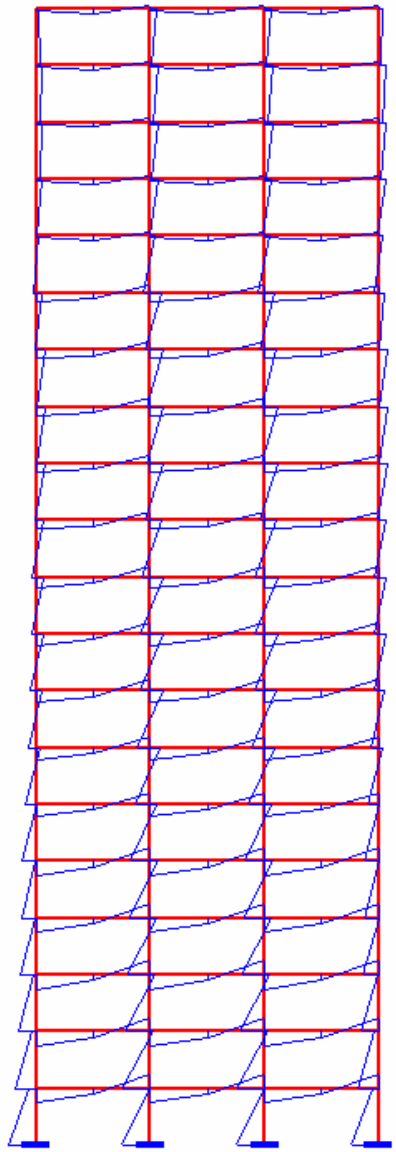

DIAGRAMME DE MOMENT FLECHISSANT

CEPAO ANALYSE - PAS A PAS

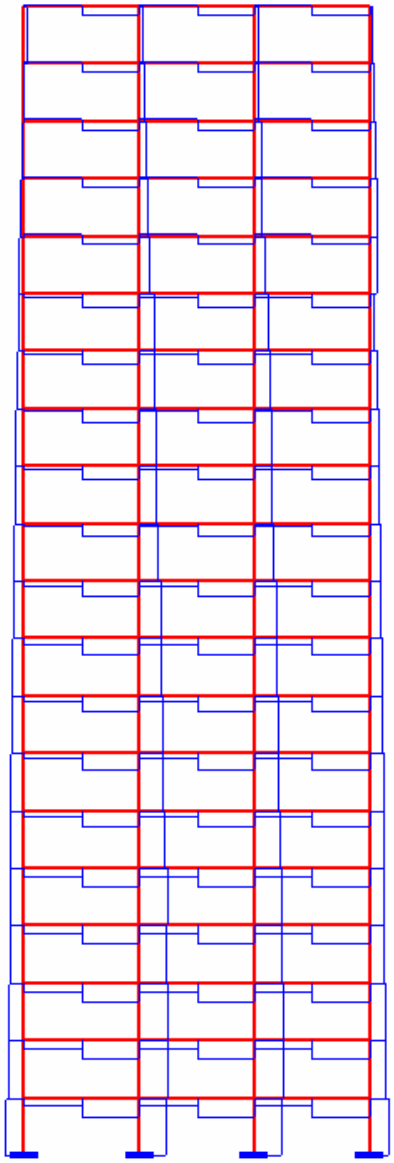

DIAGRAMME D'EFFORT TRANCHANT

CEPAO ANALYSE - PAS A PAS

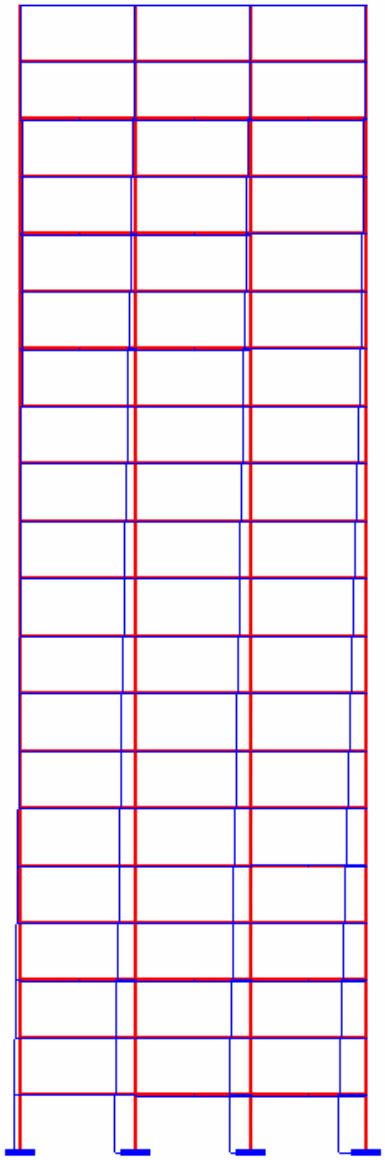

DIAGRAMME D'EFFORT NORMAL

CEPAO ANALYSE - PAS A PAS

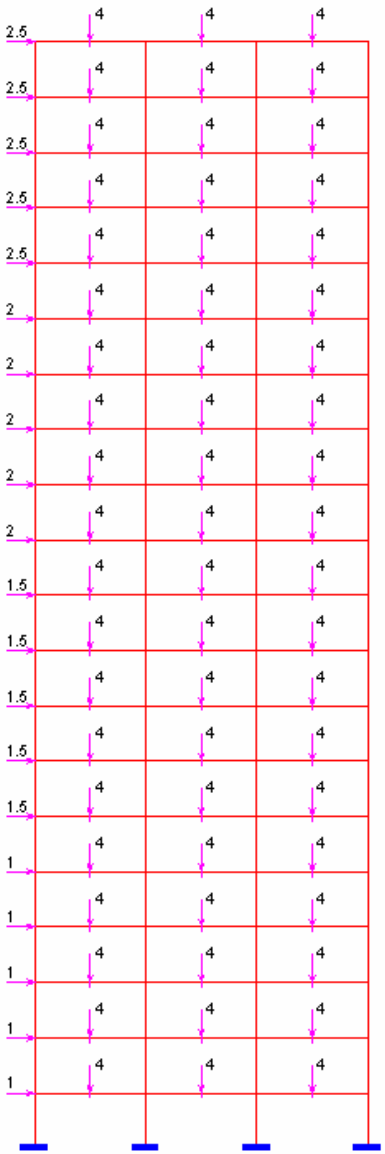

CAS DE CHARGES: 1

CEPAO ANALYSE - SECOND ORDRE

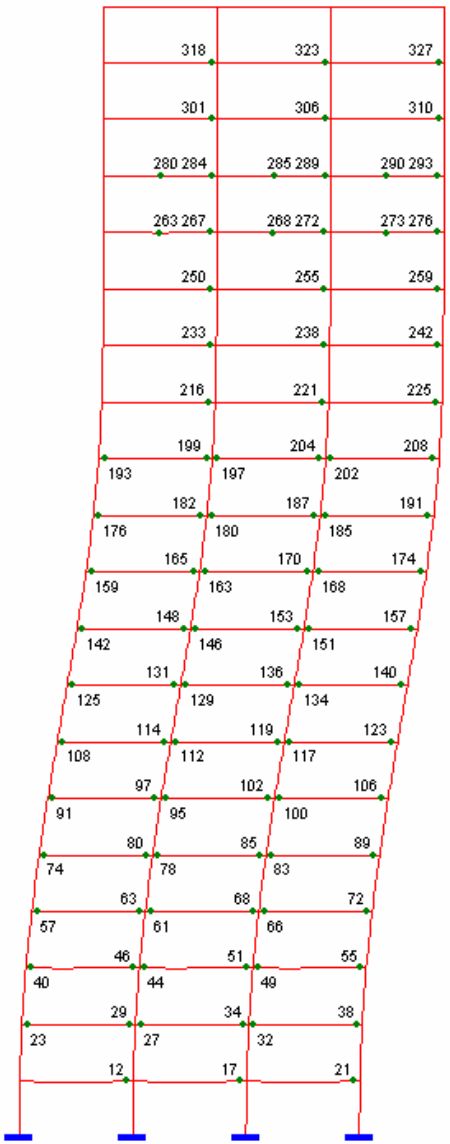

MULTIPLICATION DE LA CHARGE = 0.294

DEFORMATION JUSTE AVANT LA RUINE

CEPAO ANALYSE - SECOND ORDRE

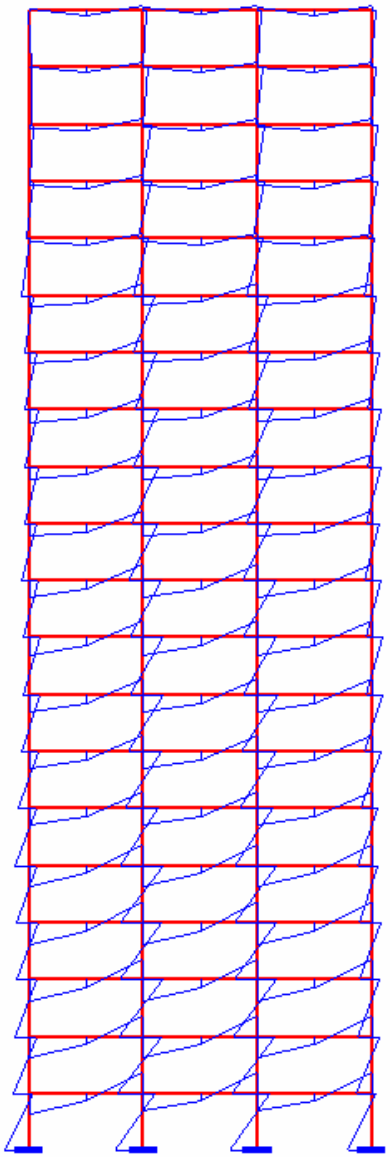

DIAGRAMME DE MOMENT FLECHISSANT

CEPAO ANALYSE - SECOND ORDRE

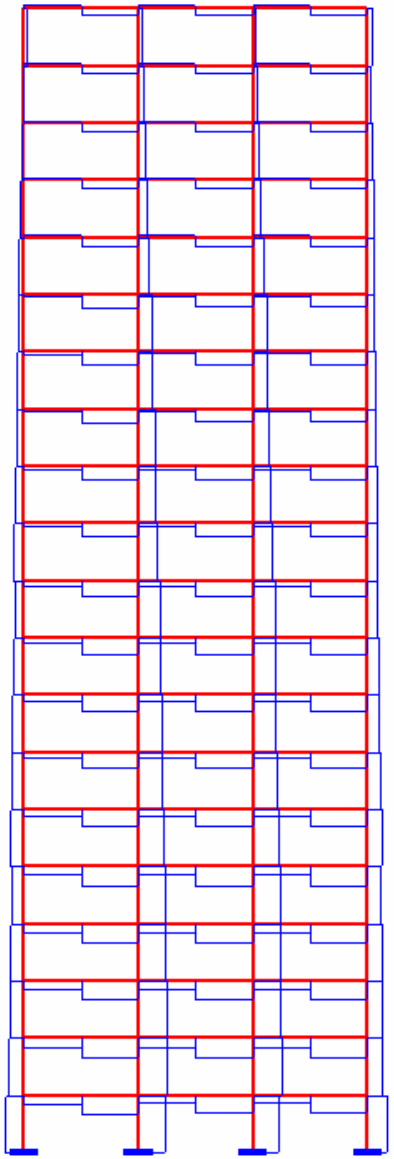

DIAGRAMME D'EFFORT TRANCHANT

CEPAO ANALYSE - SECOND ORDRE

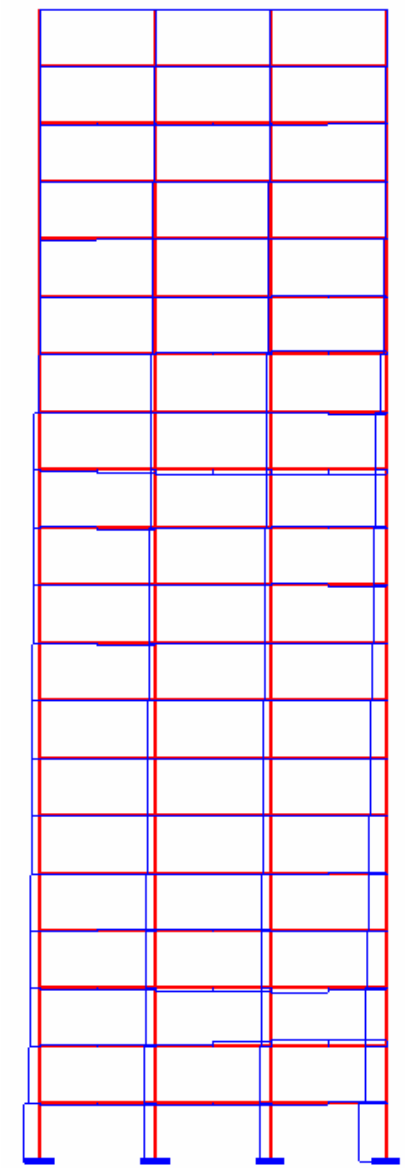

DIAGRAMME D'EFFORT NORMAL

CEPAO ANALYSE - SECOND ORDRE

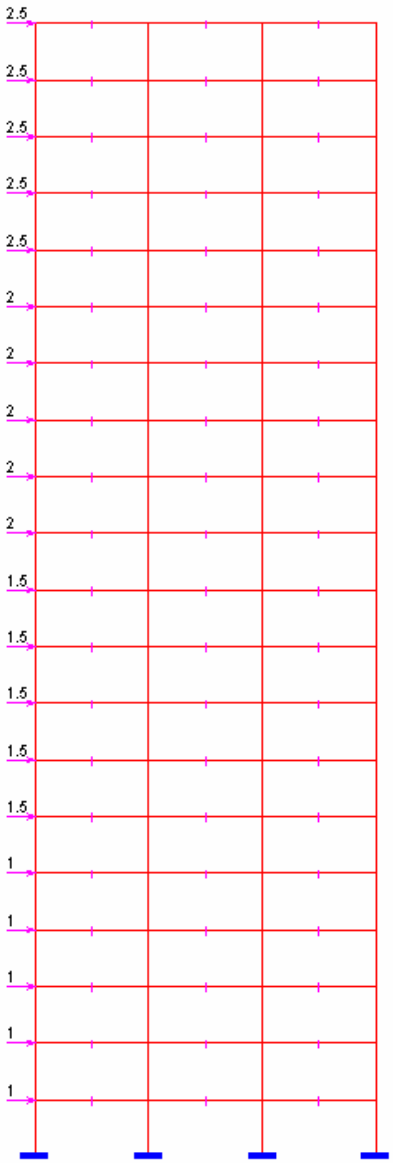

LIMITE INF. ET SUP. DE LA CHARGE = 0 ; 3

CAS DE CHARGES: 1

CEPAO ANALYSE - ADAPTATION

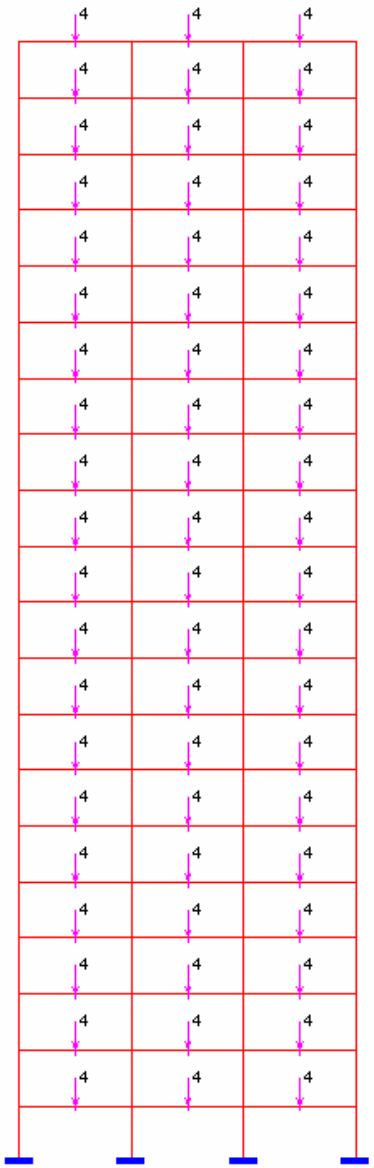

LIMITE INF. ET SUP. DE LA CHARGE = 0 ; 3

CAS DE CHARGES: 2

CEPAO ANALYSE - ADAPTATION

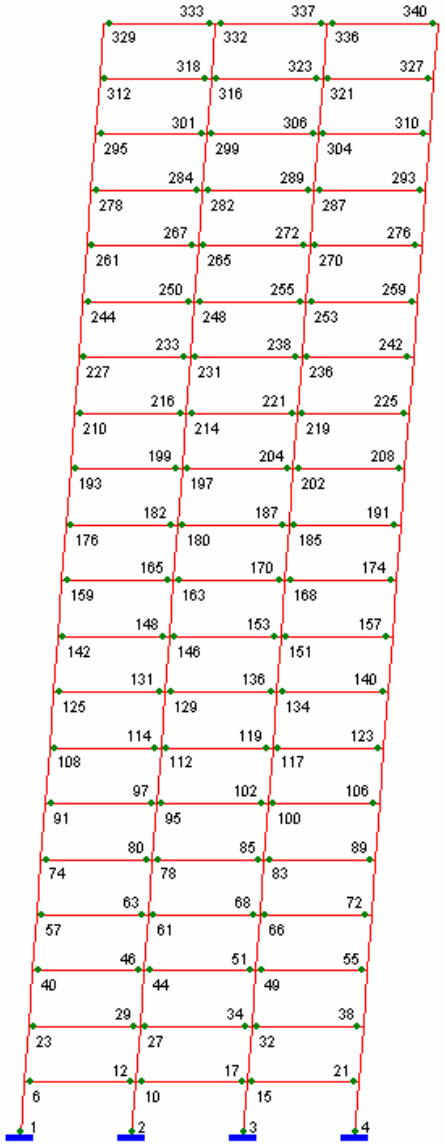

MULTIPLICATION DE LA CHARGE = 0.101

MECANISME INCREMENTAL

CEPAO ANALYSE - ADAPTATION

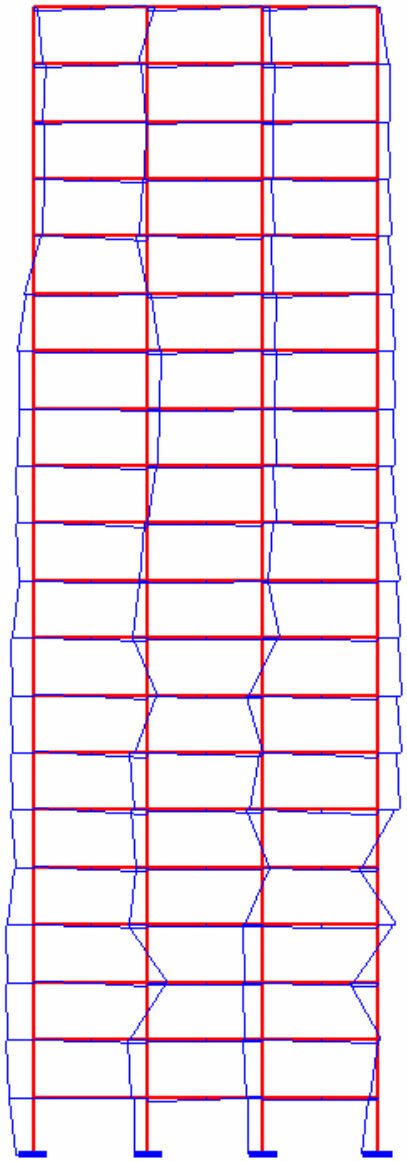

DIAGRAMME DE MOMENT RESIDUEL

CEPAO ANALYSE - ADAPTATION

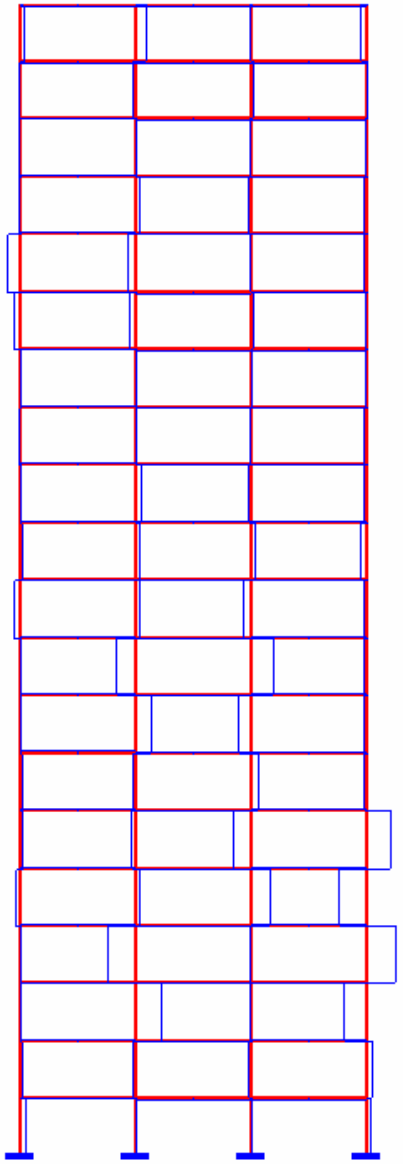

DIAGRAMME D'EFFORT TRANCHANT RESIDUEL

CEPAO ANALYSE - ADAPTATION

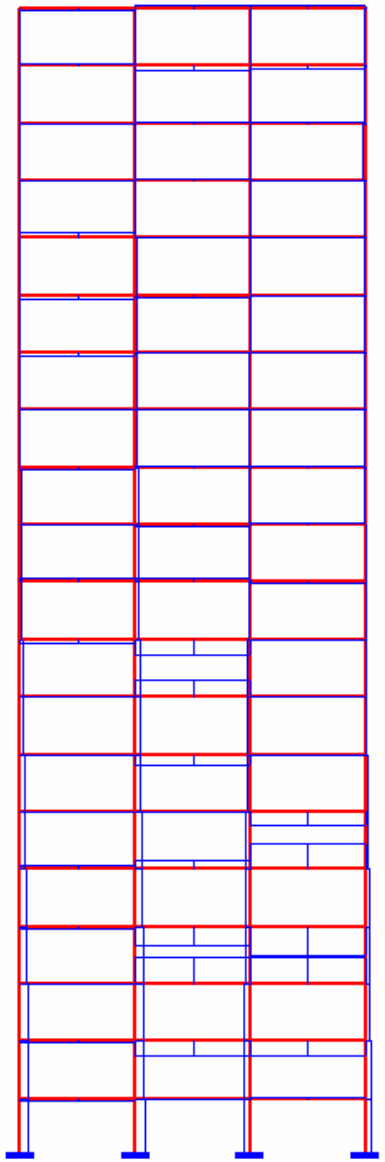

DIAGRAMME D'EFFORT NORMAL RESIDUEL

CEPAO ANALYSE - ADAPTATION

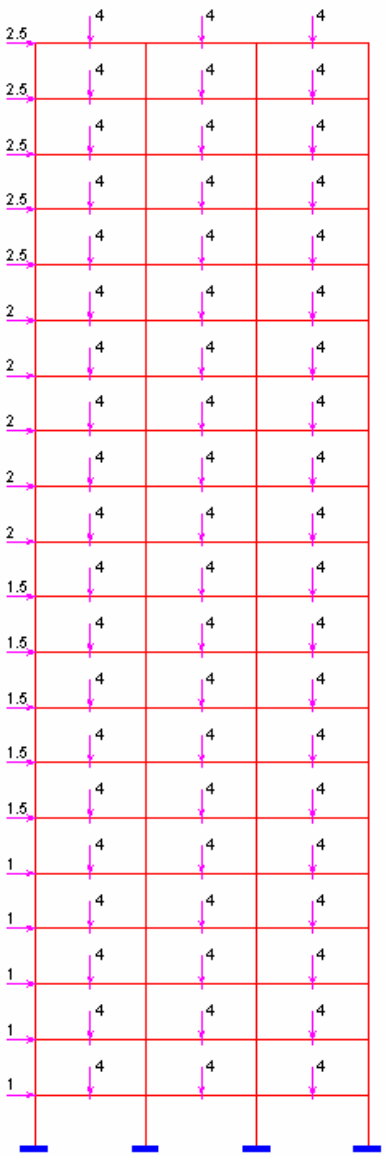

CAS DE CHARGES: 1

CEPAO OPTIMISATION - LIMITE

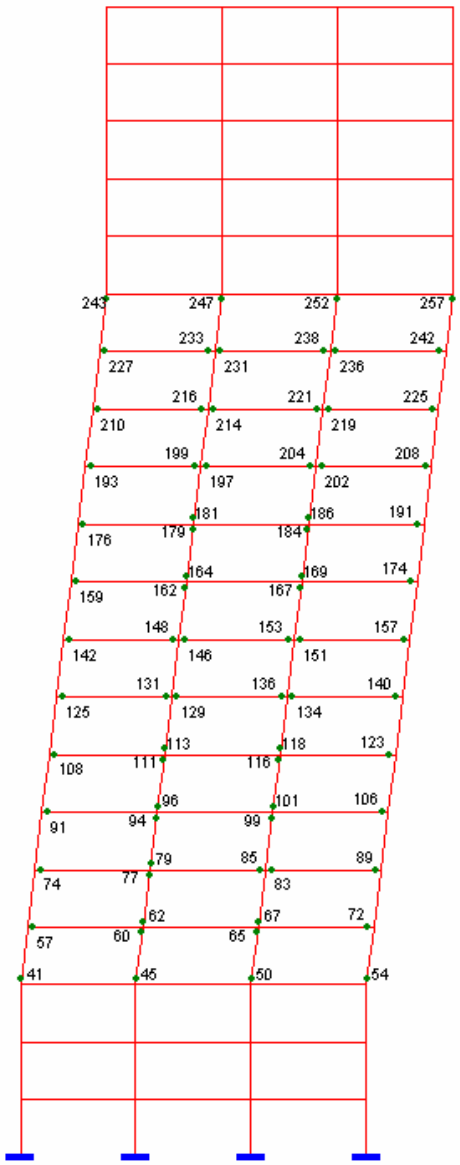

UN DES MECANISMES OPTIMALS

CEPAO OPTIMISATION - LIMITE

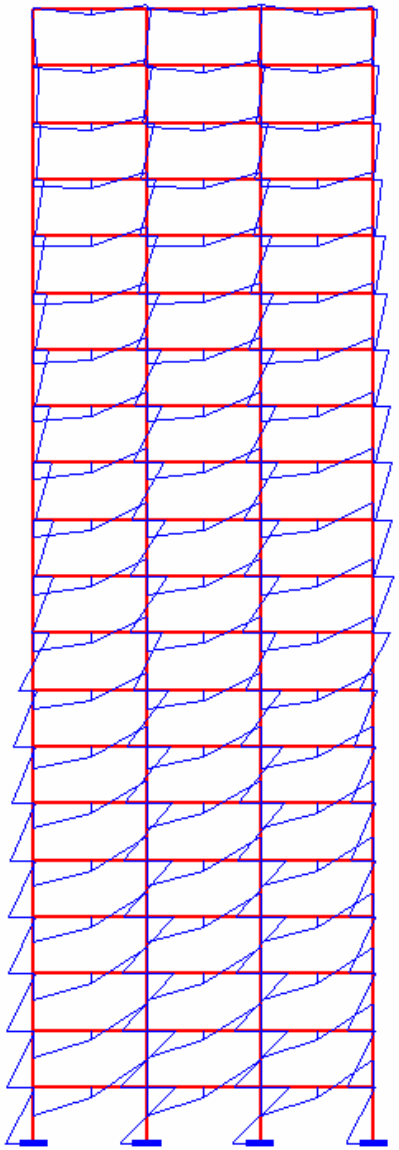

DIAGRAMME DE MOMENT FLECHISSANT

CEPAO OPTIMISATION - LIMITE

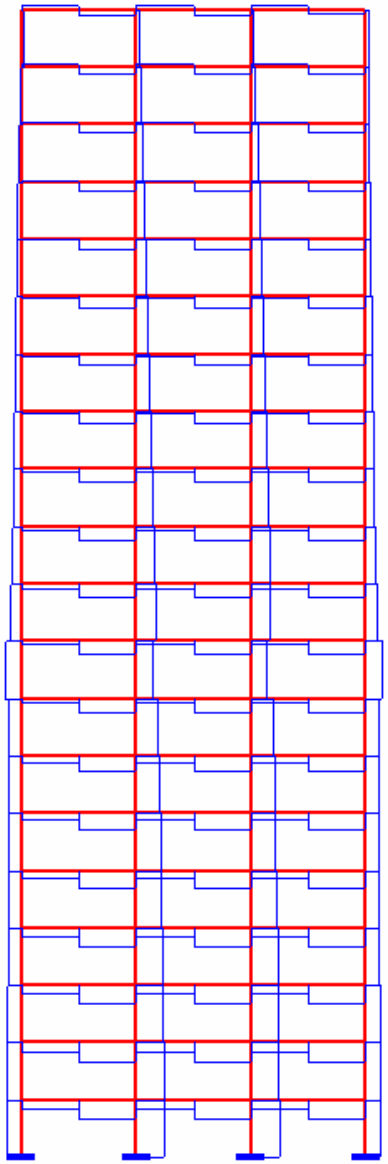

DIAGRAMME D'EFFORT TRANCHANT

CEPAO OPTIMISATION - LIMITE

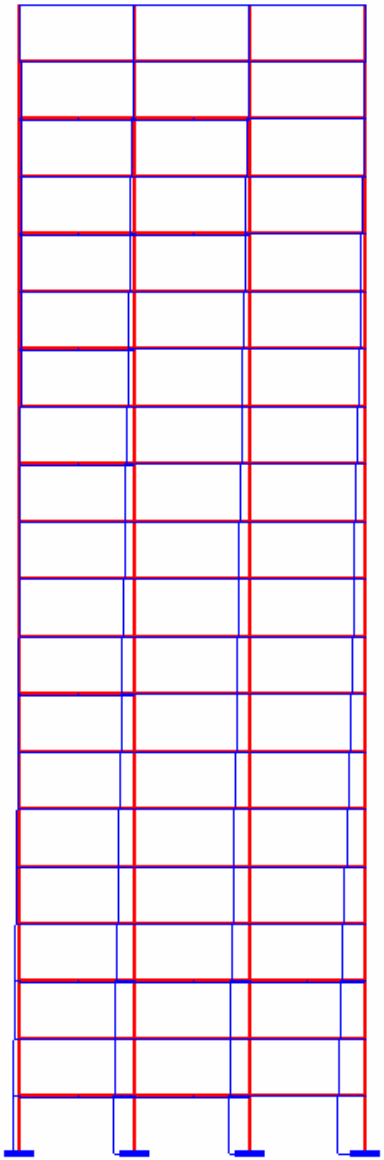

DIAGRAMME D'EFFORT NORMAL

CEPAO OPTIMISATION - LIMITE

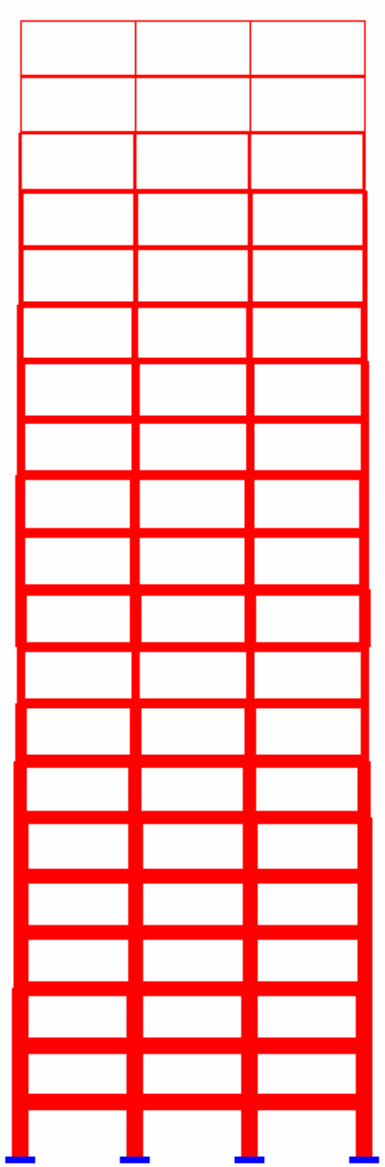

MOMENTS PLASTIQUES OPTIMALS

CEPAO OPTIMISATION - LIMITE

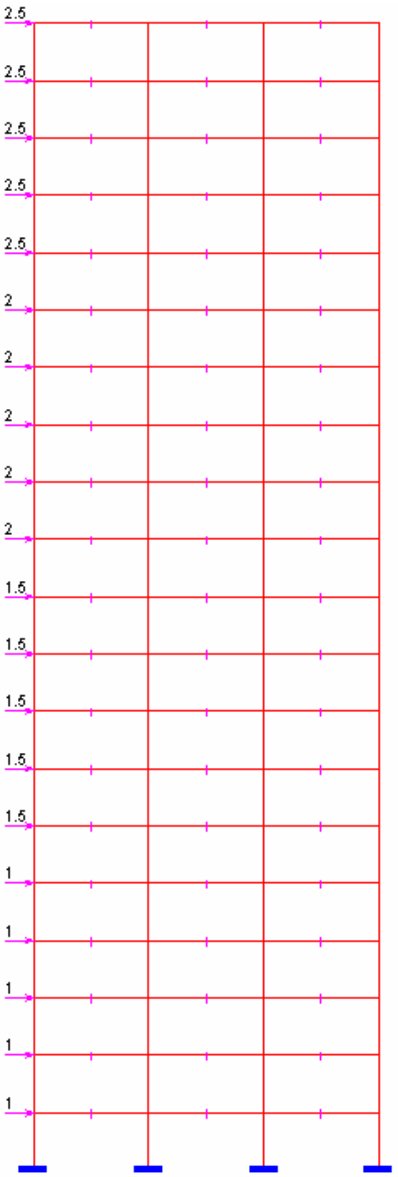

LIMITE INF. ET SUP. DE LA CHARGE = 0 ; 3

CAS DE CHARGES: 1

CEPAO OPTIMISATION - ADAPTATION

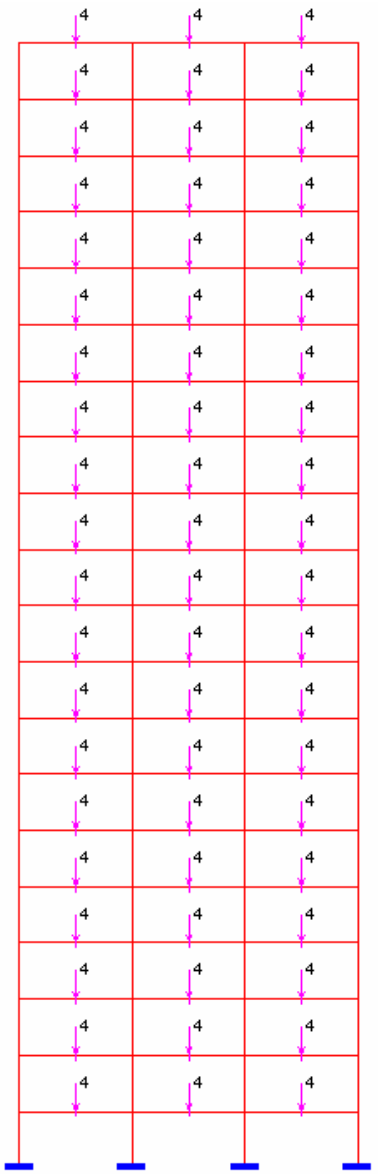

LIMITE INF. ET SUP. DE LA CHARGE = 0 ; 3

CAS DE CHARGES: 2

CEPAO OPTIMISATION - ADAPTATION

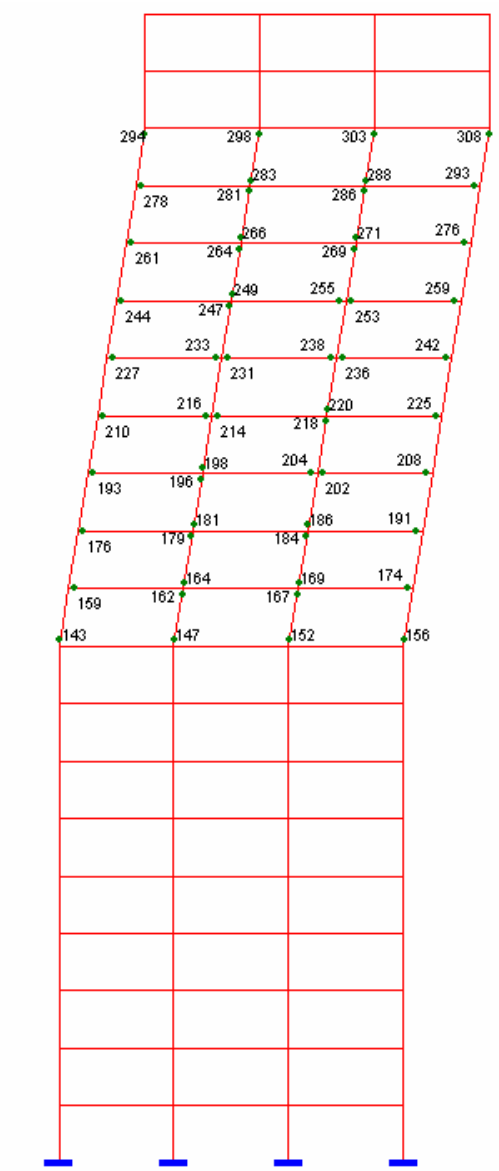

MECANISME INCREMENTAL OPTIMAL

CEPAO OPTIMISATION - ADAPTATION

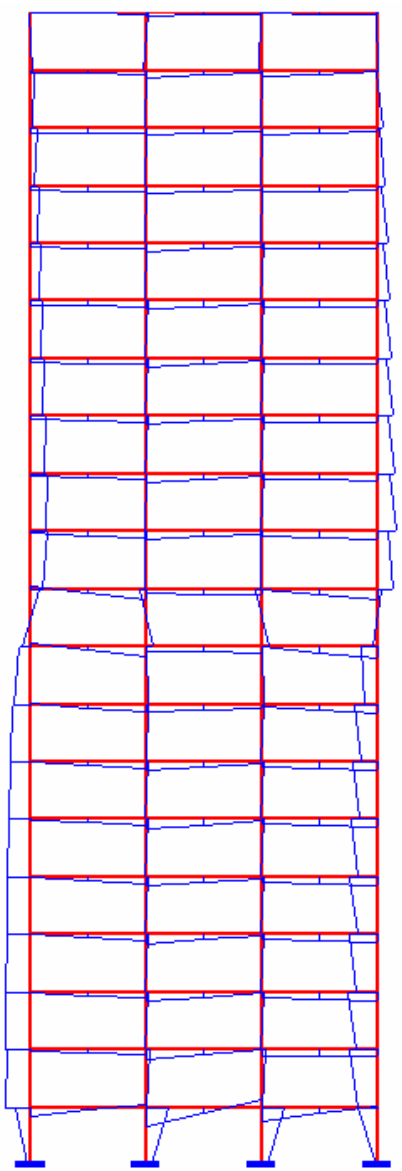

DIAGRAMME DE MOMENT RESIDUEL

CEPAO OPTIMISATION - ADAPTATION

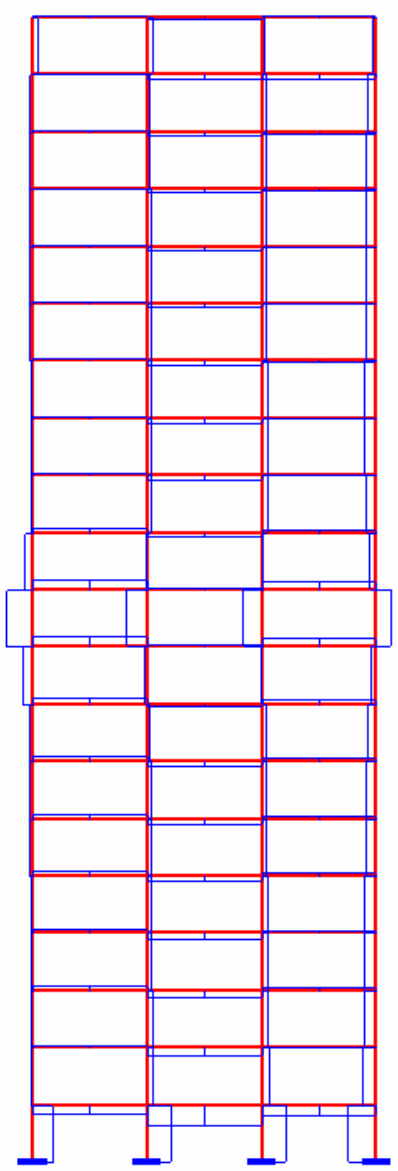

DIAGRAMME D'EFFORT TRANCHANT RESIDUEL

CEPAO OPTIMISATION - ADAPTATION

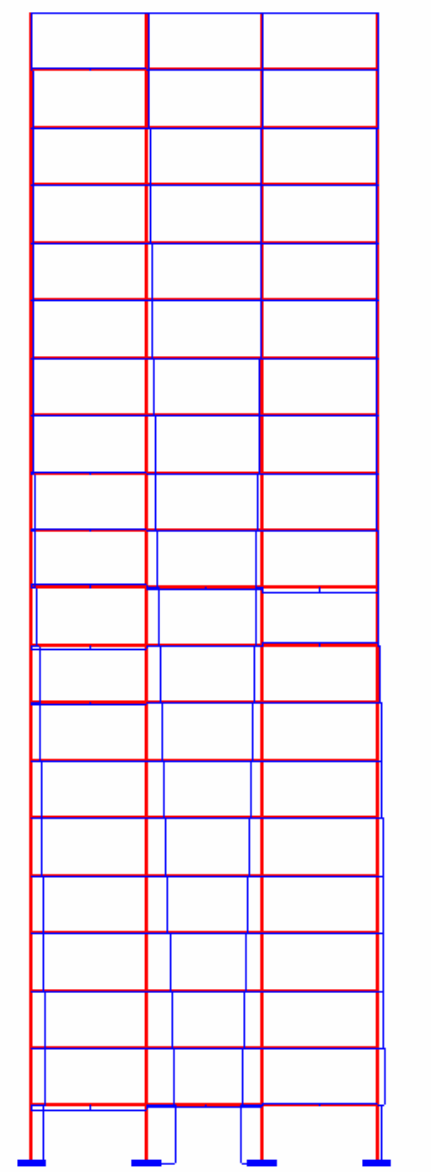

DIAGRAMME D'EFFORT NORMAL RESIDUEL

CEPAO OPTIMISATION - ADAPTATION

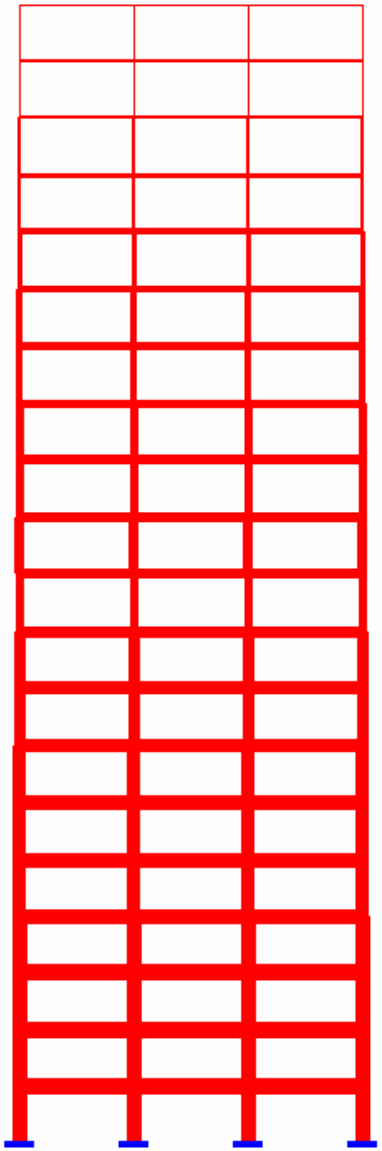

MOMENTS PLASTIQUES OPTIMALS

CEPAO OPTIMISATION - ADAPTATION

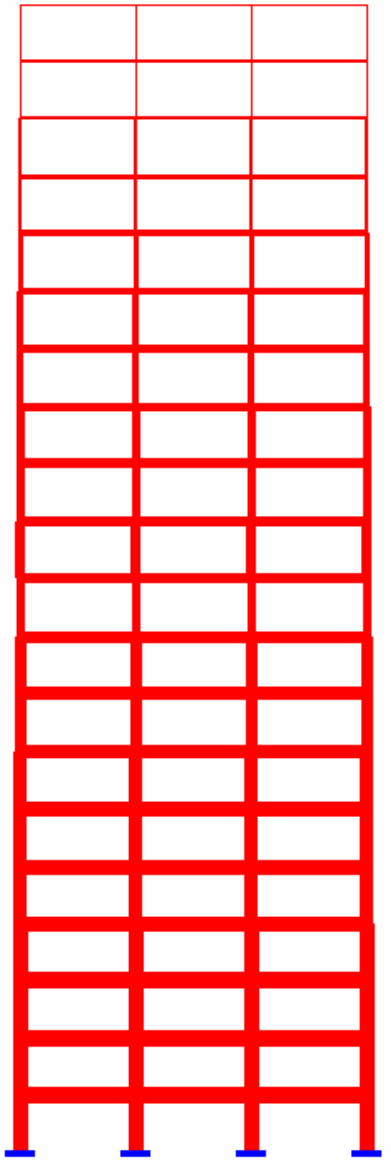

MOMENTS D"INERTIE OPTIMALS

CEPAO OPTIMISATION - ADAPTATION

Fig.9.5. Graphic images in the output of CEPAO for 2-D twenty-story frame (end)

9.4. Conclusions

On the application aspect, this chapter demonstrates the advantages of the plastic-hinge model in generally and of CEPAO in particularly. With an input that similar to which of any linear elastic analysis, one has a rather complete picture of the nonlinear analysis of frames under static load. However, for the commercial purpose, the more improvement of the input and output data system is needed.

Chapter **10**

Conclusions

A rather complete picture of the automatic plastic-hinge analysis onto steel frames under static loads is made in the present thesis. The one/two/three-linear behaviours of the mild steel are considered. The frames are submitted to fixed or repeated load. The geometric nonlinearity is taken into account. The connexions beam-to-column of structures could be rigid or semi-rigid. The compact or slender cross-sections are examined. The investigation is carried out using direct or step-by-step methods. Both analysis and optimization methodologies are applied. From the fundamental theory to the computer program aspect are presented. Various benchmarks in the open literatures are tested demonstrating the efficiency of the implementation. The final remarks are summarized as follows:

Obtaining the actual behaviour of a steel frame by every price is not an optimal solution because the time and the manpower become more and more rare. In our opinion, the application of the plastic-hinge model for the global analysis of steel frames is a reasonable choice for practical design. The plastic-zone methods are suitable to the research offices or to the design/study of the separate components of the frames, as the beam, the column, the connexions, etc.

By combining the normality-rule application for the plastic hinges with the formulation of thirteen-degree-of-freedom-beam-column element (Chapter 3), one has obtained a flexible algorithm. The fundamental relationship may be applied in both direct and step-by-step method. The internal forces are associated to the net displacements at the plastic hinges. The strain hardening behaviour may also be taken into account. The possibility to consider the axial deformation of the connexions is open.

The standard formulations of the application of linear programming in the classic plastic problems have been presented the specialized literature. However, without the necessary skills, it would be not feasible to perform the analysis of large real-world structures. Currently, five additional necessary techniques are proposed in the present work (Chapters 4 and 5): change of variables, automatic choice of the initial solution in the simplex algorithm, primal-dual technique, push-fixed technique and standard-transformation techniques. Those techniques have played the significant role and their effects are illustrated. Thank to these suggested techniques, direct method using linear programming technique becomes robust to solve large-scale problems, even under repeated loading (the shakedown problem).

The idea of the step-by-step methods is always adopted by most people because it is close to the natural process of thought. There are many texts that present the algorithms for the conventional elastic-plastic second-order of the steel frames. However, the approach described in Chapter 6 constitutes an innovative formulation. It deals with a high degree of automatization and minimizing the breaks in the program process. It allows taking into account the strain hardening behaviour in plastic-hinge analysis and seems to be a new progress for the plastic-hinge methodology.

Concerning local buckling check, there is the guidance in Standards. However, the formulation in Chapter 7 would be useful for researches and mostly consultant engineers because it leads to an extended application of direct analysis to frame design including semi-compact and slender cross-sections.

It appears from the numerical results that: The nonlinear Orbison's yield surface [126] has good correlation with the sixteen-facet polyhedron of AISC-LRFD [1]. The utilizations of the two yield surfaces, respectively, in the step-by-step and direct methods converge at the ultimate state. In the case of symmetrical horizontal loading, the alternating plasticity is generally occurs with a small load multiplier. However, the number of load cycle leading to the fatigue is not considered in the shakedown theory. For the popular frames, the augmentation of the strength may reach, at the ultimate state, from 2% to 6% due to the strain hardening effect.

Even if the formulations discussed in present work are not familiar to practical engineers, the utilisation of CEPAO should not be very difficult for them. Within two hours, a student with the elementary knowledge about the mechanic of structures could become a good user of CEPAO. Its input file is similar to those of every computer program for the linear elastic analysis of frames. On the other hand, CEPAO is an auto-control program. Indeed, with the multi-results giving by multi-methods, we may confirm the results by the verifications using alternative computation. The list of 283 European beams (IPE, IPN, HE, HL, HD, HP) and 224 American beams (W) in Arcelor Sections Commercial is introduced in the database of CEPAO.

Due to the limitation of times, although we have already certain ideas for the shape of its solutions, the following problems must be tackled in the close future:

It is necessary to consider automatically the stability and stiffness constraints in the plastic optimization problem for the 3-D steel frames. The configurations given in the output of the plastic design procedure become then more practice. The stability and stiffness conditions may be directly considered as the initial constrains of the problem (see Kaneko (1981)[75], Tin-Loi (2000)[146], Kaliszky (2002)[74], Romero (2004)[133] and Merkevičiùtê (2006)[108]). Or by other technique, they are taken into account as a post-process (see Nguyen-Dang (1984)[117]). The first technique is original while the second technique is simple and efficient. However, there are the gaps in the algorithm of the mentioned references, they need to be improved, for example: the stability condition are less considered, the 3-D steel frames are not yet examined.

Another technique to optimize the structures is the optimal design of steel frames using elastic-plastic second-order analysis. Generally, this algorithm is based on an iteration procedure: selecting the initial configuration, analyzing the frame by second-order algorithm, checking the stability and stiffness condition according to Standards, and re-selecting the new configuration (see Choi (2002)[27]). The updating the second-order algorithm of CEPAO and the requirements of Eurocode-3 in above algorithm will be considered.

The plates, shells and disks structures are also frequently used in construction. The researches on the plastic analysis of these structures are abundant (e.g. Save (1972, 1995)[135, 134], Nguyen-Dang (1984)[122] and Morelle (1984, 1986, 1989) [111, 110, 109]). We will refer to them to establish or/and improve the automatic algorithms.

Liège 19th May 2008.

References

[1] AISC - Load and Resistance Factor Design Specification for Steel Buildings. American Institute of Steel Construction, Chicago, 1993.

[2] Argyris JH, Dunne PC, Scharpf DW. On large displacement-small strain analysis of structures with rotational degrees of freedom. Computer Methods in Applied Mechanic and Engineering 1978(14):401-451, 1978(15):99-135.

[3] Baset S, Grierson DE, Lind NC. Second-Order Collapse Load Analysis: a LP Approach. Solid Mechanics Division University of Waterloo, Canada, N°117, 1973.

[4] Bathe KJ. Finite element procedures. Prentice-Hall, Englewood Cliffs, NJ, 1996.

[5] Bathe KJ. Finite element procedures in engineering analysis. Prentice-Hall, Englewood Cliffs, NJ, 1982.

[6] Battini JM, Pacoste C. Co-rotational beam elements with warping effects in stability problems. Computer Methods in Applied Mechanic and Engineering 2002(191):1755-1789.

[7] Beckers P. Les fonctions de tension dans la méthode des éléments finis. Thèse de doctorat, Université de Liège, 1972.

[8] Bjorhovde R, Colson A, Brozzetti J. Classification system for beam-to-column connections. Journal of Structural Engineering-ASCE 1990(116-11):3059-3076.

[9] Bui-Cong T. Analyse directe des états limites plastiques des structures par programmation mathématique et discrétisation par éléments finis. Thèse de doctorat, Université de Liège, 1998.

[10] Byfield MP, Davies JM, Dhanalakshmi M. Calculation of the strain hardening behaviour of steel structures based on mill tests. Journal of Constructional Steel Research 2005 (61):133-150.

[11] Cabrero JM, Bayo E. Development of practical design methods for steel structures with semi-rigid connections. Engineering Structures 2005(27):1125-1137.

[12] Cabrero JM, Bayo E. The semi-rigid behaviour of three-dimensional steel beam-to-column steel joints subjected to proportional loading. Parts I and II. Journal of Constructional Steel Research 2007(63):1241-1267.

[13] Cardona A, Géradin M. A beam finite element non-linear theory with finite rotations. International Journal for Numerical Methods in Engineering 1988 (26):2403-2438.

[14] Casciaro R, Garcea G. An iterative method for shakedown analysis. Computer Methods in Applied Mechanic and Engineering 2002 (191):5761-5792.

[15] Cescotto S. Etude par élément finis des grands déplacements et grandes déformations: Application aux problèmes spécifiques des matériaux quasi-incompressibles. Thèse de doctorat, Université de Liège, 1978.

[16] Cescotto S, Zhu YY. Large strain dynamic analysis using solid and contact finite elements based on the mixed formulation: application to metal forming. Journal of Materials Processing Technology, 1994 (45):657-663.

[17] Charnes A, Greeberg HJ. Plastic collapse and linear programming. Bulletin of the American mathematical Society 1951:p506.

[18] Chan SL, Chui PPT. A generalized design-based elastoplastic analysis of steel frames by section assemblage concept. Engineering Structures 1997(19-8):628-636.

[19] Chen WF, Yoshiaki G, Liew JYR. Stability design of semi-rigid frames. John Wiley & sons, inc, 1996.

[20] Chen WF, Atsuta T. Theory of beam-columns – volume 2. McGRAW-HILL, 1977.

[21] Chen WF, Han DJ. Plasticity for structural engineers. Springer-Verlag, N.Y, 1988.

[22] Chen WF, Lui EM (eds). Handbook of structural engineering; Chapter 5: Steel frame design using advanced analysis. CRC Press, Boca Raton, Florida, 2005.

[23] Chen WF, Kishi N. Semi-rigid steel beam-to-column connexions: data base and modelling. Structural Engineering - ASCE 1989 (115-1):105-119.

[24] Chen WF, Lui EM. Stability design of steel frames. Boca Raton, FL: CRS Press, 1991.

[25] Chen WF. Structural Engineering: Seeing the Big Picture. KSCE Journal of Civil Engineering 2008(12-1):25-29.

[26] Chen WF. Structural stability: from theory to practice. Engineering Structures 2000(22):116-122.

[27] Choi SH, Kim SE. Optimal design of steel frame using practical nonlinear inelastic analysis. Engineering Structures 2002(24):1189-1201.

[28] Chiorean CG, Barsan GM. Large deflection distributed plasticity analysis of 3D steel frameworks. Computers & Structures 2005(83):1555-1571.

[29] Cocchetti G, Maier G. Elastic-plastic and limit-state analysis of frames with softening plastic-hinge models by mathematical programming. International Journal of Solids and Structures 2003(40):7219-7244.

[30] Cohn MZ, Ghosh SK, Parimi SR. A unified approach to the theory of plastic structures. Solid Mechanic Division Report 78, University of Waterloo, Canada, 1971.

[31] Cohn MZ, Grierson DE. An automatic approach to the analysis of plastic frames under fixed or variable loading. Solid Mechanic Division Report 22, University of Waterloo, Canada, 1969.

[32] Cohn MZ, Maier G. Engineering Plasticity by Mathematical Programming. University of Waterloo, Canada, 1979.

[33] Cohn MZ, Parimi SR. Optimal design of structures for fixed and shakedown loading. Solid Mechanic Division Report 98, University of Waterloo, Canada, 1971.

[34] Colson A, Bjorhovde R. Intérêt économiques des assemblages semi-rigides. Construction Métallique 1992(2):37-41.

[35] Cuong NH, Kim SE, Oh JR. Nonlinear analysis of space frames using fibre plastic hinge concept. Engineering Structures 2006(29):649-657.

[36] Davies JM. Second-order elastic-plastic analysis of plan frames. Journal of Constructional Steel Research 2002 (58): 1315-1330.

[37] Davies JM. Strain hardening, local buckling and lateral-torsional buckling in plastic hinges. Journal of Constructional Steel Research 2006 (62):27-34.

[38] de Saxcé G, Ohandja LMA. Une méthode automatique de calcul de l'effet P-Delta pour l'analyse pas - à - pas des ossatures planes. Construction Métallique 9/1985(3).

[39] Dentzig GB. Application et prolongement de la programmation linéaire. Dunord, Paris 1966.

[40] Doghri Issam. Mechanics of deformable solids: linear and nonlinear, analytical and computational aspects. Springer 2000.

[41] Domaszewski M, Borkowski A. An automatic selection of redundancies. Computers & Structures 1979(10):577-582.

[42] Domaszewski M, Stanislawska ES. Explicit solution of limit analysis problems as interval linear programs. Engineering Analysis 1984(1-2):110-116.

[43] Domaszewski M, Stanislawska ES. Optimal shakedown design of frames by linear programming. Computers & Structures 1985(21-3):379-385.

[44] Donald WW. Plastic-hinge methods for advanced analysis of steel frames. Journal of Constructional Steel Research 1993(24):121-152.

[45] Eurocode-3: Design of steel structures – Part 1-8: Design of connexions. European Committee for Standardization, 1993.

[46] Eurocode-3: Design of steel structures – Part 1-1: General rules and rules for building. European Committee for Standardization, 1993.

[47] Foukle J. The minimum weight design of structural frames. Proc. Roy. Soc. London, série A, 1954 (223): p82.

[48] Fraijs de Veubeke B. Displacement and equilibrium models in the finite element method. Stress Ananlysis, ed. Zienkiewics OC, Wiley and Sons, 1965:145-197.

[49] Franchi A, Grierson DE, Cohn MZ. An elastic-plastic analysis computer system. Solid Mechanic Division Paper 157, University of Waterloo, Canada, 1979.

[50] Frey F. L'analyse statique non linéaire des structures par la méthode des éléments finis et son application à la construction métallique. Thèse de doctorat, Université de Liège, 1979.

[51] Géradin M, Rixen D. Mechanical vibrations: theory and application to structural dynamics. New York, NY: John Weily, 1997.

[52] Gizejowski MA, Barszcz AM, Branicki CJ, Uzoegbo HC. Review of analysis methods for inelastic design of steel semi-continuous frames. Journal of Constructional Steel Research 2006(62):81-92.

[53] Gong Y, Xu L, Grierson DE. Sensitivity analysis of steel moment frames accounting for geometric and material nonlinearity. Computer & Structures 2006(84):426-475.

[54] Grierson DE. Computer-based methods for the plastic analysis and design of building frames. ASCE-IABSE Joint Committee on Planning and Design of Tall Building, Report to Technical Committee 15, 1974.

[55] Grierson DE, Gladwell ML. Collapse load analysis using linear programming. Journal of the Structural Division - ASCE 1971(5):1561-1573.

[56] Grierson DE. Deformation analysis of Elastic-plastic frames. Journal of the Structural Division - ASCE 1972(98-10): 2247-2267.

[57] Guisse S. Quelle économie attendre de la mise en oeuvre de noeuds semi-rigides?. Construction Métallique 1993(3):19-27.

[58] Hasan R, Xu L, Grierson DE. Push-over analysis for performance-based seismic design. Computer & Structures 2002(80):2483-2493.

[59] Hayalioglu MS, Degertekin SO. Minimum cost design of steel frames with semi-rigid connection and column bases via genetic optimization. Computers & structures 2005(83):1849-1863.

[60] Hoang-Van L, Nguyen-Dang H. Limit and shakedown analysis of 3-D steel frames. Engineering Structures 2008(30):1895-1904.

[61] Hoang-Van L, Nguyen-Dang H. Plastic optimization of 3-D steel frames under fixed or repeated loading: reduction formulation. Engineering Structures, under review 2008.

[62] Hoang-Van L, Nguyen-Dang H. Local buckling check according to Eurocode-3 for plastic-hinge analysis of 3-D steel frames. Engineering Structures 2008(30): 3105-3513.

[63] Hoang-Van L, Nguyen-Dang H. Second-order plastic-hinge analysis of 3-D steel frames including strain hardening effects. Engineering Structures 2008(30): 3505-3512.

[64] Hodge PG. Plastic analysis of structures. McGraw Hill, New York, 1959.

[65] Izzuddin BA. Conceptional issues in geometrically nonlinear analysis of 3-D framed structures. Computer Methods in Applied Mechanic and Engineering 2001(191):1029-1053.

[66] Jaspart JP, Vandegans D. Application of the component method to column base. Journal of constructional steel research 1998(48):89-106.

[67] Jaspart JP, Demonceau JF. European design recommendations for simple joints in steel structures. Journal of Constructional Steel Research 2008(64):822-832.

[68] Jaspart JP. Etude de la semi - rigidité des nœuds poutre - colonne et son influence sur la résistance et la stabilité des ossatures en acier. Thèse de doctorat, Université de Liège, 1991.

[69] Jaspart JP. General report: section on connexions. Journal of Constructional Steel Research 2000(55):69-89.

[70] Jaspart JP. Recent advances in the field steel joints column - Bases and further configurations for beam-to-column joints and beam splices. Professorship thesis, University of Liège, 1997.

[71] Jiang XM, Chen H, Liew JYR. Spread-of-plasticity analysis of three-dimensional steel frames. Journal of Constructional Steel Research 2002 (58):193-212.

[72] Jirásek M, Bažant ZP. Inelastic Analysis of Structure. John Wiley & Sons, LTD, 2001.

[73] Jones SW, Kirby PA, Nethercot DA. The analysis of frames with semi-rigid connexion- a state-of-the-art-report. Journal of Constructional Steel Research 1983(3-2):2-13.

[74] Kaliszky S, Lógó J. Plastic behaviours and stability constraints in the shakedown analysis and optimal design of trusses. Structural and Multidisciplinary Optimization 2002 (24):118-124.

[75] Kaneko L, Maier G. Optimum design of plastic structures under displacement' constraints. Computer Methods in Applied Mechanic and Engineering 1981, (27-3):369-392.

[76] Kaveh A, Moez H. Analysis of frames with semi-rigid joints: A graph-theoretical approach. Engineering Strcutures 2006(28):829-836.

[77] Kim SE, Choi SH. Practical advanced analysis for semi-rigid space frames. International Journal of Solids and Structures 2001 (38):9111-9131.

[78] Kim SE, Cuong NH, Lee DH. Second-order inelastic dynamic analysis of 3-D steel frames. International Journal of Solids and Structures 2006 (43):1693-1709.

[79] Kim SE, Lee J, Part JS. 3-D second - order plastic-hinge analysis accounting for lateral torsional buckling. International Journal of Solids and Structures 2002 (39):2109-2128.

[80] Kim SE, Lee J, Part JS. 3-D second - order plastic-hinge analysis accounting for local buckling. Engineering Structures 2003 (25):81-90.

[81] Kim SE, Park MH, Choi SH. Direct design of three-dimensional frames using advanced analysis. Engineering Structures 2001(23):1491-1502.

[82] Kishi N, Chen WF. Moment-rotation relations of semi-rigid connexions with angles. Structural Engineering - ASCE 1990 (116-7):1813-1834.

[83] Koiter WT. General theorem for elastic-plastic solids. Progress in Solid Mechanic, North Holland, Amsterdam, 1960(1):165-221.

[84] König JA. Shakedown of elastic-plastic structures. Elsevier, Amsterdam, 1987.

[85] Landesmann A, Batista EM. Advanced analysis of steel buildings using the Brazilian and Eurocode-3. Journal of Constructional Steel Research 2005 (61):1051-1074.

[86] Lescouarc'h Y. Calcul en plasticité des structures à barres avec prise en compte de l'influence moment de flexion - effort normal. Annales de l'institut technique de bâtiment et des travaux publics, supplément au N^0 326 mars 1975.

[87] Lescouarc'h Y. Programme de calcul en élasto-plasticité des structures planes. Construction Métallique 1976(1):40-50.

[88] Liew JYR, Chen H, Shanmugam NE, Chen WF. Improved nonlinear plastic hinge analysis of space frame structures. Engineering Structures 2000(22): 1324-1338.

[89] Liew JYR, Chen H, Shanmugam NE. Inelastic analysis of steel frames with composite beams. Journal of Structural Engineering - ASCE 2001; 127(2): 194-202.

[90] Liew JYR, White DW, Chen WF. Second order refined plastic hinge analysis for frame design: parts 1 and 2. Journal of Structural Engineering-ASCE 1993; 119 (11): 3196-1237.

[91] Liu Y, Xu L, Grierson DE. Compound-element modelling accounting for semi-rigid connexions and member plasticity. Engineering Structures 2008(30):1292-1307.

[92] Lubliner J. Plasticity theory. Macmilan Publising Company, 1990.

[93] Maier G. A matrix structural theory of piecewise linear elastoplastic with interacting yield plan. Meccanica 1970 (5):54-66.

[94] Maier G, Garvelli V, Cocchetti G. On direct methods for shakedown and limit analysis. European Journal of Mechanics/A: Solids 2000 (19):S79-S100.

[95] Maier G, Giacomini S, Paterlini F. Combined elastoplastic and limit analysis via restricted basis linear programming. Computer Method in Applied Mechanics and Engineering 1979 (19):21-48.

[96] Maier G. Increment plastic analysis in the presence of large displacement and physical instabilizing effects. International Journal of Solids and Structures 1971 (7):345-372.

[97] Maier G. Mathematical programming applications to structural mechanics: some introductory thoughts. Key Note, Workshop of Liège, 1 june 1982.

[98] Maier G. Mathematical programming methods in structural analysis. Proc. Int. Symp. On Variational Methods in Engineering (ed. by Brebbia C, Tottenham H), Southampton Universiy Press, 1973.

[99] Maier G, Munro J. Mathematical programming applications to engineering plastic analysis. Appl Mech Rev 1982(35):1631-1643.

[100] Maier G. Piecewise linearization of yield criteria in structural plasticity. SM Archives 1976(1):239-281.

[101] Maier G. Quadratic programming and theory of elastic-perfectly plastic structures. Meccanica 1970 (3):121-130.

[102] Maier G. Shakedown theory in perfect elastoplasticity with associated and nonassocieted flow-laws: A finite element linear programming approach. Meccanica 1969 (4):250-260.

[103] Maier G, Srininavan R, Save M. On limit design of frames using linear programming. Proc. Int. On Computer-Aide Structural Design, University of Warwick, 1972.

[104] Maquoi R, Jaspart JP. Modelling of beam-to-column joints for the design of steel building frames. Constructional Steel Design Conference: World developments, Edited by Dowling PJ, Harding JE, Bjorhovde R and Martinez-Romero E, Elsevier Applied Science, 1992.

[105] Maquoi R. Semi-rigid joints: from research to design practice. In "Steel structures: Recent research and development" ed. by Lee SL, Shanmugan NE, 1991.

[106] Massonnet Ch, Save M. Calcul plastique des constructions, Volume 1, Nelissen, Belgique, 1976.

[107] Massonnet Ch. Faut-il introduire l'hypothèse de Bernoulli en résistance des matériaux? Bull. Soc. Roy. Des Sci., 12, 301, Liège 1947.

[108] Merkevičiùtê D, Atkočiùnas J. Optimal shakedown design metal structures under stiffness and stability constraints. Journal of Constructional Steel Research 2006 (62):1270-1275.

[109] Morelle P. Analyse duale de l'adaptation plastique des éléments finis et la programmation mathématique. Thèse de doctorat, Université de Lège, 1989.

[110] Morelle P. Numerical shakedown analysis of axisymmetric sandwich shells: An upper bound formulation. International Journal for Numerical Methods in Engineering 1986(23):2071-2088.

[111] Morelle P. Structural shakedown analysis by dual finite-element formulation. Engineering Structures 1984(6):70-79.

[112] Mróz Z, Weichert D, Dorosz S (eds). Inelastic behaviour of structures under variable loads. Kluwer, Dordrecht, The Netherlands, 1995.

[113] Munro J, Smith DL. Linear programming duality in plastic analysis and synthesis. Proc. Int. Symp.Computer Aided Structural Design, Coventry, 1972.

[114] Neal BG. The plastic method of structural analysis. Chapman & Hall, London, 1956.

[115] Nguyen-Dang H, König JA. A finite element formulation for shakedown problems using a yield criterion of the mean. Computer Methods in Applied Mechanics and Engineering 1976 (8):81-116.

[116] Nguyen-Dang H. Applications of mathematical programming method to structural analysis and design. Proceeding of the Workshop of Liège, 1 june 1982.

[117] Nguyen-Dang H. CEPAO-an automatic program for rigid-plastic and elastic-plastic, analysis and optimization of frame structure. Engineering Structures 1984 (6): 33-50.

[118] Nguyen-Dang H, de Saxcé G. Frictionless contact of elastic bodies by finite elements method and mathematical programming technique. Computer & Structures 1980(11):55-68.

[119] Nguyen-Dang H. Displacement and equilibrium methods in matrix analysis of trapezoidal structures. Collection des publications de la Faculté des Sciences Appliquées, Université de Liège, N^0 21, 1970.

[120] Nguyen-Dang H, Hoang Van L. A united algorithm for limit state determination of frames with semi-rigid connexion. In: Collection of papers from Pro. Nguyen-Dang Hung's former students (edited by de Saxcé G and Moës N), Ho-Chi-Minh City 2006.

[121] Nguyen-Dang H. Plastic collapse of shells of revolution by non-linear programming and finite element techniques. Journal of Engineering Mechanics Division - ASCE 1978 (104/3): 707-712.

[122] Nguyen-Dang H. Sur la plasticité et le calcul des états limites par élément finis. Thèse de doctorat spécial, Université de Liège, 1984.

[123] Nguyen-Dang H. Sur l'utilisation du simplexe dans le CEPAO. Rapport interne N133, Laboratoire de Mécanique des Matériaux et Statique des Constructions, Université de Liège, 1982.

[124] Nguyen-Dang H, Trapletti M, Ransart D. Bornes quasi-inférieure et bornes supérieures de la pression de ruine des coques de révolution par la méthode éléments finis et par la programmation non-linéaire. International Journal of Non-linear Mechanics 1978(13):79-102.

[125] Nguyen-Dang H. Une méthode automatique du calcul de déplacement élasto-plastique juste avant la ruine. Construction Métallique 1983(1):27-36.

[126] Orbison JG, McGUIRE W, Abel JF. Yield surface applications in nonlinear steel frame analysis. Computer Method in Applied Mechanics and Engineering 1982(33):557-573.

[127] Parimi SR, Ghosh SK, Cohn MZ. The computer programme DAPS for the design and analysis of plastic structures. Solid Mechanics Division Report 26, University of Waterloo, Canada, 1973.

[128] Ponthot JP. Traitement unifié de la mécanique des milieux continus solides en grandes transformations par la méthode des éléments finis. Thèse de doctorat, Université de Liège, 1994.

[129] Ponthot JP. Unified stress update algorithms for the numerical simulation of large deformation elasto-plastic and elasto-viscoplastic processes. International Journal of Plasticity 2002(18):91-126.

[130] Rondal J. Contribution à l'étude de la stabilité des profils creux à paroi minces. Thèse de doctorat, Université de Liège, 1984.

[131] Rondal J, Maquoi R. Formulations d'Ayrton-Perry pour le flambement des barres métalliques. Construction Métallique 1979(4):41-53.

[132] Rodrigues PFN, Jacob BP. Collapse analysis of steel jacket structures for offshore oil exploitation. Journal of Constructional Steel Research 2005(61):1147-1171.

[133] Romero J, Mappa PC, Herskovits J, Mota Soares CM. Optimal truss design including plastic collapse constraints. Structural and Multidisciplinary Optimization 2004(27):20-26.

[134] Save M. Atlas of limit loads of metal plates, shells and disks. ELSEVIER, 1995.

[135] Save M, Massonnet Ch. Calcul plastic des constructions, Volume 2. Nelissen, Belgique, 1972.

[136] Save M. On yield conditions in generalized stress. Quart. Of Applied Math 1961(XIX- 3).

[137] Sawczuk A. Yield surfaces. Solid Mechanic Division, Technical note 1, University of Waterloo, Canada, 1971.

[138] Sekulović M, Danilović MN. Static inelastic analysis of steel frames with flexible connexions. Theory. Appl. Mech. Belgrade 2004(31-2):101-134.

[139] Simões LMC. Optimization of frames with semi-rigid connections. Computers & structures 1996 (60-4):531-539.

[140] Smith DL (ed). Mathematical Programming Method in Structural Plasticity. Springer – Verlag, New York, 1990.

[141] Teh LH, Clarke MJ. Co-rotational and Lagrangian formulation for elastic three-dimensional beam finite elements. Journal of Constructional Steel Research 1998(48):123-144.

[142] Timoshenko SP, Goodier JM. Theory of Elasticity. McGraw-Hill, New York, 1951.

[143] Timoshenko SP, Young DH. Element of Strength of Materials. Van Nostrand, Princeton, New Jersey, 1962.

[144] Tin Loi F, Vimonsatit V. Nonlinear analysis of semi-rigid frames: a parametric complementarity approach. Engineering Structure 1996 (18-2): 115-124.

[145] Tin Loi F, Vimonsatit V. Shakedown of frame with semi-rigid connections. Journal of Structural Engineering-ASCE 1993(119-6):1694-1711.

[146] Tin-Loi F. Optimum shakedown design under residual displacement constraints. Structural and Multidisciplinary Optimization 2000(19):130-139.

[147] Vu-Duc K, Yan YM, Nguyen-Dang H. A dual form for discretized kinematic formulation in shakedown analysis. International Journal of Solids and Structures 2004 (41):267-277.

[148] Weichert D, Maier G (eds). Inelastic analysis of structures under variable repeated loads. Kluwer, Dordrecht, The Netherlands, 2000.

[149] Xu L, Grierson DE. Computer- automated design of semi-rigid steel frameworks. Journal of Structural Engineering- ASCE 1993(119-6): 1741-1760.

[150] Yan AM, Nguyen-Dang H. Limit analysis of cracked structures by mathematical programming and finite element technique. Computational Mechanics 1999(23):319-333.

[151] Zienkiewicz OC. Elasto-plastic solutions of engineering problems. Initial stress, finite element approach. International Journal for Numerical Methods in Engineering 1969 (1):75-100.

[152] Zienkiewicz OC, Taylor RL. The finite element method. Vol. 1 – Basic formulation and linear problems, 4th edition, McGraw Hill Book Co., England, 1989.

[153] Zienkiewicz OC, Taylor RL. The finite element method. Vol. 2 – Solid and fluid mechanics, dynamics and nonlinearity, 4th edition, McGraw Hill Book Co., England, 1991.